

TUM School of Engineering and Design

Development and validation of an orthogonal polarity-extended HRMS screening to detect highly polar trace organic compounds in the aquatic environment

Susanne Kathryn Minkus

Vollständiger Abdruck der von der TUM School of Engineering and Design der Technischen Universität München zur Erlangung einer Doktorin der Naturwissenschaften genehmigten Dissertation.

Vorsitz: apl. Prof. Dr. Brigitte Helmreich

Prüfer\*innen der Dissertation:

1. Prof. Dr.-Ing. Jörg E. Drewes
2. Priv.-Doz. Dr. Thomas Letzel
3. Prof. Dr. Torsten Schmidt

Die Dissertation wurde am 05.07.2022 bei der Technischen Universität München eingereicht und durch die TUM School of Engineering and Design am 30.10.2022 angenommen.



## Abstract

Highly polar trace organic compounds tend to be mobile in the aquatic environment. If they are additionally persistent, they pass natural and technical barriers, accumulate in the water cycle and eventually pose a threat to drinking water supplies. In order to analyze compounds of an extended polarity range, a serial coupling of reversed-phase liquid chromatography, hydrophilic interaction chromatography and mass spectrometric detection was used within in the scope of this study. Operating the high-resolution and high-accuracy mass spectrometer in full scan mode enabled a so-called non-target screening of samples. From the complex non-target screening data, so-called features - described by their accurate mass, chromatographic retention time and signal intensity - need to be extracted, ideally corresponding to a chemical compound.

This thesis presents an analytical method comprising of an instrumental as well as a data analysis part. It was developed to screen water samples for molecules of an extended polarity range without preselecting substances of interest. In order to meet that objective, the method needed to fulfill the following criteria:

- a) Detect as many relevant features as possible,
- b) be of controlled quality,
- c) be adaptable to different research questions,
- d) be applicable to environmental water samples.

The first criterion was tackled by optimizing the method parameters to detect a plethora of molecules but at the same time reduce false positive findings. In that sense, a robust setpoint was found for electrospray ionization parameters which maximizes the ionization efficiency of multiple model substances with diverse physico-chemical properties. The data evaluation method was applied to internal and external standard compounds in order to iteratively maximize their recovery. A tool of choice for method optimization herein was statistical design of experiment where settings of multiple parameters are varied strategically and simultaneously and the results are subsequently modeled.

Secondly, the measurement of quality control samples and standard compounds provided information on the instrumental performance and served as reference points to reduce false positive and false negative findings during data processing.

According to criterion (c), the data processing strategy needed to be flexible enough to adapt to different software tools and research questions. Therefore, a core workflow for extracting features was identified first and complemented by either prioritization and database matching for

compound identification or statistical evaluations for sample comparison.

The method was applied to comprehensive sample sets of surface water samples and (tentatively) identified highly polar and environmentally relevant compounds. Guanylurea, melamine, and 1,3-dimethylimidazolidin-2-one were verifiably detected in the Isar river. 4-hydroxy-2,2,6,6-tetramethylpiperidine-1-ethanol was a suspect of particularly high priority as it was found at 47 different locations in the Danube river basin. Finally, the method was able to give indications on the (partial) removal of highly polar compounds from surface water by treating it with three different types of powdered activated carbon.

## Kurzzusammenfassung

Hochpolare organische Spurenstoffe neigen dazu, in der aquatischen Umwelt mobil zu sein. Sind sie zudem persistent, überwinden sie natürliche und technische Barrieren, reichern sich im Wasserkreislauf an und stellen schließlich eine Gefahr für die Trinkwasserversorgung dar. Um Verbindungen eines erweiterten Polaritätsbereichs zu analysieren, wurde im Rahmen dieser Arbeit eine serielle Kopplung von Umkehrphasen-Flüssigkeitschromatographie, hydrophiler Interaktionschromatographie und massenspektrometrischer Detektion eingesetzt. Der Betrieb des hochauflösenden und akkuraten Massenspektrometers im Full-Scan-Modus ermöglichte ein sogenanntes nicht-zielgerichtetes Screening der Proben. Aus diesen komplexen Daten müssen Merkmale extrahiert werden, die durch ihre genaue Masse, chromatographische Retentionszeit und Signalintensität beschrieben werden und denen im Idealfall eine chemische Verbindung zugrunde liegt.

In Rahmen dieser Doktorarbeit wird eine Analysemethode vorgestellt, die sowohl aus einem instrumentellen als auch aus einem Datenanalyseteil besteht. Sie wurde entwickelt, um Wasserproben auf Moleküle eines erweiterten Polaritätsbereichs zu untersuchen, ohne eine molekulare Vorauswahl zu treffen. Um dieses Ziel zu erreichen, musste die Methode die folgenden Kriterien erfüllen:

- a) Erkennung möglichst vieler relevanter Merkmale,
- b) kontrollierte Qualität,
- c) Anpassungsfähigkeit an verschiedene Forschungsfragestellungen und
- d) Anwendbarkeit auf Wasserproben.

Um das erste Kriterium zu erfüllen, wurden die Methodenparameter optimiert, um eine Vielzahl von Molekülen zu erkennen und gleichzeitig die Zahl der falsch-positiven Ergebnisse zu reduzieren. In diesem Sinne wurde für die Elektrospray-Ionisation eine robuste Kombination der Einstellparameter ermittelt, die die Ionisationseffizienz mehrerer Modellsubstanzen mit unterschiedlichen physikalisch-chemischen Eigenschaften maximiert. Die Datenauswertungsmethode wurde auf interne und externe Standardverbindungen angewandt, um deren Wiederfindung iterativ zu maximieren. Ein Mittel der Wahl für die Methodenoptimierung war hier die statistische Versuchsplanung, bei der die Einstellungen mehrerer Parameter strategisch und simultan variiert und die Ergebnisse anschließend modelliert werden.

Weiterhin lieferten Messungen von Qualitätskontrollproben und Standardverbindungen Informationen über die instrumentelle Leistung und dienten als Referenzpunkt, um falsch-positive und falsch-negative Befunde während der Datenverarbeitung zu reduzieren.

Gemäß Kriterium (c) musste die Datenverarbeitungsstrategie so flexibel sein, dass sie an unterschiedliche Softwaretools und Forschungsfragestellungen angepasst werden konnte. Daher wurde zunächst ein Kernarbeitsablauf für die Extraktion von Merkmalen festgelegt, der entweder durch Priorisierung und Datenbankabgleich zur Identifizierung von Verbindungen oder durch statistische Auswertungen zum Vergleich von Proben ergänzt wurde.

Die Methode wurde auf umfassende Probensätze von Oberflächenwasserproben angewandt und identifizierte (vorläufig) hochpolare und umweltrelevante Verbindungen. Guanylarnstoff, Melamin und 1,3-Dimethylimidazolidin-2-on wurden in der Isar eindeutig nachgewiesen. 4-Hydroxy-2,2,6,6-tetramethylpiperidin-1-ethanol war ein Kandidat von besonders hoher Priorität, da er an 47 verschiedenen Probenahmestellen im Einzugsgebiet der Donau gefunden wurde. Schließlich konnte die Methode Hinweise auf die (partielle) Entfernung hochpolarer Verbindungen aus dem Oberflächenwasser durch die Behandlung mit drei verschiedenen Arten von pulverförmiger Aktivkohle geben.

## Acknowledgement

Preparing my doctoral thesis would not have been possible without the help of many people and I hereby express my gratitude for their support.

Firstly, I would like to thank the people at the Chair of Urban Water Systems Engineering, especially Prof. Dr. Jörg Drewes. Apart from supervising this thesis, he taught me how to introduce structure and logic into my work to create the bigger picture. I extend my gratitude to Dr. Oliver Knoop, Dr. Konrad Koch, Prof. Brigitte Helmreich and the other doctoral candidates like Dr. Rofida Wahman and Hanna Ulrich who all created a productive scientific environment and a friendly working atmosphere.

I am grateful to Prof. Dr. Torsten Schmidt for being an active and friendly member of my examination committee.

I acknowledge the valuable contributions to my work and the cooperative collaboration of the (former) students Bianca Waldapfel and Simon Stoß.

The statistical knowledge and forward thinking of Stefan Moser is also greatly acknowledged.

I want to thank the people of the Westfälische Wasser- und Umwelt GmbH for their fruitful cooperation. Thank you, Dr. André Liesener and Anna Maria Reineke for your support and trust in my skills. Anna-Lisa Kowalski and Jacqueline Porada always offered me a helping hand and good time at lunch.

The contributions of the International Commission for the Protection of the Danube River (ICPDR) in the form of samples and information is acknowledged.

A special thanks goes to my employers at the AFIN TS GmbH, PD Dr. Thomas Letzel and Dr. Stefan Bieber. Dr. Stefan Bieber mentored me far before my Ph.D. project started. His impressive analytical and practical knowledge are paired with outstanding teaching skills. Much of what I know and can do now when it comes to analytical chemistry, I owe to him.

And most importantly, I thank you, Thomas, for your close supervision and tireless input and discussion. Without you, this thesis would not be what it is. You contributed a great deal to shaping my career and your enthusiasm for the subject sparked my interest and motivation. Your progressive work ethic has yet to be matched by many!

And finally, I am deeply grateful for my friends and family, especially my parents. Even though she cannot see me finish anymore, my mother's smart advice still guides me. I want to thank my father for always being the rock of the family.

# Content

Abstract.....	i
Kurzzusammenfassung.....	iii
Acknowledgement.....	v
Content .....	vi
List of Figures.....	xi
List of Tables.....	xiii
Abbreviations .....	xiv
1. Introduction .....	1
1.1 Trace organic compounds in the aquatic environment .....	1
1.1.1 Occurrence and toxicological potential .....	1
1.1.2 Persistent and mobile organic compounds (PMOCs).....	2
1.2 Instrumentation to analyze (polar) organic micropollutants.....	3
1.2.1 Polarity-extended chromatography .....	3
1.2.2 Mass spectrometry .....	4
1.2.3 Ionization techniques.....	6
1.3 Non-target screening .....	7
1.3.1 Screening strategies.....	7
1.3.2 Data processing .....	7
1.3.3 Applications.....	8
1.4 Quality assurance and control for non-target screening .....	9
1.5 Design of experiment.....	10
2. Research objectives and hypothesis .....	12
3. Method optimization .....	16
3.1 Use statistical design of experiment (DoE) to find a robust setpoint for electrospray ionization parameters that maximizes ionization efficiency for a wide range of molecules.....	16
3.1.1 Introduction.....	17

---

3.1.2 Methods .....	19
3.1.2.1 Chemicals and solutions .....	19
3.1.2.2 Design of Experiment.....	19
3.1.2.3 Instrumentation .....	20
3.1.2.4 Data handling.....	21
3.1.3 Results and discussion .....	22
3.1.3.1 Strategy .....	22
3.1.3.2 Model fit and diagnostics.....	22
3.1.3.3 Prediction and Optimization .....	24
3.1.3.4 Robust setpoint validation .....	26
3.1.4 Conclusion.....	27
3.2 Adjust the parameter settings of the data processing method by applying it to standards compounds and maximizing their recall .....	28
3.2.1 Methods .....	28
3.2.2 Discussion.....	28
3.3 Use DoE to find a robust setpoint for the input parameters and filters of the data processing method that maximizes predefined performance descriptors .....	29
3.3.1 Methods .....	29
3.3.2 Discussion.....	29
4. Quality assurance of the method .....	31
4.1 Use QC samples, external and internal standards at different concentrations and in different matrices to assess the variability between RPLC-HILIC-HRMS measurements .....	32
4.1.1 Methods .....	32
4.1.2 Results and discussion.....	32
4.2 Add filters to the data processing workflow to remove noise, artefacts, redundant and false positive features.....	35
4.2.1 Methods .....	35
4.2.2 Discussion.....	36

---

4.3 Identify the points of losses of false negative features by accessing intermediate stages of the data processing workflow .....	37
4.3.1 Methods .....	37
4.3.2 Discussion.....	37
4.4 Introduce recursive target searches to the data processing workflow to retrospectively improve the quality and statistical confidence of final feature lists .....	37
4.4.1 Methods .....	37
4.4.2 Discussion.....	38
5. Method adaptation.....	40
5.1 In a top-down approach, all necessary processing tools are gathered first, identified in the specific vendor and open access software and used to construct a feature extraction workflow .....	41
5.1.1 Methods .....	41
5.1.2 Discussion.....	41
5.2 Use specialized databases to match a feature with a candidate compound using exact mass and physicochemical properties.....	44
5.2.1 Methods .....	44
5.2.2 Discussion.....	44
5.3 Add prioritization and classification steps to the feature extraction workflow to facilitate identification at a high level of confidence .....	45
5.3.1 Methods .....	45
5.3.2 Discussion.....	46
5.4 Add the necessary processing steps to the workflow and adjust related parameters for comparative analysis of samples .....	48
5.4.1 Introduction.....	48
5.4.2 Methods .....	48
5.4.3 Results and discussion.....	50
6. Application of the method .....	52

---

6.1 Evaluate the spatial and temporal distribution of polar features in the Isar river and tentatively identify them .....	53
6.1.1 Methods .....	53
6.1.2 Discussion.....	53
6.2 Classify, prioritize and tentatively identify polar features in ground and surface water samples of the Danube river basin.....	54
6.2.1 Methods .....	54
6.2.2 Discussion.....	54
6.3 Characterize different types and concentrations of powdered activated carbon by comparing the fingerprints of polar candidate molecules.....	55
6.3.1 Introduction.....	55
6.3.2 Methods .....	56
6.3.2.1 Chemicals.....	56
6.3.2.2 Samples.....	56
6.3.2.3 LC-MS analysis.....	57
6.3.2.4 Data analysis .....	58
6.3.3 Results and discussion.....	59
6.3.3.1 Targeted evaluation .....	59
6.3.3.2 Non-targeted evaluation.....	61
6.3.3.3 Further statistical analysis.....	63
6.3.4 Conclusions.....	64
7. Conclusion and final discussion.....	66
8. Outlook.....	69
9. List of further research contributions.....	70
9.1 Other articles .....	70
9.2 Oral presentations.....	70
9.3 Poster presentations .....	70
10. References.....	72

---

<b>Appendix A: Peer-reviewed publications</b> .....	A-1
Appendix A.1 Optimized hidden target screening for very polar molecules in surface waters including a compound database inquiry .....	A-2
Appendix A.2 (Very) polar organic compounds in the Danube river basin: a non-target screening workflow and prioritization strategy for extracting highly confident features .....	A-17
Appendix A.3 Spotlight on mass spectrometric non-target screening analysis: Advanced data processing methods recently communicated for extracting, prioritizing and quantifying features .....	A-29
<b>Appendix B: Supporting information</b> .....	B-40
Appendix B.1 Supplementary material - Optimization of electrospray ionization parameters in a RPLC-HILIC-MS/MS coupling by design of experiment .....	B-41
Appendix B.2 Electronic supplementary material - Optimized hidden target screening for very polar molecules in surface waters including a compound database inquiry .....	B-46
Appendix B.3 Electronic supplementary information - (Very) polar organic compounds in the Danube river basin: Non-target screening workflow and prioritization strategy for extracting highly confident features .....	B-56
Appendix B.4 Supplementary material - Characterizing powdered activated carbon treatment of surface water samples using polarity-extended non-target screening analysis.....	B-78

## List of Figures

Figure 1: The four hypothesis are presented under the four topics of developing and validating the analytical method. Each hypothesis is subdivided into tasks. The results of each task are presented in peer-reviewed articles which are listed in text above and referenced by P in brackets.....	15
Figure 2: Schematic graphic of the Sciex TurbolonSpray™ probe used in this study. Setting parameters that were subject of the statistical adaption are depicted in bolt. ....	18
Figure 3: The serial coupling of RPLC and HILIC. The mobile phases are transported by two binary pumps and the reference solution by an isocratic pump. The diagrams below each partial system display the flow and solvent gradients. ....	21
Figure 4: Normal probability plot for linuron. The deleted studentized residuals of all experiments were ordered by size and plotted against their normal probability. Since thy are following a straight line, it can be assumed that residuals in the case of linuron are approximately normal distributed. There are no outliers that exceed the $\pm 4$ SD mark. ....	24
Figure 5: Factor effects of the declustering potential and temperature on the signal intensity of linuron (response 16). The yellow bullets mark the robust settings. All other factors values were kept at the robust setpoint as well. The 95 % prediction interval is depicted by the dotted lines and the specification limits by the dashed lines ....	26
Figure 6: The robust setpoint was validated by comparing the predicted and observed signal intensities of the 30 model substances. Response 14 (flurtamone) is not displayed since it is an outlier with a predicted an observed peak height > 2,000,000 cps.....	27
Figure 7: Scores plot of the PCA based on the normalized peak heights of the feature extracted from each individual measurement. ....	35
Figure 8: The methods for extracting features from data acquired with polarity-extended chromatography coupled to ESI-HRMS are presented schematically. The workflow was built into three different software tools: A) MassHunter Workstation Profinder, B) MarkerView and C) MZmine 2. The core procedural modules are depicted in colored boxes along with the relevant setting parameters. Additional processing steps which were necessary to adapt the workflow to the respective software and data set are displayed in dashed boxes.....	43
Figure 9: For the RTI normalization, nine standard compounds were measured three times. Their log D values were plotted against the mean RTs and a linear calibration function was fitted. The trend line (solid black line) was extrapolated to a log D (pH 7) value of 0 (dashed red line). This Figure has been previously published elsewhere [101]. ....	45

- Figure 10: The dot plot displays features that were detected in the March samples either upstream or downstream of Munich (circles, location IDs 8 and 9, Table S1; Appendix B.2) or just downstream of Munich (crosses). The features eluted from the HILIC column and were proposed by the STOFF-IDENT database. Only matches with a negative log  $D$  value were considered. The numbers indicate the ID of the database queries as are listed in Table 2 of Appendix A.1. This figure was published as presented in Appendix A.1. .... 47
- Figure 11: NTS data processing workflow for comparing a treated and an untreated surface water sample. The processing steps for extracting and filtering features from the technical replicates of a single sample are depicted in black. The orange boxes are processing steps that enable the comparative analysis of the treated and the untreated sample. .... 50
- Figure 12: The base-2 logarithm of the fcs of the HILIC standards (added prior to PAC treatment, blue diamonds) and the internal standards (added prior to analysis, orange circles) are plotted versus their RTs. The dashed lines mark the consistency interval where no compound removal is assumed. .... 61
- Figure 13: Non-target features (black crosses) and polar standard compounds (blue diamonds) are plotted by their base-2 logarithmic fcs and RT. The dashed lines mark the consistency interval.  $\text{Log}_2(\text{fc})$  values  $< -1$  and  $> 1$  are defined as a decrease and increase in signal intensity, respectively. Here the sample treated with  $30 \text{ mg L}^{-1}$  of PAC H121 was compared to the untreated blank sample, both measured in positive ionization mode. .... 63
- Figure 14: The volcano plot depicts features extracted during the comparative analysis of the sample treated with PAC type H121 at  $30 \text{ mg L}^{-1}$  and the respective blank sample. The horizontal dashed line marks the cut-off p-value of  $-\log_{10}(0.05)$  and the vertical dashed lines the consistency interval. Features which were annotated with polar standard compounds are marked with blue diamonds. .... 64

## List of Tables

Table 1: Six factors of the ESI that were statistically evaluated and optimized (see also Figure 2). For each factor the upper and lower limit of the interval and the setting precision are given. ....	20
Table 2: Robust setpoint value for each factor along with the hypercube range and its contribution percentage. ....	25
Table 3: Maximum values of RT precision, mass precision and mass accuracy assessed on 177 reference compounds measured three times on the RPLC-HILIC-QTOF-MS setup. Standard compounds are classified by their polarity. Log <i>D</i> values are given for a pH of 7. This table has been published before [101]. ....	33
Table 4: The types of PAC used for the batch sorption experiments.....	57
Table 5: Means and standard deviations of log <sub>2</sub> ( <i>f</i> <sub>c</sub> ) values for the internal standards and the polar standard compounds measured in positive ionization mode. H118, H120 and H121 are the laboratory names of the different PAC types (Table 4) which were tested for surface water treatment at three different concentrations. ....	60
Table 6: Means and standard deviations of log <sub>2</sub> ( <i>f</i> <sub>c</sub> ) values for the non-target features in positive ionization mode. H118, H120 and H121 are the laboratory names of the different PAC types which were tested for surface water treatment at three different concentrations. ....	62

## Abbreviations

CSV	Comma-separated Values
DBP	Disinfection Byproducts
DF	Degrees of Freedom
DOC	Dissolved Organic Carbon
DoE	Design of Experiment
EIC	Extracted Ion Chromatogram
ESI	Electrospray Ionization
fc	Fold Change
HILIC	Hydrophilic Interaction Liquid Chromatography
HRMS	High-Resolution Mass Spectrometry
IDA	Independent Data Acquisition
MAPE	Mean Absolute Percentage Error
MLR	Multiple Linear Regression
<i>m/z</i>	Mass-to-charge ratio
NTS	Non-target screening
OFAT	One Factor At a Time
PAC	Powdered Activated Carbon
PCA	Principal Component Analysis
PFAS	Per- and Polyfluoroalkyl Substances
PMT	Persistent, Mobile and Toxic
PVDF	Polyvinylidene Fluoride
QC	Quality Control

QToF	Quadrupole Time-of-Flight
RPLC	Reversed-Phase Liquid Chromatography
RT	Retention Time
RTI	Retention Time Index
SFC	Supercritical Fluid Chromatography
SPE	Solid Phase Extraction
TIC	Total Ion Chromatogram
TOrC	Trace Organic Compounds
TP	Transformation Product
vPvM	Very persistent, very mobile
WWTP	Wastewater Treatment Plant

# 1. Introduction

## 1.1 Trace organic compounds in the aquatic environment

### 1.1.1 Occurrence and toxicological potential

Over the past 100 years, global freshwater withdrawals increased by a factor of six with an expected future growth rate of 1 % per year [1, 2]. At the same time, the global water quality is deteriorating, especially for less developed countries, as 80 % of industrial and municipal wastewater is introduced into the environment without any prior treatment [1]. Accompanied therewith is the release of trace organic compounds (TOrcs) of anthropogenic origin into the aquatic environment. Since the publication of “Silent Spring” [3] in 1962, there is an ever-growing public concern of chemical pollution and its effects on the aquatic life and on human health. In natural waters, millions of tons of synthetic or natural TOrcs might be universally present at low concentrations like those used in industrial or consumer products, biocides and transformation products (TPs) [4]. These compounds enter the aquatic environment mainly through wastewater treatment plant (WWTP) effluents but also through diffuse sources like urban and agricultural surface runoff [5–9]. The number of publications on TOrcs in groundwater and drinking water supplies is limited. Nevertheless, a variety of TOrcs (i.e. carbamazepine, sulfamethoxazole, ibuprofen, bisphenol A and caffeine) are present at environmentally significant concentrations ( $\text{ng L}^{-1}$  to  $\mu\text{g L}^{-1}$ ) in groundwater [10]. Low quantities of TOrcs have already been detected in drinking water sources as well [9, 11].

TOrcs include per- and polyfluoroalkyl substances (PFAS) and disinfection byproducts (DBPs). PFAS are used in almost all industry branches with over 200 use cases identified for more than 1400 individual PFAS [12]. Andrew *et al.* estimated that 8 – 22 % of the U.S. population receive tap water with  $\geq 10 \text{ ng L}^{-1}$  of perfluorooctanoic acid (PFOA) and perfluorooctanesulfonate (PFOS) [13]. DBPs, on the other hand, do not *enter* the environment like most TOrcs but are *formed* during the water treatment process when disinfectants react with natural organic matter (NOM) as the main precursor [14].

The long-term exposure of water consumers to TOrcs raises concerns of adverse effects on the environment as well as on human health. Especially, endocrine disrupting chemicals or hormones bioaccumulate into the upper trophic levels of the food chain and modulate hormone functions even at trace concentrations [14, 15]. To name one example: Ecotoxicological effects were observed on zebra fish when exposed to glucocorticoids as they lead to a decrease in muscle contractions, increase in heart rate or expressional alterations of some genes [16, 17].

When considering human health, it is hypothesized that exogenous endocrine disruptors partially cause a deterioration in male reproductive health, involving an increase in testicular cancer cases [18].

### **1.1.2 Persistent and mobile organic compounds (PMOCs)**

For quite some time, research has been focusing on non-polar to mid-polar TOrcs, such as polycyclic aromatic hydrocarbons (PAHs). This is mirrored in the EU regulation on the registration, evaluation, authorization and restriction (REACH, EC no. 1907/2006) that requires an assessment of the persistent, bioaccumulative and toxic (PBT) properties of a registered chemical. However, the focus recently broadened, including now organic compounds which are polar and soluble in water and thus mobile and recalcitrant to degradation and thus persistent. They are often referred to as PMOCs (“persistent mobile organic compounds”) [19]. A PMOC with toxicological potential is considered a PMT-type of substance (i.e. “persistent in the environment, mobile in the aquatic environment, and toxic”) [20]. A compound’s mobility in water can be described by its water solubility and its sorption tendency. The German Federal Ministry for the Environment, suggested the  $\log K_{OC}$ , namely the coefficient for distribution between organic carbon and water, as an approximate measure for aquatic mobility [21]. The  $\log D_{OC}$  is an even more appropriate descriptor as it accounts for the different ionization states of a compound. It should be noted that these one-parameter relationships for the prediction of equilibrium partitioning do not account for variability between different compound classes or between different natural organic phases [22]. Nevertheless, Arp *et al.* defined a minimum mobility criterion of  $\log D_{OC} < 4.5$  (pH 4 – 10). They ranked 5155 TOrcs registered under the EU REACH legislation (December 2014) and assigned 21% with the highest PMOC score as their degradation half-life was  $> 40$  days and  $\log D_{OC} < 1.0$  for pH 4 – 10 [23]. Building on that work, Schulze *et al.* recognized a potential of being emitted into the environment for 43 % of PMOCs based on tonnage and on certain use characteristics [24]. Polar organic compounds enter surface waters through various sources and spread in the aquatic environment due to their persistency and mobility: Their intrinsic physico-chemical properties enable PMOCs to pass natural or technical barriers such as WWTPs; thereby accumulate in water cycles and threaten drinking water resources [25].

PMOCs could originate from pharmaceuticals, products of consumer or industrial use or pesticides. In addition to that, TPs and metabolites are formed by biotic or abiotic reactions which tend to be more polar than the precursor molecules [26]. Among environmentally relevant PMT substances are for example the antidiabetic drug metformin or the industrial chemical trifluoroacetic acid (TFA) [27]. Metformin is insufficiently removed by WWTPs and therefore

detected in recipient waters of Europe at a median measured environmental concentration of  $\sim 235 \text{ ng L}^{-1}$  along with its TP guanyurea at  $\sim 2000 \text{ ng L}^{-1}$  [28, 29]. TFA caught attention as it was detected at a concentration of  $>100 \text{ } \mu\text{g L}^{-1}$  in a German river where an industrial company was identified as the point source. Municipal WWTPs or degradation of precursor compounds are suspected as alternative sources of discharge [30]. The occurrence and potential risks of PMT substances for drinking water production is reflected by calls to the EU to identify, prioritize and regulate these chemicals under REACH considering the precautionary principle [31].

## 1.2 Instrumentation to analyze (polar) organic micropollutants

### 1.2.1 Polarity-extended chromatography

Over the last decades, liquid chromatography (LC) improved the selectivity of analytical methods for TOxCs in general. The most widespread technique is reversed-phase liquid chromatography (RPLC) in which analytes are retained due to hydrophobic interactions with typically C18-bonded stationary phases. However, highly polar and permanently charged compounds are poorly retained and separated by RPLC and consequently are ineffectively detected; a fact famously described as the “analytical gap” by Reemtsma *et al.* in 2016 [19]. A compound’s polarity is closely related to its mobility in water and often described by the logarithmic octanol-water partition coefficient  $\log P$  or its pH-sensitive pendant  $\log D$ . The data presented by Arp *et al.* suggests that of all persistent and mobile compounds with a  $\log D \leq 0$ , more than 95 % are either ionizable or permanently charged [23, 27]. It can be concluded that the analysis of approximately half of PMT/ vPvM (very persistent and very mobile) substances requires an alternative method to conventional RPLC-MS analysis [27]. In an attempt to remedy this lack of retention, the typical C18 chemistry has been modified to polar-embedded (i.e. amide group) or polar-endcapped (i.e. alcohol group) phases. However, these phases show slightly reduced (polar-endcapped) and significantly reduced (polar-embedded) hydrophobicity [32] and thus seem to be a compromise at the expense of the retention of non-polar and mid-polar compounds. An orthogonal separation technique to RPLC is hydrophilic interaction liquid chromatography (HILIC). It was originally introduced as a variant of normal-phase chromatography that works on hydrophilic partitioning between the mobile phase and a water layer partially immobilized on the surface of the stationary phase [33]. Thus, polar analytes tend to be retained longer and can be eluted using mobile compositions with no more than 50 % water due to its high elution strength. The high organic solvent content supports electrospray ionization and increases the sensitivity of subsequent mass detection [34]. However, several studies have proven the retention process to be multiparametric including adsorption

mechanisms such as hydrogen bonding and dipole-dipole interactions and ionic contributions with differences in selectivity between various column phases [35–37]. Changing the pH of the mobile phase, changes the ionization state of analytes and can therefore influence their retention on some HILIC phases [38]. Nevertheless, HILIC has proven to reproducibly separate very polar ( $\log D < -2.5$ ) TOrcs [39]. Alternatively, ion chromatography (IC) has been applied in environmental analysis to separate polar and charged compounds [40]. Mixed-mode liquid chromatography combines different retention mechanisms, i.e. RP and IC extend the application range towards charged compounds [27]. An alternative to LC in the separation of compounds that fall into the “analytical gap”, appears to be supercritical fluid chromatography (SFC). Bieber *et al.* used SFC to separate 245 out of 274 standard compounds covering a  $\log D$  range of -7.7 to 5.4 (pH 7) within an elution window of < 18 min [39].

### **1.2.2 Mass spectrometry**

Analytes separated by LC are frequently detected using mass spectrometry (MS) by measuring their mass-to-charge ratios ( $m/z$ ). Over the past decades, the capabilities of MS developed vastly from low-resolution (LR) to high-resolution (HR) instruments. For quantitative analysis of TOrcs as in environmental monitoring studies, LRMS instruments like triple quadrupoles (QqQ) or quadrupole ion trap (QIT) analyzers are well-established, performing selected reaction monitoring (SRM) for precursor-product ion transitions. Reference standards and an *a priori* selection of target analytes are prerequisites. LC hyphenated with HRMS has emerged as a powerful tool for the analysis of known and unknown compounds in complex environmental matrices. With the introduction of time-of-flight (TOF), Fourier transform ion cyclotron resonance or Orbitrap and finally hybrid technologies; resolving power, mass accuracy, linear dynamic range and sensitivity were improved [41].

Two frequently applied hybrid HRMS technologies are described in more detail in the following: When commercially introduced in 2005, the Orbitrap mass analyzer was presented with a preconnected external injection device (LTQ) that traps and stores ions in a C-shaped quadrupole and subsequently injects them as pulsed beams into the Orbitrap [42]. There, the ions tangentially enter the space between two coaxially arranged electrodes: An outer barrel-like electrode and a central spindle-like electrode sustained at high voltage. The electric field induces axial harmonic oscillations and the frequencies of the ions are measured and Fourier transformed [43]. The Q(q)TOF is another hybrid mass analyzer frequently applied in environmental analysis [44]. In the usual configuration three quadrupoles Q0, Q1 and Q2 are followed by a TOF analyzer. The Q0 serves the purpose of collisional cooling and focusing after the ions entered the instrument. The Q1 can filter masses to transmit only selected precursor

ions, before they undergo collision-induced dissociation (CID) in the Q2 usually with argon or nitrogen as collision gas. Remaining precursors as well as product ions are cooled and focused before they are orthogonally injected by an ion modulator into the acceleration column and finally arrive in the field-free drift space of the TOF analyzer. Lastly, a mirror focusses the ions onto a horizontal plane at the detector entrance [45].

After the introduction of the aforementioned hybrid HRMS instruments, they have been predominantly used for qualitative analysis of unknown and unexpected TOCs in the aquatic environment [44]. Hybrid HRMS instruments operated in full scan mode or at MS1 level are able to screen a broad mass range, i.e. from 60 – 1000 Da. On the MS2 level, spectra enclose structural information in the form of characteristic fragmentation patterns. There are two experimental approaches to record such MS2 spectra: Data-dependent or data-independent acquisition, DDA or DIA, respectively. In DDA mode, the most intense precursor ions are usually automatically selected from the MS1 scan for fragmentation if they exceed a predefined intensity threshold [46, 47]. In contrast, all analytes are supposed to be fragmented in DIA mode of which SWATH is a widely used example: For SWATH, the MS continuously cycles through sequential wide isolation windows covering the entire  $m/z$  range [48]. The increased selectivity and accuracy in combination with the MS2 information enabled confirmation and structural elucidation of compounds at a much higher degree of certainty and reduced the false positive rate. Accurately screening samples and extracting exact masses from the resulting raw data allows to detect a large number of compounds, even if analytical standards are lacking like for TPs [49].

For years, QqQ-MS was considered the gold standard of quantitative analysis due to its high sensitivity and selectivity in SRM mode. However, state-of-the-art HRMS instruments are capable of reliable and routine quantification with generally similar performance characteristics but the advantage of greater selectivity and the possibility of retrospectively analyzing the full-scan data [50]. Cavaliere *et al.* compared QqQ-MS operated in SRM mode and Q-Orbitrap-MS with data-dependent acquisition of MS2 spectra for the quantification of polyphenols in rosé wine [51]. They observed generally lower limits of quantification for HRMS, as well as a better overall performance in terms of interday and intraday precision and the ability to cope with matrix effects. Only a slightly lower linear dynamic range was observed mostly for negative polarity. A recent example of a multi-residue quantitative target screening was presented by Gago-Ferrero *et al.* [52]: They developed a method for the simultaneous detection of 2316 TOCs including pharmaceuticals, pesticides, illicit drugs, industrial chemicals and TPs and validated it for 195 representative substances. The instrumental method involved mixed mode solid phase extraction for sample preparation and subsequent LC-QTOF-HRMS analysis with data-

independent acquisition of MS2 information. Applying the method to the wastewater influent and effluent samples yielded 395 findings at concentrations ranging from 0.14 ng L<sup>-1</sup> to 431 µg L<sup>-1</sup>.

### **1.2.3 Ionization techniques**

In order for an MS analyzer to determine the  $m/z$  of molecular species, their ionization is a prerequisite. For gas chromatography this is traditionally done by electron impact (EI). On the other hand, condensed-phase analytes need to be transferred to the gas phase prior to MS detection. For matrix-assisted laser desorption/ionization (MALDI) a laser pulse forms gaseous ions from molecules embedded in a solid matrix [53, 54]. Ionization techniques that are able of converting liquid-phase chemical species into gas-phase ions and hence are suitable to connect LC and MS, include: Atmospheric pressure chemical ionization (APCI), atmospheric pressure photoionization (APPI) [55] and electrospray ionization (ESI). So-called “soft” ionization techniques are a common choice for screening methods that run on LC-MS systems since they preserve the pseudo-molecular ion.

Since the introduction of ESI [56], its working principle has been the subject of extensive investigations and discussions and was reviewed in detail elsewhere [57–59]. The primary mechanistic steps of ESI include formation and charging droplets of the sample solution, droplet evaporation and producing gaseous ions. In its basic configuration the ESI source is a two-electrode system operated at atmospheric pressure with a high potential difference between the spray capillary (working electrode) and the MS (counter electrode). The sample solution is emitted from the capillary tip as a fine mist of charged droplets supported by a coaxial nebulizer gas flow. As the solvent rapidly evaporates, the droplets shrink and the charge density increases. Close to or at the Rayleigh limit repulsion between charges overcomes the cohesive force of the surface tension and the instability causes fissions of progeny droplets. Finally, ions are ejected from the nanodroplets (< 10 nm) into the gas phase following the ion evaporation model [60]. This theory is well supported for small analytes. Large globular species and non-polar polymer chains, however, are released into the gas phase following the charged residue model and the chain ejection model, respectively. Krueve *et al.* conducted a thorough comparison of four ion sources for LC-MS under the same conditions using 40 pesticides of a wide range of polarity and basicity [61]. Compared to APCI, APPI and multimode ionization, ESI and thermally focused/heated ESI (HESI) obtained the lowest limits of detection. HESI appeared to be more prone to matrix effects, showing ion suppression or enhancement depending on the run. The authors concluded that for trace analysis conventional ESI is a solid choice. Nevertheless, in line with the ion evaporation model, a theory was put forward that assumes an enhanced ESI response for nonpolar analytes. Compared to more polar analytes, they have higher affinities for

the droplet air interface, carry more excess charge and therefore enter the gas phase quicker [62, 63].

### 1.3 Non-target screening

#### 1.3.1 Screening strategies

Due to the aforementioned technological advantages, LC and high-resolution/high-accuracy tandem mass spectrometry connected via ESI is now widely applied for multiresidue trace analysis. LC-MS expands the analysis repertoire from target screening to suspect and non-target screening [41]. Other than target screening, suspect screening does not use reference standards but rather the accurate mass and other structural information like the isotopic pattern or the MS<sub>2</sub> spectrum. Based on the theoretical information, the LC-HRMS raw data is then searched for pre-defined substances of interest. The non-target screening (NTS) approach was introduced by Hernández *et al.* [64] and refined by Krauss *et al.* [41]. In 2019, an expert committee of the German Water Chemistry Society released for the first time a guideline on the “Use of non-target screening by means of LC-ESI-HRMS in water analysis” [65]. NTS was described therein as a “[...] procedure without limitation to pre-select substances”. Based on the ISO norm ISO/DIS 21253-1:2018(E) and the decision of the European Commission 2002/657/EG, the authors defined a minimum resolving power for NTS using mass spectrometers of 20,000 (full width at half maximum of the mass peak height) and mass accuracy < 5 ppm at  $m/z$  200 and recommended the measurements of MS<sub>2</sub> spectra. In the subsequent data evaluation, so-called features are extracted from LC-HRMS chromatograms, which are defined by their accurate mass, chromatographic retention time (RT) and signal intensity (peak height or peak area).

NTS investigations can be a valuable addition to the routine monitoring of surface water quality, as was proven by the International Commission for the Protection of the Danube River (ICPDR). A periodic survey is conducted, namely the Joint Danube Survey, which was repeated for the fourth time in 2019 [66]. Its main purpose was to collect additional data, compare and harmonize it between adjacent countries and regions and raise public awareness for protection efforts.

#### 1.3.2 Data processing

HRMS measurements including full scan as well as MS<sub>2</sub> experiments, generate massive amounts of complex data. Hundreds of thousands features might be initially extracted from the NTS raw data [67], illustrating the need for further data processing in order to reduce noise,

artefacts or redundant features. For data processing, there are open source tools such as MZmine 2 [68] or XCMS [69], but also commercial and often market-oriented software solutions, such as MassHunter Profinder (Agilent Software) or MarkerView (AB Sciex). Building a basic NTS data evaluation workflow and possibly being restricted to the software available at the institution presents a challenge that needs to be tackled so that NTS approaches can be integrated into routine monitoring. General workflows for NTS data evaluation to obtain reliable feature lists are presented elsewhere [65, 70]. Letzel and Drewes gathered several environmental studies screening for suspects, hidden targets or unknowns and extracted the key procedural data processing steps: Peak picking or feature extraction, alignment, integration or chromatogram deconvolution, background comparison and componentization [71]. Recent trends in data pretreatment and feature extraction are discussed in Appendix A.3.

### **1.3.3 Applications**

The NTS approach developed quite diversely in the different fields of research and application. Whereas highly specialized techniques using advanced statistics are common in metabolomics, NTS approaches in water analysis are often more practical and effect-driven. The approach either aims at identifying unknown or unexpected TOxCs or reveal general trends or patterns in comparative studies.

Features which were extracted in an untargeted manner and subsequently annotated with substances stated in the literature or chemical databases but unknown to the investigator, are called “known unknowns” [72] or “hidden targets” [73]. Analytical information on a feature such as accurate mass, isotopic pattern or fragmentation pattern are used to connect it to a real compound and create a feature-candidate pair. Additionally, further instrumental constraints such as retention behavior can support an unambiguous allocation of features. All the information gathered on a feature may be compared to a compound database.

When aiming at finding *relevant* feature-candidate pairs, filtering, ranking, and prioritization strategies are needed. The relevance is an important criterion to make the hidden-target screening approach more feasible. Ideally, only those features should be considered for validation with reference material that are

- a) annotated with a high degree of confidence and
- b) relevant to the investigated sample set.

All the amenable information is accommodated by several filters which allow to rank and classify features according to their identification confidence. In NTS analysis of water samples, feature-

candidate pairs are further prioritized by considering meta-data on a sample, such as proximity to conurbations [74]. Additionally, prioritizing features based on their detection frequency in larger sample sets has been applied in LC-HRMS screening investigations of surface waters before [75].

A non-target screening approach can complement the assessment of water treatment processes [76, 77]. Instead of focusing on the fate of preselected target compounds, all features extracted before and after the treatment are considered. A comparison of the fingerprints reveals the removal or transformation/desorption of features during the treatment process or an increase or decrease in signal intensities. Individual features that are of interest for the process could be further identified. In future investigations, those recently identified features could serve as indicators for typically underrepresented compound groups such as TPs. The data evaluation process for a comparative NTS analysis needs to be adapted in order to classify features based on fold changes (fcs) of their signal intensities and at the same time takes matrix effects under consideration.

#### **1.4 Quality assurance and control for non-target screening**

Measures specifically introduced to assure and control the quality of results are imperative to an analytical method. Due to varying research objectives in non-target analysis, universally valid quality control (QC) guidelines are lacking. Still, the need for appropriate QC strategies was recognized and several procedures proposed and reviewed in the field of metabolomics [78] and more recently also within the environmental analysis community [79].

Over time the general performance of an LC-MS setup could be compromised by column degradation or a decline in mass spectrometric response which contributes to the total variability of an analytical method. These effects on repeatability of RT, mass and signal intensity can be monitored in a targeted analysis of multiple standard compounds. Those are spiked into an external quality control (QC) sample at known concentrations and analyzed throughout a measurement campaign, as was established early on for validated metabolomic methods [46]. Furthermore, (isotopically-labelled) internal standards can be spiked into each sample for optimizing the method and assessing the system's accuracy and stability, especially considering matrix effects. It should be noted though that a typical NTS approach covers a vast amount of compounds whose identity is not disclosed prior to the analysis. A limited number of internal standards might not be representative for the entire chemical space. Ideally, the set of standard compounds represents a broad mass range and diverse physicochemical properties.

Moreover, including blank samples in the measurement sequence, allows to correct for features

which originate from the laboratory background, contamination (i.e. carry-over) and thus reduce the false positive rate.

In 2006, Sangster *et al.* suggested to combine aliquots of every sample one and repeatedly measure it throughout the sequence [80]. These pooled QC samples might provide a more representative matrix when, i.e. evaluating the stability of the system on the internal standards. For processing the data of pooled QC samples, multivariate statistical methods such as principal component analysis (PCA) allow to reveal potential variabilities throughout the measurement sequence such as gradual shifts or sudden changes. Ideally, the QC samples would cluster closely together in the PCA score plot.

Through replicate injections of QC samples precision values of mass, RT and intensity can be determined. Three technical replicates of each real sample are recommended to increase the statistical power of feature recognition [81].

The two focus points of the QC regime for NTS data processing are reducing the type I (false positive) as well as the type II (false negative) error. To achieve the former, data complexity is reduced by adding noise thresholds, replicate filter, componentization steps or blank correction. When later on compound candidates are assigned to extracted features, a high level of identification confidence is sought and the community agreed on a universal scale to communicate it [82–84]. In order for the NTS approach to be unbiased it is equally important to control the false negative rate. Creating a feature extraction method requires setting up several quantitative parameters and filters which affect the quality of the final feature list. In addition to controlling the quality of an analytical run, data on standard compounds can be used to optimize an NTS method by maximizing their recall.

### 1.5 Design of experiment

Throughout the analytical process, there are multiple parameters that need to be set robustly and optimally. Choosing default settings, trial and error or changing one factor at a time (OFAT) are common optimization approaches, but strongly rely on the personal experience of the experimenter and assume the absence of statistical interaction [85]. Statistical design-of-experiment (DoE) constitutes a more systematic and efficient approach as it significantly reduces the number of necessary experiments. The general idea is to vary parameter settings simultaneously following a strategic experimental plan. Subsequently, a model is built based on the results, i.e. by Multiple Linear Regression (MLR) [86], which can be used for interpretation, prediction, and optimization of the input parameters. Since the foundational work of Ronald Fisher [87], numerous experimental designs have been proposed like by Plackett and Burman [88] or fractional factorial designs [89] for initial first-order, linear screenings of the investigated

input parameters. Since full factorial designs are often resource-intensive, screening designs can be augmented by model-specific D-optimal designs [90] in order to fit non-linear models for optimization purposes but keeping the experimental effort as low as possible.

DoE has been picked-up for investigating and optimizing LC-MS method parameters. In various applications the effects (main and interactions) of ESI source parameters on the analyte response were evaluated and an adequate combination of settings was found to increase sensitivity in detection [91, 92]. For processing metabolomics data, DoE was used to optimize parameter settings of XCMS software [69] based on a reliability index for assessing the peak quality [93, 94]. Hu *et al.* used a central composite face design and response surface modeling to optimize critical peak detection parameters of MZmine 2 software [68]. They validated the optimized peak detection method on real surface water samples against a manual target screening of a list of TOrCs and found 75 – 100 % of the peaks at an intensity level of  $10^5$  [95].

## 2. Research objectives and hypothesis

In this thesis, an analytical method was developed comprising of an instrumental and data processing part. It is supposed to be suited for screening water samples for analytes of an extended polarity range in an untargeted manner. The workflow is considered to be suited if it fulfills the following criteria which translate to the research objectives of this work:

- a) The method detects as many relevant features as possible.
- b) The quality of the method is controlled.
- c) The method can be adapted to different research questions.
- d) The method is applicable to environmental water samples.

As was outlined in the chapters 1.1.2 and 1.2, recognition of the “analytical gap” [19], analytical techniques emerged within the field of LC-MS, able to detect highly polar compounds [27]. Polarity intrinsically implies a compound’s mobility in water. Mobility paired with persistency and toxicity characteristics in a molecule render it a risk for surface and drinking waters. The serial RPLC-HILIC coupling introduced by Greco *et al.* [96], covers an extended polarity range and is a key instrumental element of this work. Referring to chapter 1.3.1, the molecular scope was further expanded by changing the way of investigating a sample from a target screening to a non-target/suspect target screening [41]. Following criterion a), aspects of the instrumental as well as the data processing method needed to be optimized to exploit the full potential of the aforementioned analytical approaches. As a consequence, hypothesis 1 was formulated:

*By optimizing selected parameters of the instrumental as well data processing method, unexpected molecules with diverse properties can be detected.*

Since in non-target screening the true composition of sample is unknown to the investigator, fixed reference points need to be artificially established for the method. This can be achieved by incorporating quality control and assurance measures into the measurement sequence as well as the data analysis process (compare chapter 1.4 and references [78, 79]). In order to address criterion b), the following hypothesis (#2) was postulated:

*Through introducing quality control (QC) measures, the robust operation of the instrumental method can be monitored and the ability of the data processing method to detect molecules assured.*

As discussed in the chapters 1.3.2 and 1.3.3, as well as in Appendix A.3, NTS is subjected to diverse research questions and analytical platforms. The environmental analyst could either aim

at identifying unknown or unexpected compounds or globally assess water treatment processes – both entailing entirely different methodological requirements [97]. Furthermore, the instrumentation available in the different laboratories could include different front-end systems and range from QTOF- to Q-Orbitrap HRMS instruments of various subordinate series equipped with ionization sources of different types and designs. Depending on the laboratory, there might be access to either commercial software provided by the MS vendor or open source tools for feature extraction with specific parameters based on different algorithms. Thus, the NTS data processing strategy needs to be flexible and able to adapt to the given circumstances as claimed by criterion c). This claim was addressed by hypothesis 3:

*The data processing strategy can be adapted to fit different software tools as well as to different non-target screening applications such as identification, trend analysis and comparative analysis.*

Finally, the analytical method developed under chapters 3 – 5 (corresponding to hypotheses 1 - 3) was validated on real applications. That meant screening surface water samples taken from two German rivers and a reservoir for polar compounds. Criterion d) was addressed by hypothesis 4:

*The optimized and adopted workflow is universally able to tentatively identify unexpected (very) polar candidate compounds and can be applied to surface water samples and samples after water treatment processes.*

The hypotheses are discussed in the chapters 3 – 6 and were tested by 3 – 4 tasks per hypothesis, outlined in **Fehler! Verweisquelle konnte nicht gefunden werden.** The following peer-reviewed papers were prepared while testing these four hypotheses:

- **P1:** Minkus S, Grosse S, Bieber S, Veloutsou S, Letzel T (2020) Optimized hidden target screening for very polar molecules in surface waters including a compound database inquiry. *Anal Bioanal Chem* 412:4953–4966. <https://doi.org/10.1007/s00216-020-02743-0> (Appendix A.1 and 0)
- **P2:** Minkus S, Bieber S, Letzel T (2021) (Very) polar organic compounds in the Danube river basin: Non-target screening workflow and prioritization strategy for extracting highly confident features. *Anal Methods* 13:2044–2054. <https://doi.org/10.1039/D1AY00434D> (Appendix A.2 and Appendix B.3)
- **P3:** Minkus S, Bieber S, Letzel T (2022) Spotlight on mass spectrometric non-target screening analysis: Advanced data processing methods recently communicated for

extracting, prioritizing and quantifying features. *Anal Sci Adv* 3:103–112.

<https://doi.org/10.1002/ansa.202200001> (Appendix A.3)

### Method optimization - chapter 3

- **Hypothesis 1: By optimizing selected parameters of the instrumental as well data processing method, unexpected molecules with diverse properties can be detected.**
  - Task 1: Use DoE to find a robust setpoint for electrospray ionization parameters that maximizes ionization efficiency for a wide range of molecules.
  - Task 2: Adjust the parameter settings of the data processing method by applying it to standard compounds and maximizing their recall (**P2**).
  - Task 3: Use DoE to find a robust setpoint for the input parameters and filters of the data processing method that maximizes predefined performance descriptors (**P1**).

### Quality assurance of the method - chapter 4

- **Hypothesis 2: Through introducing QC measures, the robust operation of the instrumental method can be monitored and the ability of the data processing method to detect molecules assured.**
  - Task 1: Use QC samples, external and internal standards at different concentrations and in different matrices to assess the variability between RPLC-HILIC-HRMS measurements (**P1, P2**).
  - Task 2: Add filters to the data processing workflow to remove noise, artefacts, redundant and false positive features (**P1, P2**).
  - Task 3: Identify the points of losses of false negative features by accessing intermediate stages of the data processing workflow (**P2**).
  - Task 4: Introduce recursive target searches to the data processing workflow to retrospectively improve the quality and statistical confidence of final feature lists (**P1**).

### Method adaptation - chapter 5

- **Hypothesis 3: The data processing strategy can be adapted to fit different software tools as well as to different non-target screening applications such as identification, trend analysis and comparative analysis.**
  - Task 1: In a top-down approach, all necessary processing tools are gathered first, identified in the specific vendor and open access software and used to construct a feature extraction workflow (**P1, P2, P3**).
  - Task 2: Use specialized databases to match a feature with a candidate compound using exact mass and physicochemical properties (**P1, P2, P3**).
  - Task 3: Add prioritization and classification steps to the feature extraction workflow to facilitate identification at a high level of confidence (**P1, P2, P3**).
  - Task 4: Add the necessary processing steps to the workflow and adjust related parameters for comparative analysis of samples.

### Application of the method - chapter 6

- **Hypothesis 4: The optimized and adopted workflow is universally able to tentatively identify unexpected (very) polar candidate compounds and can be applied to surface water samples and samples after water treatment processes.**
  - Task 1: Evaluate the spatial and temporal distribution of polar features in the Isar river and tentatively identify them (**P1**).
  - Task 2: Classify, prioritize and tentatively identify polar features in ground and surface water samples of the Danube river basin (**P2**).
  - Task 3: Characterize different types and concentrations of powdered activated carbon by comparing the fingerprints of polar candidate molecules.

Figure 1: The four hypotheses are presented under the four topics of developing and validating the analytical method. Each hypothesis is subdivided into tasks. The results of each task are presented in peer-reviewed articles which are listed in text above and referenced by P in brackets.

### 3. Method optimization

Hypothesis 1: By optimizing selected parameters of the instrumental as well data processing method, unexpected molecules with diverse properties can be detected.

The hypothesis has been addressed in the following peer-reviewed papers:

- **P1:**
  - Reference: Minkus S, Grosse S, Bieber S, Veloutsou S, Letzel T (2020) Optimized hidden target screening for very polar molecules in surface waters including a compound database inquiry. *Anal Bioanal Chem* 412:4953–4966. <https://doi.org/10.1007/s00216-020-02743-0> (Appendix A.1 and B.2)
  - Author contributions: Author contributions: Susanne Minkus curated the data, planned and performed the DoE and the NTS data processing workflow, interpreted the data and drafted the manuscript. Stefan Bieber contributed to collecting the samples and performing the measurements, edited the manuscript and contributed to the discussion. Sylvia Grosse contributed to the laboratory work. Sofia Veloutsou prepared the samples and contributed to the measurements. Thomas Letzel supervised the research project, contributed to the discussion and edited the manuscript.
  
- **P2:**
  - Reference: Minkus S, Bieber S, Letzel T (2021) (Very) polar organic compounds in the Danube river basin: Non-target screening workflow and prioritization strategy for extracting highly confident features. *Anal Methods* 13:2044–2054. <https://doi.org/10.1039/D1AY00434D> (Appendix A.2 and Appendix B.3)
  - Author contributions: Susanne Minkus contributed to the sample preparation and analysis, curated the data, planned, optimized and performed the NTS data processing, interpreted the data and prepared the manuscript. Stefan Bieber edited the manuscript and contributed to the sample preparation and analysis. Thomas Letzel supervised the research project, contributed to the discussion and edited the manuscript.

#### **3.1 Use statistical design of experiment (DoE) to find a robust setpoint for electrospray ionization parameters that maximizes ionization efficiency for a wide range of molecules**

This chapter has been previously published as an application note with minor modifications.

Reference: Minkus S, Bieber S, Moser S, Letzel T (2020) Optimization of electrospray ionization parameters in an RPLC-HILIC-MS/MS coupling by design of experiment. AFIN-TS Forum March:1–17.

Author contributions: Susanne Minkus contributed to planning and performing the DoE and the sample preparation and analysis. She curated, processed and interpreted the data and prepared the manuscript. Stefan Bieber contributed to planning and performing the DoE as well as to the sample preparation and analysis. He edited the manuscript. Stefan Moser contributed to planning and performing the DoE and edited the manuscript. Thomas Letzel supervised the analytical part of the work, contributed to the discussion and edited the manuscript.

### 3.1.1 Introduction

LC-MS analysis benefitted from the advent of ESI that converts liquid-phase chemical species of a broad mass range into gas-phase ions [56]. ESI is considered a “soft” ionization technique as it induces very little fragmentation. The working principle is described elsewhere in detail (chapter 1.2.3 and references [57, 58]) and the ionization source used in this study is schematically depicted in Figure 2.

Briefly, the sample solution is emitted from the tip of the *spray capillary* as a fine mist of charged droplets. The surface tension of the solvent in the spray is pneumatically counteracted by a coaxial *nebulizer gas* flow. The solvent evaporation is accelerated by a heated gas flow from the *heater*. Based on the ion evaporation model ions start to separate from the shrinking nanodroplet as charge density increases [60]. The ions follow a decreasing pressure gradient towards the ion optics of the mass spectrometer. The so-called *curtain gas* stream which is introduced between the curtain plate and the orifice prevents ambient air, solvent and uncharged compounds and particles from entering as well. Additionally, the *declustering potential* is applied to the orifice and hinders ions to cluster from cooling after passing the orifice.

There are multiple adjustable parameters that influence the ionization efficiency. That raises the question of the most suitable combination of settings for a general, but sensitive operation. Accordingly, the objective of the present study was to optimize a new ESI source coupled to LC. The essential parameters heater gas, temperature, ion spray voltage, nebulizer gas, curtain gas and declustering potential were investigated (Figure 2).

The scientific issue gains more depth when considering that the ionization efficiency depends on the physicochemical properties of the analytes as well as on the composition of the mobile phase. Herein, a serial coupling of RPLC and HILIC was employed to separate molecules of a wide polarity-range [98]. Accordingly, rather heterogeneous elution profiles of the solvents can

be expected. The optimization was based on the signal intensities of a set of 30 model substances. They covered the entire retention time window of the RPLC-HILIC separation to represent the complex and inconsistent solvent composition.

A common optimization approach is to change one factor at a time (OFAT) which is also applicable for ESI optimization. OFAT works well for the optimization of a single ion transfer. However, that method strongly relies on the experimenter's personal experience but what is more problematic, implicitly assumes the absence of statistical interaction [85]. Moreover, some analytical strategies, like a non-target screening, require efficient ionization of whole spectrum of compounds [39]. In such cases, a more systematic approach has to be chosen like statistical DoE. The general idea is to vary the relevant input parameters within their appropriate factor ranges simultaneously in a methodically designed set of experiments. By using state of the art investigation designs the number of necessary experiments can be reduced in a very efficient way. The results can be connected by means of a regression model that allows interpretation, prediction and finally optimization of the parameters.

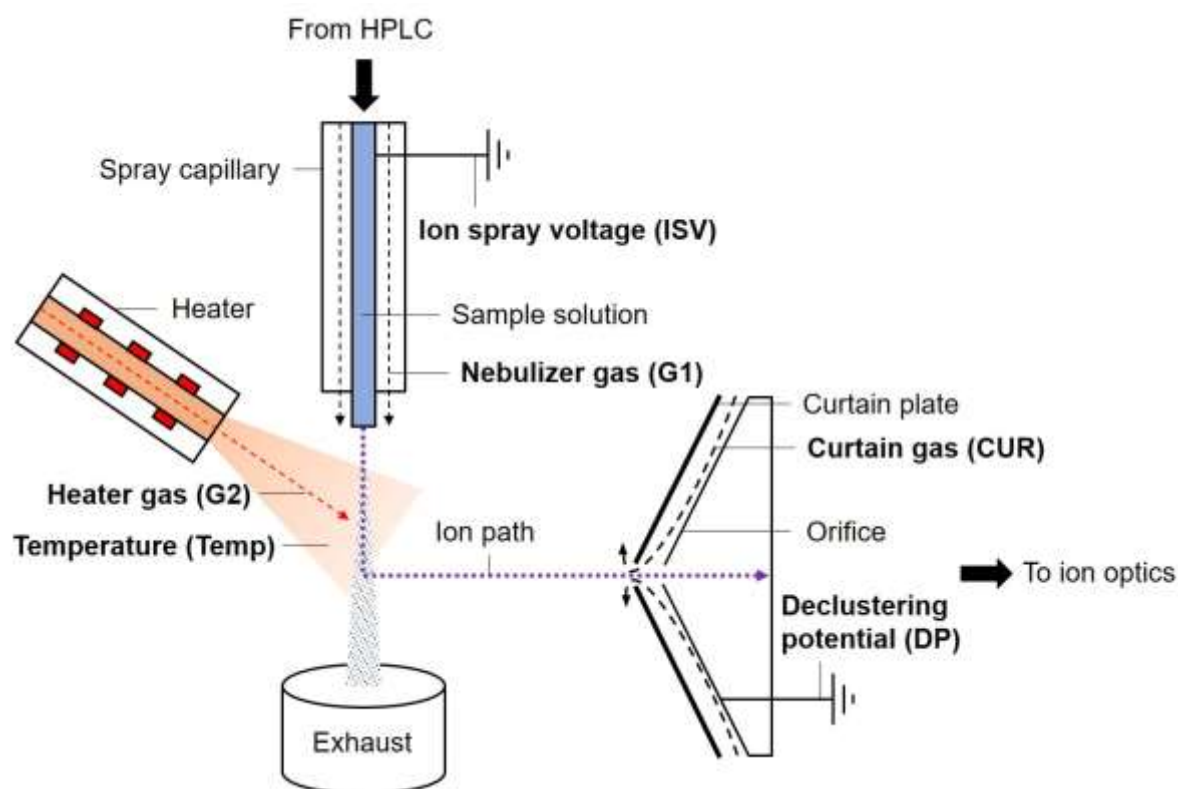


Figure 2: Schematic graphic of the Sciex TurbolonSpray™ probe used in this study. Setting parameters that were subject of the statistical adaption are depicted in bolt.

### 3.1.2 Methods

#### 3.1.2.1 Chemicals and solutions

LC-MS grade acetonitrile and water were obtained from Honeywell (Morristown, USA) and VWR (Darmstadt, Germany). Ammonium acetate was obtained from Sigma-Aldrich (Merck KGaA, Darmstadt, Germany). Standard compounds were purchased from Alfa Aesar (Thermo Fisher Scientific, Karlsruhe, Germany), Fluka (Buchs, Switzerland), Merck KGaA (Darmstadt, Germany) and Sigma-Aldrich. Individual standard stock solutions were prepared at 1 mM in either acetonitrile or, in case a compound had a log D at pH 7 < 2.0, in acetonitrile/water (50/50, v/v). A working mix at 10  $\mu$ M per compound was prepared in acetonitrile from the stock solutions.

#### 3.1.2.2 Design of Experiment

Planning and evaluating the experimental design were done with MODDE Pro software (version 12.1.0.5491; Sartorius Stedim Data Analytics AB, Umeå, Sweden).

Six setting parameters of the ESI source (represented graphically in Figure 2) referred to as *factors* were screened and optimized by DoE. They are listed together with the range within they were varied in Table 1. Each experiment represents a distinct combination of factor settings.

They were varied simultaneously by following the system of a fractional factorial design with resolution IV [89] complemented by a D-optimal design [90]. The design matrix consisted of 46 experimental runs and is given in Table S1 (see supplementary material in Appendix B.1). The experiments were conducted in random order to prevent systematic noise variation.

The result of each experiment is reflected in so-called response values. In this case, the performance of a certain combination of ESI settings was evaluated by means of the signal intensities of 30 model substances. They are listed in Table S2 in Appendix B.1.

The relationship between the ESI settings and the signal intensities of the 30 molecules was modeled using MLR [86]. A quadratic process model was estimated which allows optimizing the response values. Therefore, a default minimum peak height of 10,000 Cps was defined similar to a study by Bieber et al. where they optimized an ESI source integrated in a SFC-MS system [99]. The specification target of each response was set slightly below the predicted maximum value. With the implemented optimization algorithm in the software, specification limits were adjusted if a response exceeded a probability of failure of 0.5 %. The exact values are summarized in Table S2 of the supplementary material (Appendix B.1). A robust setpoint was calculated using Monte Carlo simulations. Coming from this setpoint a design space was generated with the use of the Manhattan distance algorithm at a resolution of 8, 1000 iterations and an acceptance limit of 1 %.

The robust setpoint was validated by measuring the model mix three times at the robust ESI settings (Table 2).

Table 1: Six factors of the ESI that were statistically evaluated and optimized (see also Figure 2). For each factor the upper and lower limit of the interval and the setting precision are given.

<b>Factor</b>	<b>Abbreviation</b>	<b>Lower limit (-1)</b>	<b>Upper limit (+1)</b>	<b>Precision</b>
<b>Nebulizer gas</b>	G1	30 psi	50 psi	1 psi
<b>Heater gas</b>	G2	20 psi	50 psi	1 psi
<b>Curtain gas</b>	CUR	25 psi	40 psi	1 psi
<b>Ion spray voltage</b>	ISV	2000 V	5500 V	100 V
<b>Temperature</b>	Temp	300 °C	650 °C	10 °C
<b>Declustering potential</b>	DP	20 V	200 V	10 V

### 3.1.2.3 Instrumentation

The chromatographic separation was performed on a serial coupling of RPLC and HILIC, which is described in detail elsewhere [39].

In short, two binary pumps and two online degassers were used (Agilent Technologies, Waldbronn, Germany). For RP separation a Poroshell 120 EC-C18 column was used (50.0 x 3.0 mm, 2.7 µm; Agilent Technologies). The HILIC Separation was performed on a ZIC-HILIC (150 x 2.1 mm, 5 µm 200 Å; Merck Sequant, Umea, Sweden). A T-piece connects the two columns and a second binary pump. The injection volume was 10 µL. The mobile phase for RPLC comprises 10 mM ammonium acetate in water/acetonitrile at a volumetric ratio of 90/10 (solvent A) and 10/90 (solvent B). For the HILIC column acetonitrile (solvent C) and water (solvent D) were used.

A schematic representation of the entire set-up along with the flow rates and gradients is given in Figure 3.

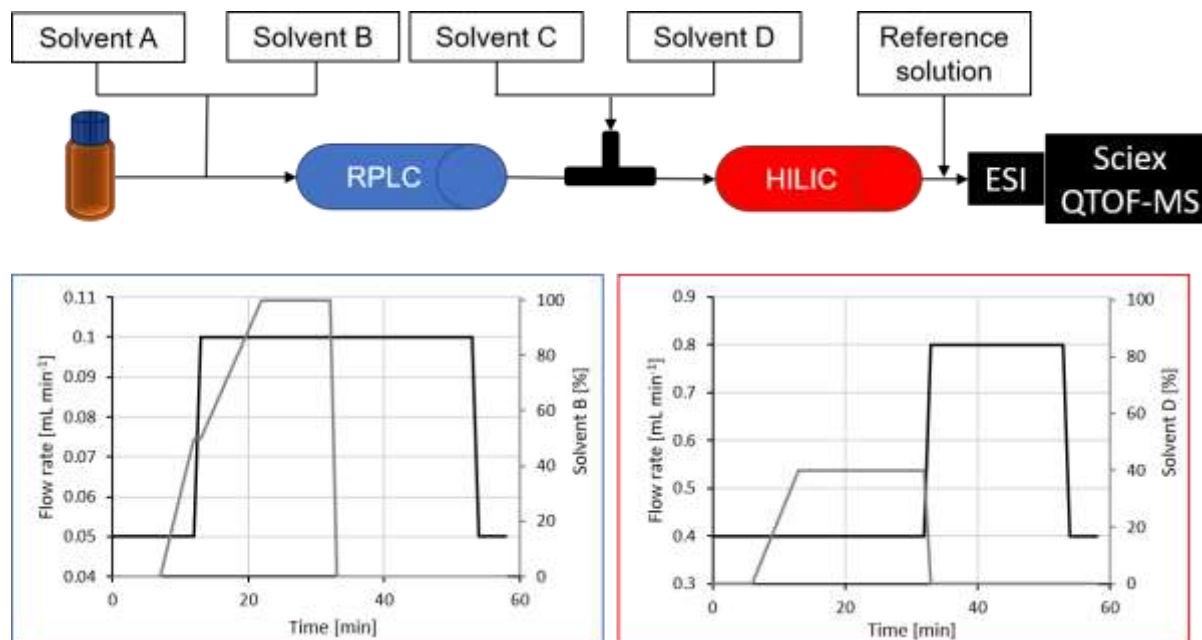


Figure 3: The serial coupling of RPLC and HILIC. The mobile phases are transported by two binary pumps and the reference solution by an isocratic pump. The diagrams below each partial system display the flow and solvent gradients.

The standard molecules were detected with a QTOF (TripleTOF 4600; AB Sciex, Darmstadt, Germany). It was equipped with a DuoSpray™ ion source with a TurbolonSpray™ probe for ESI experiments. The probe was operated in positive ionization mode and the source parameters were set according to the designed plan (Table S1, Appendix B.1). Prior to each experimental run the source was equilibrated for 20 min. A full scan of the mass range from 65 Da to 1000 Da was acquired with an accumulation time of 0.25 s. To gather fragmentation information, eight independent data acquisition (IDA) experiments were performed with an accumulation time of 0.10 s. The QTOF was recalibrated automatically every five runs using an implemented atmospheric pressure chemical ionization probe.

#### 3.1.2.4 Data handling

For HRMS data evaluation SCIEX OS software (version 1.4.0.18069, AB Sciex) was used. The protonated ion mass was calculated from the elemental formula of each substance and ion chromatograms (EICs) were extracted. Chromatographic peaks were accepted if the mass error was < 5 ppm, nearly Gaussian shaped and the MS and MS/MS spectra showed an isotopic pattern and a fragmentation pattern that both fitted the analyte. A compound's peak height was determined for each experimental run and recorded as the respective response value for modeling and optimization.

### **3.1.3 Results and discussion**

The ESI parameters temperature (Temp), declustering potential (DP), ion spray voltage (ISV), the pressures of the nebulizer gas (G1), heater gas (G2) as well as the curtain gas (CUR) were optimized with regards to maximizing the signal intensities of 30 model substances. These compounds are likely to occur in environmental samples. The six factors influence the ionization efficiency to a varying but significant degree and have partly opposing effects or interactions. Thus, they pose a classical optimization problem which was solved in this study by a DoE approach.

#### **3.1.3.1 Strategy**

It is necessary to ensure, that all factor combinations of the investigation are measurable in order to derive a valid cause-effect-model. Therefore, certain extreme setting combinations were tested in an in-house preliminary study to evaluate the largest possible ranges. The upper and lower limits of the setting intervals differed from the operational range specified by the vendor. The tests showed that in some cases the QTOF did not get ready for operation due to not reachable factor values. Once the minimum and maximum factor values were determined (Table 1) an experimental plan was successively generated:

Initially, the factors were screened at two levels (minimum and maximum) in order to investigate main effects and get indications for potential non-linearities and interactions. Therefore, an efficient fractional factorial design with a resolution of IV was chosen. It consisted of 18 experimental runs and supported a linear model. The nonlinear effect of the ion spray voltage was investigated by three additional runs. Subsequently, the screening model was complemented D-optimally to an optimization design. For the D-optimal design a modified K-exchange algorithm [12] chose an optimal set of 18 design runs out of a candidate set including extreme vertices, edge points and centroids of high dimensional surfaces. The optimality criterion seeks to maximize the information in a selected set of experiments by maximizing the determinant of the matrix  $X'X$  with respect to a pre-specified model  $Y = Xb + \varepsilon$ . With this approach the final experimental setup was maximized according to orthogonality, balance and symmetry, to get the best base for the regression model. Finally, two center point runs, and four replicate experiments were added. Even though as many as 30 molecules were investigated, the total number of runs is not affected by the number of response variables.

#### **3.1.3.2 Model fit and diagnostics**

For each experimental run the EICs of the 30 response molecules were extracted from the mass spectrometric data and the peak heights were determined. Based on these results a basic model

was fitted for each individual response variable using MLR. As further described in the following, the basic model was iteratively refined by inspecting and adjusting a couple of diagnostic screws:

First, the response distribution was checked for skewness, which describes the degree of asymmetry of the distribution around the mean, or more figuratively speaking: The degree of distortion from the Gaussain curve. Skewed data might impair model estimates and therefore needs to be transformed close to a normal distribution. The responses that triggered the skewness test were log transformed according to the formula  $10\text{Log}(Y)$  and are marked in Table S2 (Appendix B.1).

Furthermore, residuals  $r_i$  were examined as part of the total variation that cannot be explained by the model. They should not display patterns that are not accounted for by the model. For all 30 responses, residuals were roughly independent of the run order, predicted values and factor settings. Moreover, they were approximately normally distributed, as is exemplified on the model substance linuron in Figure 4. A total of four outliers that exceeded  $\pm 4$  standard deviations were identified via the residual analysis and excluded from the experiments. Two outliers (dapsone, N,N'-trimethyleneurea ) occurred during experiment 8, one during experiment 11 (moroxydine) and one during experiment 22 (panthenol). Experiment 8 was repeated twice and added as the additional runs 43 and 46 to the design matrix. Both runs did not exhibit further outliers. Experiments 3 and 30 were duplicated as well, since they showed outliers in an earlier stage auf the investigation.

The coefficient of determination  $R^2$  was consulted to assess the model's goodness-of-fit. It describes the fraction of variation that cannot be explained by the model and is defined as:

$$R^2 = 1 - \frac{\sum_{i=1}^n (y_i - \hat{y}_i)^2}{\sum_{i=1}^n (y_i - \bar{y})^2}$$

With the observed values  $y_i$ , the predicted values  $\hat{y}_i$ , the mean value  $\bar{y}$ .

The predictive ability of the model was estimated by  $Q^2$  with the predicted response  $\hat{y}_{i/i}$  when leaving out the  $i$ -th object from the training set (cross-validation) [100]:

$$Q^2 = 1 - \frac{\sum_{i=1}^n (y_i - \hat{y}_{i/i})^2}{\sum_{i=1}^n (y_i - \bar{y}_i)^2}$$

A model with a value of 1 for both,  $R^2$  and  $Q^2$ , would fit the data perfectly. The basic models were refined by eliminating non-significant model terms and adding model supported terms that would increase the  $Q^2$  value. At the same time, the number of degrees of freedom (DF) of each response was maintained above  $> 20$ , where replicate DFs are not counted. That means the risk of overfitted data is low. For all final models  $R^2$  was  $> 0.75$  and  $Q^2 > 0.56$

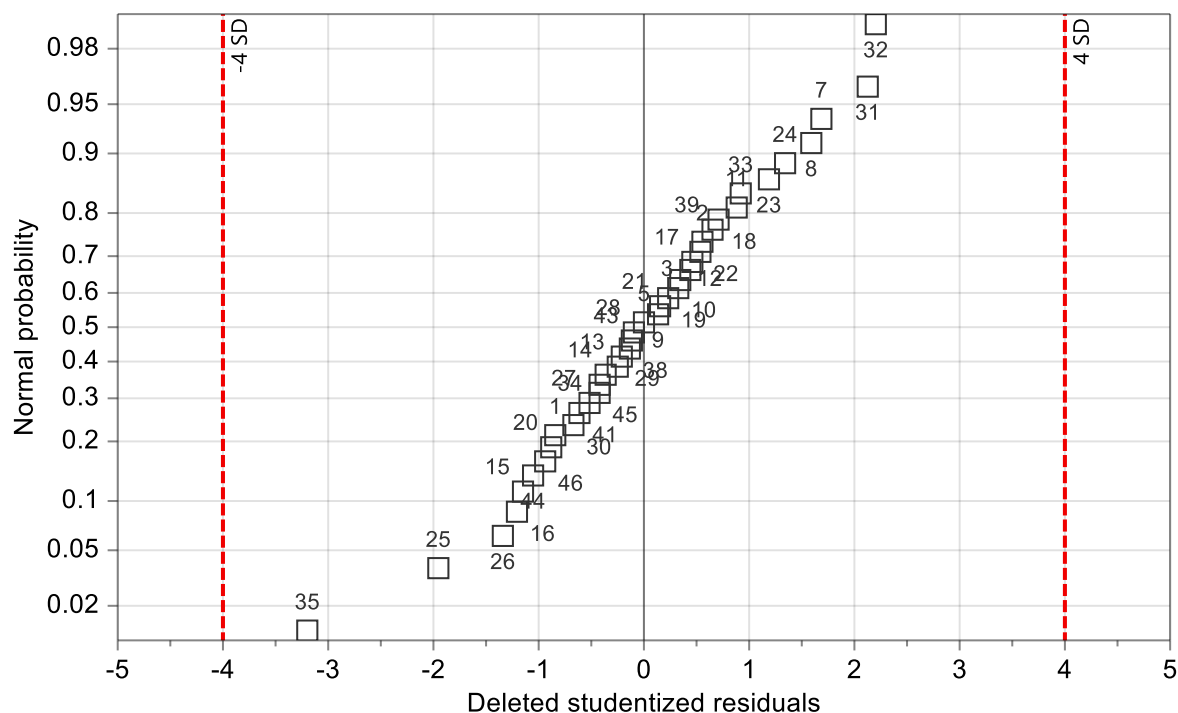


Figure 4: Normal probability plot for linuron. The deleted studentized residuals of all experiments were ordered by size and plotted against their normal probability. Since they are following a straight line, it can be assumed that residuals in the case of linuron are approximately normal distributed. There are no outliers that exceed the  $\pm 4$  SD mark.

### 3.1.3.3 Prediction and Optimization

After the model was fitted, the six factors influencing the ionization performance were optimized. For the optimization desirability functions were used with the objective of maximizing the signal intensities of the 30 model substances. These search functions run on specification limits that were adjusted iteratively in order to assure that each limit is possible to reach for the search functions (Table S2, Appendix B.1). Afterwards, a six-dimensional design space was generated. The robust setpoint was found by maximizing the distance from the acceptance boundaries. The results are presented in Table 2. The probability of failure was 0.67 %, cumulated over all 30 responses for the given robust setpoint. Moreover, the hypercube is given: A volume where all factors can be changed at the same time without violating the response specifications. It does not include the factors heater gas, temperature and declustering potential. However, the

acceptance limit was as low as 1 %, which means 99 % of the samples were within specification limits. Moreover, the factors without a hypercube range had short robust distances to the design space limit which were limited by the resolution.

Table 2: Robust setpoint value for each factor along with the hypercube range and its contribution percentage.

<b>Factor</b>	<b>Setpoint</b>	<b>Hypercube low edge</b>	<b>Hypercube high edge</b>	<b>Factor contribution [%]</b>
<b>Nebulizer gas</b>	44 psi	30 psi	47 psi	5
<b>Heater gas</b>	50 psi	50 psi	50 psi	12
<b>Curtain gas</b>	29 psi	27 psi	31 psi	2
<b>Ion spray voltage</b>	2000 V	2000 V	2500 V	12
<b>Temperature</b>	650 °C	650 °C	650 °C	27
<b>Declustering potential</b>	46 V	46 V	46 V	42

The most significant impact on the ionization efficiency had the factors temperature (27 %) and declustering potential (42 %) which will be discussed in more detail: The effect of both factors on an analyte's peak height is exemplarily depicted for linuron (response 16) in Figure 5. First of all, higher temperatures lead to higher signal intensities, which could be explained by more efficient solvent evaporation and ultimately more ions reaching the detector. Secondly, the declustering potential: It is applied to the orifice at the transition from atmospheric pressure to vacuum and assures the analytes' entry into the MS optics by preventing ions from clustering together. There was an optimal declustering potential for each individual analyte that ranged from 50 to 90 V. Figure 5 clarifies that from that highest point on the signal intensity decreases with increasing declustering potential which could be attributed to in-source fragmentation.

Still, it should be noted that the effect of a factor is also affected by the difference between its minimum and maximum value.

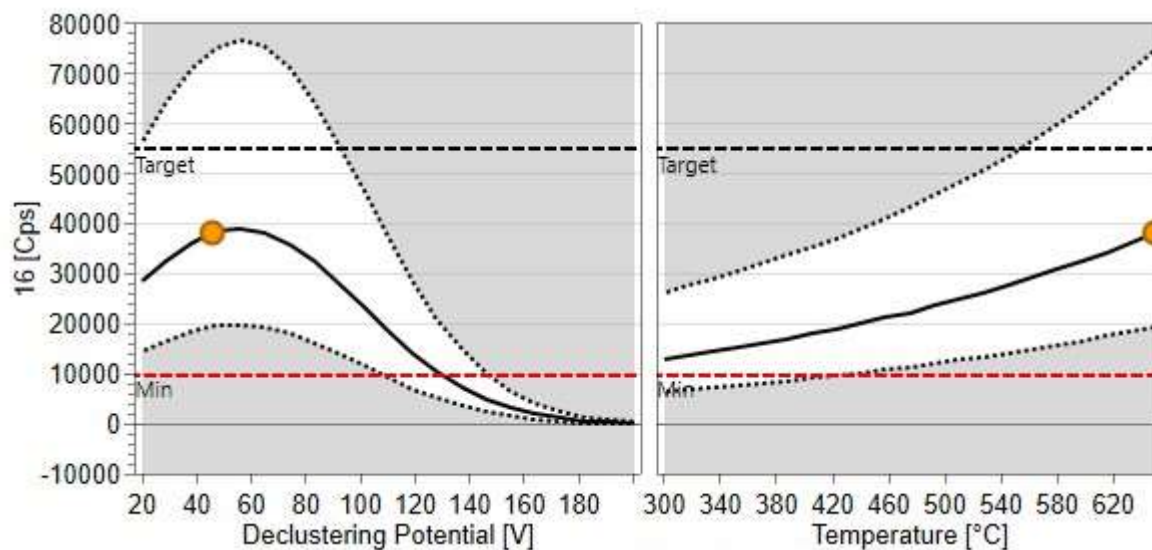


Figure 5: Factor effects of the declustering potential and temperature on the signal intensity of linuron (response 16). The yellow bullets mark the robust settings. All other factors values were kept at the robust setpoint as well. The 95 % prediction interval is depicted by the dotted lines and the specification limits by the dashed lines

#### 3.1.3.4 Robust setpoint validation

The last step was to validate the robust ESI settings that were previously calculated. Therefore, the same mixture including the 30 model substances was injected three times on the RPLC-HILIC-coupling. The predicted values for signal intensity were plotted against the mean of the three observed values (Figure 6). The trend line (blue) displays very little bias from the identity line (black). Furthermore, to summarize the forecast accuracy for signal intensity the mean absolute percentage error (MAPE) was calculated at 29 % for the  $n = 30$  mean observations according to the following equation:

$$MAPE = \left( \frac{1}{n} \sum_{i=1}^n \left| \frac{r_i}{y_i} \right| \right) \cdot 100\%$$

Somehow, the model accomplished to predict weaker signals more adequately than stronger ones.

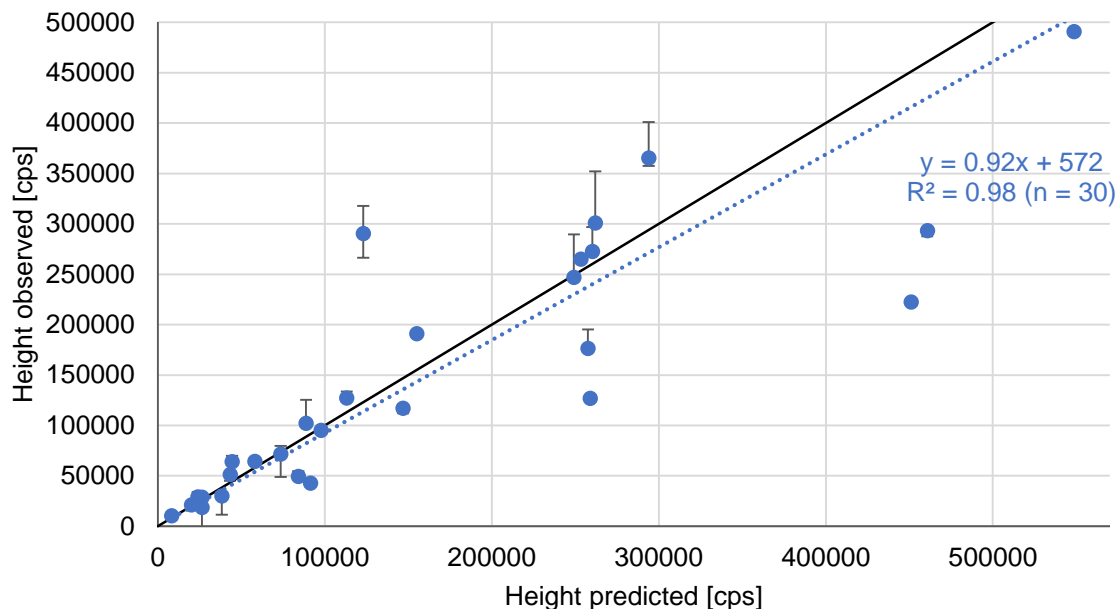


Figure 6: The robust setpoint was validated by comparing the predicted and observed signal intensities of the 30 model substances. Response 14 (fluritamone) is not displayed since it is an outlier with a predicted an observed peak height > 2,000,000 cps.

### 3.1.4 Conclusion

The objective of this task was to increase the ionization efficiency by optimizing the essential input factors of an ESI source by means of DoE. The ESI source was part of an RPLC-HILIC serial coupling hyphenated with a high-resolution tandem mass spectrometer. The optimization aimed for maximizing the signal intensities of 30 model substances – so-called response variables. By considering an entire set of molecules instead for just one, the ionization conditions suit the challenges of NTS: When a broad mass range is scanned, compounds covering the whole spectrum of physiochemical properties can be expected.

The experimental plan was based on a fractional factorial screening design with a resolution of IV that was complemented by a D-optimal design to create a design capable of response surface modeling. For each response variable a model was fitted with MLR with an  $R^2 > 0.75$ . A robust setpoint was computed for the six ESI factors and revealed a major effect of the temperature and the declustering potential on the compounds' signal intensity.

The setpoint was validated by measuring at the respective combination of factor settings in triplicate. The forecast accuracy of the model was adequate (MAPE = 29 %), especially for compound with a peak height < 100,000 Cps.

The ESI method was optimized to ensure a robust and sensitive detection of molecules of a broad mass and log  $D$  range and therefore hypothesis 1 can be accepted.

## **3.2 Adjust the parameter settings of the data processing method by applying it to standards compounds and maximizing their recall**

### **3.2.1 Methods**

Firstly, data processing parameters were optimized with respect to recovering a subset of 51 out of 177 external standard compounds prepared in solvent at a concentration of 10  $\mu\text{M}$  per compound. They were analyzed along with the environmental samples in question as part of a study published elsewhere [101]. The approach for finding suitable parameter settings was refined by preparing two synthetic samples where 34 standard compounds were spiked into a tap water matrix at concentration levels of 10 nM and 100 nM, respectively (Appendix A.2). The parameters of the NTS data evaluation implemented in MZmine 2 [68] were adjusted iteratively with the objective of maximum recovery. The parameters were later on adjusted to fit the requirements of the process evaluation study (compare chapters 5.4, 6.3), given for example by a different type of high-resolution mass spectrometer or research objective. Mass and RT tolerances were set based on the targeted analysis of the internal standards as well as the spiked HILIC standards. The parameter settings were validated and if necessary optimized on the three blank samples with the objective of obtaining full recall of the standard compounds and reducing the total feature number as well as the processing time.

### **3.2.2 Discussion**

When optimizing the NTS data processing parameters of a preliminary study, the required recovery rate for external standard compounds was defined at 75 % [101]. However, the matrix as well as the concentration of the external multicomponent standards do not represent realistic conditions. As a consequence, TOxCs present in a real surface water sample, might not be extracted by the peak picking algorithm or false positives might be erroneously detected. Within the scope of the study Appendix A.2, the parameters of the feature extraction method intensity threshold, mass tolerance, peak duration range and RT wavelet range (Appendix B.3, Table S4) were adjusted based on the synthetic samples. Therefore, target compounds were analyzed in matrix and at concentrations realistic for surface waters. The acquired data was handled as an NTS test set and the parameters iteratively adjusted to maximize the recovery of standard compounds. The final feature extraction method was validated on both synthetic samples, leading to a > 90% recovery at higher concentrations and > 60% at lower concentrations. This difference could be attributed to an increased variability in feature properties at lower concentrations. The RT threshold for the feature extraction method needed to account for some outliers in RT repeatability by specifying relatively conservative values of 0.9

min (Appendix A.1) and 1.6 min (Appendix A.2), compare also chapter 4.1. The parameter settings were transferred to the NTS data processing strategy of the process evaluation study (chapters 5.4 and 6.3), and adjusted until all of the internal standards were recovered.

Alterations were necessary due to a different study design and different instrumental conditions:

- a) Orbitrap Exploris 120 mass spectrometer (Thermo Fisher Scientific) was used instead of a TripleTOF series 4600 (AB Sciex)
- b) The research aimed at evaluation a water treatment process instead of (tentatively) identifying TOrCs

The results are presented in Appendix B.4, page Table S3.

The input parameters and filter criteria of the NTS data processing method can readily be adjusted based on fixed reference points, namely standard compounds. To address hypothesis 1, they can be chosen to cover a wide range of masses, RTs and log  $D$  values. As a consequence, the hypothesis can be accepted since unexpected molecules with diverse properties can be detected. However, the assortment most likely does still not cover the entire chemical space.

### **3.3 Use DoE to find a robust setpoint for the input parameters and filters of the data processing method that maximizes predefined performance descriptors**

#### **3.3.1 Methods**

Eight critical parameters and filters of the feature extraction method presented in Appendix A.1, Figure 1 were optimized using MODDE Pro software (version 12.1.0.5491; Sartorius Stedim Biotech GmbH). Features were extracted from HRMS full scan data of a subset of six out of 33 real samples. The eight factors were varied simultaneously following a Plackett-Burman screening design [48]. Six response variables were calculated from the feature lists which resulted from each experiment (0, Table S6). A model was fitted to connect all the results using multiple linear regression. The eight responses were minimized using desirability functions based on specified limits (0, Table S6).

#### **3.3.2 Discussion**

The optimization of the feature extraction parameters was performed on a sample subset in order to reduce the time that would be required to process the entire sample batch. Five input parameters and three filters were identified as critical and optimizable factors: Noise threshold, charge state, RT tolerance, mass tolerance and mass tolerance for EIC extraction and three

peak intensity filters. Six response variables in the form of numerical descriptors were defined to assess the performance of each feature extraction experiment. For each individual response, the coefficient of determination  $R^2$  was  $> 0.7$  and the predictive ability  $Q^2 > 0.6$ , suggesting that the general model was sufficiently significant (0, Table S7). A robust combination of factor settings was calculated and is presented in Appendix A.1, Table 1. For a more general result, the initial noise threshold for the peak picking was found to be optimal at zero and was counteracted by two rather rigid signal intensity filter applied further downstream of the workflow (compare chapter 4.2). In contrast, the tolerance windows for mass and RT are more specific to the mass analyzer used for this study (6230 TOF-MS, Agilent Technologies) and the five-month time period it took to measure the entire sample set. A systematically designed experimental plan was presented that is able to optimally adapt the feature extraction method to fluctuating data quality. The thorough statistical analysis of a DoE approach could deepen the understanding of complex and sometimes undisclosed algorithms.

When trying to find the optimal combination of software settings as claimed by hypothesis 1, conflicts might arise: Distinguishing between reliable features from artefacts and noise, introducing statistical value but also reducing experimental efforts, or customizing the workflow to the individual data set by keeping it reproducible. Statistical DoE offered the possibility of systematically compromising on these problems by finding an optimal combination of software settings for critical parameters and filters. In conclusion, in the study presented in Appendix A.2, again unexpected TOrCs were identified and thus hypothesis 2 can be accepted.

## 4. Quality assurance of the method

Hypothesis 2: Through introducing quality control (QC) measures, the robust operation of the instrumental method can be monitored and the ability of the data processing method to detect molecules assured.

The hypothesis has been addressed in the following peer-reviewed papers:

- **P1:**
  - Reference: Minkus S, Grosse S, Bieber S, Veloutsou S, Letzel T (2020) Optimized hidden target screening for very polar molecules in surface waters including a compound database inquiry. *Anal Bioanal Chem* 412:4953–4966. <https://doi.org/10.1007/s00216-020-02743-0> (Appendix A.1 and B.2)
  - Author contributions: Author contributions: Susanne Minkus curated the data, planned and performed the DoE and the NTS data processing workflow, interpreted the data and drafted the manuscript. Stefan Bieber contributed to collecting the samples and performing the measurements, edited the manuscript and contributed to the discussion. Sylvia Grosse contributed to the laboratory work. Sofia Veloutsou prepared the samples and contributed to the measurements. Thomas Letzel supervised the research project, contributed to the discussion and edited the manuscript.
- **P2:**
  - Reference: Minkus S, Bieber S, Letzel T (2021) (Very) polar organic compounds in the Danube river basin: Non-target screening workflow and prioritization strategy for extracting highly confident features. *Anal Methods* 13:2044–2054. <https://doi.org/10.1039/D1AY00434D> (Appendix A.2 and Appendix B.3)
  - Author contributions: Susanne Minkus contributed to the sample preparation and analysis, curated the data, planned, optimized and performed the NTS data processing, interpreted the data and prepared the manuscript. Stefan Bieber edited the manuscript and contributed to the sample preparation and analysis. Thomas Letzel supervised the research project, contributed to the discussion and edited the manuscript.

## 4.1 Use QC samples, external and internal standards at different concentrations and in different matrices to assess the variability between RPLC-HILIC-HRMS measurements

### 4.1.1 Methods

Generally, solvent and matrix blank samples were injected throughout the analytical sequence (Appendix A.1, Appendix A.2, reference [101]). Analytical standards were handled in stock solutions at a concentration of 1 mM per compound in acetonitrile or acetonitrile/water (50/50, v/v) and subsequently combined to mixtures of 10  $\mu$ M per compound in acetonitrile. The external multicomponent standards were injected multiple times, evenly spread over the course of the measurement sequence. The raw data was evaluated to generally assess the performance of the RPLC-HILIC coupling with special focus on the RT precision (Appendix A.1, Appendix A.2). Within the scope of a study not presented here but was part of the fourth Joint Danube Survey [101], 177 reference standards covering a polarity range of  $-5.60 \leq \log D (\text{pH } 7) \leq 4.90$  were measured in triplicates to assess the stability of the serial coupling hyphenated to QTOF-MS (TripleTOF 4600; AB Sciex, Darmstadt, Germany). The approach was further advanced by preparing two synthetic samples in tap water matrix and spiking them with 34 standard compounds (Appendix B.3, Table S2) at two concentration levels ( $c_1 = 10 \text{ nM}$ ,  $c_2 = 100 \text{ nM}$ ; Appendix A.2).

In the process evaluation study presented in chapter 6.3, internal standards covering a  $\log D$  range at pH 7 of  $-2.47 - 3.59$  were prepared in stock solutions (Appendix B.4, Table S1). Subsequently, they were spiked into treated and untreated samples for activated carbon treatment evaluation at a final concentration of 5  $\mu$ M. Aliquots of all the samples were combined at equal volumes and also spiked with internal standards. Two triplicates of the pooled QC samples were measured at the beginning and the end of the sequence. In R (version 4.0.2) [102] and RStudio (version 1.3.959) [103], PCA was carried out for the blank samples, the treated samples and six pooled QC samples for each ionization mode. The data comprised normalized peak heights and "0" was put for missing values. The data was scaled and centered before being submitted to the *prcomp* function.

### 4.1.2 Results and discussion

The instrumental performance of the RPLC-HILIC coupling was assessed on external multicomponent standards in solvent and matrix and is presented in Appendix B.2, Table S3 and Appendix B.3, Tables S1 and S2. Precision values of mass, RT, peak height and peak width are given, as well as mass accuracy values. Those, however, could differ from study to study since throughout the course of thesis three HRMS instruments were used (TOF, QTOF and Orbitrap-

MS). Compounds that were retained from the RPLC column exhibited an average standard deviation of 0.3 min (0.9%,  $n = 43$ ). The RTs of the external HILIC standards deviated by 0.2 min (1.9%,  $n = 25$ , Appendix A.1) and 0.1 min (1.0%,  $n = 100$ , Appendix A.2). However, in some isolated cases, like for gabapentin or histamine, the RTs shifted  $> 1.0$  min. These “jumps” could be caused by switching between water samples and matrix-free QC samples, as the equilibrium at the HILIC stationary phase might be disturbed [104]. 177 target analytes were measured three times on the RPLC-HILIC-QTOF-MS system and the repeatability and accuracy determined separately for very polar ( $\log D < -2.50$ ), polar ( $-2.50 < \log D < 2.00$ ) and non-polar ( $\log D > 2.00$ ) [39, 101]. The results are summarized in Table 3. The probability of RT outliers seems to increase for highly polar compounds ( $\log D < 2.5$ , pH 7, Table 3).

Table 3: Maximum values of RT precision, mass precision and mass accuracy assessed on 177 reference compounds measured three times on the RPLC-HILIC-QTOF-MS setup. Standard compounds are classified by their polarity. Log  $D$  values are given for a pH of 7. This table has been published before [101].

	<b>Number of reference standards</b>	<b>Maximum RT shift [%]</b>	<b>Maximum deviation from average mass [%]</b>	<b>Maximum deviation from target mass [ppm]</b>
<b>Very polar (<math>\log D &lt; -2.5</math>)</b>	29	6.2	2.4	3.8
<b>Polar (<math>-2.5 &lt; \log D &lt; 2.0</math>)</b>	117	3.0	5.0	5.0
<b>Non-polar (<math>\log D &gt; 2.0</math>)</b>	31	2.3	1.6	4.2

In addition to causing instabilities at the HILIC stationary phase, external multicomponent standards do not factor matrix effects into the mass spectrometric response. This creates a need for an advanced QC regime in environmental analysis, such as internal standards and pooled QC samples [79, 80, 105] as was done in the process evaluation study presented in the chapters 5.4 and 6.3. Internal standards allow to monitor matrix effects and – if necessary – can be used for intensity normalization. Including external and internal standards in a measurement sequence allows to control the total variability of an analytical method and adjust the respective settings accordingly (Appendix A.1, Appendix A.2, reference [101] and Table S3 of Appendix B.4).

Checking field, transport, procedural or analytical blank samples for contamination or carry-over is common procedure. For process evaluation, however, the untreated samples served as blank samples.

As part of the study described in chapter 6.3, a PCA was computed using the feature lists prior to alignment in order to determine how individual samples group together based on the normalized peak heights. As an unsupervised, multivariate method, it further served the purpose to examine the pooled QC samples which were measured at the beginning and the end of sequence, as suggested by Sangster et al [80]. Figure 7 displays the score plot for the data acquired in positive ionization mode. The equivalent for the negative mode is given in Figure S3 of the supplementary material (Appendix B.4). The first dimension (principal component 1, PC 1) explains 22.4 % of the variation and the second dimension (PC 2) 16.5 %. Technical replicates are overall grouped closely together in both ionization modes. Samples subjected to different treatments (PAC of different types and at different concentrations) are mostly separated on the first principal component whereas the isotherm of PAC H118 (Table 4, chapter 6.3) is also separated on the second dimension. The samples of the H120 isotherm (green) are grouped together suggesting very little treatment effects. It was expected that the QC samples cluster tightly together and thus the variability among the test samples reflects the differences caused by treatment effects. However, the samples (black crosses) are positioned far apart on the PC 1 axis. In summation, these findings indicate that the run order is responsible for some variability between measurements. That a gradual change throughout the analytical sequence rendered the results less reproducible cannot be fully excluded at this point. On the other hand, the feature lists were investigated by PCA prior to alignment and the recursive gap filling (compare Figure 11, chapter 6.3). Consequently, some of the observed effects might be softened later on in the data processing regime.

Hypothesis 2 can be accepted since the aforementioned efforts give information on the variability of the instrumental setup and thus allow to monitor its robust operation.

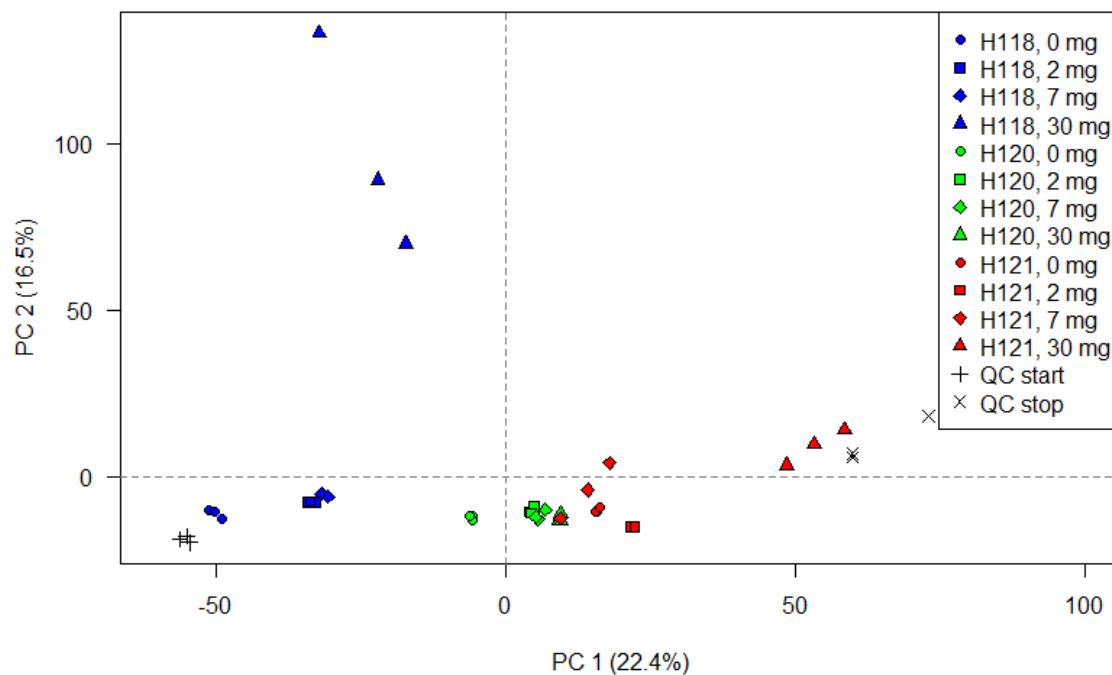


Figure 7: Scores plot of the PCA based on the normalized peak heights of the feature extracted from each individual measurement.

## 4.2 Add filters to the data processing workflow to remove noise, artefacts, redundant and false positive features

### 4.2.1 Methods

As presented in the articles of Appendix A.1, Appendix A.2 and the process evaluation study (chapters 5.4 and 6.3), componentization and alignment steps were added to the NTS data processing workflows. Thereby, peaks such as adducts or isotopes, belonging to the same mother compound (i.e. the  $[M+H]^+$  ion) are either grouped together or removed based on their RT and mass. Similarly, features that are assumed to represent the same compound are aligned across technical replicates and samples. After the alignment step, a replicate filter was incorporated in the workflows to eliminate features detected in less than a defined number of times. Noise filters remove peaks below a user-defined intensity threshold and had to be set at different points of the workflow (Appendix A.1 Figure 1, Appendix B.3 Table S4, Appendix B.4 Table S3). The feature extraction method was applied to the blank samples just like to the real samples and the detected features were excluded from the final list based on their RTs and masses (Appendix A.1 and Appendix A.2). A peak filter and a duplicate filter were added to the process evaluation NTS workflow, depicted in Figure 11.

### 4.2.2 Discussion

Processing steps like componentization, alignment and several filters are supposed to reduce redundant peaks [65]. On the one hand, prioritization of features for their identification is supported since false positive findings decrease. When comparing samples by their molecular fingerprint for process evaluation (chapter 5.4), rather than filtering for features that could readily be matched with real compounds, it is important to curate the data to avoid skewness and create a final feature list that is statistically reliable. Thus, the data needs to be cleaned from noise, artefacts and redundant peaks when comparing samples treated with activated carbon to untreated samples (compare chapter 6.2.2). Regions of increased data density were observed in the total ion chromatogram (Figure S2, Appendix B.4), i.e. around RT 25.6 min, where non-target peaks accumulate. Within these regions the peak quality deteriorates and the probability for the algorithm to erroneously extract artefacts might be increased. Therefore, an additional peak filter was applied after the initial peak picking step. Peaks were filtered by shape and number of data points before further processing. However, parameter ranges had to be set relatively wide to avoid false negative features. As a result, the bands of high feature density persist even after completing the full data processing regime (Figure 13, chapter 6.3). This matter is arguably better resolved by adapting the chromatographic separation rather than on a data processing level.

Another filtering step for refining the NTS data processing workflow for sample comparison was the duplicate filter. It was included after the alignment of replicates and created consensus rows from features that were missed by the alignment algorithm. Thereby, false negative detects caused by the replicate filter as explained in chapter 4.3, can be reduced.

In Appendix A.1 critical input parameters and filters were modeled based on the DoE approach (chapter 3.3). The results suggest to keep the initial noise threshold low but include a more rigid intensity filter further downstream of the process. This avoids missing peaks and at the same time reduces the number of falsely deconvoluted peaks and single ions. Consequently, noise thresholds at early stages of the NTS data analysis workflow are critical to the false negative rate. Nevertheless, when using open source software without parallelization strategies to speed up the processing times, thresholds close to zero might not be feasible. The open source platform patRoön is addressing this problem [106] as is further discussed in Appendix A.3. Depending on the algorithm more than 10,000 peaks might be detected per sample during initial peak picking [107]. Data reduction by componentization and filtering is imperative to obtain features that likely represent a real compound.

These steps improve the quality of the final feature list as they mitigate the risk of false positive findings and increase the statistical reliability of the data. Consequently, hypothesis 2 can be

accepted as the ability of extracting molecules from the raw HRMS data is assured. Still, the true amount of false positives in a sample is unknown.

### **4.3 Identify the points of losses of false negative features by accessing intermediate stages of the data processing workflow**

#### **4.3.1 Methods**

Synthetic samples, comprising standard compounds spiked into a tap water sample at two concentration levels (10 nM and 100 nM), were subjected to the feature extraction method for retrospective validation as part of the study presented in Appendix A.2. The 34 target analytes were tracked throughout the data analysis workflow.

#### **4.3.2 Discussion**

For false negative compounds the points of losses in the data treatment process were determined and are presented in Appendix B.3, Table S5. At the higher concentration level, > 90 % of the standard compounds were recovered, at the lower level > 60 %. Generally speaking, more variability in the data occurs for compounds at lower concentrations which leads to more losses during feature extraction.

Most of these false negatives were caused by the replicate filter applied after the alignment step. In cases like vidarabine, L-glutamic acid or lisinopril, a peak could not be deconvoluted in one of the replicates which constitutes a complex step during feature extraction and is thus prone to missing peaks. These findings highlight the need for retrospective targeted peak searches to fill these gaps as well as a duplicate filter to compensate for misalignments (compare chapters 4.4 and 4.2).

Retrospectively determining the processing steps within the workflow where known reference points (standard compounds) were lost, is a useful strategy to control the quality of the data processing method as proposed in hypothesis 2 which can consequently be accepted. However, it requires NTS software such as MZmine 2 [68] or patRoon [106] that is accessible at intermediate stages of the workflow.

### **4.4 Introduce recursive target searches to the data processing workflow to retrospectively improve the quality and statistical confidence of final feature lists**

#### **4.4.1 Methods**

Post-hoc target screenings based on non-target features were implemented into the NTS data analysis strategies developed as parts of the studies presented in reference [101], Appendix A.1

and chapters 5.4, 6.3. For the first approach, peak picking and alignment was performed on MarkerView software (version 1.3.1; AB Sciex) and afterwards chemical formulae were derived from matching the features' accurate masses with entries of a compound database. Based on the list of chemical formulae, EICs were extracted from the raw data using SCIEX OS software (version 1.4.0.18067; AB Sciex).

Secondly, MassHunter Workstation Profinder software (Agilent Technologies) includes a recursive algorithm as well that uses median mass and RT values of a previously extracted feature to search for missing peaks in a targeted manner [105, 108]. A similar step was added to the workflow developed for comparative NTS analysis using the open source software MZmine 2 [68]. Missing peaks are searched for within the  $m/z$  and RT ranges given by the other peaks of the feature. An extra  $m/z$  tolerance of 0.0015 Da (for an Orbitrap Exploris 120 HRMS instrument, Thermo Fisher Scientific) was added to each range to achieve full recovery of the internal standards during method optimization.

#### **4.4.2 Discussion**

Recursive target screening algorithms are considered to be more precise and thus complement a non-targeted one. They soften the replicate filter as they fill in single peaks missing from one of multiple sample injections as discussed in chapter 4.3. Peak integration can be improved by targeted integration algorithms such as MQ4 implemented in the SCIEX OS software and additional information can be gained on isotopes and MS2 spectra [101]. Because the search criteria depend on preceding processing steps, they should be applied rather late in the workflow when the data has already been cleaned-up. Parameter settings of the non-targeted and the targeted part of the feature extraction method were coordinated by means of DoE in Appendix A.1. Comparing the feature lists of two samples based on fcs of the feature intensity (chapters 5.4, 6.3), can give indications on concentration changes. However, there are several reasons why a feature could not be detected in one of the two samples:

- a) It was only present in one.
- b) Its concentration fell under the limit of detection of the instrumental setup.
- c) It was not extracted by the data processing method.

In the case of option c), a recursive target screening could recover the feature as it is more focused, simplistic and robust than the NTS algorithm. In the cases a) and b) it might still be more beneficial to subsequent statistical analysis to integrate baseline signal to fill the gaps than imputing assumed non-zero values.

A recursive target screening step within an NTS workflow improve the reliability in non-target

features and improve the statistical confidence as it is able to detect peaks previously missed by the peak picking algorithm. Through this measure, the quality of the data processing method can be controlled and hypothesis 2 accepted. However, the majority of available software tools do not offer gap filling solutions and performing missing value imputation is critical to univariate and multivariate statistical analysis [109].

Through introducing quality control (QC) measures, the robust operation of the instrumental method can be monitored and the ability of the data processing method to detect molecules assured.

## 5. Method adaptation

Hypothesis 3: The data processing strategy can be adapted to fit different software tools as well as to different non-target screening applications such as identification, trend analysis and comparative analysis.

The hypothesis has been addressed in the following peer-reviewed papers:

- **P1:**
  - Reference: Minkus S, Grosse S, Bieber S, Veloutsou S, Letzel T (2020) Optimized hidden target screening for very polar molecules in surface waters including a compound database inquiry. *Anal Bioanal Chem* 412:4953–4966. <https://doi.org/10.1007/s00216-020-02743-0> (Appendix A.1 and B.2)
  - Author contributions: Author contributions: Susanne Minkus curated the data, planned and performed the DoE and the NTS data processing workflow, interpreted the data and drafted the manuscript. Stefan Bieber contributed to collecting the samples and performing the measurements, edited the manuscript and contributed to the discussion. Sylvia Grosse contributed to the laboratory work. Sofia Veloutsou prepared the samples and contributed to the measurements. Thomas Letzel supervised the research project, contributed to the discussion and edited the manuscript.
- **P2:**
  - Reference: Minkus S, Bieber S, Letzel T (2021) (Very) polar organic compounds in the Danube river basin: Non-target screening workflow and prioritization strategy for extracting highly confident features. *Anal Methods* 13:2044–2054. <https://doi.org/10.1039/D1AY00434D> (Appendix A.2 and Appendix B.3)
  - Author contributions: Susanne Minkus contributed to the sample preparation and analysis, curated the data, planned, optimized and performed the NTS data processing, interpreted the data and prepared the manuscript. Stefan Bieber edited the manuscript and contributed to the sample preparation and analysis. Thomas Letzel supervised the research project, contributed to the discussion and edited the manuscript.
- **P3:**
  - Reference: Minkus S, Bieber S, Letzel T (2022) Spotlight on mass spectrometric non-target screening analysis: Advanced data processing methods recently

communicated for extracting, prioritizing and quantifying features. *Anal Sci Adv* 3:103–112. <https://doi.org/10.1002/ansa.202200001>

- Author contributions: Susanne Minkus searched, reviewed and managed the literature and drafted the manuscript. Stefan Bieber contributed to the discussion and edited the manuscript. Thomas Letzel contributed to the literature search and the discussion and edited the manuscript.

## **5.1 In a top-down approach, all necessary processing tools are gathered first, identified in the specific vendor and open access software and used to construct a feature extraction workflow**

### **5.1.1 Methods**

The feature extraction core method was realized so far on three different software tools:

- MassHunter Workstation Profinder (version B.06.00, Agilent Technologies) using the proprietary “Molecular Feature Extraction” algorithm coupled to the recursive “Find by Ion” algorithm with the “Agile 2” integration method (Appendix A.1)
- MarkerView (version 1.3.1, AB Sciex) (Reference [101])
- MZmine 2 using the algorithms of the “Automated Data Analysis Pipeline” (ADAP) [110] (Appendix A.2 and chapters 5.4, 6.3)

### **5.1.2 Discussion**

A feature extraction workflow was developed and refined as part of a hidden-target screening for polar, small and organic molecules.

It was realized on three different software tools – two commercial and one open source. Letzel and Drewes defined the five key processing steps as peak picking, alignment, integration, background comparison and componentization [71]. They formed the core of a workflow which was then adjusted and extended to serve the following research objective:

Suggesting relevant polar, organic, and small candidate molecules detected in environmental real samples for validation *via* reference material. The key processing steps were identified in the NTS workflows and are shown in Figure 8. It should be noted that “peak picking” often describes a technique where data points are binned together within defined limits. There are alternative feature extraction methods, such as ROIMCR, as is discussed in more detail in Appendix A.3. “Integration” herein is replaced by “deconvolution” since some programs employ

different methods for peak detection such as the “centWave” algorithm that applies continuous wavelet transformation [111]. All the modules were somehow integrated into each of the three workflows, but the underlying algorithms, especially for peak picking and deconvolution differed considerably. That is reflected in a portion of very software-specific parameters, such as the subtraction offset in MarkerView or the minimum scan group size in MZmine 2. It can be concluded that information on the RT and mass tolerance, the noise threshold or the charge state was required for all the tools. Hohrenk *et al.* found that the overlap of features extracted with four different processing tools was about 10% [112]. Accordingly, there is a need for quality control in NTS data processing workflows as discussed in chapter 4. The core workflow was somehow identified in a process evaluation study as well (compare Figure 11). Rather than identifying individual features, a global comparison of treated and untreated samples was pursued. The workflow is similar to the one presented in Figure 8C. However, for background comparison the untreated sample that has undergone the entire feature extraction and clean-up process was considered instead of dedicated blank samples as part of the QC regime as was also discussed by Schollée *et al.* [70]. Treated and untreated samples were measured under the same conditions and in the same sequence. Hence laboratory background was assumed to be the same for both. Since only features of which the signal intensities presented significant differences between treated and untreated sample were considered, artefacts and background noise would be of no consequence. However, grouping redundant peaks by alignment and componentization became all the more important to maintain statistical accuracy for further interpretations.

With respect to hypothesis 3, a core workflow as identified in different NTS investigations and was implemented in different software tools. Hypothesis 3 can therefore be accepted. However, the order of processing steps and the parameters might differ substantially. Especially, for research goals other than feature identification, further data treatment is necessary. In conclusion, the claim of 5.1 can only be partially accepted.

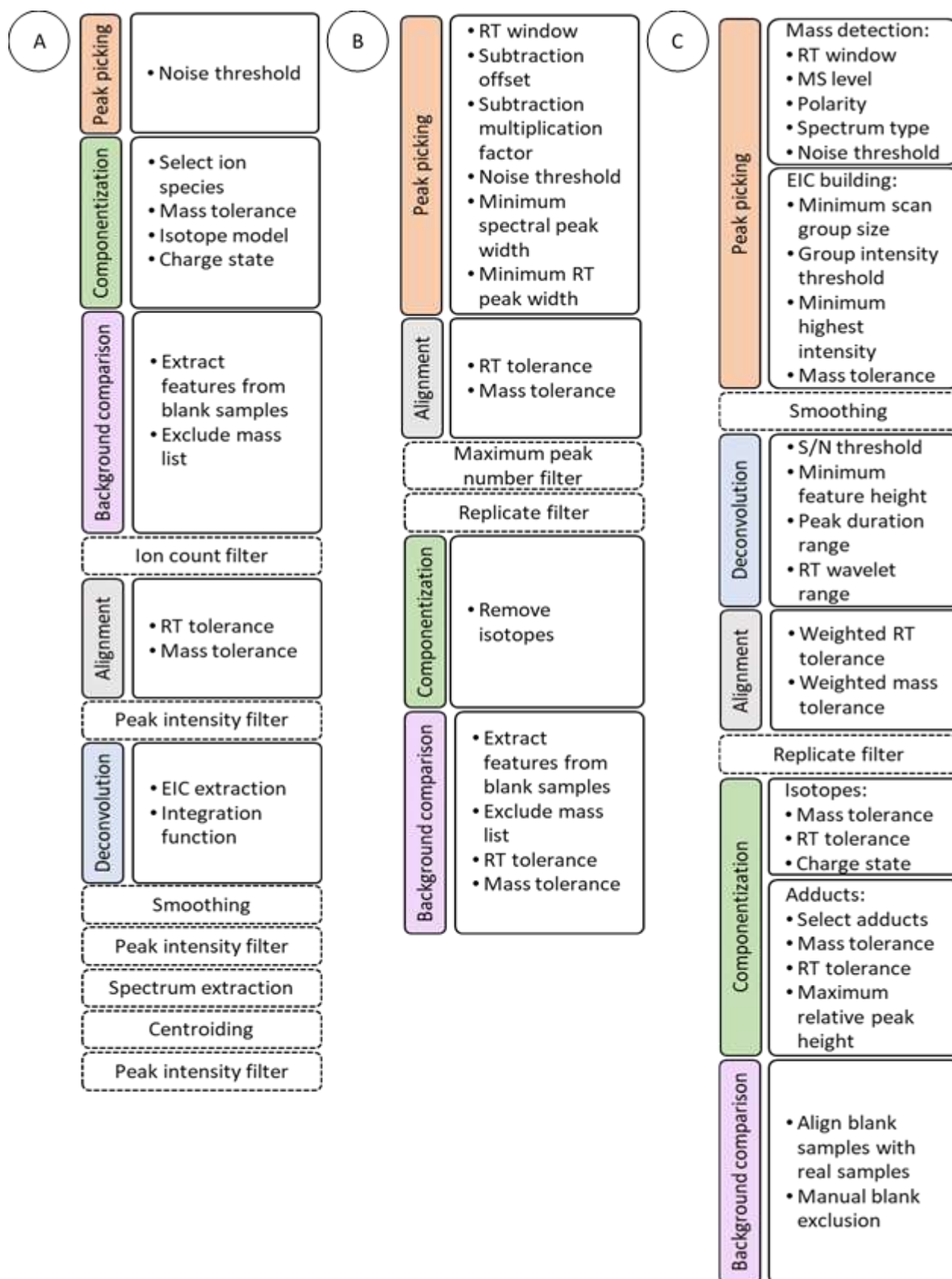


Figure 8: The methods for extracting features from data acquired with polarity-extended chromatography coupled to ESI-HRMS are presented schematically. The workflow was built into three different software tools: A) MassHunter Workstation Profinder, B) MarkerView and C) MZmine 2. The core procedural modules are depicted in colored boxes along with the relevant setting parameters. Additional processing steps which were necessary to adapt the workflow to the respective software and data set are displayed in dashed boxes.

## 5.2 Use specialized databases to match a feature with a candidate compound using exact mass and physicochemical properties

### 5.2.1 Methods

Features of the HILIC or the RPLC retention interval were uploaded separately to the FOR-IDENT platform [113] and compared to trace organic compounds of anthropogenic origin stored in the STOFF-IDENT database [73]. If available, detected MS2 spectra were matched with *in silico* spectra predicted by MetFrag (version 2010) [114]. As for the input parameters, a pH level of 7 was selected and the mass tolerance for precursor and fragment ions was adjusted to the specific data set (Appendix A.1, Appendix A.2). For RPLC features log *D* values were calculated by means of retention time indexing (RTI) [101]. Therefore, the log *D* values of nine standard compounds were related to their normalized RTs by linear calibration. The log *D* values of charged molecules were corrected following the rules explained elsewhere [115]. Compounds assigned to features retained on the HILIC column were matched with compound database entries by accurate mass and subsequently filtered for compound candidates with a negative log *D* value.

### 5.2.2 Discussion

Features were extracted from the HILIC and the RPLC elution windows and handled separately in the annotation process. Firstly, features extracted from the HRMS raw data were matched by accurate mass with trace organic compounds of anthropogenic origin stored in the database. The STOFF-IDENT database specializes in anthropogenic TOrcs that are relevant to the aquatic environment. Confining the chemical space for compound annotation by using reduced compound databases is discussed in Appendix A.3.

An elemental composition and at least one candidate substance were assigned to a successfully matched feature. If available, MS2 spectra observed for a feature were compared to the *in silico* spectrum predicted for a matched compound (see Appendix A.2). In case of multiple hits, MS2 scores between 0 and 1 were calculated which indicate structural similarity between feature and compound. For RPLC features an RTI score between 0 and 1 was calculated. It expresses the difference between the real log *D* value of a compound and the log *D* value calculated by a linear correlation with the observed RTs of nine standard compounds. The regression line as presented in Figure 9, was extrapolated to a log *D* of 0 whereas an RT window from 22.7 to 31.6 min was covered.

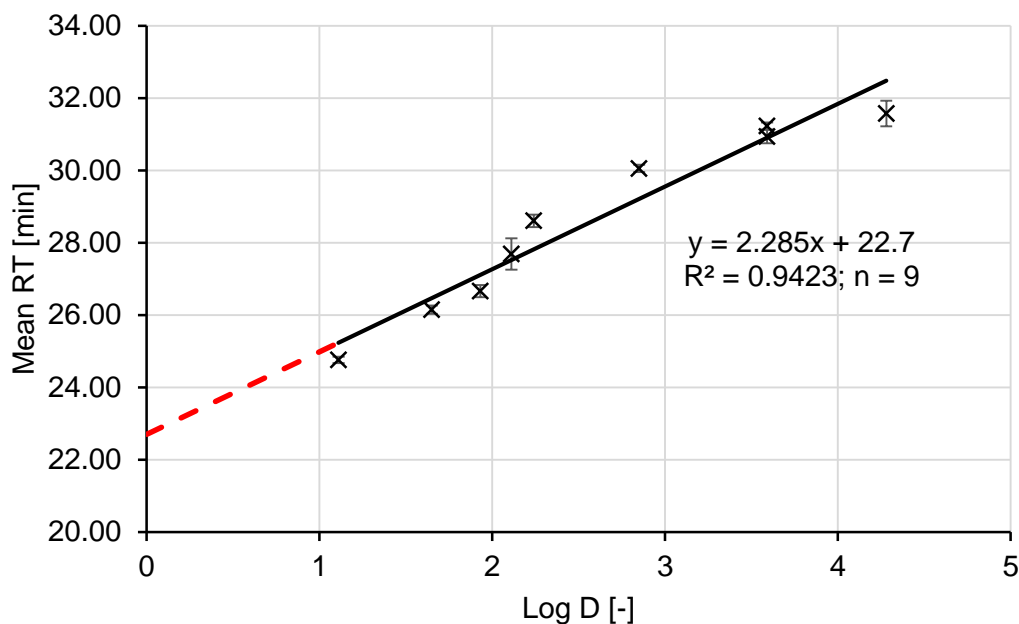


Figure 9: For the RTI normalization, nine standard compounds were measured three times. Their log  $D$  values were plotted against the mean RTs and a linear calibration function was fitted. The trend line (solid black line) was extrapolated to a log  $D$  (pH 7) value of 0 (dashed red line). This Figure has been previously published elsewhere [101].

Candidate lists generated for HILIC features were filtered by their log  $D$  value at pH 7. Compounds predominantly retained by the HILIC column are expected to be (very) polar and accordingly have a negative log  $D$  value. Three different targeted analysis on the RPLC-HILIC coupling using multicomponent standards, showed that > 97% of the targets which eluted from the HILIC column had a log  $D < 0$  [39, 116, 117]. Besides accurate mass screening, MS2 and RTI scorings as well as a log  $D$  filter were successfully used to reduce the number of candidate compounds assigned to features detected on the RPLC-HILIC-ESI-HRMS system. A feature annotation workflow was presented which was able to differentiate between polar and nonpolar candidate molecules. As stated by hypothesis 3, the NTS data processing strategy can adapt to the purpose of identifying features: A compound database search is simply added to the feature extraction core workflow.

### 5.3 Add prioritization and classification steps to the feature extraction workflow to facilitate identification at a high level of confidence

#### 5.3.1 Methods

The first data set derived from 33 surface water sample taken on three different dates from eleven sites (Table S1, Appendix B.2). The feature fingerprints upstream and downstream of an

urban area were compared.

For the second data set which comprised of 51 surface water samples (Appendix B.3, Table S3), a classification system was introduced. It ranked features and their potential annotations based on their identification confidence by considering the analytical factors accurate mass, fragmentation pattern and retention behavior. Furthermore, they were prioritized on how frequently they were detected in the sample set.

### 5.3.2 Discussion

As anticipated for urban areas, a local increase of polar features was observed and investigated in more detail within the first study (Figures 3 and 4, Appendix A.1). Features which were detected before and after the urban area are depicted in Figure 10 (see below). They were compared based on their mere presence or absence as well as their absolute signal intensities. Using this prioritization method, a feature was suggested for validation as its absolute peak height increased by a factor of 34. However, due to the lack of calibration data no definite quantitative statement can be made.

In the second surface water study, a two-step prioritization strategy was applied. For one, features extracted from the 51 samples were divided into six classes indicating how much analytical information was available and how certainly they were allocated to candidate compounds. The highest class (A) was attributed to four features “[...] which were unequivocally annotated by querying the compound database and were assigned an MS2 score > 0.6” (Appendix A.2). Class A complies with a level 2-3 in identification confidence according to Schymanski *et al.* [82]. For querying the compound database, it was differentiated between features eluting during the RPLC or HILIC retention interval. If the latter were matched with one or more compound candidates, only those with a negative log  $D$  were considered. Features retained by the RPLC column can be prioritized based on the RTI score as described in the previous chapter and in reference [101]. An unambiguous allocation by matching features by their accurate mass with entries of a compound database is often not possible due to i.e. structural isomers. The  $\Delta \log D$  value as implemented on the FOR-IDENT platform is calculated from RTI normalization and experimental data. Rostkowski *et al.* suggested an acceptance interval of  $\Delta \log D \pm 0.70$  during a collaborative trial performing NTS on house dust samples [118]. Thereby, it was possible to distinguish between structural isomers allocated with a feature (RT 31.6 min/ mass 301.1768 Da) detected in the Danube river (Austria, rkm 2113). It was assigned with dapoxetine (InChI key USRHYDPUVLEVMC-FQEVSTJZSA-N) since its  $\Delta \log D$  was 0.62 and thus < 0.70 [101]. Chromatographic parameters like RT for complementing accurate mass diagnostic evidence during feature identification is discussed in more detail in

## Appendix A.3.

In a further prioritization step, features which were detected at the most sampling sites were marked as high priority for validation by reference standard. Eight features occurred in ten or more samples out of a total of 51 samples (Table 2, Appendix A.2). The frequent detection of polar features in coherent surface waters indicates their persistence and mobility and thus their environmental relevance.

It was hypothesized that the NTS data processing workflow can adapt to different research objectives which in this case was tentatively identifying relevant candidate substances. However, the data analysis method needs adjustments such as additional prioritization steps and thus hypothesis 3 must be rejected considering the outcome of this task.

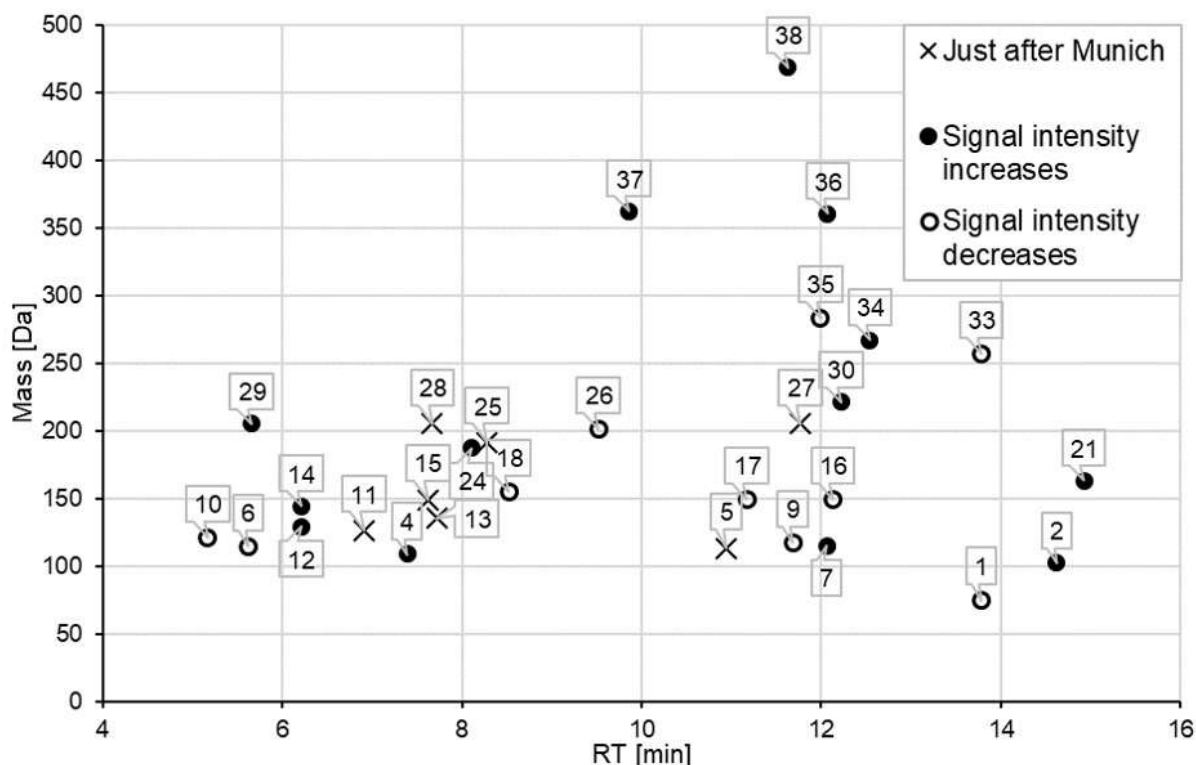


Figure 10: The dot plot displays features that were detected in the March samples either upstream or downstream of Munich (circles, location IDs 8 and 9, Table S1; Appendix B.2) or just downstream of Munich (crosses). The features eluted from the HILIC column and were proposed by the STOFF-IDENT database. Only matches with a negative log  $D$  value were considered. The numbers indicate the ID of the database queries as are listed in Table 2 of Appendix A.1. This figure was published as presented in Appendix A.1.

## 5.4 Add the necessary processing steps to the workflow and adjust related parameters for comparative analysis of samples

### 5.4.1 Introduction

The occurrence and fate of TOrcs throughout treatment processes is typically assessed *via* targeted analyses. Focusing on a limited number of prioritized or probably already regulated target analytes could cause a partially distorted view of the molecular fingerprint as unknown or unexpected TOrcs are missed. At this point, it cannot be determined whether a decrease in concentration of a target analyte indicates its removal or merely its transformation. This leads to TPs being underestimated, even though they tend to be more polar (and thus mobile) and might even have enhanced toxicity potential compared to their parent compounds [26, 119–121]. The NTS approach, powered by HRMS often in combination with LC, allows a more comprehensive assessment of TOrcs as it refrains from preselecting substances [41, 65]. When evaluating NTS data, features characterized by their RT, mass and signal intensity are extracted from full scan HRMS data and further processed following two general objectives:

- Identification with the methodological consequence of prioritizing features based on i.e. the amount and quality of information available and their environmental relevance [97, 107, 117].
- Bulk characterization by a non-discriminatory feature extraction workflow followed by statistical analysis [70].

The latter is a suitable method to globally evaluate water treatment processes, often based on features' signal intensities, that gives indications of the removal of TOrcs and formation of TPs [67, 122, 123].

### 5.4.2 Methods

The non-targeted data analysis were performed in MZmine 2 [68]. Figure 11 schematically presented the workflow for extracting features from NTS data, filtering and bringing the feature lists of the treated and untreated sample together for comparative analysis. The workflow is shortly outlined in the following:

First, masses were detected on MS1 and MS2 level whereas the RPLC as well as the HILIC retention intervals (5 min – 33 min) were considered (for the instrumental method compare chapter 6.3). Then, chromatograms were built and peaks deconvoluted using the ADAP algorithm (“Automated Data Analysis Pipeline”) [110]. Chromatograms were smoothed by applying a Savitzky-Golay filter. Peaks were filtered out if the number of data points, tailing factor

and/or asymmetry factor fell outside a predefined range. Thereafter, isotopic patterns of singly charged molecular ions were detected and isotopic peaks as well as sodium, potassium and ammonium adducts were removed. The feature lists were aligned across the three technical replicates using the RANSAC aligner [68, 124] and subsequently duplicates were removed. Finally, the features that were detected in less than three replicates were eliminated.

The cleaned-up feature lists of the treated and the untreated sample were subsequently aligned for comparative analysis. For features which were only present or detected in one of the two samples, the respective gap was filled by a recursive targeted search in the raw data. Feature rows whose gaps could not be filled, were removed from the list. Finally, the features' signal intensities (peak heights) were normalized using the internal standards. All the standard compounds contributed to the normalization factor, but were weighted based on the  $m/z$  and RT distance to the feature [125]. The final feature list was exported to comma-separated values (CSV) format.

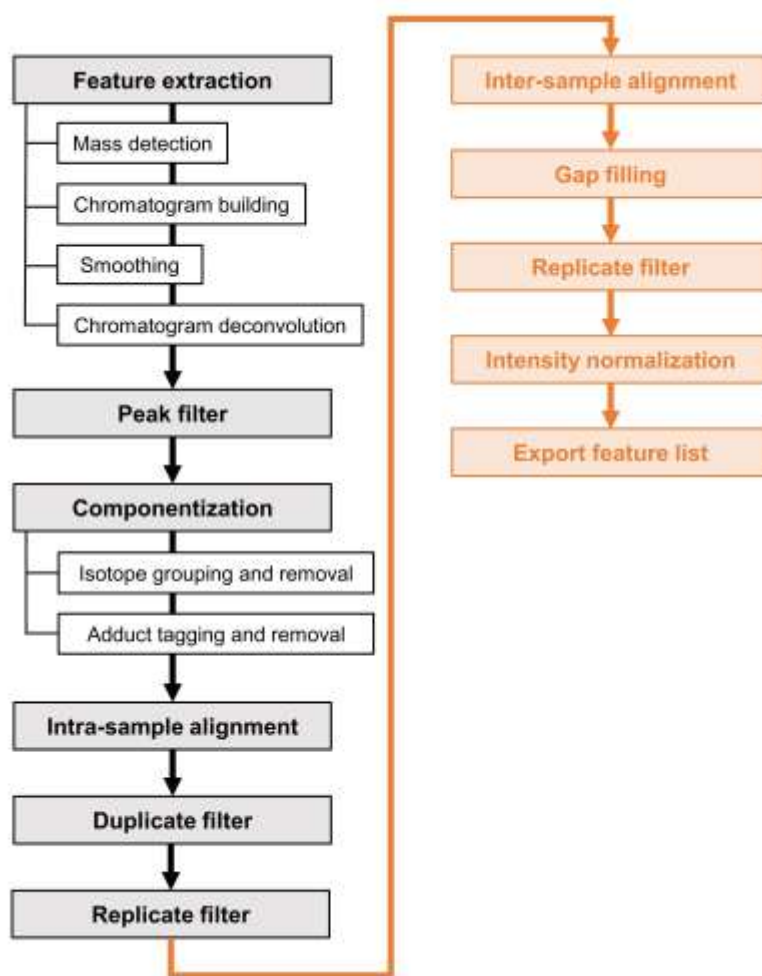


Figure 11: NTS data processing workflow for comparing a treated and an untreated surface water sample. The processing steps for extracting and filtering features from the technical replicates of a single sample are depicted in black. The orange boxes are processing steps that enable the comparative analysis of the treated and the untreated sample.

### 5.4.3 Results and discussion

The method for extracting features from HRMS full scan data as depicted by the black and grey boxes in Figure 11. The core workflow presented in chapter 5.1, was extended to meet the requirements for analyzing fcs of features between a treated and an untreated sample. In order to minimize statistical errors, additional processing steps were added as are depicted in the yellow boxes.

Chromatographic peaks which were identified as isotopologues or adducts of features were removed in order to reduce redundancy in the feature lists. Features were aligned in two separate steps, first across technical replicates and then across both samples. An alignment method was chosen based on the iterative RANSAC (“random sample consensus”) algorithm

[68, 124]. It allows to correct for some RT deviations which were observed for some HILIC-influenced analytes (compare chapter 4.1). In an attempt to eliminate misaligned features, the list was searched for duplicates which might occur due to misalignment. Duplicates were then merged to consensus rows.

There are features which are only detected in one or the other sample, either because they were only present in one, their concentrations fell below the limit of detection or the feature was not extracted from the data. Missing values pose an issue in comparative non-target screening analysis, as they hamper the calculation of fcs. Missing value imputation to replace zeros should be chosen with care as different univariate or multivariate analysis require different methods [109]. Instead, a gap filling step was implemented into the data processing workflow that conducts a targeted search to retrospectively pick missed peaks or baseline from the raw data. The first replicate filter removed features that were found in less than three technical replicates and the second one caught features missed by the second gap filling step.

The single intensities of the features were normalized based on the internal standards in order to mitigate matrix effects that might otherwise affect the fcs. Where a bulk characterization of the NTS data is favored over extracting single features for identification, advanced statistical analysis (i.e. PCA) facilitates revealing general patterns [70].

The NTS workflow that was developed according to this task enables the comparative analysis of samples, ranging from spatial and temporal trends to two-sample comparisons (before and after treatment). But here again, the core workflow had to be complemented by additional processing steps and some were considerably adapted (handling the untreated sample as a blank rather than conventional background subtraction). Consequently, hypothesis 3 must be rejected.

## 6. Application of the method

Hypothesis 4: The optimized and adopted workflow is universally able to tentatively identify unexpected (very) polar candidate compounds and can be applied to surface water samples and samples after water treatment processes.

The hypothesis has been addressed in the following peer-reviewed papers:

- **P1:**
  - Reference: Minkus S, Grosse S, Bieber S, Veloutsou S, Letzel T (2020) Optimized hidden target screening for very polar molecules in surface waters including a compound database inquiry. *Anal Bioanal Chem* 412:4953–4966. <https://doi.org/10.1007/s00216-020-02743-0> (Appendix A.1 and B.2)
  - Author contributions: Author contributions: Susanne Minkus curated the data, planned and performed the DoE and the NTS data processing workflow, interpreted the data and drafted the manuscript. Stefan Bieber contributed to collecting the samples and performing the measurements, edited the manuscript and contributed to the discussion. Sylvia Grosse contributed to the laboratory work. Sofia Veloutsou prepared the samples and contributed to the measurements. Thomas Letzel supervised the research project, contributed to the discussion and edited the manuscript.
- **P2:**
  - Reference: Minkus S, Bieber S, Letzel T (2021) (Very) polar organic compounds in the Danube river basin: Non-target screening workflow and prioritization strategy for extracting highly confident features. *Anal Methods* 13:2044–2054. <https://doi.org/10.1039/D1AY00434D> (Appendix A.2 and Appendix B.3)
  - Author contributions: Susanne Minkus contributed to the sample preparation and analysis, curated the data, planned, optimized and performed the NTS data processing, interpreted the data and prepared the manuscript. Stefan Bieber edited the manuscript and contributed to the sample preparation and analysis. Thomas Letzel supervised the research project, contributed to the discussion and edited the manuscript.

## 6.1 Evaluate the spatial and temporal distribution of polar features in the Isar river and tentatively identify them

### 6.1.1 Methods

Grab samples were taken from the Isar river in southern Germany at eleven locations (Appendix B.2, Table S1). Each sampling pass was completed within a single day and repeated in March, May and July of 2015. Samples were prepared following a two-step solid-phase extraction (SPE) protocol involving two cartridges: An RP C18-encapped (Strata-X, Phenomenex, Aschaffenburg, Germany) for non-polar analytes and a ZIC-HILIC (DiChrom GmbH, Appendix A.1). The extracts were filtered (22  $\mu\text{m}$ ; polyvinylidene fluoride, PVDF) and stored at 4 °C until the analysis. The samples were measured on the RPLC-HILIC serial coupling connected to a TOF-MS. Polar features were extracted from the HILIC retention interval by applying the method presented in Figure 2 A (chapter 5.1). They were annotated by querying a compound database followed by a filtering step for compounds with a negative log  $D$  value at pH 7 (chapter 5.2).

### 6.1.2 Discussion

Processing the data of 33 environmental samples yielded 46 HILIC features that were assigned with 64 candidate substances with a log  $D < 0$  at pH 7 (Appendix A.1, Table 1). The Isar river was sampled starting near the spring at the Austrian-German border, covered the metropolitan area of Munich and ended in the town of Dingolfing. The estimated wastewater effluent contribution in the river varied from 5 to >50% after the discharge points of wastewater treatment plants (WWTP) [126]. There, an increase in anthropogenic trace organic compounds was expected including polar ones. The spatial distribution is presented in Appendix A.1, Figure 3 and illustrates a significant amplitude of polar features at the sampling location downstream of Munich. Furthermore, the campaign unraveled seasonal differences as the number of polar features was higher in March than in May or July due to relatively low precipitation in February. Three tentative polar compounds, listed in Appendix A.1, Table 3, were confirmed by RT and accurate mass matching with reference standards. The respective EICs and isotopic ratios are given in Figures S1-S3 and Table S8 of Appendix B.2. Among these substances was guanylurea which was prioritized based on its absolute abundance as was described under chapter 5.3. It is an aerobic bacterial degradation product of the antidiabetic drug metformin [127] which was also observed in this study. Guanylurea has already been detected in the North Sea [128] pointing to its mobility in water cycles. Thus, it is expected to be a high-risk candidate for affecting drinking water supplies.

This application sought to accommodate the central research objective: Finding and validating

relevant polar, organic, and small candidate molecules in real environmental samples. Of further interest was their spatial and temporal distribution along the Isar river in southern Germany. Therefore, the hidden-target screening method as described above was applied to real samples of the Isar river. Three polar, organic small molecules were definitely identified. Consequently, hypothesis 4 can be accepted.

## **6.2 Classify, prioritize and tentatively identify polar features in ground and surface water samples of the Danube river basin**

### **6.2.1 Methods**

The Danube and its major tributaries were sampled as part of the fourth Joint Danube survey (JDS4) in 2019 [66]. Grab samples for direct injection were taken from 51 locations and 20 mL aliquots were sent to our laboratory [129]. The samples were filtered (0.22  $\mu\text{m}$ , PVDF) and stored at 4 °C until the measurement. The chromatographic separation was carried out on the serial RPLC-HILIC coupling and masses were analyzed on a QTOF-MS instrument (Appendix A.2). Besides the full scan experiment to acquire NTS data, product ion scans were recorded using an information-dependent acquisition (IDA) method to gather fragmentation information on automatically selected precursor ions.

### **6.2.2 Discussion**

In total, 77 features (class B) which were extracted from the HILIC retention interval were unequivocally assigned to 67 candidate substances with a negative log  $D$  value which are listed in Table S6 of Appendix B.3. The classification system describes how reliably a feature was identified, is explained in further detail in chapter 5.3. The spatial binary trends of features assigned to different classes are shown in Appendix A.2, Figure 2. A binary trend describes the mere presence or absence of feature at the individual sampling points. A trend analysis of a continuous variable such as a feature's signal intensity was not possible since only qualitative or at best semi-quantitative data can be derived from an NTS investigation. The binary trend of polar features (class C) could disclose potential sources of discharge. An elevated number of polar features was observed in the samples JDS4-7 (rkm 2113) and JDS4-37 (rkm 488) which were taken 7 km and 9 km downstream of the WWTPs of Asten (Austria) and Giurgiu (Romania), respectively. Loos *et al.* found that the highest concentrations of polar organic compounds are often detected in the Danube's tributaries [130]. In line with their findings, an amplitude of polar features was detected in the Hron river (Slovakia; sample JDS4-20, confluence rkm 1716). In direct comparison to tributaries of lower discharge, the number of polar

features is often significantly lower in the Danube river itself (JDS4-22, rkm 1707) due to dilution effects. Of the 67 polar candidate compounds, eleven features listed in the Tables 1 and 2 of Appendix A.2 were prioritized for validation *via* reference material. Among these high-priority suspects was 4-hydroxy-2,2,6,6-tetramethylpiperidine-1-ethanol (class A) which was detected in 47 out of 51 samples. It was described as ecotoxicologically relevant and highly mobile and persistent in ground and surface waters and could thus pose a risk to drinking water supplies [23, 131].

In the study presented in Appendix A.1, 64 candidate substances were assigned to 46 features which were extracted from the HILIC retention interval of chromatograms acquired from analyzing 33 environmental samples. 18 features had more than one candidate compound annotated to them. This example illustrates the need for additional amenable information on a feature in order to reduce the number of annotations. The approach for finding polar, organic, and small compounds in surface water samples presented in the previous task was extended by MS2 experimentation. Additionally, the feature extraction and prioritization strategies were developed further. The method was successful in detecting polar, organic and small features in real samples of the Danube river and thus hypothesis 4 can be accepted.

### **6.3 Characterize different types and concentrations of powdered activated carbon by comparing the fingerprints of polar candidate molecules**

#### **6.3.1 Introduction**

TOrCs, i.e. pharmaceuticals, enter the aquatic environment frequently through municipal or industrial wastewater and have already been detected in drinking water at  $\text{ng L}^{-1}$  levels [9, 11]. In urbanized areas in Germany the contributions of wastewater effluents to streams can in some cases be  $> 50\%$  in the summer months [126]. The *de facto* reuse of wastewater could increase the risk of introducing TOrCs into drinking water sources. Conventional water treatment processes have been reported to ineffectively remove certain TOrCs, such as hydrophilic compounds [9]. Measures that aim at further reducing the discharge of TOrCs include upgrading WWTPs with advanced treatments like ozonation or powdered activated carbon (PAC), a strategy currently pursued by Switzerland [132, 133].

PAC is commonly used for drinking water purification due to its adsorptive qualities: In batch experiments, Hernández-Leal *et al.* treated ultrapure water spiked with TOrCs of personal care products ( $20 - 1600 \mu\text{g L}^{-1}$ ) with PAC at a dose of  $1.25 \text{ g L}^{-1}$  and found the removal efficiency to be  $> 94\%$  for all compounds after 5 min of contact time [134]. Kovalova *et al.* showed that  $23 \text{ mg L}^{-1}$  of PAC (hydraulic residence time of one day) removed  $62\%$  of the load of 56 TOrCs

including pharmaceuticals, metabolites and industrial chemicals from hospital wastewater pre-treated by a membrane bioreactor. In their investigation, all compounds with a  $\log D > 2$  (pH 9) were eliminated completely or fell below the limit of quantification [135]. Adsorption capacities of polar TOrcs are expected to be lower than those of non-polar or mid-polar ones, in some cases up to one order of magnitude [136]. However, depending on the pH, some charged or zwitterionic polar compounds exhibit strong sorption, probably due to electrostatic interactions [135].

In this study, three different types of PAC at three different concentrations are assessed in batch experiments using the NTS approach. The polarity range of the analytical method is extended by coupling RPLC to HILIC in series and screening a mass window for small molecules using HRMS equipped ESI. It should be noted that this study does not provide adsorption kinetics but rather presents a non-target screening method that enables a comprehensive comparison of untreated and treated samples, explicitly considering (very) polar compounds.

### **6.3.2 Methods**

#### *6.3.2.1 Chemicals*

Ultrapure water and acetonitrile were obtained at LC-MS grade from Supelco (Darmstadt, Germany) and Honeywell (Morristown, New Jersey, U.S.A). Ammonium acetate was purchased from Sigma-Aldrich (Seelze, Germany). Information on (internal) standard compounds is given in Tables S1 and S2 of the supplementary material (Appendix B.4). The polar standard compounds for spike-in ( $\log D$  at pH 7 of 0.30 to -4.10) were obtained from Neochema (Bodenheim, Germany), handled in four stock solutions at  $10 \mu\text{g mL}^{-1}$  in methanol and stored at  $-18 \text{ }^\circ\text{C}$ . The compounds that served as internal standards were purchased from Sigma-Aldrich (Seelze Germany) and Dr. Ehrenstorfer (Augsburg, Germany). They were prepared in individual stock solutions at  $1000 \mu\text{M}$ , except for sotalol ( $586 \mu\text{M}$ ), vidarabine ( $337 \mu\text{M}$ ) and monuron ( $970 \mu\text{M}$ ). They were dissolved in acetonitrile (etilefrine, sotalol, chlortoluron and metobromuron), acetonitrile/water (50/50, v/v; 6-amino-1,3-dimethyl-5-(formylamino)uracil, vidarabine and chloridazon) or methanol (chlorbromuron, metconazol and monuron) and stored at  $4 \text{ }^\circ\text{C}$ .

#### *6.3.2.2 Samples*

For bench-scale batch sorption experiments, a surface water sample was taken from a German reservoir and filtered with a glass fiber filter (type GF 9; Schleicher & Schuell GmbH, Whatman, NH, U.S.A) The dissolved organic carbon (DOC) concentration of the sample was  $6.1 \text{ mg L}^{-1}$ , the pH 8.02 and the conductivity  $526 \mu\text{S cm}^{-1}$  at  $25 \text{ }^\circ\text{C}$ . The sample was spiked with 12 polar standard compounds at a final concentration of  $50 \mu\text{g L}^{-1}$  per compound prior to treatment. The

sample was separated into aliquots and treated with three different types of PAC (Table 4) at different concentrations. For each of the three PAC types, four 1 L-batches were prepared in beakers, adding no carbon (blank), 2 mg, 7 mg and 30 mg to the surface water sample. The batches were stirred at 250 rpm for 4 h at room temperature. Aliquots of all the batches were passed through a syringe filter (GF and 0.45  $\mu\text{m}$  cellulose acetate, Minisart NML; Sartorius, Göttingen Germany) and transferred to baked-out vials (450  $^{\circ}\text{C}$ ). Treated samples were spiked with internal standards to a final concentration of 5  $\mu\text{M}$  per compound prior to LC-MS analysis.

Table 4: The types of PAC used for the batch sorption experiments.

Laboratory name	H118	H120	H121
Commercial name	Hydraffin CCP 90 plus	Carbopal AP supra	Aquasorb MP 23 PAC-S
Manufacturer	Donau Carbon GmbH (Frankfurt am Main, Germany)	Donau Carbon GmbH	Jacobi (Frankfurt am Main, Germany)
Water content	8.1 %	1.5 %	2.0 %
Ash content	6.7 %	13.6 %	10.2 %
Contact pH	10.79	9.85	10.14
Iodine number	1088 $\text{mg g}^{-1}$	1019 $\text{mg g}^{-1}$	944 $\text{mg g}^{-1}$
Particle size distribution (wet sieving)			
<150 $\mu\text{m}$	99.1	99.1	99.7
<50 $\mu\text{m}$	72.0	88.6	70.2

### 6.3.2.3 LC-MS analysis

The LC setup consisted of a HILIC and a RPLC system coupled in series via a T-piece with a mixing frit (Upchurch, IDEX Europe GmbH, Erlangen, Germany) [96].

Each LC system (1260 Infinity series; Agilent Technologies, Waldbronn, Germany) consisted of a binary pump, an online degasser and a mixing chamber. The RP separation was carried out on a Poroshell 120 EC-C18 column (50.0  $\times$  3.0 mm, 2.7  $\mu\text{m}$ ; Agilent Technologies). The mobile phase consisted of 10 mM ammonium acetate in aqueous solution and acetonitrile at volumetric ratios of 90/10 and 10/90. For the HILIC subsystem a ZIC-HILIC column was employed (150.0  $\times$  2.1mm, 5  $\mu\text{m}$ , 200  $\text{\AA}$ ; Merck Sequant, Umeå, Sweden) and the mobile phase consisted of

acetonitrile and water. Information on the gradients can be found in previous publications [39, 116]. The injection volume was 10  $\mu\text{L}$ .

The chromatographic system was connected to an Orbitrap Exploris 120 mass spectrometer (Thermo Fisher Scientific; Waltham, MA, U.S.A) equipped with an ESI source. The source was operated at spray voltages of 3.5 and -2.5 kV in positive and negative mode, respectively. Sheath gas, auxiliary gas and sweep gas were set to 50, 8 and 0 (arbitrary units). The capillary temperature and the vaporizer temperature were set to 320 and 400  $^{\circ}\text{C}$ , respectively. In order to obtain NTS data, a mass range of 70 – 1000 Da was scanned at a resolution of 60,000 (full width at half maximum at  $m/z$  200). MS2 spectra were acquired in data-dependent acquisition mode at a resolution of 30,000 by employing a collision energy ramp of 15 – 45 eV. The four most abundant precursor ions were selected to trigger after one scan cycle and afterwards excluded for 7 s.

#### 6.3.2.4 Data analysis

The targeted analysis was performed in MZmine 2 [68]. The internal standards as well as the polar standard compounds were extracted at a mass tolerance of 3 ppm and a RT tolerance of 5 min. For further confirmation, detected MS2 spectra were compared to experimental MS2 spectra stored in the mass spectral databases MassBank [137, 138] and MassBank of North America (MoNA) [139]. For the RTs and masses of the internal standards the precision values were calculated, expressing the closeness of observed values to each other. Additionally, the mass accuracy was determined, expressing the closeness of detected masses to theoretical masses.

After a target screening for the polar standard compounds, the HMRS raw data was processed employing the NTS method described in chapter 5.4 including QC measures detailed in chapter 4.1. The samples treated with 2, 7 and 30  $\text{mg L}^{-1}$  of activated carbon were compared to the untreated sample. The processing steps along with the parameter settings and explanatory comments are listed in Table S3 of the supplementary material (Appendix B.4). The parameters were optimized as part of the study presented in Appendix A.2 on two synthetic water samples containing environmentally relevant and polar standard compounds at different concentration levels and adapted to fit the requirements of the present study (chapter 3.2).

For further statistical analysis, the fcs were calculated as the ratio of the mean signal intensities across the technical replicates in the treated and the untreated sample. For each comparison (e.g. H118, (7/0) mg) the mean fc and the standard deviation of all the features were calculated. The threshold values for signal increase and decrease of a feature after activated carbon

treatment were defined at  $\log_2(fc) > 1$  and  $\log_2(fc) < -1$ , respectively [123]. Further statistical evaluations were performed in R (version 4.0.2) [102] and RStudio (version 1.3.959) [103]. Whether the feature intensities are significantly different between the treated and the untreated sample was evaluated using Welch's t-test [140] and Benjamini-Hochberg adjustment [141] at a significance level of 0.05.

### **6.3.3 Results and discussion**

In the following, the results of the target evaluation are presented considering the internal standards and the polar standard compounds. Moreover, features extracted before and after PAC treatment are globally assessed with the objective of getting indications on removal and/or transformation/desorption of TOrcs. Therefore, fcs and multiple hypothesis tests were interpreted. Variabilities throughout the measurement sequence were evaluated based on the feature lists of all samples including pooled QC samples.

#### *6.3.3.1 Targeted evaluation*

A targeted search for the internal standards ( $n = 10$ , added prior to sample analysis) and the polar standard compounds ( $n = 10$ , added prior to PAC treatment) was performed on the ESI(+) data. The RT and mass precision as well as the mass accuracy of the RPLC-HILIC-HRMS system was evaluated on the internal standards. In positive ionization mode, the precision was better than 1.5 % for RT ( $n = 35$  injections) and better than 1.5 ppm for mass. The mass accuracy was  $< 2.1$  ppm for all compounds. One measurement (absorbent H118 at  $7 \text{ mg L}^{-1}$ , third replicate) appeared to be an outlier in the three parameters mass, RT and signal intensity, and was therefore discarded. In negative ionization mode, precision values for RT and mass were  $< 0.8$  % and 1.5 ppm, respectively. The masses of the internal standards were detected more accurately than 2.0 ppm ( $n = 36$  injections). Based on these findings, the instrumental setup performed reproducibly and accurately.

Furthermore, the consistency interval for the fcs of the signal intensities was validated on the internal standards. It was defined as  $-1.00 \leq \log_2(fc) \leq 1.00$  which corresponds to  $0.50 \leq fc \leq 2.00$  [123]. Since the internal standards were spiked into the samples after treatment and prior to analysis, the  $\log_2(fc)$  was expected to fall into the consistency interval and be close to 0. In all of the sample comparisons in positive ionization mode, all internal standards fell into the consistency interval with at least  $\pm 9$  standard deviations (see Table 5). The same was observed in negative ionization mode with at least  $\pm 8$  standard deviations (see Table S4, Appendix B.4). The polar standard compounds were spiked into the samples prior to PAC treatment. In positive ionization mode, their mean  $\log_2(fc)$  decreased with increasing PAC load and the variability of

fcs increased (Table 5). It can therefore be assumed that some of the standard compounds absorbed onto the activated carbon. Figure 12 represents the  $\log_2(\text{fc})$ -RT plots of the PAC type H121 at different concentrations (2, 7 and 30 mg L<sup>-1</sup>). The internal standards (orange circles) all fall into the consistency interval (dashed lines). The polar standard compounds (blue diamonds) eluted earlier than 15.6 min have  $\log D$  values  $\leq 0.30$  and are thus expected to be primarily retained by the HILIC column. At 2 mg L<sup>-1</sup> of PAC H121, they did not show any increase or decrease. At 7 mg L<sup>-1</sup>, a decrease in signal intensity ( $\log_2(\text{fc}) < -1$ ) was observed for famotidine and 2,4-diamino-6-(hydroxymethyl)pteridine, complemented by 2-aminopyridine and 3-pyridinemethanol at 30 mg L<sup>-1</sup>. The respective plots for PAC H118 and H120 are given in Figure S1, Appendix B.4. Only miglitol and acamprosate were detected in all measurements conducted in negative ionization mode and their fcs did not suggest any removal. Other polar standard compounds were partially filtered out during data processing.

Table 5: Means and standard deviations of  $\log_2(\text{fc})$  values for the internal standards and the polar standard compounds measured in positive ionization mode. H118, H120 and H121 are the laboratory names of the different PAC types (Table 4) which were tested for surface water treatment at three different concentrations.

	<b>H118</b>	<b>H120</b>	<b>H121</b>
<b>Internal standards</b>	n = 10	n = 10	n = 10
<b>2 mg L<sup>-1</sup></b>	0.09 ± 0.05	-0.20 ± 0.07	0.03 ± 0.04
<b>7 mg L<sup>-1</sup></b>	-0.04 ± 0.09	-0.25 ± 0.14	0.08 ± 0.04
<b>30 mg L<sup>-1</sup></b>	-0.03 ± 0.10	-0.21 ± 0.16	-0.01 ± 0.10
<b>Polar standard compounds</b>	n = 10	n = 10	n = 10
<b>2 mg L<sup>-1</sup></b>	-0.40 ± 0.49	-0.21 ± 0.49	-0.17 ± 0.22
<b>7 mg L<sup>-1</sup></b>	-1.22 ± 1.46	-0.70 ± 1.30	-0.65 ± 0.95
<b>30 mg L<sup>-1</sup></b>	-2.31 ± 2.21	-2.07 ± 2.45	-1.59 ± 1.88

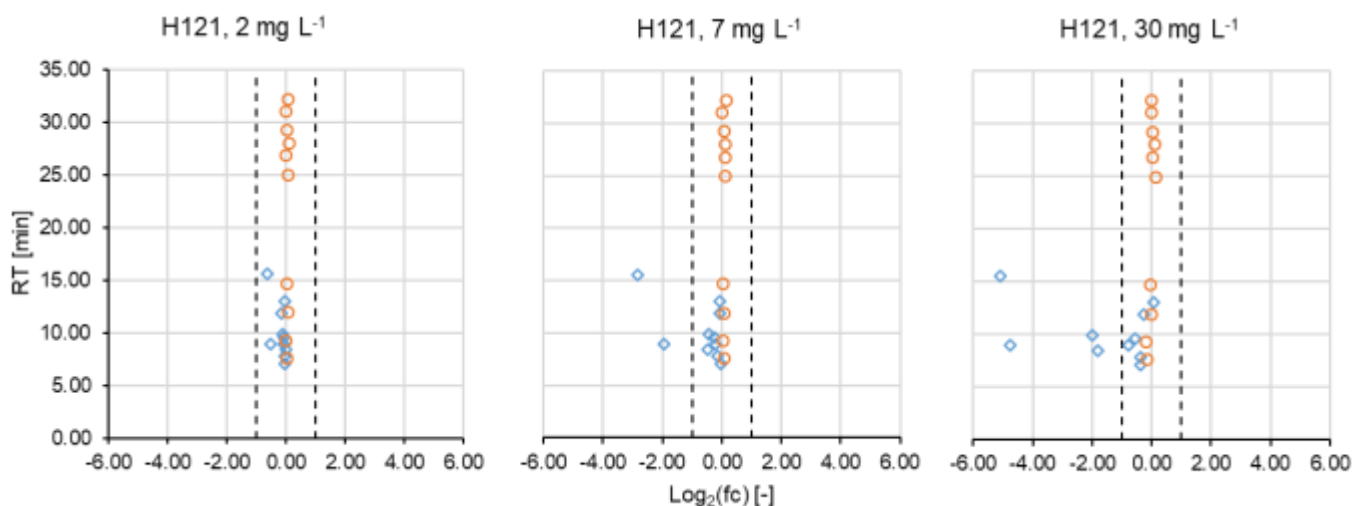


Figure 12: The base-2 logarithm of the fcs of the HILIC standards (added prior to PAC treatment, blue diamonds) and the internal standards (added prior to analysis, orange circles) are plotted versus their RTs. The dashed lines mark the consistency interval where no compound removal is assumed.

### 6.3.3.2 Non-targeted evaluation

The results of the NTS investigation were nine final feature lists for each ionization mode (three PAC types, three concentrations). For each feature list the mean  $\log_2(\text{fc})$ -value and the respective standard deviation were calculated and are listed in Table 6 for positive ionization mode and Table S5 (supplementary material Appendix B.4) for negative mode. In contrast to what was suggested by the target compounds, no general decrease in signal intensity was observed as result of PAC treatment. On the contrary, the portion of non-target features with a  $\log_2(\text{fc}) > 1$  increased at higher concentrations to a maximum of 13.4 % at 30 mg L<sup>-1</sup> of PAC H121. This result are visualized in Figure 13. The portion of predominantly HILIC-influenced features with RTs < 17 min exhibit an increase in signal intensity rather than a decrease. This could be attributed to contaminations desorbing from the PAC or, even though less likely, formation of TPs. For post-treatments with granulated activated carbon and PAC dosed onto a sand filter, formation of TPs has been observed before, possibly due to biological degradation [67, 122]. Nevertheless, variability in the gap filling results due to a noisy baseline could impair a clear distinction of consistent and increasing features. Our partner laboratory investigated the adsorption characteristics of (among others) the same PAC types under comparable experimental conditions, except they did not include a HILIC separation into their analytical platform [142]. For samples treated with 7 mg L<sup>-1</sup> PAC compared to untreated samples they found median fcs of 0.54, 0.49 and 0.69 for H118, H120 and H121, respectively. Since these

values are in or close to the defined lower limit of the consistency interval, no or little adsorption can be derived from these findings as well.

Table 6: Means and standard deviations of  $\log_2(fc)$  values for the non-target features in positive ionization mode. H118, H120 and H121 are the laboratory names of the different PAC types which were tested for surface water treatment at three different concentrations.

	<b>Number of features</b>	<b>Mean <math>\log_2(fc)</math></b>	<b>Increasing/ decreasing features [%]</b>	<b>Significant features</b>
<b>H118</b>				
2 mg L <sup>-1</sup>	2981	-0.16 ± 0.38	0.6/2.7	38
7 mg L <sup>-1</sup>	3366	-0.26 ± 0.43	0.4/5.1	0
30 mg L <sup>-1</sup>	3000	0.07 ± 0.57	4.5/2.7	13
<b>H120</b>				
2 mg L <sup>-1</sup>	2941	0.11 ± 0.39	2.1/0.8	40
7 mg L <sup>-1</sup>	2856	0.11 ± 0.39	1.7/1.2	29
30 mg L <sup>-1</sup>	3058	0.17 ± 0.42	3.0/0.7	95
<b>H121</b>				
2 mg L <sup>-1</sup>	2842	-0.04 ± 0.37	1.1/1.8	28
7 mg L <sup>-1</sup>	2886	0.17 ± 0.41	3.5/0.7	2
30 mg L <sup>-1</sup>	3099	0.36 ± 0.62	13.4/0.8	336

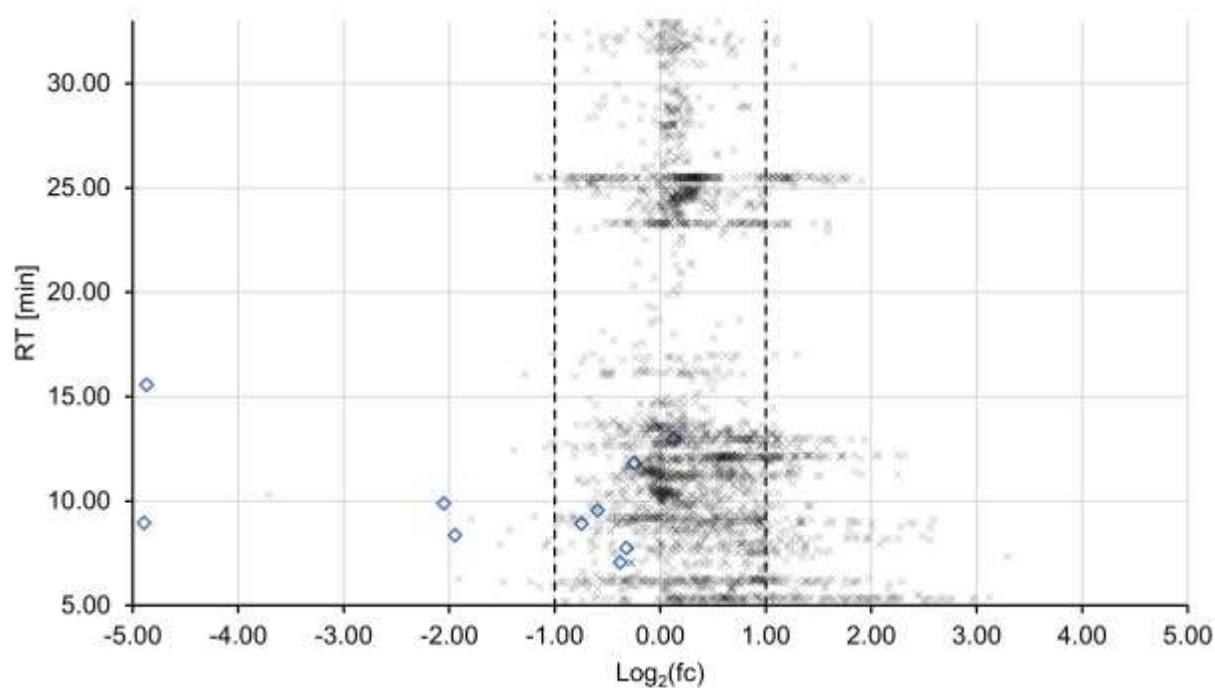


Figure 13: Non-target features (black crosses) and polar standard compounds (blue diamonds) are plotted by their base-2 logarithmic fcs and RT. The dashed lines mark the consistency interval.  $\text{Log}_2(\text{fc})$  values  $< -1$  and  $> 1$  are defined as a decrease and increase in signal intensity, respectively. Here the sample treated with  $30 \text{ mg L}^{-1}$  of PAC H121 was compared to the untreated blank sample, both measured in positive ionization mode.

### 6.3.3.3 Further statistical analysis

To figure out whether the features' signal intensities were significantly different between the untreated and the treated sample, a Welch's test was performed on signal intensities. Since the probability of wrongfully rejecting a true hypothesis increases for multiple comparisons (here around 3000 features), p-values need to be corrected [143, 144]. In this study, the Benjamini-Hochberg method for controlling the false discovery rate was applied [141]. Finally, an exemplary volcano plot for PAC H121 at a concentration of  $30 \text{ mg L}^{-1}$  was constructed and presented in Figure 14. The features' negative  $\log_{10}$ -transformed and adjusted p-values were plotted against the corresponding  $\log_2$ -transformed fcs. Features with adjusted p-values  $< 0.05$  (horizontal dashed line) and  $\log_2(\text{fc})$ -values  $< -1$  and  $\log_2(\text{fc}) > 1$  (vertical dashed lines) were considered to be of significant decrease and significant increase, respectively. Out of a total of 439 features that fell outside the consistency interval, 340 were statistically significant, of which four were annotated with standard compounds. This additional level of security substantiates the assumption that either TPs were built or compounds desorbed from the H121 PAC material. However, for PAC H118 only 13 significant features with decreasing or increasing feature intensities were detected (Table 6), even though the PCA suggested otherwise. Features with

signal intensities close to the limit of detection as well as background signals deconvoluted by the gap filling algorithm, tend to introduce variability into the data. Since the standard error factors into the denominator of the t-statistic, the t-value decreases and the degrees of freedom increase which leads to higher p-values. For this reason, fcs need to be considered as a criterion besides significance testing.

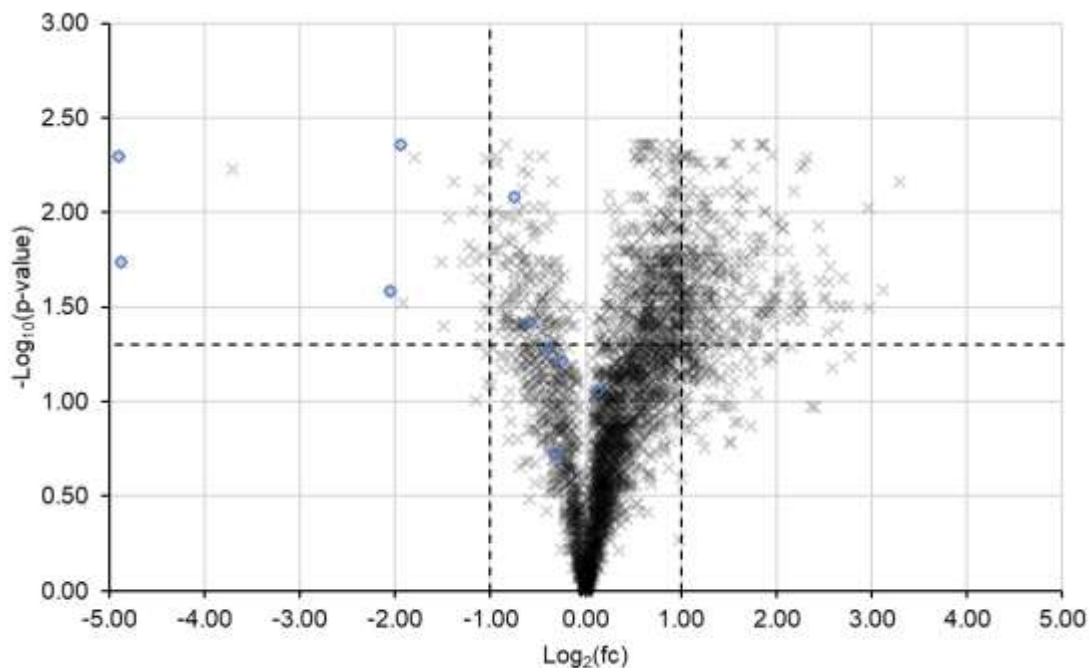


Figure 14: The volcano plot depicts features extracted during the comparative analysis of the sample treated with PAC type H121 at  $30 \text{ mg L}^{-1}$  and the respective blank sample. The horizontal dashed line marks the cut-off p-value of  $-\log_{10}(0.05)$  and the vertical dashed lines the consistency interval. Features which were annotated with polar standard compounds are marked with blue diamonds.

### 6.3.4 Conclusions

NTS was carried out in order to evaluate the treatment of surface water samples with PAC. A target screening in ESI(+) mode of the polar standard compounds, spiked into the samples prior to PAC treatment, indicated the reduction of famotidine, 2,4-diamino-6-(hydroxymethyl)pteridine, 2-aminopyridine and 3-pyridinemethanol. No reduction was observed for 4-(2-hydroxyethyl)morpholine when treated with PAC H120 in contrast to PAC types H118 and H121. 2,2,6,6-tetramethyl-4-piperidone was only reduced by PAC H118. According to criteria defined within this study, PAC treatment did not affect 1,3-dimethyl-2-imidazolidinone, ectoine, miglitol and N,N'-ethylenebisacetamide.

Non-target screening data was evaluated using fcs, principal component analysis and multiple hypothesis testing. Derived from the results, features exhibit repeatable peak heights across technical replicates, however, the run order appeared to introduce some variability throughout

the sequence of measurements. The mean fcs of non-target features fall into the consistency interval, overall suggesting no removal or occurrence of compounds due to transformation or desorption. However, the variability increases with PAC concentration indicating removal or transformation/desorption of individual compounds. The fraction of features with increasing signal intensities ( $fc > 2.00$ ) was elevated at the highest tested PAC concentration of  $30 \text{ mg L}^{-1}$  with up to 13 % and the highest number of significant features (based on differences in their signal intensities) observed for PAC type H121.

Different types and concentrations of PAC for treating real samples were assessed by comparing the molecular fingerprints with a particular focus on polar features. In this aspect, hypothesis 4 can be accepted as it is applicable to an investigation subjected to a research objective other than compound identification.

For future references, the priority features (showing significant increase or decrease in feature intensities) could be identified and their (eco)toxicological relevance assessed.

## 7. Conclusion and final discussion

This thesis strived to develop a methodological concept for the non-targeted analysis of TOrcs in water, with special focus on polar and very polar compounds.

The method needs to meet certain criteria and thus four research hypotheses were formulated and tested by tackling specific tasks derived from the hypotheses (compare chapter 2).

The first hypothesis can be accepted as the input parameters of the polarity-extended NTS method can be optimized to widen the scope of detectable compounds. What is more, facing multiple parameters and having to satisfy several requirements (i.e. increase sensitivity, decrease the false positive and false negative rates), poses a classical optimization problem. DoE offers the possibility of strategically managing several input and response variables. Firstly, DoE was employed to optimize six instrumental parameters of an ESI source for non-targeted LC-HRMS analysis. This approach has been reported before, however, the response variables are often limited to maximizing the signal intensity of one or two substances [91, 92, 145]. Even though time-consuming, this might be sufficient for developing a targeted and/or quantitative LC-MS method. Since in an NTS measurement a broad range of molecules is supposed to be detected, the study presented in chapter 3.1 optimized the signal intensities of 30 model substances. To ensure sensitive analysis of highly polar TOrcs retained by the polarity-extended chromatographic setup, model substances with  $\log D$  values down to -5.42 (moroxydine at pH 7) were included. Considering the complexity of setting NTS data processing, the DoE approach was applied extracting features from HRMS raw data as well (Appendix A.1). A similar approach has been published in the field of environmental analysis by Hu *et al.* [95] who maximized the recovery of target compounds spiked into synthetic samples. However, the presented method does not reflect the false negative rate. Moreover, there might be other compounds present in the sample besides the spiked-in target substances. The fact that the true composition of a sample is unknown to the analyst poses a general problem in NTS investigations, and is discussed in sections below. The authors of the study presented as part of this theses, defined numerical descriptors as response variables for DoE that were based on actually observed non-target features. These descriptors give indications on the quality of componentization of peaks as well as missed and wrongfully detected peaks and artefacts. Finally, the accuracy of the recursive algorithm to improve the overall quality of extracted features (chapter 4.4) was assessed. Nevertheless, study designs and constraints vary from case to case and need to be adapted for DoE optimization as becomes evident in this thesis.

Hypothesis 2 dealt with controlling and assuring the quality of the instrumental as well as the data processing method. Monitoring the robust and accurate operation of the analytical platform

is well-established and a prerequisite also for NTS. The system's suitability can be assessed based on external and internal standards and blank samples. Measuring pooled QC samples in combination with subsequent PCA allowed to check for inter- and intra-sample variability. Besides the representative matrix, all of the detectable non-target features are considered rather than a limited number of pre-selected standard compounds which renders this QC method suitable for NTS [78, 79]. Hypothesis 2 can be accepted with some reservations concerning the QC for data analysis. A feature list containing only true positives would comply with the highest theoretical quality. This standard can only be approximated since the actual false positive and false negative rates in NTS are unknown to the investigator. Apart from well-established filtering steps [70, 71] (chapter 4.2), the author would suggest tracking standard compounds (internal or in synthetic samples) throughout the data processing workflow and performing recursive target searches to decrease the false negative rate.

A general data analysis workflow including peak picking, alignment, deconvolution, background comparison and componentization was found to be applicable to multiple study designs. Having a more or less universal starting point might lower the barrier for new researchers to enter the NTS field. Nevertheless, as discussed in chapter 5.1, the order of processing steps, algorithms and parameters and finally results differ considerably between different software tools [112]. Further individual processing is required for the different objectives overarching every NTS investigation of environmental water samples. Of those, two can be generally identified in this thesis:

- Suggesting relevant polar, organic, and small candidate molecules detected in environmental real samples for validation via reference material.
- Comparative analysis of the molecular fingerprint of samples in order to evaluate a water treatment process.

For the first NTS objective, the RPLC-HILIC chromatographic setup used throughout this thesis allowed for a polarity-dependent extraction of non-target features. The differentiation can be picked up by compound databases STOFF-IDENT [73] storing physico-chemical information (log *D*, RTI score) on compounds. Another crucial aspect of the STOFF-IDENT was the fact that it specializes in environmentally relevant TOxCs of anthropogenic origin and by this means streamlines the feature annotation process as it confines the chemical space. Similarly, Schymanski *et al.* distilled the PubChem database [146] down to a selection of compounds stored in the PubChemLite [147] (compare also Appendix A.3).

Special attention must be paid to the clean-up process of extracted features lists when attempting to globally assess the molecular fingerprint of a sample (compare chapter 5.4).

Reducing the amount of artefacts, redundant and missed peaks to a minimum is beneficial to subsequent statistical interpretation of the data. In conclusion, hypothesis 3 can only be partially accepted since the rudimentary core workflow needs considerable adjustments depending on the software tool and its implemented algorithms and parameters as well as the research objective.

The analytical method developed under hypotheses 1 – 3 was finally applied on real environmental water samples. As a result, 46 non-target features detected in 33 samples taken from the Isar river and were allocated with 64 candidate compounds. Melamine (InChI key JDSHMPZPIAZGSV-UHFFFAOYSA-N,  $\log D$  at pH 7 of -2.0), guanylurea (BKMMTJMQCTUHRP-UHFFFAOYSA-N, -2.1) and the solvent 1,3-dimethylimidazolidin-2-one (CYSGHNMQYZDMIA-UHFFFAOYSA-N, -0.6) were exemplarily confirmed with reference material (Appendix A.1).

4-hydroxy-2,2,6,6-tetramethylpiperidine-1-ethanol (STEYNUVPFMIUOY-UHFFFAOYSA-N, -2.62) is an especially concerning TOxC which was identified by our group in the Danube river basin as part of the fourth Joint Danube survey [66]. It was detected at 47 out of a total of 51 sampling locations. It is acutely harmful to aquatic organisms [131] and was assigned the highest scores for persistence in surface and ground waters as well as mobility [23].

According to the results presented for the evaluation of PAC treatment (chapter 6.3) half of the highly polar standard compounds ( $\log D < 0.30$  at pH 7) adsorbed onto the PAC, possibly due to electrostatic interactions [135]. However, more and quantitative data is necessary to substantiate these findings. NTS results suggest that either compounds were transformed or desorbed from the PAC material. It should be noted, that the results could be affected by the feature extraction and data clean-up process, especially the gap filling step.

Concluding from these applications, hypothesis 4 can be accepted since the analytical method presented in this thesis, was successfully applied to real surface water samples. It (tentatively) identified polar, organic and small compounds in samples of the Isar and the Danube rivers and gave indications on the treatment effectiveness when considering features of an extended polarity range.

## 8. Outlook

As NTS evolved from the trial phase to complement monitoring activities, parameter optimization and QC must be part of a comprehensive data processing phase. Developers have picked up on that by integrating automated parameter optimization into analytical workflows, like patRoön with IPO [106, 148] or SLAW [149]. The matter was also discussed in the literature study presented in Appendix A.3. Further efforts are required when defining response variables for NTS to base the optimization on since the true sample composition is unknown to the investigator. Using internal or external compounds as reference points might be an obvious choice, however, covering the entire chemical space seems unfeasible [79]. As a consequence, more work could be invested in designing synthetic samples as were discussed in chapter 3.2. Artificial matrices, ultra-pure chemicals and a large set of carefully chosen standard compounds at different concentrations, could serve as a more universal and clearly defined model sample to build the NTS workflow on.

The review in Appendix A.3 discusses regions of interest – multivariate curve resolution as an alternative feature extraction method that might gain relevance in the future.

Besides accurate mass, RT can serve as evidence for compound annotation. It can be connected to the physico-chemical properties of a candidate compound by means of a compound database. The matter is also reviewed in more detail in Appendix A.3. It facilitates the prioritization of relevant features and enables the (tentative) identification of highly polar compounds.

To improve the reproducibility of NTS studies general instructions are helpful, especially to users outside of the research community [65]. To further remedy the problem, transparency could be promoted through good reporting practice which as of now, mainly entails communicating the confidence in feature identification *via* the Schymanski system [82]. More recently the reporting tool BP4NTA was developed to guide researches, reviewers and editors through NTS studies [150].

Finally, trend analyses and two-sample comparisons based on NTS data might benefit from quantitative data. The group of Anneli Krüve presented a quantification without reference standards based on ionization efficiency [151] which is presented in the review article in Appendix A.3.

## 9. List of further research contributions

### 9.1 Other articles

- Minkus S, Bieber S, Moser S, Letzel T (2020) Optimization of electrospray ionization parameters in an RPLC-HILIC-MS/MS coupling by design of experiment. AFIN-TS Forum March:1–17.
- Minkus S, Bieber S, Letzel T (2021) Polarity-extended non-target screening using RPLC-HILIC-ESI-QToF-MS/MS and tailor-made data handling. In: Liška I, Wagner F, Sengl M, Deutch K, Slobodnik J, Paunović M (eds) Joint Danube Survey 4 Scientific Report: A Shared Analysis of the Danube River. International Commission for the Protection of the Danube River, Vienna, pp 363–372.
- Bieber S, Minkus S, Letzel T (2022) Non-Target-Screening im Routinebetrieb: Analytik von „unbekannten“ persistenten und (sehr) polaren Substanzen in wässrigen Proben, chrom+food forum 06, pp 34-36
- Minkus S, Bieber S, Letzel T (2021) In-silico modelling of a gas chromatographic method for thirteen pesticides. AFIN-TS Forum. January(4):1-18. <https://afin-ts.de/programm/afin-ts-forum-2021-jan4/>

### 9.2 Oral presentations

- Minkus S, Bieber S, Letzel T (2021) Hidden-target screening of the Danube river basin employing polarity-extended chromatography and high-resolution mass spectrometry. Testing the Waters 5 conference
- Minkus S, Bieber S, Letzel T (2021) Serial coupling of two liquid chromatography systems for polarity-extended non-target screening. 12th Multidimensional Chromatography Virtual Workshop
- Minkus S, Bieber S, Moser S, Letzel T (2020) Using statistical design of experiment to optimize complex analytical workflows. 14th Interdisciplinary Ph.D. Seminar of the working group process analytics (GDCh)

### 9.3 Poster presentations

- Minkus S, Bieber S, Letzel T (2021) Flexible feature extraction data processing workflow as part of a non-target screening strategy for (very) polar small molecules. ICNTS21

- 
- Minkus S, Bieber S, Letzel T (2021) Flexible feature extraction data processing workflow as part of a non-target screening strategy for (very) polar small molecules. Langenauer Wasserforum
  - Bieber S, Minkus S, Letzel T (2021) Sample preparation of salty aqueous samples for non-target screening analysis. Langenauer Wasserforum
  - Minkus S, Bieber S, Letzel T (2020) A mass spectrometric non-target screening workflow using the FOR-IDENT platform and the compound database STOFF-IDENT for very polar compound recognition in the aqueous environment. Analytica Conference
  - Minkus S (202) A mass spectrometric non-targeted workflow using a compound database for very polar compound recognition in the aqueous environment. Doctoral Candidates' Day of the Department Graduate Center of Civil, Geo and Environmental Engineering (TUM)
  - Minkus S, Kaufmann C, Graßmann J, Letzel T (2019) The open source e-learning platform "Analytics+": An essential training in analytical chemistry. Langenauer Wasserforum
  - Minkus S, Kaufmann C, Graßmann J, Letzel T (2019) The open source e-learning platform "Analytics+": An essential training in analytical chemistry. ANAKON

## 10. References

1. UNESCO World Water Assessment Programme (2021) The United Nations world water development report 2021: valuing water. Paris
2. Burek P, Satoh Y, Fischer G, Kahil, M.T. Scherzer, A. Tramberend, S. Nava LF, Wada Y, Eisner Y, Flörke M, Hanasaki N, Magnuszewski, P. Cosgrove, B. Wiberg D (2016) Water Futures and Solution - Fast Track Initiative (Final Report). Laxenburg, Austria
3. Carson R (1962) *Silent Spring*. Houghton Mifflin Company, Boston
4. Schwarzenbach RP, Escher BI, Fenner K, Hofstetter TB, Johnson CA, von Gunten U, Wherli B (2006) The Challenge of Micropollutants in Aquatic Systems. *Science* (80- ) 313:1072–1077.
5. Heberer T (2002) Tracking persistent pharmaceutical residues from municipal sewage to drinking water. *J Hydrol* 266:175–189. [https://doi.org/10.1016/S0022-1694\(02\)00165-8](https://doi.org/10.1016/S0022-1694(02)00165-8)
6. Koplín D, Furlong E, Meyer MT, Thurman EM, Zaugg S, Barber L, Buxton H (2002) Pharmaceuticals, hormones, and other organic wastewater contaminants in U.S. streams, 1999-2000: a national reconnaissance. *Environ Sci Technol* 36:1202–1211. <https://doi.org/10.1021/es0200903>
7. Heberer T, Feldmann D (2005) Contribution of effluents from hospitals and private households to the total loads of diclofenac and carbamazepine in municipal sewage effluents—modeling versus measurements. *J Hazard Mater* 122:211–218. <https://doi.org/10.1016/j.jhazmat.2005.03.007>
8. Tian Z, Wark DA, Bogue K, James CA (2021) Suspect and non-target screening of contaminants of emerging concern in streams in agricultural watersheds. *Sci Total Environ* 795:148826. <https://doi.org/10.1016/j.scitotenv.2021.148826>
9. Luo Y, Guo W, Ngo HH, Nghiem LD, Hai FI, Zhang J, Liang S, Wang XC (2014) A review on the occurrence of micropollutants in the aquatic environment and their fate and removal during wastewater treatment. *Sci Total Environ* 473–474:619–641. <https://doi.org/10.1016/j.scitotenv.2013.12.065>
10. Lapworth DJ, Baran N, Stuart ME, Ward RS (2012) Emerging organic contaminants in groundwater: A review of sources, fate and occurrence. *Environ Pollut* 163:287–303. <https://doi.org/10.1016/j.envpol.2011.12.034>
11. Mompelat S, Le Bot B, Thomas O (2009) Occurrence and fate of pharmaceutical products and by-products, from resource to drinking water. *Environ Int* 35:803–814. <https://doi.org/10.1016/j.envint.2008.10.008>
12. Glüge J, Scheringer M, Cousins IT, Dewitt JC, Goldenman G, Herzke D, Lohmann R, Ng CA, Trier X, Wang Z (2020) An overview of the uses of per- And polyfluoroalkyl substances (PFAS). *Environ Sci Process Impacts* 22:2345–2373. <https://doi.org/10.1039/d0em00291g>
13. Andrews DQ, Naidenko O V. (2020) Population-Wide Exposure to Per- And Polyfluoroalkyl Substances from Drinking Water in the United States. *Environ Sci Technol Lett* 7:931–936. <https://doi.org/10.1021/acs.estlett.0c00713>

14. Richardson SD, Ternes TA (2021) Water Analysis: Emerging Contaminants and Current Issues. *Anal Chem.* <https://doi.org/10.1021/acs.analchem.1c04640>
15. Bolong N, Ismail AF, Salim MR, Matsuura T (2009) A review of the effects of emerging contaminants in wastewater and options for their removal. *Desalination* 239:229–246. <https://doi.org/10.1016/j.desal.2008.03.020>
16. Willi RA, Salgueiro-González N, Carcaiso G, Fent K (2019) Glucocorticoid mixtures of fluticasone propionate, triamcinolone acetonide and clobetasol propionate induce additive effects in zebrafish embryos. *J Hazard Mater* 374:101–109. <https://doi.org/10.1016/j.jhazmat.2019.04.023>
17. Faltermann S, Hettich T, Küng N, Fent K (2020) Effects of the glucocorticoid clobetasol propionate and its mixture with cortisol and different class steroids in adult female zebrafish. *Aquat Toxicol* 218:<https://doi.org/10.1016/j.aquatox.2019.105372>
18. Joffe M (2001) Are problems with male reproductive health caused by endocrine disruption? *Occup Environ Med* 58:281–288. <https://doi.org/10.1136/oem.58.4.281>
19. Reemtsma T, Berger U, Arp HPH, Gallard H, Knepper TP, Neumann M, Quintana JB, Voogt P De (2016) Mind the Gap: Persistent and Mobile Organic Compounds - Water Contaminants That Slip Through. *Environ Sci Technol* 50:10308–10315. <https://doi.org/10.1021/acs.est.6b03338>
20. German Environment Agency (UBA) (2019) Protecting the sources of our drinking water - The criteria for identifying Persistent, Mobile, and Toxic (PMT) substances and very Persistent, and very Mobile (vPvM) substances under EU REACH Regulation (EC) No 1907/ 2006
21. Kalberlah F, Oltmanns J, Schwarz M, Baumeister J, Striffler A (2014) Guidance for the precautionary protection of raw water destined for drinking water extraction from contaminants regulated under REACH, Project (UFOPLAN) FKZ 371265416, German Federal Ministry for the Environment, Building and Nuclear Safety
22. Goss K-U, Schwarzenbach RP (2001) Linear Free Energy Relationships Used To Evaluate Equilibrium Partitioning of Organic Compounds. 35:1–9. <https://doi.org/10.1021/es000996d>
23. Arp HPH, Brown TN, Berger U, Hale SE (2017) Ranking REACH registered neutral, ionizable and ionic organic chemicals based on their aquatic persistency and mobility. *Environ Sci Process Impacts* 19:939–955. <https://doi.org/10.1039/c7em00158d>
24. Schulze S, Sättler D, Neumann M, Arp HPH (2018) Using REACH registration data to rank the environmental emission potential of persistent and mobile organic chemicals. *Sci Total Environ* 625:1122–1128. <https://doi.org/https://doi.org/10.1016/j.scitotenv.2017.12.305>
25. Reemtsma T, Weiss S, Mueller J, Petrovic M, Gonzalez S, Barcelo D, Francesc V, Knepper TP (2006) Polar Pollutants Entry into the Water Cycle by Municipal Wastewater : A European Perspective. *Environ Sci Technol* 40:5451–5458. <https://doi.org/10.1021/es060908a>
26. Boxall A, Sinclair C, Fenner K, Koplín D, Maund S (2004) When synthetic chemicals degrade in the environment. *Environ Sci Technol* 38:368–375. <https://doi.org/10.1117/1.3589100>
27. Zahn D, Neuwald IJ, Knepper TP (2020) Analysis of mobile chemicals in the aquatic

- environment—current capabilities, limitations and future perspectives. *Anal Bioanal Chem* 412:4763–4784. <https://doi.org/10.1007/s00216-020-02520-z>
28. Scheurer M, Michel A, Brauch HJ, Ruck W, Sacher F (2012) Occurrence and fate of the antidiabetic drug metformin and its metabolite guanlyurea in the environment and during drinking water treatment. *Water Res* 46:4790–4802. <https://doi.org/10.1016/j.watres.2012.06.019>
  29. Caldwell DJ, D'Aco V, Davidson T, Kappler K, Murray-Smith RJ, Owen SF, Robinson PF, Simon-Hettich B, Straub JO, Tell J (2019) Environmental risk assessment of metformin and its transformation product guanlyurea: II. Occurrence in surface waters of Europe and the United States and derivation of predicted no-effect concentrations. *Chemosphere* 216:855–865. <https://doi.org/10.1016/j.chemosphere.2018.10.038>
  30. Scheurer M, Nödler K, Freeling F, Janda J, Happel O, Riegel M, Müller U, Storck FR, Fleig M, Lange FT, Brunsch A, Brauch HJ (2017) Small, mobile, persistent: Trifluoroacetate in the water cycle – Overlooked sources, pathways, and consequences for drinking water supply. *Water Res* 126:460–471. <https://doi.org/10.1016/j.watres.2017.09.045>
  31. Rüdell H, Körner W, Letzel T, Neumann M, Nödler K, Reemtsma T (2020) Persistent, mobile and toxic substances in the environment: a spotlight on current research and regulatory activities. *Environ Sci Eur* 32:<https://doi.org/10.1186/s12302-019-0286-x>
  32. Layne J (2002) Characterization and comparison of the chromatographic performance of conventional, polar-embedded, and polar-endcapped reversed-phase liquid chromatography stationary phases. *J Chromatogr A* 957:149–164. [https://doi.org/10.1016/S0021-9673\(02\)00193-0](https://doi.org/10.1016/S0021-9673(02)00193-0)
  33. Alpert AJ (1990) Hydrophilic-interaction chromatography for the separation of peptides, nucleic acids and other polar compounds. *J Chromatogr A* 499:177–196. [https://doi.org/10.1016/S0021-9673\(00\)96972-3](https://doi.org/10.1016/S0021-9673(00)96972-3)
  34. Nguyen HP, Schug KA (2008) The advantages of ESI-MS detection in conjunction with HILIC mode separations: Fundamentals and applications. *J Sep Sci* 31:1465–1480. <https://doi.org/10.1002/jssc.200700630>
  35. Berthod A, Chang SSC, Kullman JPS, Armstrong DW (1998) Practice and mechanism of HPLC oligosaccharide separation with a cyclodextrin bonded phase. *Talanta* 47:1001–1012. [https://doi.org/10.1016/S0039-9140\(98\)00179-9](https://doi.org/10.1016/S0039-9140(98)00179-9)
  36. McCalley D V. (2010) Study of the selectivity, retention mechanisms and performance of alternative silica-based stationary phases for separation of ionised solutes in hydrophilic interaction chromatography. *J Chromatogr A* 1217:3408–3417. <https://doi.org/10.1016/j.chroma.2010.03.011>
  37. Dinh NP, Jonsson T, Irgum K (2011) Probing the interaction mode in hydrophilic interaction chromatography. *J Chromatogr A* 1218:5880–5891. <https://doi.org/10.1016/j.chroma.2011.06.037>
  38. Chirita RI, West C, Finaru AL, Elfakir C (2010) Approach to hydrophilic interaction chromatography column selection: Application to neurotransmitters analysis. *J Chromatogr A* 1217:3091–3104. <https://doi.org/10.1016/j.chroma.2010.03.001>
  39. Bieber S, Greco G, Grosse S, Letzel T (2017) RPLC-HILIC and SFC with Mass Spectrometry: Polarity-Extended Organic Molecule Screening in Environmental (Water)

- Samples. *Anal Chem* 89:7907–7914. <https://doi.org/10.1021/acs.analchem.7b00859>
40. Haddad PR, Nesterenko PN, Buchberger W (2008) Recent developments and emerging directions in ion chromatography. *J Chromatogr A* 1184:456–473. <https://doi.org/10.1016/j.chroma.2007.10.022>
  41. Krauss M, Singer H, Hollender J (2010) LC-high resolution MS in environmental analysis: From target screening to the identification of unknowns. *Anal Bioanal Chem* 397:943–951. <https://doi.org/10.1007/s00216-010-3608-9>
  42. Makarov A, Denisov E, Kholomeev A, Balschun W, Lange O, Strupat K, Horning S (2006) Performance evaluation of a hybrid linear ion trap/orbitrap mass spectrometer. *Anal Chem* 78:2113–2120. <https://doi.org/10.1021/ac0518811>
  43. Hu Q, Noll RJ, Li H, Makarov A, Hardman M, Cooks RG (2005) The Orbitrap: A new mass spectrometer. *J Mass Spectrom* 40:430–443. <https://doi.org/10.1002/jms.856>
  44. Petrovic M, Barceló D (2006) Application of liquid chromatography/quadrupole time-of-flight mass spectrometry (LC-QqTOF-MS) in the environmental analysis. *J Mass Spectrom* 41:1259–1267. <https://doi.org/10.1002/jms.1103>
  45. Chernushevich I V., Loboda A V., Thomson BA (2001) An introduction to quadrupole-time-of-flight mass spectrometry. *J Mass Spectrom* 36:849–865. <https://doi.org/10.1002/jms.207>
  46. Sandhu C, Hewel JA, Badis G, Talukder S, Liu J, Hughes TR, Emili A (2008) Evaluation of data-dependent versus targeted shotgun proteomic approaches for monitoring transcription factor expression in breast cancer. *J Proteome Res* 7:1529–1541. <https://doi.org/10.1021/pr700836q>
  47. Hilaire PB Saint, Rousseau K, Seyer A, Dechaumet S, Damont A, Junot C, Fenaille F (2020) Comparative evaluation of data dependent and data independent acquisition workflows implemented on an orbitrap fusion for untargeted metabolomics. *Metabolites* 10:<https://doi.org/10.3390/metabo10040158>
  48. Gillet LC, Navarro P, Tate S, Röst H, Selevsek N, Reiter L, Bonner R, Aebersold R (2012) Targeted data extraction of the MS/MS spectra generated by data-independent acquisition: A new concept for consistent and accurate proteome analysis. *Mol Cell Proteomics* 11:1–17. <https://doi.org/10.1074/mcp.O111.016717>
  49. Kern S, Fenner K, Singer HP, Schwarzenbach RP, Hollender J (2009) Identification of transformation products of organic contaminants in natural waters by computer-aided prediction and high-resolution mass spectrometry. *Environ Sci Technol* 43:7039–7046. <https://doi.org/10.1021/es901979h>
  50. Anumol T, Lehotay SJ, Stevens J, Zweigenbaum J (2017) Comparison of veterinary drug residue results in animal tissues by ultrahigh-performance liquid chromatography coupled to triple quadrupole or quadrupole–time-of-flight tandem mass spectrometry after different sample preparation methods, including use of . *Anal Bioanal Chem* 409:2639–2653. <https://doi.org/10.1007/s00216-017-0208-y>
  51. Cavaliere C, Antonelli M, Capriotti AL, La Barbera G, Montone CM, Piovesana S, Laganà A (2019) A Triple Quadrupole and a Hybrid Quadrupole Orbitrap Mass Spectrometer in Comparison for Polyphenol Quantitation. *J Agric Food Chem* 67:4885–4896. <https://doi.org/10.1021/acs.jafc.8b07163>
  52. Gago-Ferrero P, Bletsou AA, Damalas DE, Aalizadeh R, Alygizakis NA, Singer HP,

- Hollender J, Thomaidis NS (2020) Wide-scope target screening of >2000 emerging contaminants in wastewater samples with UPLC-Q-ToF-HRMS/MS and smart evaluation of its performance through the validation of 195 selected representative analytes. *J Hazard Mater* 387:121712. <https://doi.org/10.1016/j.jhazmat.2019.121712>
53. Karas M, Hillenkamp F (1988) Laser Desorption Ionization of Proteins with Molecular Masses Exceeding 10 000 Daltons. *Anal Chem* 60:2299–2301. <https://doi.org/10.1021/ac00171a028>
  54. Knochenmuss R (2006) Ion formation mechanisms in UV-MALDI. *Analyst* 131:966–986. <https://doi.org/10.1039/b605646f>
  55. Robb DB, Covey TR, Bruins AP (2000) Atmospheric pressure photoionization: An ionization method for liquid chromatography-mass spectrometry. *Anal Chem* 72:3653–3659. <https://doi.org/10.1021/ac0001636>
  56. Fenn JB, Mann M, Meng CKAI, Wong SF, Whitehouse CM (1989) Electrospray Ionization for Mass Spectrometry of Large Biomolecules. *Science* (80- ) 246:64–71.
  57. Van Berkel GJ, Kertesz V (2007) Using the electrochemistry of the electrospray ion source. *Anal Chem* 79:5510–5520. <https://doi.org/10.1021/ac071944a>
  58. Konermann L, Ahadi E, Rodriguez AD, Vahidi S (2013) Unraveling the mechanism of electrospray ionization. *Anal Chem* 85:2–9. <https://doi.org/10.1021/ac302789c>
  59. Kebarle P, Verkerk UH (2009) Electrospray: From ions in solution to ions in the gas phase, what we know now. *Mass Spectrom Rev* 28:898–917. <https://doi.org/10.1002/mas>
  60. Iribarne J V., Thomson BA (1976) On the evaporation of small ions from charged droplets. *J Chem Phys* 64:2287–2294. <https://doi.org/10.1063/1.432536>
  61. Laaniste A, Leito I, Kruve A (2019) ESI outcompetes other ion sources in LC/MS trace analysis. *Anal Bioanal Chem* 411:3533–3542. <https://doi.org/10.1007/s00216-019-01832-z>
  62. Oss M, Kruve A, Herodes K, Leito I (2010) Electrospray ionization efficiency scale of organic compound. *Anal Chem* 82:2865–2872. <https://doi.org/10.1021/ac902856t>
  63. Cech NB, Enke CG (2001) Practical implications of some recent studies in electrospray ionization fundamentals. *Mass Spectrom Rev* 20:362–387. <https://doi.org/10.1002/mas.10008>
  64. Hernández F, Pozo JÓ, Sancho J V, López FJ, Harín JM, Ibáñez M (2005) Strategies for quantification and confirmation of multi-class polar pesticides and transformation products in water by LC – MS 2 using triple quadrupole and hybrid quadrupole time-of-flight analyzers. *Trends Anal Chem* 24:596–612. <https://doi.org/10.1016/j.trac.2005.04.007>
  65. “Non-Target Screening” expert committee of the German Water Chemistry Society (2019) Use of non-target screening by means of LC-ESI-HRMS in water analysis
  66. Liška I, Wagner F, Sengl M, Deutch K, Slobodnik J, Paunović M (Eds) (2021) Joint Danube Survey 4 Scientific Report: A Shared Analysis of the Danube River. International Commission for the Protection of the Danube River, Vienna
  67. Schollée JE, Hollender J, McArdell CS (2021) Characterization of advanced wastewater treatment with ozone and activated carbon using LC-HRMS based non-target screening with automated trend assignment. *Water Res* 200:<https://doi.org/10.1016/j.watres.2021.117209>

68. Pluskal T, Castillo S, Villar-Briones A, Orešič M (2010) MZmine 2: Modular framework for processing, visualizing, and analyzing mass spectrometry-based molecular profile data. *BMC Bioinformatics* 11:<https://doi.org/10.1186/1471-2105-11-395>
69. Smith CA, Want EJ, O'Maille G, Abagyan R, Siuzdak G (2006) XCMS: Processing mass spectrometry data for metabolite profiling using nonlinear peak alignment, matching, and identification. *Anal Chem* 78:779–787. <https://doi.org/10.1021/ac051437y>
70. Schollée JE, Schymanski EL, Hollender J (2016) Statistical Approaches for LC-HRMS Data to Characterize, Prioritize, and Identify Transformation Products from Water Treatment Processes. In: *ACS Symposium Series*. pp 45–65
71. Letzel T, Drewes JE (2016) Holistic and detailed view on workflow strategies applied in this book. In: *ACS Symposium Series*. pp 175–181
72. Little JL, Williams AJ, Pshenichnov A, Tkachenko V (2012) Identification of “known unknowns” utilizing accurate mass data and chemspider. *J Am Soc Mass Spectrom* 23:179–185. <https://doi.org/10.1007/s13361-011-0265-y>
73. Letzel T, Bayer A, Schulz W, Heermann A, Lucke T, Greco G, Grosse S, Schüssler W, Sengl M, Letzel M (2015) LC – MS screening techniques for wastewater analysis and analytical data handling strategies : Sartans and their transformation products as an example. *Chemosphere* 137:198–206. <https://doi.org/10.1016/j.chemosphere.2015.06.083>
74. Müller A, Schulz W, Ruck WKL, Weber WH (2011) A new approach to data evaluation in the non-target screening of organic trace substances in water analysis. *Chemosphere* 85:1211–1219. <https://doi.org/10.1016/j.chemosphere.2011.07.009>
75. Zonja B, Delgado A, Pérez S, Barceló D (2015) LC-HRMS suspect screening for detection-based prioritization of iodinated contrast media photodegradates in surface waters. *Environ Sci Technol* 49:3464–3472. <https://doi.org/10.1021/es505250q>
76. Merel S, Anumol T, Park M, Snyder SA (2015) Application of surrogates, indicators, and high-resolution mass spectrometry to evaluate the efficacy of UV processes for attenuation of emerging contaminants in water. *J Hazard Mater* 282:75–85. <https://doi.org/10.1016/j.jhazmat.2014.09.008>
77. Nürenberg G, Schulz M, Kunkel U, Ternes TA (2015) Development and validation of a generic nontarget method based on liquid chromatography - high resolution mass spectrometry analysis for the evaluation of different wastewater treatment options. *J Chromatogr A* 1426:77–90. <https://doi.org/10.1016/j.chroma.2015.11.014>
78. Broadhurst D, Goodacre R, Reinke SN, Kuligowski J, Wilson ID, Lewis MR, Dunn WB (2018) Guidelines and considerations for the use of system suitability and quality control samples in mass spectrometry assays applied in untargeted clinical metabolomic studies. *Metabolomics* 14:1–17. <https://doi.org/10.1007/s11306-018-1367-3>
79. Schulze B, Jeon Y, Kaserzon S, Heffernan AL, Dewapriya P, O'Brien J, Gomez Ramos MJ, Ghorbani Gorji S, Mueller JF, Thomas K V., Samanipour S (2020) An assessment of quality assurance/quality control efforts in high resolution mass spectrometry non-target workflows for analysis of environmental samples. *TrAC - Trends Anal Chem* 133:<https://doi.org/10.1016/j.trac.2020.116063>
80. Sangster T, Major H, Plumb R, Wilson AJ, Wilson ID (2006) A pragmatic and readily implemented quality control strategy for HPLC-MS and GC-MS-based metabonomic

- analysis. *Analyst* 131:1075–1078. <https://doi.org/10.1039/b604498k>
81. Bader T, Schulz W, Kümmerer K, Winzenbacher R (2016) General strategies to increase the repeatability in non-target screening by liquid chromatography-high resolution mass spectrometry. *Anal Chim Acta* 935:173–186. <https://doi.org/10.1016/j.aca.2016.06.030>
  82. Schymanski EL, Jeon J, Gulde R, Fenner K, Ruff M, Singer HP, Hollender J (2014) Identifying small molecules via high resolution mass spectrometry: Communicating confidence. *Environ Sci Technol* 48:2097–2098. <https://doi.org/10.1021/es5002105>
  83. Psoma AK, Rousis NI, Georgantzi EN, Thomaidis NS (2021) An integrated approach to MS-based identification and risk assessment of pharmaceutical biotransformation in wastewater. *Sci Total Environ* 770:<https://doi.org/10.1016/j.scitotenv.2020.144677>
  84. Wang S, Perkins M, Matthews DA, Zeng T (2021) Coupling Suspect and Nontarget Screening with Mass Balance Modeling to Characterize Organic Micropollutants in the Onondaga Lake–Three Rivers System. *Environ Sci Technol* 55:15215–15226. <https://doi.org/10.1021/acs.est.1c04699>
  85. Riter LS, Vitek O, Gooding KM, Hodge BD, Julian RK (2005) Statistical design of experiments as a tool in mass spectrometry. *J Mass Spectrom* 40:565–579. <https://doi.org/10.1002/jms.871>
  86. Draper N, Smith H (1981) *Applied Regression Analysis*, 2nd ed. Wiley, New York
  87. Fisher RA (1926) The Arrangement of Field Experiments. *J Minist Agric Gt Britain* 505–513. [https://doi.org/10.1007/978-1-4612-4380-9\\_8](https://doi.org/10.1007/978-1-4612-4380-9_8)
  88. Plackett RL, Burman JP (1946) The Design of Optimum Multifactorial Experiments. *Biometrika* 33:305–325.
  89. Box GEP, Hunter JS (1961) The 2 k-p Fractional Factorial Designs Part I. *Technometrics* 3:311–351. <https://doi.org/10.2307/1266725>
  90. Kiefer J (1959) Optimum Experimental Designs. *J R Stat Soc* 21:272–319.
  91. Raji MA, Schug KA (2009) Chemometric study of the influence of instrumental parameters on ESI-MS analyte response using full factorial design. *Int J Mass Spectrom* 279:100–106. <https://doi.org/10.1016/j.ijms.2008.10.013>
  92. Moreiras G, Leão JM, Gago-Martínez A (2018) Design of experiments for the optimization of electrospray ionization in the LC-MS/MS analysis of ciguatoxins. *J Mass Spectrom* 53:1059–1069. <https://doi.org/10.1002/jms.4281>
  93. Eliasson M, Rännar S, Madsen R, Donten MA, Marsden-Edwards E, Moritz T, Shockcor JP, Johansson E, Trygg J (2012) Strategy for Optimizing LC-MS Data Processing in Metabolomics: A Design of Experiments Approach. *Anal Chem* 84:6869–6879. <https://doi.org/10.1016/j.ijpharm.2011.11.009>
  94. Zheng H, Clausen MR, Dalsgaard TK, Mortensen G, Bertram HC (2013) Time-saving design of experiment protocol for optimization of LC-MS data processing in metabolomic approaches. *Anal Chem* 85:7109–7116. <https://doi.org/10.1021/ac4020325>
  95. Hu M, Krauss M, Brack W, Schulze T (2016) Optimization of LC-Orbitrap-HRMS acquisition and MZmine 2 data processing for nontarget screening of environmental samples using design of experiments. *Anal Bioanal Chem* 408:7905–7915. <https://doi.org/10.1007/s00216-016-9919-8>

96. Greco G, Grosse S, Letzel T (2013) Serial coupling of reversed-phase and zwitterionic hydrophilic interaction LC/MS for the analysis of polar and nonpolar phenols in wine. *J Sep Sci* 36:1379–1388. <https://doi.org/10.1002/jssc.201200920>
97. Hollender J, Schymanski EL, Singer HP, Ferguson PL (2017) Nontarget Screening with High Resolution Mass Spectrometry in the Environment: Ready to Go? *Environ Sci Technol* 51:11505–11512. <https://doi.org/10.1021/acs.est.7b02184>
98. Rajab M, Greco G, Heim C, Helmreich B, Letzel T (2013) Serial coupling of RP and zwitterionic hydrophilic interaction LC-MS: suspects screening of diclofenac transformation products by oxidation with a boron-doped diamond electrode. *J Sep Sci* 36:3011–3018. <https://doi.org/10.1002/jssc.201300562>
99. Bieber S, Moser S, Bilke H-W, Letzel T (2019) Design of Experiment Strategy for an Electrospray Ionization Optimization in Supercritical Fluid Chromatography–Mass Spectrometry Coupling. *LCGC* 32:526–535.
100. Golub GH, Heath M, Wahba G (1979) Generalized cross-validation as a method for choosing a good ridge parameter. *Technometrics* 21:215–223. <https://doi.org/10.1080/00401706.1979.10489751>
101. Minkus S, Bieber S, Letzel T (2021) Polarity-extended non-target screening using RPLC-HILIC-ESI-QToF-MS/MS and tailor-made data handling. In: Liška I, Wagner F, Sengl M, Deutch K, Slobodnik J, Paunović M (eds) *Joint Danube Survey 4 Scientific Report: A Shared Analysis of the Danube River*. International Commission for the Protection of the Danube River, Vienna, pp 363–372
102. R Core Team (2021) *R: A language and environment for statistical computing*. R Foundation for Statistical Computing
103. RStudio Team (2020) *RStudio: Integrated Development for R*. RStudio, PBC
104. Wernisch S, Pennathur S (2016) Evaluation of coverage, retention patterns, and selectivity of seven liquid chromatographic methods for metabolomics. *Anal Bioanal Chem* 408:6079–6091. <https://doi.org/10.1007/s00216-016-9716-4>
105. Godzien J, Alonso-Herranz V, Barbas C, Armitage EG (2015) Controlling the quality of metabolomics data: new strategies to get the best out of the QC sample. *Metabolomics* 11:518–528. <https://doi.org/10.1007/s11306-014-0712-4>
106. Helmus R, ter Laak TL, van Wezel AP, de Voogt P, Schymanski EL (2021) patRoön: open source software platform for environmental mass spectrometry based non-target screening. *J Cheminform* 13:1–25. <https://doi.org/10.1186/s13321-020-00477-w>
107. Schymanski EL, Singer HP, Longrée P, Loos M, Ruff M, Stravs MA, Ripollés Vidal C, Hollender J (2014) Strategies to characterize polar organic contamination in wastewater: Exploring the capability of high resolution mass spectrometry. *Environ Sci Technol* 48:1811–1818. <https://doi.org/10.1021/es4044374>
108. Agilent Technologies (2016) *MassHunter Profinder Software, Quick Start Guide*. G3835-90027 31–32
109. Di Guida R, Engel J, Allwood JW, Weber RJM, Jones MR, Sommer U, Viant MR, Dunn WB (2016) Non-targeted UHPLC-MS metabolomic data processing methods: a comparative investigation of normalisation, missing value imputation, transformation and scaling. *Metabolomics* 12:1–14. <https://doi.org/10.1007/s11306-016-1030-9>

110. Myers OD, Sumner SJ, Li S, Barnes S, Du X (2017) One Step Forward for Reducing False Positive and False Negative Compound Identifications from Mass Spectrometry Metabolomics Data: New Algorithms for Constructing Extracted Ion Chromatograms and Detecting Chromatographic Peaks. *Anal Chem* 89:8696–8703. <https://doi.org/10.1021/acs.analchem.7b00947>
111. Tautenhahn R, Bottcher C, Neumann S (2008) Highly sensitive feature detection for high resolution LC/MS. *BMC Bioinformatics* 9:1–16. <https://doi.org/10.1186/1471-2105-9-504>
112. Hohrenk LL, Itzel F, Baetz N, Tuerk J, Vosough M, Schmidt TC (2020) Comparison of Software Tools for Liquid Chromatography-High-Resolution Mass Spectrometry Data Processing in Nontarget Screening of Environmental Samples. *Anal Chem* 92:1898–1907. <https://doi.org/10.1021/acs.analchem.9b04095>
113. Letzel T, Sengl M (2016) FOR-IDENT - Platform International hunt for unknown molecules combining international workflows and software tools. In: *NORMAN Bulletin*. pp 20–21
114. Wolf S, Schmidt S, Müller-Hannemann M, Neumann S (2010) In silico fragmentation for computer assisted identification of metabolite mass spectra. *BMC Bioinformatics* 11:<https://doi.org/10.1186/1471-2105-11-148>
115. Grosse S, Letzel T (2017) User Manual for FOR-IDENT Database
116. Minkus S, Grosse S, Bieber S, Veloutsou S, Letzel T (2020) Optimized hidden target screening for very polar molecules in surface waters including a compound database inquiry. *Anal Bioanal Chem* 412:4953–4966. <https://doi.org/10.1007/s00216-020-02743-0>
117. Minkus S, Bieber S, Letzel T (2021) (Very) polar organic compounds in the Danube river basin: Non-target screening workflow and prioritization strategy for extracting highly confident features. *Anal Methods* 13:2044–2054. <https://doi.org/10.1039/D1AY00434D>
118. Rostkowski P, Haglund P, Aalizadeh R, Alygizakis N, Thomaidis N, Arandes JB, Nizzetto PB, Booij P, Budzinski H, Brunswick P, Covaci A, Gallampos C, Grosse S, Hindle R, Ipolyi I, Jobst K, Kaserzon SL, Leonards P, Lestremau F, Letzel T, Magnér J, Matsukami H, Moschet C, Oswald P, Plassmann M, Slobodnik J, Yang C (2019) The strength in numbers: comprehensive characterization of house dust using complementary mass spectrometric techniques. *Anal Bioanal Chem*. <https://doi.org/10.1007/s00216-019-01615-6>
119. Schmitt-Jansen M, Bartels P, Adler N, Altenburger R (2007) Phytotoxicity assessment of diclofenac and its phototransformation products. *Anal Bioanal Chem* 387:1389–1396. <https://doi.org/10.1007/s00216-006-0825-3>
120. Petrie B, Barden R, Kasprzyk-Hordern B (2015) A review on emerging contaminants in wastewaters and the environment: Current knowledge, understudied areas and recommendations for future monitoring. *Water Res* 72:3–27. <https://doi.org/10.1016/j.watres.2014.08.053>
121. Gómez MJ, Sirtori C, Mezcuca M, Fernández-Alba AR, Agüera A (2008) Photodegradation study of three dipyrone metabolites in various water systems: Identification and toxicity of their photodegradation products. *Water Res* 42:2698–2706. <https://doi.org/10.1016/j.watres.2008.01.022>
122. Brunner AM, Bertelkamp C, Dingemans MML, Kolkman A, Wols B, Harmsen D, Siegers W, Martijn BJ, Oorthuizen WA, ter Laak TL (2020) Integration of target analyses, non-target screening and effect-based monitoring to assess OMP related water quality

- changes in drinking water treatment. *Sci Total Environ* 705:135779. <https://doi.org/10.1016/j.scitotenv.2019.135779>
123. Bader T, Schulz W, Kümmerer K, Winzenbacher R (2017) LC-HRMS Data Processing Strategy for Reliable Sample Comparison Exemplified by the Assessment of Water Treatment Processes. *Anal Chem* 89:13219–13226. <https://doi.org/10.1021/acs.analchem.7b03037>
  124. Fischler M a, Bolles RC (1981) Random Sample Consensus: A Paradigm for Model Fitting with Applications to Image Analysis and Automated Cartography. *Commun ACM* 24:381–395. <https://doi.org/10.1145/358669.358692>
  125. Katajamaa M, Orešič M (2005) Processing methods for differential analysis of LC/MS profile data. *BMC Bioinformatics* 6:<https://doi.org/10.1186/1471-2105-6-179>
  126. Karakurt S, Schmid L, Hu U, Drewes JE (2019) Dynamics of Wastewater Effluent Contributions in Streams and Impacts on Drinking Water Supply via Riverbank Filtration in Germany - A National Reconnaissance. *Environ Sci Technol* 53:6154–6161. <https://doi.org/10.1021/acs.est.8b07216>
  127. Trautwein C, Kümmerer K (2011) Incomplete aerobic degradation of the antidiabetic drug Metformin and identification of the bacterial dead-end transformation product Guanylurea. *Chemosphere* 85:765–773. <https://doi.org/10.1016/j.chemosphere.2011.06.057>
  128. Trautwein C, Berset J, Wolschke H, Kümmerer K (2014) Occurrence of the antidiabetic drug Metformin and its ultimate transformation product Guanylurea in several compartments of the aquatic cycle. *Environ Int* 70:203–212. <https://doi.org/http://dx.doi.org/10.1016/j.envint.2014.05.008> 0160-4120/©
  129. Slobodnik J, Höbart A (2021) Survey logistics. In: International Commission for the Protection of the Danube River (ed) Joint Danube Survey 4 Scientific Report: A Shared Analysis of the Danube River. Vienna, pp 9–20
  130. Loos R, Tavazzi S, Paracchini B, Fick J (2015) Target analysis of emerging polar organic substances in water, fish and SPM using solid-phase extraction followed by UHPLC-MS-MS analysis. In: Joint Danube Survey 3: A Comprehensive Analysis of Danube Water Quality. pp 240–248
  131. European Chemicals Agency REACH registered substance factsheets. <https://echa.europa.eu/de/registration-dossier/-/registered-dossier/13887/6/2/1>. Accessed 29 Nov 2020
  132. Eggen RIL, Hollender J, Joss A, Schärer M, Stamm C (2014) Reducing the discharge of micropollutants in the aquatic environment: The benefits of upgrading wastewater treatment plants. *Environ Sci Technol* 48:7683–7689. <https://doi.org/10.1021/es500907n>
  133. 814.201 Gewässerschutzverordnung (GSchV) of 10/28/1998, status of 01/01/2021. Der Schweizerische Bundesrat
  134. Hernández-Leal L, Temmink H, Zeeman G, Buisman CJN (2011) Removal of micropollutants from aerobically treated grey water via ozone and activated carbon. *Water Res* 45:2887–2896. <https://doi.org/10.1016/j.watres.2011.03.009>
  135. Kovalova L, Siegrist H, Von Gunten U, Eugster J, Hagenbuch M, Wittmer A, Moser R, McArdell CS (2013) Elimination of micropollutants during post-treatment of hospital wastewater with powdered activated carbon, ozone, and UV. *Environ Sci Technol* 47:7899–7908. <https://doi.org/10.1021/es400708w>

136. Kovalova L, Knappe DRU, Lehnberg K, Kazner C, Hollender J (2013) Removal of highly polar micropollutants from wastewater by powdered activated carbon. *Environ Sci Pollut Res* 20:3607–3615. <https://doi.org/10.1007/s11356-012-1432-9>
137. Horai H, Arita M, Kanaya S, Nihei Y, Ikeda T, Suwa K, Ojima Y, Tanaka K, Tanaka S, Aoshima K, Oda Y, Kakazu Y, Kusano M, Tohge T, Matsuda F, Sawada Y, Hirai MY, Nakanishi H, Ikeda K, Akimoto N, Maoka T, Takahashi H, Ara T, Sakurai N, Suzuki H, Shibata D, Neumann S, Iida T, Tanaka K, Funatsu K, Matsuura F, Soga T, Taguchi R, Saito K, Nishioka T (2010) MassBank: A public repository for sharing mass spectral data for life sciences. *J Mass Spectrom* 45:703–714. <https://doi.org/10.1002/jms.1777>
138. European MassBank mass spectral database of the NORMAN network. <https://massbank.eu/MassBank/>. Accessed 2 Feb 2022
139. MassBank of North America. <https://mona.fiehnlab.ucdavis.edu/>. Accessed 2 Feb 2022
140. Welch BL (1947) The Generalization of “Student’s” Problem when Several Different Population Variances are Involved. *Biometrika* 34:28–35. <https://doi.org/10.1093/biomet/34.1-2.28>
141. Benjamini Y, Hochberg Y (1995) Controlling the False Discovery Rate: A Practical and Powerful Approach to Multiple Testing. *J R Stat Soc Ser B* 57:289–300. <https://doi.org/10.1111/j.2517-6161.1995.tb02031.x>
142. Reineke A, Liesener A, Betz L (2021) Anwendung von Nontarget-Screening und Wirkungsbezogener Analytik in der Charakterisierung von Aktivkohle zur Aufbereitung von Trinkwasser. *Vom Wasser* 119:78–81
143. Chen SY, Feng Z, Yi X (2017) A general introduction to adjustment for multiple comparisons. *J Thorac Dis* 9:1725–1729. <https://doi.org/10.21037/jtd.2017.05.34>
144. Bender R, Lange S (2001) Adjusting for multiple testing—when and how? *Stat Med* 20:1459–1468. [https://doi.org/10.1016/S0895-4356\(00\)00314-0](https://doi.org/10.1016/S0895-4356(00)00314-0)
145. Bheemanapally K, Ibrahim MMH, Briski KP (2021) HPLC–electrospray ionization–mass spectrometry optimization by high-performance design of experiments for astrocyte glutamine measurement. *J Mass Spectrom* 56:<https://doi.org/10.1002/jms.4680>
146. Kim S, Chen J, Cheng T, Gindulyte A, He J, He S, Li Q, Shoemaker BA, Thiessen PA, Yu B, Zaslavsky L, Zhang J, Bolton EE (2021) PubChem in 2021: New data content and improved web interfaces. *Nucleic Acids Res* 49:D1388–D1395. <https://doi.org/10.1093/nar/gkaa971>
147. Schymanski EL, Kondić T, Neumann S, Thiessen PA, Zhang J, Bolton EE (2021) Empowering large chemical knowledge bases for exposomics: PubChemLite meets MetFrag. *J Cheminform* 13:1–15. <https://doi.org/10.1186/s13321-021-00489-0>
148. Libiseller G, Dvorzak M, Kleb U, Gander E, Eisenberg T, Madeo F, Neumann S, Trausinger G, Sinner F, Pieber T, Magnes C (2015) IPO: A tool for automated optimization of XCMS parameters. *BMC Bioinformatics* 16:1–10. <https://doi.org/10.1186/s12859-015-0562-8>
149. Delabriere A, Warmer P, Brennsteiner V, Zamboni N (2021) SLAW: A Scalable and Self-Optimizing Processing Workflow for Untargeted LC-MS. *Anal Chem*. <https://doi.org/10.1021/acs.analchem.1c02687>
150. Peter KT, Phillips AL, Knolhoff AM, Gardinali PR, Manzano CA, Miller KE, Pristner M,

- 
- Sabourin L, Sumarah MW, Warth B, Sobus JR (2021) Nontargeted Analysis Study Reporting Tool: A Framework to Improve Research Transparency and Reproducibility. *Anal Chem* 93:13870–13879. <https://doi.org/10.1021/acs.analchem.1c02621>
151. Jaanus Liigand, Wang T, Kellogg JJ, Smedsgaard J, Cech NB, Kruve A (2020) Quantifying the unquantifiable : Quantification for non-targeted LC / MS screening without standards. *Sci Rep* in press. <https://doi.org/10.1038/s41598-020-62573-z>

## Appendix A: **Peer-reviewed publications**

---

## **Appendix A.1 Optimized hidden target screening for very polar molecules in surface waters including a compound database inquiry**

The following research article has undergone a peer-review process and has been previously published as presented below.

Reference: Minkus S, Grosse S, Bieber S, Veloutsou S, Letzel T (2020) Optimized hidden target screening for very polar molecules in surface waters including a compound database inquiry. *Anal Bioanal Chem* 412:4953–4966. <https://doi.org/10.1007/s00216-020-02743-0>



# Optimized hidden target screening for very polar molecules in surface waters including a compound database inquiry

Susanne Minkus<sup>1,2</sup> · Sylvia Grosse<sup>1,3</sup> · Stefan Bieber<sup>2</sup> · Sofia Veloutsou<sup>1,4</sup> · Thomas Letzel<sup>1,2</sup>Received: 18 March 2020 / Revised: 26 May 2020 / Accepted: 27 May 2020  
© Springer-Verlag GmbH Germany, part of Springer Nature 2020

## Abstract

Highly polar trace organic compounds, which are persistent, mobile, and toxic (PMT) or are very persistent and very mobile (vPvM) in the aquatic environment, may pose a risk to surface water, ground water, and drinking water supplies. Despite the advances in liquid chromatography-mass spectrometry, there often exists an analytical blind spot when it comes to very polar chemicals. This study seeks to make a broad polarity range analytically accessible by means of serially coupling reversed-phase liquid chromatography (RPLC) and hydrophilic interaction liquid chromatography (HILIC) to high-resolution mass spectrometry (HRMS). Moreover, a workflow is presented using optimized data processing of nontarget screening (NTS) data and subsequently generating candidate lists for the identification of very polar molecules via an open-access NTS platform and implemented compound database. First, key input parameters and filters of the so-called feature extraction algorithms were identified, and numerical performance indicators were defined to systematically optimize the data processing method. Second, all features from the very polar HILIC elution window were uploaded to the STOFF-IDENT database as part of the FOR-IDENT open-access NTS platform, which contains additional physicochemical information, and the features matched with potential compounds by their accurate mass. The hit list was filtered for compounds with a negative log *D* value, indicating that they were (very) polar. For instance, 46 features were assigned to 64 candidate compounds originating from a set of 33 samples from the Isar river in Germany. Three PMT candidates (e.g., guanylurea, melamine, and 1,3-dimethylimidazolidin-2-one) were illustratively validated using the respective reference standards. In conclusion, these findings demonstrate that polarity-extended chromatography reproducibly retards and separates (very) polar compounds from surface waters. These findings further indicate that a transparent and robust data processing workflow for nontarget screening data is available for addressing new (very) polar substances in the aqueous environment.

**Keywords** Hydrophilic interaction liquid chromatography · High-resolution mass spectrometry · PMTs · vPvMs · DoE · Optimization

Published in the topical collection *Persistent and Mobile Organic Compounds – An Environmental Challenge* with guest editors Torsten C. Schmidt, Thomas P. Knepper, and Thorsten Reemtsma.

**Electronic supplementary material** The online version of this article (<https://doi.org/10.1007/s00216-020-02743-0>) contains supplementary material, which is available to authorized users.

✉ Thomas Letzel  
t.letzel@afin-ts.de

<sup>1</sup> Technical University of Munich (Chair of Urban Water Systems Engineering), Am Coulombwall 3, 85748 Garching, Germany

<sup>2</sup> Analytisches Forschungsinstitut für Non-Target Screening GmbH (AFIN-TS), Am Mittleren Moos 48, 86167 Augsburg, Germany

<sup>3</sup> Present address: Thermo Fisher Scientific, Dornierstraße 4, 82110 Germering, Germany

<sup>4</sup> Present address: N. Votsi 35, 10445 Athens, Greece

## Introduction

Trace organic compounds (TOCs) are widely known for being ubiquitous in the aquatic environment [1]. Recently, attention was drawn to one specific group of very polar and poorly degradable TOCs—classified as “persistent in the environment, mobile in the aquatic environment, and toxic” (PMT) or “very persistent in the environment and very mobile in the aquatic environment” (vPvM)—because they give rise to environmental concerns [2, 3]. PMTs and vPvMs originate from household or industrial chemicals, pharmaceuticals, or pesticides, and enter the aquatic environment through point sources like municipal and industrial wastewater discharge [4] or diffuse sources such as runoff from agricultural fields or urban surfaces. Additionally, biotic or abiotic reactions from both

metabolites and transformation products tend to be more polar than the precursor molecule [5]. Whereas nonpolar chemical compounds can often be efficiently eliminated by sorption to sludge or biotransformation/biodegradation, conventional wastewater treatment fails to significantly remove PMTs and vPvMs [6]. Being highly polar and thus mobile in water, these compounds spread along partially closed water cycles and are able to overcome technical and biological barriers. The result is that PMTs and vPvMs are high-risk candidates for eventually reaching drinking water supplies.

The advent of liquid chromatography (LC) coupled to mass spectrometry (MS) has created new opportunities for detecting polar substances in complex samples. Nevertheless, a large fraction of PMTs and vPvMs still constitute a blind spot in terms of analysis, monitoring, and regulation [7]. Recognition of this “analytical gap” led to an increasing demand for chromatographic techniques which complement classical reversed-phase liquid chromatography (RPLC). Supercritical fluid chromatography (SFC) appears to be a promising technology because it is able to separate compounds of a broad polarity range within a relatively small elution window [8]. Furthermore, hydrophilic interaction liquid chromatography (HILIC) seems to be predestined for coupled separations because of its orthogonality to RPLC [9, 10]. Alpert originally postulated a partitioning mechanism between a hydrated layer partially immobilized on a hydrophilic stationary phase and a relatively hydrophobic bulk eluent [11]. Later on, a theory of a multimodal separation was put forward in which retention occurs through partitioning interactions as well as hydrogen bonding and ion exchange [12, 13]. Despite having a complex retention mechanism, applications already exist which prove that HILIC can effectively separate very polar and environmentally relevant molecules [8, 14, 15]. In 2013, Greco et al. developed a serial coupling of RPLC and HILIC that takes advantage of the complementarity of both techniques and enables both highly polar and nonpolar compounds to be separated within a single run [16]. Injecting large volumes of aqueous sample on a HILIC column might render elution patterns. However, the injection on the RPLC column of the polarity-extended chromatographic system presented here overcomes this issue, and the final eluent containing a high acetonitrile content is very suitable for mass spectrometric electrospray ionization (ESI).

In order to widen the analytical window in favor of more polar molecules, the overall approach regarding how to handle a sample and the respective data requires adjustment. The nontarget screening strategy as initially introduced by Hernández et al. [17] and further refined by Krauss et al. [18] is well-suited for revealing unknown molecules of interest in complex matrices without prior information or reference standards. The German Water Chemical Society recently described it as a “[...] procedure without limitation to pre-select substances” [19]. The nontarget approach was essentially

driven by the evolution of high-accuracy and high-resolution mass spectrometers (HRMS) able to acquire full scan data within a remarkably large mass range. However, even though high mass accuracy reduces the chance of erroneously assigning a molecular formula to a detected mass, further constraints need to be applied for an unambiguous allocation. Kind and Fiehn generated a comprehensive *in silico* test set of molecular formulae using the elements C, H, N, O, S, and P while complying with chemical and mathematical rules. They showed that the upper mass limit for unique formula assignment is still as low as 185.9760 Da at a theoretical accuracy of 0.1 parts per million (ppm) [20]. It becomes obvious that the results of a nontargeted measurement need to undergo further filtering steps. Criteria can be derived from instrumental boundary conditions and physicochemical properties specific to a compound group. In addition to the predefined mass range, chromatographic information like a retention time (RT) window and/or retention time indexing (RTI) also constitutes instrumental constraints beneficial to data filtering. In parallel with a suspect screening approach, the gathered data may be compared with entries of potential PMTs/vPvMs in a compound database. The search is facilitated by polarity indicators like the logarithmic distribution coefficient between octanol and water ( $\log D$ ). Substances which are known in chemical databases but unknown to the investigator are referred to as “known unknowns” [21] or “hidden targets” [22]. In contrast to the hidden target strategy, a suspect screening commonly targets the suspected ions already at the data acquisition stage, for instance, by conducting “multiple reaction monitoring” experiments.

Alongside the hidden target screening workflow—from planning an experiment to a final list of tentative PMTs/vPvMs found in a sample—several issues typically arise that require some form of compromise:

- (a) Introducing statistical value to the conducted study versus maintaining feasibility in terms of total measurement time and HRMS data volume
- (b) Reducing false positive allocations by applying a set of restrictive parameters and filters to the data processing method versus avoiding information loss by choosing overly rigid threshold values
- (c) Optimizing the data processing method according to individual needs versus keeping the process transparent and reproducible

These conflicts pose a classical optimization problem and become apparent when composing a method for extracting features from nontarget screening data. Such a feature extraction (FE) method has several quantitative parameters and filters upon which the quality of the resulting feature list depends. Despite the complexity of setting these parameters, the common approaches include either using default settings

or optimizing by “trial and error,” or changing “one factor at a time.” Not only do these approaches strongly rely on the investigator’s personal experience, they frequently also disregard statistical interactions between parameters. A more efficient and systematic approach is the statistical design of experiment (DoE): The maximum amount of information is extracted from complex nontarget screening data while simultaneously reducing experimental effort. The idea is to vary relevant peak picking parameters simultaneously over a reduced set of experiments. Cause-and-effect correlations are described by a mathematical model that can in turn be used for the interpretation, prediction, and optimization of these parameters. Since the pioneering work of Fisher in 1926 [23], the field has developed several methodological instruments such as the Plackett-Burman screening design [24], upon which the experimental plan used in this study was based.

In the following, an analytical workflow is suggested for facilitating the identification of PMTs and vPvMs in aqueous environments. Data was acquired by an RPLC-HILIC-ESI-time of flight (TOF)-MS coupling. Features were extracted by means of a systematically optimized method, then followed by a database inquiry and a filtering step for polar and very polar substances.

## Material and methods

In the following, polarity is approximated by the pH-dependent octanol-water partition coefficient  $\log D$ . Substances are referred to as either “nonpolar” for a  $\log D > +2$ , “polar” for values between  $-2.5$  and  $+2$ , or “very polar” for a  $\log D < -2.5$ ” at pH 7 as described elsewhere [8]. It should be kept in mind that a one-parameter coefficient like the  $\log D$  can only describe the compound variability within a single substance class and does not consider interactions involved in partitioning [25].

## Chemicals

Acetonitrile and water (both LC-MS grade) were purchased from Fluka (Buchs, Switzerland). Reference compounds with a purity of  $> 99\%$  were purchased from Sigma-Aldrich (Seelze, Germany). First, they were dissolved individually into stock solutions of 1 mM in either acetonitrile (nonpolar compounds) or in acetonitrile/water (50/50, v/v) (polar or very polar compounds). Afterwards, they were combined into a standard working mixture of 10  $\mu\text{M}$  per compound.

## Water sampling and sample preparation

The samples used in this study were collected from the Isar river in Germany during March, May, and July 2015, respectively. Grab samples were taken at eleven locations between

the Austrian-German border and the Bavarian city of Dingolfing, respectively (exact coordinates and descriptions of the sites are given in Table S1 in the Electronic Supplementary Material, ESM). Each monthly sampling pass and subsequent filtration were completed within a single day.

The samples were enriched using an offline polarity-extended solid-phase extraction (SPE) method. Therefore, two different extraction steps were sequentially conducted: (a) Reversed Phase (RP) Strata-X C18-encapped from Phenomenex (Aschaffenburg, Germany) for nonpolar compounds and (b) ZIC-HILIC from Dichrom GmbH (Haltem am See, Germany) for (very) polar compounds. Firstly, the preconditioned RP cartridges were loaded with 150 mL of water sample. After passing through the column, it was freeze-dried with an Alpha 1 – 4 LSC freeze dryer (Christ, Osterode am Harz, Germany). The nonpolar fraction of the sample was eluted from the RP cartridge with 3 mL of acetonitrile/water (80/20, v/v), followed by 3 mL of pure acetonitrile. The eluate was dried in a vacuum until the solvents were completely evaporated. The remaining freeze-dried water sample was reconstituted in 12 mL acetonitrile/water (95/5, v/v) and centrifuged. Afterwards, the supernatant was loaded onto the preconditioned ZIC-HILIC cartridge. Three milliliters of acetonitrile/water (50/50, v/v) was used to elute the sample’s polar fraction from the ZIC-HILIC column into the tube containing the same dried nonpolar fraction of the sample. The combined extracts were dried again and finally reconstituted in 0.5 mL acetonitrile/water (50/50, v/v). The resulting solution was filtered through a 22  $\mu\text{m}$  PVDF filter into a glass vial and stored at 4 °C prior to analysis.

Pure water (LC-MS grade) was processed the same way and served as a blank sample.

## Analytical instrumentation

The chromatographic separation was performed by a serial coupling of RPLC and HILIC. Detailed information on the setup of the system and the robustness thereof is provided elsewhere [15, 16].

In short, two binary pumps and two online degassers were used (Agilent Technologies, Waldbronn, Germany). The RP separation was performed on a Poroshell 120 EC-C18 (50.0  $\times$  3.0 mm, 2.7  $\mu\text{m}$ ; Agilent Technologies) column and the HILIC separation on a ZIC-HILIC (150  $\times$  2.1 mm, 5  $\mu\text{m}$ , 200 Å; Merck Sequant, Umea, Sweden). The two columns were connected in series via a T-piece with a mixing frit (Upchurch, IDEX Europe GmbH, Erlangen, Germany). The third port of the T-piece was connected to a second binary pump. The following solvents were used as mobile phases: Solvent A was 10 mM ammonium acetate in water/acetonitrile (90/10, v/v) and solvent B was 10 mM ammonium acetate in acetonitrile/water (10/90, v/v) for the RPLC separation. For HILIC, acetonitrile (solvent C) and water (solvent D)

were used. Information on the gradients is provided in Table S2 of the ESM. The injection volume was 10  $\mu\text{L}$ .

The chromatographic system was coupled to an Agilent 6230 TOF-MS equipped with a Jet Stream ESI interface (Agilent Technologies, Santa Clara, CA, USA). The ESI source was operated in positive mode under the following conditions: gas temperature 325  $^{\circ}\text{C}$ , drying gas flow 8.0  $\text{L min}^{-1}$ , nebulizer gas pressure 45 psi, sheath gas temperature 250  $^{\circ}\text{C}$ , sheath gas flow 5.5  $\text{L min}^{-1}$ , capillary voltage 3 kV, fragmentor voltage 175 V. Nitrogen was used as both the drying and the sheath gas. During the analysis, a mass range up to 1700  $m/z$  was scanned in high-resolution mode. The instrument was continuously calibrated on 125 nM purine and 6.25 nM HP-921 MS tuning mix (Agilent Technologies, Waldbronn, Germany) [16]. The instrument's resolution is specified at 22,000 (full width at half maximum, FWHM) at  $m/z$  1522 after automatic tuning procedure [26]. The accuracy was below 10 ppm.

Each sample was measured once. Interday repeatability of the chromatographic system was investigated on 68 standard substances by measuring them four times over the course of the campaign (ESM Table S3). For each compound, the mean value and standard deviations were calculated for RT, mass error, and the peak's full width at half maximum (FWHM) and its height, respectively.

### Data processing and (tentative) molecule identification

The software that acquired the raw mass spectrometric data and controlled the system was MassHunter Workstation LC/MS Data Acquisition (version B.05.01, Agilent Technologies).

### Feature extraction

Chromatographic peaks were binned together across all samples by RT and accurate mass. This compound bin is referred to as a feature which is characterized by the median values of RT, accurate mass, and signal intensity. Had MS/MS data been available, the spectrum would have been a further part of the feature.

The mass spectrometric raw data was processed by MassHunter Workstation Profinder (version B.06.00, Agilent Technologies) software. The feature extraction (FE) method is composed of two consecutive algorithms: The first which processes the HRMS data is an untargeted matter, deconvoluting all peaks that exceed an intensity limit defined by the investigator. Subsequently, ion species (molecular ions, isotopes, and adducts) that display the same chromatographic behavior are grouped together and aligned across all samples. Median values for masses, RTs, and composite spectra are calculated and fed into the second, recursive algorithm. This

second algorithm uses these values to perform a targeted extraction and thereby improves reliability in features [27].

Within the above program, a "batch recursive FE" method for small molecules was built in order to generate a list of features. Each feature contains peaks of defined mass and RT aligned across the respective number of samples. Isotope grouping was performed on the basis of the common organic molecule model with a peak spacing tolerance of 0.0025  $m/z$  + 7.0 ppm. The critical FE parameters thereby were optimized by means of DoE (see the "Optimization of the FE parameter using the design of experiment strategy" section), and the results are shown in Table 1.

### Optimization of the FE parameter using the design of experiment strategy

Prior to the FE, critical method parameters referred to as quantitative factors (F) were identified and optimized by means of DoE using MODDE Pro software (version 12.1.0.5491; Sartorius Stedim Biotech GmbH, Göttingen, Germany). The optimization was based on the HRMS raw data from a subset of six river water samples (due to extensive data processing times): The March and July samples were each taken at locations 1, 7, and 10 (ESM Table S1), respectively. The following critical quantitative FE factors were optimized and are illustrated in Fig. 1:

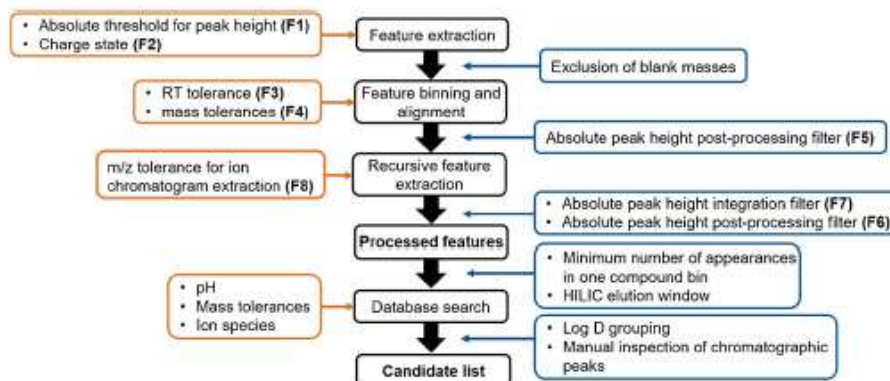
- F1) Absolute threshold for peak height prior to the FE
- F2) Charge state of the ions
- F3) RT tolerance for the binning and alignment of features
- F4) Mass tolerance for the binning and alignment of features
- F5) Absolute peak height filter applied after the untargeted algorithm
- F6) Absolute peak height filter applied after the targeted algorithm
- F7) Absolute peak height filter after integration

**Table 1** The robust setpoint is presented as a result of optimizing the critical FE parameters. For each quantitative factor, the respective value and the factor contribution were calculated

Quantitative factor	Value	Contribution (%)
F1	0 counts	9.0
F2	1	5.4
F3	0.87 min	46.1
F4	50 ppm	0.0
F5	0 counts	0.0
F6	5000 counts	2.0
F7	5000 counts	26.6
F8	10 ppm	10.9

Optimized hidden target screening for very polar molecules in surface waters including a compound database...

**Fig. 1** Workflow to evaluate nontarget screening data including a compound database search. Input parameters and filtering steps which significantly influence the output after each step are depicted in orange and blue boxes, respectively. The bolt numbers in brackets mark the critical parameters that were optimized



F8) Symmetric  $m/z$  tolerance for the recursive chromatogram extraction

These eight FE factors were varied according to a strategically designed experimental plan of 28 runs which is provided in Table S4 of the ESM. Optimization was based on six response factors (R) in the form of numerical descriptors which were chosen to assess the performance of the FE method:

- R1) The RT span of all peaks binned into a compound group across all samples. After every experimental run, the median value was calculated for the final feature list
- R2) The relative standard deviation (RSD) of masses within a compound group across all samples. Again, the median value was calculated
- R3) The number of single ions relative to the total number of extracted features
- R4) The mass difference between the median mass within a compound group and the target mass used by the recursive algorithm
- R5) The number of erroneously integrated chromatographic peaks out of a sample of ten features, which covered broad mass and RT ranges and appeared in more than ten experiments (ESM Table S5). The extracted ion chromatograms (EICs) were checked manually
- R6) The number of missed chromatographic peaks out of the same sample of ten features

For each experiment, the response variables were calculated from the extracted feature list out of the sample subset. A model was fitted using multiple linear regression. The optimization was based on desirability functions with the objective of minimizing all responses. These desirability functions ran on the specification limits for each response variable given in Table S6 (see ESM) along with the experimental results. To search for the robust setpoint, a design space was generated with a resolution of 8, with 1000 iterations and a 1% acceptance limit.

### (Tentative) molecule identification

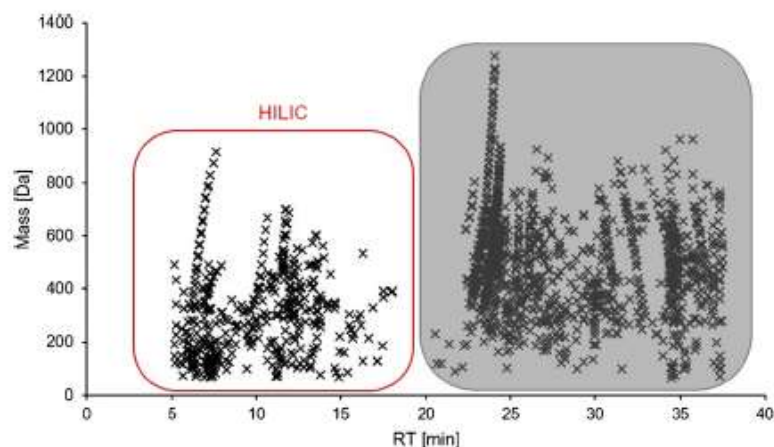
The exact masses of the features retained by the HILIC column were uploaded and processed by the FOR-IDENT platform [28] using the STOFF-IDENT compound database [29]. The transition from the HILIC to the RPLC retention window was between 16 and 21 min (Fig. 2). A hard limit was defined at the RT of metformin 17.0 min since it was the last standard compound eluting from the HILIC column (ESM Table S3). A pH level of 7 and a 10.0 ppm mass tolerance for the molecular ion were selected as input parameters. The resulting list of compounds, including their physiochemical properties, was downloaded. That list was then filtered for compounds with a log  $D$  value (at pH 7) below 0. Afterwards, the underlying chromatographic peaks of successfully matched features were manually checked. Compound lists were processed in Microsoft Excel (version 1902).

## Results and discussion

This study sought to combine a polarity-extended chromatographic method, i.e., the serial coupling of RPLC and HILIC, using a hidden target screening approach for tentatively identifying PMTs/PvMs.

A set of environmental data was used in order to exemplify a novel data processing and molecule identification strategy for very polar anthropogenic compounds. It is being presented with an emphasis on key parameters for ensuring transparency and reproducibility. Consequently, the study focused on data processing and tried to explicitly highlight the importance of transparently communicating the FE method. Since a large variety of data analysis software tools exist, the key peak picking parameters need to be identified and clearly stated. Therefore, a data-specific optimization is suggested for parameters and filters which are critical to extracting features from HRMS raw data. Subsequently, a compound database was consulted in order to tentatively identify (very) polar molecules by comparing physiochemical properties of the

**Fig. 2** Mass-RT plot of features obtained from measuring 33 environmental samples with a RPLC-HILIC-TOF-MS coupling. All blank masses were excluded in the extraction method. The features can be separated into two distinct groups, the first of which represents those that eluted from the HILIC column



observed analytical data with compounds stored in the database. The data processing strategy for going from mass spectrometric raw data to a list of potential compounds of the very polar fraction of the sample is illustrated in Fig. 1. Every step along the workflow is characterized by several input parameters (orange boxes) and filters (blue boxes) acting as variables influencing the outcome in the form of a feature list.

Features are characterized by the median RT, accurate mass, and signal intensity, as described in the experimental section.

### Environmental samples studied

The workflow was built on 33 environmental samples that were taken during early 2015 from the Isar river in southern Germany (Bavaria). The eleven sites sampled started at the German-Austrian border close to the river's source, then covered the urban area of Munich and finished in the town of Dingolfing. The exact locations are specified and commented on in Table S1 (see ESM). Each sampling pass was performed during a single day and repeated during the months of March, May, and July, respectively. Karakurt et al. [30] calculated the relative wastewater effluent contribution at different gauging stations along the Isar river from the accumulated discharge of upstream wastewater treatment plants under mean minimum annual discharge conditions. Their results showed that the wastewater effluent contribution was <1% in Mittenwald, near the source. It jumped from 5 to >50% after the plants treating the wastewater of Munich and recovered to 11% at the gauging station of the town of Landshut, 40 km downstream (probably due to dilution) [30]. Judging from the substantial portions of treated wastewater in densely populated areas, an elevated amount of anthropogenic PMTs and vPvMs was expected in the samples taken shortly downstream of Munich. Furthermore, this campaign was designed to unravel seasonal differences between the spring and summer samples.

The hidden target screening approach is well-suited for such global surveys of surface waters because it creates

options for comparing samples by their molecular fingerprint. The aqueous samples were analyzed using the polarity-extended chromatographic separation technique RPLC-HILIC coupled with accurate TOF-MS.

### Analytical robustness

Robust operation of the analytical setup is a prerequisite for successfully handling the observed nontarget screening data and the evaluation thereof.

As a result, the data on the interday repeatability of the RPLC-HILIC-TOF coupling is presented in Table S3 of the ESM.

For the 43 standard compounds eluting from the RPLC column between 23.7 and 35.1 min, the mean standard deviation of RT was 0.3 min (RSD 0.9%). Norfluoxetine showed the largest variability at 0.6 min (2.1%). The mass spectrometric accuracy can be expressed by the mass error which corresponds to the relative deviation of the detected mass from the monoisotopic mass. All RPLC standard compounds displayed a mean mass error of <7 ppm.

Twenty-five compounds were retained on the HILIC column and eluted between 5.9 and 17.0 min. The mean standard deviation of RT was 0.2 min (1.9%) whereas gabapentin and metformin exhibited the highest values at 0.5 min (4.6%) and 0.8 min (4.4%), respectively. The mean mass error was below 9 ppm for all HILIC compounds, which is in good agreement with an expected accuracy of 10 ppm for the applied time of flight mass spectrometer.

The overall scattering of the RTs for the standard compounds is considerably low, which indicates a reliable and robust separation of both the RPLC and the HILIC parts. Retention time stability is an important parameter when dealing with nontarget screening data since it directly factors into the componentization during the feature-finding process. Accordingly, for all features detected in the real samples during this 5-month project, the RSD of RTs was below 4% (Table 2). Moreover, the mass errors observed in the test set justify

Optimized hidden target screening for very polar molecules in surface waters including a compound database...

**Table 2** Features described by their detected accurate masses and mean RTs with RSDs. They are presented along with the respective database hit(s). The features eluted from the HILIC column of the RPLC-HILIC-TOF-MS coupling and therefor only compounds with a negative log *D* value were considered

ID	Detected median mass	Detected mean RT (min)	Number of samples	RSD RT (%)	Compound name (STOFF-IDENT)	InChi key	Relative mass difference (ppm)	Log <i>D</i> (pH 7)
1	75.0688	13.8	10	0.3	3-Aminopropan-1-ol	WUQZFFCHPXWKQ-UHFFFAOYSA-N	5.3	-3.9
					1-Aminopropan-2-ol	HXKKHQJGIAFBHI-UHFFFAOYSA-N	5.3	-3.4
					2-Methylaminoethanol	OPKOK-AMJFNKNAS-UHFFFAOYSA-N	5.3	-3.6
					2-Amino-1-propanol	BKMMTJMOCUHRP-UHFFFAOYSA-N	5.3	-3.5
2	102.0547	14.6	13	1.6	Guanylurea	SQSPRWMERUQXNE-UHFFFAOYSA-N	4.9	-2.1
3	103.1001	12.4	3	0.6	3-Ethoxypropylamine	SOYBEXQHNRJRCGE-UHFFFAOYSA-N	3.9	-3.0
					1-Dimethylaminoopropan-2-ol	NCXUNZWLEYGOAH-UHFFFAOYSA-N	3.9	-2.3
					3-Dimethylaminoopropan-1-ol	PYSGFFTXMUWEOT-UHFFFAOYSA-N	3.9	-2.6
4	109.0532	7.4	9	0.2	(1 <i>R</i> ,4 <i>S</i> )-2-Azabicyclo[2.2.1]hept-5-en-3-one	DDUFYKNOXPZZIWI-UHFFFAOYSA-N	3.7	-0.2
					Nicotinylalcohol	MVQVNTPHUGQQHK-UHFFFAOYSA-N	3.7	0.0
5	113.1205	11.0	3	2.8	1-Ethylpiperidine	HTLVHNRZJPSMI-UHFFFAOYSA-N	0.9	-1.5
6	114.0795	5.6	11	0.5	1,3-Dimethylimidazolidin-2-one	CYSGHNMQY ZDMIA-UHFFFAOYSA-N	1.8	-0.6
7	115.0627	12.1	11	0.8	N-(2-Hydroxyethyl)methacrylamide	DNTMOTKNSEIFO-UHFFFAOYSA-N	-5.2	-0.2
					4-Morpholinocarbaldehyde	LCEDQNDFOCWGG-UHFFFAOYSA-N	-5.2	-0.9
					N-(2-Hydroxyethyl)prop-2-enamide	UUORUTJPDJXST-UHFFFAOYSA-N	-5.2	-0.7
8	115.0995	7.9	15	1.7	Methyl-3-aminocrotonate	XKORCTHIRYKLLG-ONEGZZNKSAN	-5.2	-0.24
					2,6-Dimethylmorpholine	HNVIQLPOGUDBSU-UHFFFAOYSA-N	-1.7	-1.3
					Trans-4-Aminocyclohexan-1-ol	IMLXLGZJLAOKIN-UHFFFAOYSA-N	-1.7	-3.0
					2-Pyrrolidin-1-ylethanol	XBRDBODLCHKXHI-UHFFFAOYSA-N	-1.7	-2.7
9	117.0798	11.7	30	0.8	L-Valine	KZSNWVFEVHDMF-BYPYZUCNSAN	6.8	-2.0
					L-Norvaline	SNDPXSYPESP GGI-BYPYZUCNSAN	6.8	-1.9
					2-Hydroxy-N,N-dimethyl-propanamide	YEBLAXBYVYV COL T-UHFFFAOYSA-N	6.8	-0.8
10	121.0883	5.2	8	0.1	D-alpha-Methylbenzylamine	RQEUFK YXDPUSK-SSDOTTSWSAN	-6.6	-1.0
					Benzyl(methyl)amine	RIWRFSMVU AEBX-UHFFFAOYSA-N	-6.6	-1.1
					L-alpha-Methylbenzylamine	RQEUFK YXDPUSK-ZETCQYMHSA-N	-6.6	-1.0
					Phendylamine (PEA)	BHHGXPLMPWC GHP-UHFFFAOYSA-N	-6.6	-1.2
					Melamine	JD SHMPZPIAZGSV-UHFFFAOYSA-N	-2.4	-2.0
11	126.0651	7.2	5	1.6			0.8	
	126.0655	6.9	4	0.5			8.7	
	126.0665	8.4	9	0.2			6.2	-1.1
12	129.0182	6.3	8	2.9	1,3,5-Triazine-2,4,6-trione	ZFSLDLOARCGLHUHFFFAOYSA-N	6.2	-1.1
13	135.0554	7.7	4	0.3	Adenine	GFFGJBGJISGV-UHFFFAOYSA-N	6.7	-0.6
14	144.0904	6.3	17	2.1	N,N'-Ethylenedi(diacetamide)	WN YIBZHOMZDKNUHFFFAOYSA-N	3.5	-1.8
15	149.0709	7.6	4	0.6	3-Methyladenine	ZPBYV FQJHWLTFB-UHFFFAOYSA-N	5.4	-0.3

Table 2 (continued)

ID	Detected median mass (min)	Detected mean RT (min)	Number of samples	RSD RT (%)	Compound name (STOFF-IDENT)	InChi key	Relative mass difference (ppm)	Log D (pH 7)
16	149.1046	12.2	10	1.0	1-Methyladenine	SATCOUWSAZBIO-UHFFFAOYSA-N	5.4	-0.5
					9-Methyladenine	WRXCXOUDSPTXNX-UHFFFAOYSA-N	5.4	-0.3
					7-Methyladenine	HCGHYQLFMPXSDU-UHFFFAOYSA-N	5.4	-0.4
17	149.1052	11.2	17	1.0	2,2',2''-Nitritotriethanol	GSEJCLTVZPLZKY-UHFFFAOYSA-N	-4.0	-3.3
					2-(Dimethylamino)-2-(hydroxymethyl)propane-1,3-diol	FLZLZYVVTBQJ-UHFFFAOYSA-N	-4.0	-3.4
					2,2',2''-Nitritotriethanol	GSEJCLTVZPLZKY-UHFFFAOYSA-N	0.0	-3.3
					2-(Dimethylamino)-2-(hydroxymethyl)propane-1,3-diol	FLZLZYVVTBQJ-UHFFFAOYSA-N	0.0	-3.4
18	155.1311	8.6	19	3.0	2,2,6,6-Tetramethyl-4-piperidone	JWUXYZVKZKLTJ-UHFFFAOYSA-N	0.6	-0.3
					2-[(Dimethylamino)methyl]cyclohexanone	QDHLFBSGUGHCL-UHFFFAOYSA-N	0.6	-0.3
19	155.1316	6.2	17	1.7	2,2,6,6-Tetramethyl-4-piperidone	JWUXYZVKZKLTJ-UHFFFAOYSA-N	3.9	-0.3
					2-[(Dimethylamino)methyl]cyclohexanone	QDHLFBSGUGHCL-UHFFFAOYSA-N	3.9	-0.3
20	161.1413	15.1	3	0.9	2-[2-(Diethylamino)ethoxy]ethanol	VKBVRNHODPFVHK-UHFFFAOYSA-N	-1.9	-2.2
					(2,2-Diethoxyethyl)dimethylamine	SSFUAOAOQOISRQ-UHFFFAOYSA-N	-1.9	-0.1
					7,7-Dimethyl-3-oxa-6-azabicyclo[1.1.0]	YDEDDFNFOOPRQJ-UHFFFAOYSA-N	-1.9	-2.6
21	163.0859	15.0	6	0.5	Bicine	FSVCELGFZIQNCK-UHFFFAOYSA-N	8.6	-4.4
22	170.0932	7.3	3	0.4	3,4,5-Piperidinetriol, 2-(hydroxymethyl)-, (2R,3R,4R,5S)-	LXBIFFVIBLOUGU-JGWLITMUSA-N	8.6	-4.0
					(1R,3S)-2,2-Dimethyl-3-(2-oxopropyl)cyclopropanecarboxylic acid	BKUHNVYPRVILOX-BOBZGAKWSA-N	-6.5	-1.6
23	171.0907	7.9	8	0.3	Ethyl 2-oxopyrrolidine-1-acetate	AQZWKPDVWJWRY-UHFFFAOYSA-N	7.0	-0.4
24	187.1211	8.1	10	0.2	(3R)-3-(2-Amino-2-oxoethyl)-5-methylhexanoic acid	NPDKTSLVWGFPOG-UHFFFAOYSA-N	1.6	-1.5
25	191.1518	6.6	11	1.8	1,1',1''-Nitritotripropan-2-ol	SLNHMFUFWBEMU-UHFFFAOYSA-N	-1.6	-2.9
	191.1523	8.3	3	1.3			1.1	
26	201.1733	9.5	33	2.1	4-Hydroxy-2,2,6,6-tetramethylpiperidine-1-ethanol	STEYNUVPFMIUOY-UHFFFAOYSA-N	2.0	-2.6
	201.1734	10.9	11	0.3			2.5	
	201.1737	8.4	3	2.1			4.0	
	201.1740	9.8	5	0.7			5.5	
	201.1742	10.9	11	0.3			6.5	
27	205.0599	11.8	6	0.9	Methylglycinediacetic acid	CIEZGWLIBXOTE-UHFFFAOYSA-N	6.3	-9.9
28	205.1304	7.7	7	0.5	Panthenol, DL-form	SNPLKNRPHDVJA-UHFFFAOYSA-N	-4.9	-1.7
					Dexpanthenol	SNPLKNRPHDVJA-ZETCQYMHSA-N	-4.9	-1.7
29	205.1327	5.7	11	0.1	Panthenol, DL-form	SNPLKNRPHDVJA-UHFFFAOYSA-N	6.3	-1.7
					Phenformin	ICFJFFQJTFMIBG-UHFFFAOYSA-N	0.0	-3.8
					Dexpanthenol	SNPLKNRPHDVJA-ZETCQYMHSA-N	6.3	-1.7
30	221.1402	12.2	5	0.2	3,4-Methylenedioxypropylamphetamine	LFXMQBTXOLBCCA-UHFFFAOYSA-N	-6.3	-0.3
31	222.1475	6.0	7	0.3	Bis[2-(2-Methoxyethoxy)ethyl] ether	ZUHZGEOKBKGPSW-UHFFFAOYSA-N	3.6	-0.1

Optimized hidden target screening for very polar molecules in surface waters including a compound database..

Table 2 (continued)

ID	Detected median mass	Detected mean RT (min)	Number of samples	RSD RT (%)	Compound name (STOFF-IDENT)	InChi key	Relative mass difference (ppm)	Log D (pH 7)
32	234,1106	6.6	8	3.9	2-Ethyl-1-(2-(1,3-dioxanyloxy)ethyl)-pyridinium	HNGQYA WKWBGDR-UHFFF AOYSA-N	-6.3	-2.4
33	257,1052	13.7	9	0.7	2,2'-(Ethane-1,2-diylbis(oxy)bisethyl diacetate	OVOLKWFJRHALDD-UHFFF AOYSA-N	1.3	-0.4
34	267,1475	12.5	8	0.6	Tolmetin	UPSPUYADGBWSHF-UHFFFAOYSA-N	0.0	-0.2
35	283,1775	12.0	11	0.1	Metoprolol acid	PUQRTNPRFRZ-UHFFFAOYSA-N	1.5	-1.2
36	360,2144	12.1	7	0.3	Alpha-Hydroxymetoprolol	OFRYBPCSEMMZHR-UHFFFAOYSA-N	-3.2	-1.7
					Butylscopolamin	YBCNXCRZPWQOBR-FAOYLHNAS-A-N	-7.0	-1.9
					Butylscopolammonium	YBCNXCRZPWQOBR-MWGADRMYS-A-N	-7.0	-1.9
37	362,1668	9.9	16	0.5	Protirelin	XNSAINXGIZQOO-SRVKXCTJSA-N	-9.7	-3.4
38	468,2676	11.6	4	0.2	6,6',6''-(1,3,5-Triazine-2,4,6-triylimino)tris-hexanoic acid	BKKWPPMEXIXECW-UHFFFAOYSA-N	-4.3	-5.3
39	475,2971	6.4	22	2.2	Netilmicin	CIDUJQMULVCIBT-IULVMANBSA-N	-7.4	-12.8

adopting a maximum mass difference of 10 ppm as a criterion for matching features with database compounds by accurate mass. More details on stability testing of the coupling can be found in the previous work published by Bieber et al. [8].

## Data processing strategy and optimization

### Optimization of FE parameters and filters

The two FE algorithms applied have differing objectives:

- The nontargeted one that should allow a less restricted search in order to reduce the number of missed chromatographic peaks and
- the targeted one that should be more precise in order to introduce statistical confidence to the features. Since the target criteria of the second algorithm depend on the componentization of the first one, the parameter settings need to be coordinated.

Therefore, critical input parameters and filters (called factors) were identified and optimized before applying the FE method to real samples. The optimization was based on six responses which characterize the performance of a certain combination of factors: R1, R2, and R3 (see the “Optimization of the FE parameter using the design of experiment strategy” section for a definition) assess the quality of the feature componentization. Consequently, given closer binning and alignment tolerances, the percentage of single ions (R3) is likely to increase. Nevertheless, a fraction of observed single ions might also derive from a low signal intensity. R4 provides information on the accuracy of the recursive algorithm. R5 and R6 indicate whether integrated peaks are correctly allocated to a compound bin.

Based on the results of all 28 experiments included in the strategically designed plan, a model was fitted for each individual response by means of multiple linear regression. For model diagnostics, the coefficient of determination  $R^2$  was considered. The latter represents the fraction of a response that can be explained by the model. The predictive ability of a model can be estimated by  $Q^2$  [31]. For each response,  $R^2$  was  $>0.7$  and  $Q^2 >0.6$ . Furthermore, the FE algorithms generate the same feature lists for repeated processing attempts given that the same data set was used, and the same parameter values were set. Considering all three performance characteristics ( $R^2$ ,  $Q^2$ , and reproducibility), the model was considered to be sufficiently significant. The formula for  $R^2$  and  $Q^2$ , along with the individual values for each response, can be found in Table S7 (see ESM). Moreover, the model terms are also listed therein along with their respective coefficients.

A robust setpoint for the critical FE input parameters and filters was iteratively calculated with the objective of minimizing the six response variables. The resulting factor settings are

presented in Table 1. Some results can be transferred to other data analysis workflows applied for HRMS, e.g., setting the initial threshold for the signal intensity (F1) to zero in order to decrease the number of missed chromatographic peaks while simultaneously applying a rigid post-processing filter (F6, F7) in order to reduce the number of falsely integrated peaks and single ions. Further findings are specific to the data set at hand, the measurement campaign which was conducted over a period of 5 months. The chromatographic and mass spectrometric conditions shifted slightly as a result. It is generally accepted that tolerance windows need to be implemented in feature-building algorithms which account for these RT and mass drifts [32]. Accordingly, an optimized EIC tolerance (F8) of 10 ppm was calculated from the model and is in good agreement with the mass errors found for the HILIC standard compounds in the TOF system (see “Environmental samples studied” section and ESM Table S3). Even though the average interday RT variability over the 25 standard compounds was < 2%, in some rare cases (such as for gabapentin and metformin), the RT shifted over an absolute span of > 1.0 min. As a result, an optimal and robust binning and alignment tolerance of 0.9 min was determined for RT (F3). Another way of coping with shifting instrumental conditions would be to split data sets into homogeneous blocks, with each block containing data from successively measured samples. On the one hand, this approach could lead to smaller tolerance windows for RT and accurate mass. On the other hand, however, it would mean an inability to handle the data from a consecutive campaign as one batch.

These findings prove that FE parameter settings need to adapt to fluctuating data quality. In this context, the concept of optimizing these parameters by DoE introduces flexibility into a workflow that processes nontarget data. A DoE approach is inherently accompanied by a thorough statistical evaluation of a parameter's significance, effect, or potential interactions with other parameters and, as a result, leads to a better understanding of the algorithm in general. Examples of DoE are already being used for the purpose of optimizing peak picking parameters for XCMS software [33] in metabolomics [34, 35]. The present study shows that the concept is not limited to specific software and could serve as an add-on for improving a preexisting nontarget or hidden target screening strategy in environmental analysis. Moreover, it has the potential to become a fully automated element within an FE workflow.

### Polarity-dependent feature extraction

The final FE method was applied twice: First, on the raw HRMS data of the blank sample and afterwards to the real sample set. The masses found in the blank sample were excluded from the feature list of the real river water samples. That way, 179 features were eliminated from the sample results table. One would anticipate more lost features after a blank exclusion compared with a blank subtraction, but there

actually appears to be no significant differences between both methods [36]. One other option would be to define a sample-to-blank intensity ratio. However, blank exclusion is easier to implement into automated workflows. As depicted in the RT-mass plot in Fig. 2, the remaining 1739 features can be separated into two groups: The first group represents compounds retained by the HILIC column and the second those retained by the RPLC column. Thus, the features eluting in the first section of the run were expected to be polar or very polar [8]. Accordingly, all features with RTs > 17.0 min were eliminated from the feature list. Preliminary tests showed that the last very polar reference compound eluted from the HILIC column at that time (ESM Table S3).

The RPLC fraction of features that were detected by the serial coupling was not further considered in this study. Consequently, the instrumental setup implicitly set boundary conditions that could be used as a filter criterion with respect to the research question at hand.

Features able to be found in fewer than three different water samples were excluded in a further filter step prior to the database search. Although triplicates are in contemporary nontarget analysis considered to be the optimal with regard to replicate injections [36], each sample was measured only once. An elevated number of samples in addition to the already high data output of a nontargeted HRMS screening requires measures for increasing the feasibility of studies while simultaneously minimizing the number of false positive allocations. In the aforementioned study from 2015, the statistical need for triplicate injections of the same sample was not clearly proven and, further, single measurements reduce the expenditure of measurement time and resources. Instead, a threshold for features was introduced specifying the minimum number of appearances across all samples. The approach of filtering by “detection frequency” in real samples has been successfully applied in order to prioritize features for further investigations under different research questions [37, 38]. It works well for large sample sets, as was the case in this study, because eleven locations were sampled at several dates over 1 year (see ESM Table S1). In addition to the binning and alignment of peaks within a sample group, such a detection frequency threshold introduces more statistical confidence to a feature. However, this approach is not applicable in all situations since, for example, short-term emission of TOxCs from point sources will be missed. The number of eligible features was reduced to 408 after removing those eluting later than 17.0 min and those that were detected in fewer than three samples.

### (Tentative) compound identification in water samples

#### Inquiry of a compound database

These features were uploaded to the open-access platform FOR-IDENT handling the compound database STOFF-

IDENT. Providing physicochemical properties of more than 11,000 anthropogenic compounds, this database was developed to support identification of pollutants and emerging contaminants relevant to the aquatic environment [39]. The database search was performed based on accurate mass  $\pm 10$  ppm on the platform. Thus, 132 features were successfully located in the database, and 287 anthropogenic trace organic compounds suggested. The difference derives from the given mass window, so multiple compounds were matched with a single feature. In some cases, it was the other way around: Various features were assigned to one compound. A list of compounds was proposed together with information on their polarity expressed by pH-dependent  $\log D$  value. The list served as a basis for further filtering and investigation of the underlying peaks.

### Polarity filtering of the FOR-IDENT results

Due to the complex retention mechanism of HILIC, the relationship between the analytes' RTs and the related  $\log D$  values has yet to be determined in detail. However, Bieber et al. tested a mix of 262 standard compounds on the RPLC-HILIC coupling and found that all of the 136 compounds that eluted from the HILIC column have a negative  $\log D$  value [8]. In the current investigation, this was also true for the 25 reference compounds that eluted earlier than 17.0 min (ESM Table S3). Knowing that, 287 database hits were filtered for compounds that have a  $\log D$  value  $< 0$  at a pH value 7. One hundred nine remaining compound candidates had polar to very polar properties as indicated by their negative  $\log D$  values and consequently were expected to elute from the HILIC column.

### Manual evaluation

Finally, the 68 features that led to the 109 candidates were manually reevaluated in order to ensure that they originated from chromatographically acceptable peaks. For a feature to be classified as "acceptable," it had to fulfill the following criteria:

- The spread of relative mass differences within the compound bin of the feature is lower than  $\pm 10$  ppm.
- The chromatographic peaks are approximately Gaussian shaped.
- Each peak's mass spectrum comprises at least two ions to increase the reliability of single features.
- For at least one chromatographic peak in the compound bin, the peak's mass spectrum displays an isotopic pattern.

Our approach assigned 64 PMT/vPvM candidates to 46 features (Table 2) detected in Isar river samples from March, May, and July of 2015. The numerous filtering steps for feature lists throughout this workflow reduced the effort of manually evaluating chromatographic peaks. Nevertheless, 18 features had multiple components allocated to them. That number could probably have been reduced by comparing MS/MS spectra. A validation with reference standards is still pending at this time.

The spatial and temporal distribution of these features across all 33 samples is illustrated in Fig. 3. The study indicates that the overall number of features in the Isar river was significantly higher in March than in May or July of 2015. This result could be attributed to a concentration effect due to a relatively low precipitation (26 mm) in February of the same year. In contrast, there

**Fig. 3** Spatial distribution along the Isar river of 46 features found in 33 environmental samples of 2015. They represent the portion of features that eluted from the HILIC column and have a database match with a  $\log D < 0$  at pH 7

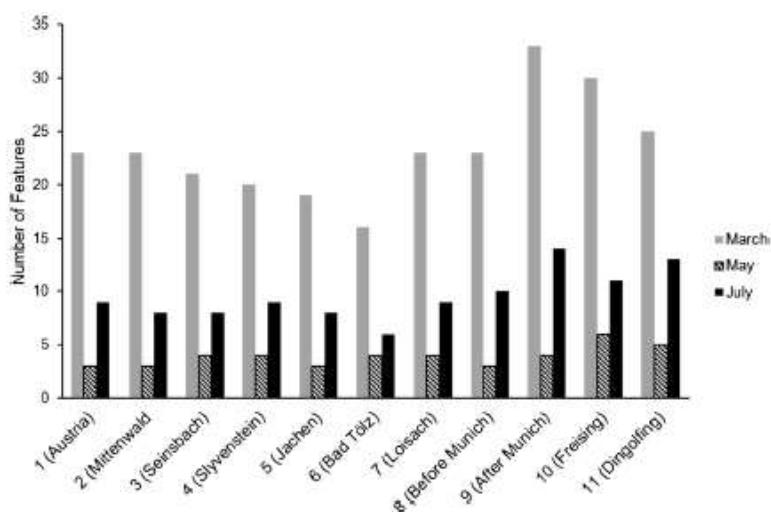
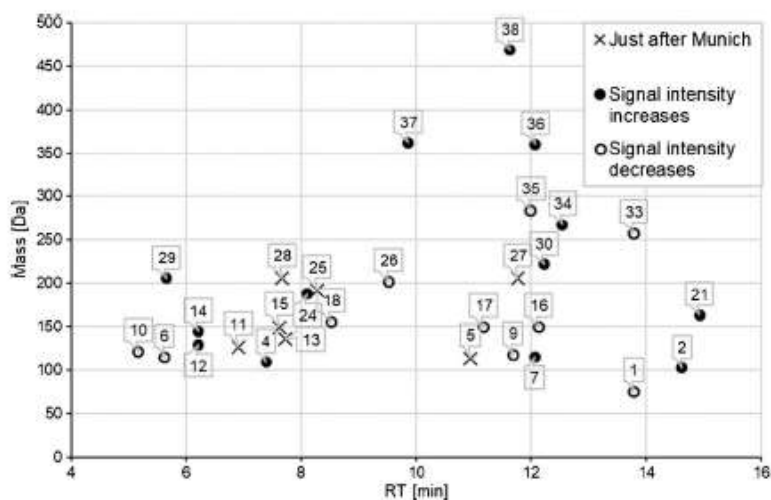


**Fig. 4** The dot plot shows features that were detected in the March samples either upstream or downstream of Munich (circles, location IDs 8 and 9, Table S1) or just downstream of Munich (crosses). The features eluted from the HILIC column and were proposed by the STOFF-IDENT database. Only matches with a negative log *D* value were considered. The numbers indicate the ID of the database queries as are listed in Table 2



were 80 mm and 58 mm of rainfall in April and May, respectively (measured in Garmisch by the Bavarian State Ministry for the Environment) [40]. However, in all campaigns, the number of features sharply increased downstream of the city of Munich. As an example, the dot plot in Fig. 4 shows the polar features detected in March around Munich. It indicates whether the feature's absolute abundance increases or decreases downstream of Munich. Even though no definite quantitative statement can be made, comparing the signal intensities at different locations or dates could help in prioritizing features. For example, the peak height of the feature with the mass/RT coordinate (102.0547 Da/14.62 min) increased by a factor of 34. The compound proposed for that feature (ID 2 in Table 2) by the STOFF-IDENT database was guanylurea, which is an aerobic bacterial degradation product of the antidiabetic drug metformin [41]. Since guanylurea is stable against further photo- and biodegradation, it distributes over the entire regional water cycle, to such an extent that it has already been detected in the North Sea [42].

### Confirmation using a reference standard

By using the feature's signal intensity for rudimentary prioritization, we uncovered guanylurea (ID 2) as a compound of interest because its signal intensity increased significantly downstream of the city of Munich. In order to achieve a higher level of confidence in compound identification, a reference standard was measured under the same chromatographic and mass spectrometric conditions. Additionally, melamine (ID 11) and 1,3-dimethylimidazolidin-2-one (DMI, ID 6) were exemplarily confirmed by matching their RT and accurate mass matching with the respective reference standards. The respective EICs (Figs. S1–S3) and isotopic ratios (Table S8) are provided in the ESM. The information is summarized in Table 3. In each case, the RT deviation was below 5%, and the mass difference was below 5 ppm. MS/MS matching would be additionally required for a level 1 identification according to Schymanski et al. [43].

However, validation by means of RT and MS matching could resolve ambiguous allocations, as the example of melamine shows: For the three features A (126.0655 Da/6.9 min),

**Table 3** Three tentative compounds found by the nontarget screening approach that were confirmed via RT and accurate mass matching with a reference standard. For each compound, the monoisotopic mass of the underlying feature is shown as well as the mass difference. The reference

RT is the mean value of the reference standard's RT measured *n* times.  $\Delta$ RT describes the RT deviation of the molecular feature from the reference standard

Name	InChi key	Elemental formula	Log <i>D</i> (pH 7)	Monoisotopic mass (Da)	Mass difference (ppm)	Reference RT (min)	$\Delta$ RT (%)
Guanylurea	BKMMTJMQCTUHRP-UHFFFAOYSA-N	C <sub>2</sub> H <sub>6</sub> N <sub>4</sub> O	-2.1	102.0542	4.9	14.4 ( <i>n</i> = 5)	1.4
Melamine	JDSHMPZPIAZGSV-UHFFFAOYSA-N	C <sub>3</sub> H <sub>6</sub> N <sub>6</sub>	-2.0	126.0654	0.8	7.0 ( <i>n</i> = 5)	-1.3
1,3-Dimethylimidazolidin-2-one	CYSGHNMQYZDMIA-UHFFFAOYSA-N	C <sub>5</sub> H <sub>10</sub> N <sub>2</sub> O	-0.6	114.0793	1.8	5.9 ( <i>n</i> = 2)	-4.8

B (126.0651 Da/7.2 min), and C (126.0665 Da/8.4 min), the STOFF-IDENT database output was melamine. The RT of the reference standard of 7.0 min closely matched the RT of feature A. In addition, the absolute mass deviation of 0.0001 Da was the lowest of the three.

The feature of guanylurea was detected 13 times in total at locations 2, 7, 8, 9, and 10 (ESM Table S1).

The feature allocated to melamine was found in four samples at locations 9, 10, and 11. The findings are in line with the expectation that pharmaceuticals and their transformation products primarily occur downstream of urban areas.

One newfound polar substance of emerging interest is 1,3-dimethylimidazolidin-2-one (DMI). The feature of DMI was detected in all eleven samples from March 2015 and compared with the reference standard. It is a high-boiling aprotic solvent that, according to the European Chemicals Agency (ECHA), is used in pH regulators, water treatment products, and laboratory chemicals. It is registered by six active suppliers under REACH and 100–1000 t is brought into the European Economic Area per year. The Predicted No-Effect Concentration in freshwater is  $100 \mu\text{g L}^{-1}$  [44]. To the best of our knowledge, there is currently no detailed information available regarding the occurrence and distribution of DMI in the aquatic environment.

**Acknowledgments** We would like to thank the “Westfälische Wasser- und Umweltanalytik GmbH” for financial support and Dr. Andre Liesener for fruitful discussions. Moreover, the authors are thankful to Stefan Moser for software support and scientific solutions. Particular thanks go to Prof. Dr.-Ing. Jörg E. Drewes, Dr. Giorgia Greco, and various colleagues at the “Chair of Urban Water Systems Engineering” for their contributions and support. Finally, we appreciate the reviewers’ detailed comments and suggestions.

**Funding information** This study received financial support from the German Federal Ministry of Education and Research for funding FOR-IDENT (02WRS1354A) and FOR-IDENT - Nachhaltigkeit (02WRS1456).

## Compliance with ethical standards

**Conflict of interest** The authors declare that they have no conflict of interest.

## References

- Schwarzenbach RP, Escher BI, Fenner K, Hofstetter TB, Johnson CA, von Gunten U, Wherli B. The challenge of micropollutants in aquatic systems. *Science*. 2006;313(80-):1072–1077.
- German Environment Agency (UBA) Protecting the sources of our drinking water - the criteria for identifying persistent, mobile, and toxic (PMT) substances and very persistent, and very mobile (vPvM) substances under EU REACH Regulation (EC) No 1907. 2006.
- Schmidt TC. Recent trends in water analysis triggering future monitoring of organic micropollutants. *Anal Bioanal Chem*. 2018;410:3933–41.
- Comero S, Loos R, Carvalho R, Anto DC, Locoro G, Tavazzi S, et al. EU-wide monitoring survey on emerging polar organic contaminants in wastewater treatment plant effluents. *Water Res*. 2013;47:6475–87. <https://doi.org/10.1016/j.watres.2013.08.024>.
- Boxall A, Sinclair C, Fenner K, Koplin D, Maund S. When synthetic chemicals degrade in the environment. *Environ Sci Technol*. 2004;38:368–75. <https://doi.org/10.1117/1.3589100>.
- Reemtsma T, Weiss S, Mueller J, Petrovic M, Gonzalez S, Barcelo D, et al. Polar pollutants entry into the water cycle by municipal wastewater: a European perspective. *Environ Sci Technol*. 2006;40:5451–8. <https://doi.org/10.1021/es060908a>.
- Reemtsma T, Berger U, Arp HPH, Gallard H, Knepper TP, Neumann M, et al. Mind the gap: persistent and mobile organic compounds - water contaminants that slip through. *Environ Sci Technol*. 2016;50:10308–15. <https://doi.org/10.1021/acs.est.6b03338>.
- Bieber S, Greco G, Grosse S, Letzel T. RPLC-HILIC and SFC with mass spectrometry: polarity-extended organic molecule screening in environmental (water) samples. *Anal Chem*. 2017;89:7907–14. <https://doi.org/10.1021/acs.analchem.7b00859>.
- Chalcraft KR, McCarty BE. Tandem LC columns for the simultaneous retention of polar and nonpolar molecules in comprehensive metabolomics analysis. *J Sep Sci*. 2013;36:3478–85. <https://doi.org/10.1002/jssc.201300779>.
- Hemström P, Irgum K. Hydrophilic interaction chromatography. *J Sep Sci*. 2006;29:1784–821. <https://doi.org/10.1002/jssc.200600199>.
- Alpert AJ. Hydrophilic-interaction chromatography for the separation of peptides, nucleic acids and other polar compounds. *J Chromatogr A*. 1990;499:177–96. [https://doi.org/10.1016/S0021-9673\(00\)96972-3](https://doi.org/10.1016/S0021-9673(00)96972-3).
- Berthod A, Chang SSC, Kullman JPS, Armstrong DW. Practice and mechanism of HPLC oligosaccharide separation with a cyclodextrin bonded phase. *Talanta*. 1998;47:1001–12. [https://doi.org/10.1016/S0039-9140\(98\)00179-9](https://doi.org/10.1016/S0039-9140(98)00179-9).
- McCalley DV. Study of the selectivity, retention mechanisms and performance of alternative silica-based stationary phases for separation of ionised solutes in hydrophilic interaction chromatography. *J Chromatogr A*. 2010;1217:3408–17. <https://doi.org/10.1016/j.chroma.2010.03.011>.
- Tang Y, Xu Y, Li F, Jmaiff L, Hrudey SE, Li X. Nontargeted identification of peptides and disinfection byproducts in water. *J Environ Sci*. 2016;42:259–66.
- Greco G, Grosse S, Letzel T. Robustness of a method based on the serial coupling of reversed-phase and zwitterionic hydrophilic interaction LC – MS for the analysis of phenols. *J Sep Sci*. 2014;37:630–4. <https://doi.org/10.1002/jssc.201301112>.
- Greco G, Grosse S, Letzel T. Serial coupling of reversed-phase and zwitterionic hydrophilic interaction LC/MS for the analysis of polar and nonpolar phenols in wine. *J Sep Sci*. 2013;36:1379–88. <https://doi.org/10.1002/jssc.201200920>.
- Hernández F, Pozo JÓ, Sancho JV, López FJ, Harín JM, Ibáñez M. Strategies for quantification and confirmation of multi-class polar pesticides and transformation products in water by LC – MS 2 using triple quadrupole and hybrid quadrupole time-of-flight analyzers. *Trends Anal Chem*. 2005;24:596–612. <https://doi.org/10.1016/j.trac.2005.04.007>.
- Krauss M, Singer H, Hollender J. LC – high resolution MS in environmental analysis: from target screening to the identification of unknowns. 2010:943–51. <https://doi.org/10.1007/s00216-010-3608-9>.

19. "Non-Target Screening" expert committee of the German Water Chemistry Society. Use of non-target screening by means of LC-ESI-HRMS in water analysis, 1.0. 2019.
20. Kind T, Fiehn O. Metabolomic database annotations via query of elemental compositions: mass accuracy is insufficient even at less than 1 ppm. *BMC Bioinformatics*. 2006;1–10. <https://doi.org/10.1186/1471-2105-7-234>.
21. Little JL, Williams AJ, Pshenichnov A, Tkachenko V. Identification of "known unknowns" utilizing accurate mass data and chemspider. *J Am Soc Mass Spectrom*. 2012;23:179–85. <https://doi.org/10.1007/s13361-011-0265-y>.
22. Letzel T, Bayer A, Schulz W, Heemann A, Lucke T, Greco G, et al. LC – MS screening techniques for wastewater analysis and analytical data handling strategies: Sartans and their transformation products as an example. *Chemosphere*. 2015;137:198–206. <https://doi.org/10.1016/j.chemosphere.2015.06.083>.
23. Fisher RA. The arrangement of field experiments. *J Minist Agric Gt Britain*. 1926:505–13. [https://doi.org/10.1007/978-1-4612-4380-9\\_8](https://doi.org/10.1007/978-1-4612-4380-9_8).
24. Plackett RL, Burman JP. The design of optimum multifactorial experiments. *Biometrika*. 1946;33:305–25.
25. Goss K-U, Schwarzenbach RP. Linear free energy relationships used to evaluate equilibrium partitioning of organic compounds. 2001;35:1–9. <https://doi.org/10.1021/es000996d>.
26. Agilent Technologies. Agilent 6230B Accurate-Mass TOF LC / MS Data Sheet. 5991-1347EN, 2012.
27. Agilent Technologies. MassHunter Profinder Software, Quick Start Guide. G3835-90027 31–32. 2016.
28. Open Access Platform FOR-IDENT. <https://www.for-ident.org/>. Accessed 28 Oct 2019.
29. Compound Database STOFF-IDENT. <https://www.lfu.bayern.de/stoffident/#home>. Accessed 28 Oct 2019.
30. Karakurt S, Schmid L, Hu U, Drewes JE. Dynamics of wastewater effluent contributions in streams and impacts on drinking water supply via riverbank filtration in Germany - a national reconnaissance. *Environ Sci Technol*. 2019;53:6154–61. <https://doi.org/10.1021/acs.est.8b07216>.
31. Golub GH, Heath M, Wahba G. Generalized cross-validation as a method for choosing a good ridge parameter. *Technometrics*. 1979;21:215–23. <https://doi.org/10.1080/00401706.1979.10489751>.
32. Schollée JE, Schymanski EL, Hollender J. Statistical approaches for LC-HRMS data to characterize, prioritize, and identify transformation products from water treatment processes. In: ACS Symposium Series; 2016. p. 45–65.
33. Smith CA, Want EJ, O'Maille G, Abagyan R, Siuzdak G. XCMS: processing mass spectrometry data for metabolite profiling using nonlinear peak alignment, matching, and identification. *Anal Chem*. 2006;78:779–87. <https://doi.org/10.1021/ac051437y>.
34. Eliasson M, Rännar S, Madsen R, Donten MA, Marsden-Edwards E, Moritz T, et al. Strategy for optimizing LC-MS data processing in metabolomics: a design of experiments approach. *Anal Chem*. 2012;84:6869–79. <https://doi.org/10.1016/j.jpchem.2011.11.009>.
35. Zheng H, Clausen MR, Dalsgaard TK, Mortensen G, Bertram HC. Time-saving design of experiment protocol for optimization of LC-MS data processing in metabolomic approaches. *Anal Chem*. 2013;85:7109–16. <https://doi.org/10.1021/ac4020325>.
36. Nürenberg G, Schulz M, Kunkel U, Temes TA. Development and validation of a generic nontarget method based on liquid chromatography - high resolution mass spectrometry analysis for the evaluation of different wastewater treatment options. *J Chromatogr A*. 2015;1426:77–90. <https://doi.org/10.1016/j.chroma.2015.11.014>.
37. Zonja B, Delgado A, Pérez S, Barceló D. LC-HRMS suspect screening for detection-based prioritization of iodinated contrast media photodegradates in surface waters. *Environ Sci Technol*. 2015;49:3464–72. <https://doi.org/10.1021/es505250q>.
38. Müller A, Schulz W, Ruck WKL, Weber WH. A new approach to data evaluation in the non-target screening of organic trace substances in water analysis. *Chemosphere*. 2011;85:1211–9. <https://doi.org/10.1016/j.chemosphere.2011.07.009>.
39. Huckle S, Track T. Risk management of emerging compounds and pathogens in the water cycle (RISKWa). *Environ Sci Eur*. 2013;25:1.
40. Bavarian State Ministry for the Environment Precipitation Gammisch-Partenkirchen-Griesen. <https://www.gkd.bayern.de/en/meteo/precipitation/isar/gammisch-partenkirchen-griesen-6307/download>. Accessed 29 Oct 2019.
41. Trautwein C, Kümmerer K. Incomplete aerobic degradation of the antidiabetic drug metformin and identification of the bacterial dead-end transformation product guanlylurea. *Chemosphere*. 2011;85:765–73. <https://doi.org/10.1016/j.chemosphere.2011.06.057>.
42. Trautwein C, Berset J, Wolschke H, Kümmerer K. Occurrence of the antidiabetic drug metformin and its ultimate transformation product guanlylurea in several compartments of the aquatic cycle. *Environ Int*. 2014;70:203–12. <https://doi.org/10.1016/j.envint.2014.05.008> 0160–4120©.
43. Schymanski EL, Jeon J, Gulde R, Fenner K, Ruff M, Singer HP, et al. Identifying small molecules via high resolution mass spectrometry: communicating confidence. *Environ Sci Technol*. 2014;48:2097–8. <https://doi.org/10.1021/es5002105>.
44. European Chemicals Agency Brief Profile of 1,3-dimethylimidazolidin-2-one. <https://echa.europa.eu/brief-profile/-/briefprofile/100.001.187>. Accessed 29 Oct 2019.

**Publisher's note** Springer Nature remains neutral with regard to jurisdictional claims in published maps and institutional affiliations.

## **Appendix A.2 (Very) polar organic compounds in the Danube river basin: a non-target screening workflow and prioritization strategy for extracting highly confident features**

The following research article has undergone a peer-review process and has been previously published as presented below.

Reference: Minkus S, Bieber S, Letzel T (2021) (Very) polar organic compounds in the Danube river basin: Non-target screening workflow and prioritization strategy for extracting highly confident features. *Anal Methods* 13:2044–2054. <https://doi.org/10.1039/D1AY00434D>.



Cite this: DOI: 10.1039/d1ay00434d

## (Very) polar organic compounds in the Danube river basin: a non-target screening workflow and prioritization strategy for extracting highly confident features†

Susanne Minkus,<sup>ab</sup> Stefan Bieber<sup>id b</sup> and Thomas Letzel<sup>id \*ab</sup>

Recently, more and more research has been focused on the analysis of polar organic compounds as they tend to be persistent and mobile in the aquatic environment. The serial coupling of reversed-phase and hydrophilic interaction liquid chromatography allows the separation of analytes of an extended polarity range within a single run. The non-target screening approach was driven by high-resolution mass spectrometry and is able to detect unexpected compounds. It is therefore capable of complementing regular monitoring of surface water. Non-target screening, however, can produce massive data sets. Here, a data processing method is presented focusing on unravelling tentative polar compounds from the full scan data of 51 samples of the Danube river and its tributaries. The feature extraction method was optimized to 34 reference compounds at two concentration levels and was then applied to real samples. Features were matched by accurate mass with anthropogenic substances stored in the compound database STOFF-IDENT located on the FOR-IDENT platform. In order to extract polar candidates, the retention time interval corresponding to the HILIC separation was connected to compounds with a negative  $\log D$  value. As a result, 67 candidates were detected which were found to be plausible. Finally, features were prioritized based on an identification certainty classification system as well as their frequency of occurrence. Therefore, several feature-candidate compound pairs could be suggested for confirmation *via* reference materials. The presented non-target screening strategy followed by a database query is transferrable to other sample sets and other data evaluation tools.

Received 15th March 2021  
Accepted 22nd March 2021DOI: 10.1039/d1ay00434d  
rsc.li/methods

### Introduction

The occurrence of anthropogenic micropollutants in ground and surface water has been of major public concern for decades now.<sup>1,2</sup>

Therefore, the water quality is monitored and regulated with the objective of assessing and minimizing risks for the environment and human health. The International Commission for the Protection of the Danube River (ICPDR) sets an example of complementing routine monitoring activities by conducting a periodic survey, the Joint Danube Survey (JDS). This survey was last completed in 2015 (ref. 3) and recently repeated for the fourth time. Its purpose is to collect additional data that are comparable across all adjacent countries and create a basis for harmonizing methods and raising public awareness.

The better understanding of the introduction and fate of chemical compounds of anthropogenic origin into the environment, along with analytical advances, led to an ever-increasing number of detected compounds and newly identified environmentally relevant compound classes. Among them is a particularly concerning group of polar molecules appearing to be “persistent in the environment, mobile in the aquatic environment, and toxic” (PMT) or “very persistent in the environment and very mobile in the aquatic environment” (vPvM).<sup>4</sup> Technical barriers in wastewater treatment plants (WWTPs) struggle to retain polar micropollutants, which then enter surface water.<sup>5</sup> Loos *et al.* analyzed more than 100 European rivers for the presence of 35 polar compounds and showed that the average percentile frequency detecting all compounds was at 61%.<sup>6</sup> There is a rapidly increasing number of publications and studies documenting the presence of new, so far unexpected polar compounds in the aquatic environment.<sup>7,8</sup> Since environmental waterbodies can serve as a source for drinking water, polar organic compounds can also impair drinking water quality and might become a concern for human health.

Non-target screening (NTS) is a useful strategy to monitor the occurrence of unexpected or unknown compounds in water

<sup>a</sup>Technical University of Munich (Chair of Urban Water Systems Engineering), Garching, Germany

<sup>b</sup>Analytisches Forschungsinstitut für Non-Target Screening GmbH (AFIN-TS), Augsburg, Germany. E-mail: t.letzel@afin-ts.de

† Electronic supplementary information (ESI) available. See DOI: 10.1039/d1ay00434d

## Analytical Methods

samples. Currently, NTS is mostly performed using reversed-phase liquid chromatography (RPLC) coupled to mass spectrometry (MS),<sup>2</sup> allowing the detection of medium polar to nonpolar organic compounds in aqueous samples. Analytical techniques like hydrophilic interaction chromatography (HILIC) combined with MS facilitate the detection of (very) polar molecules in environmental water samples.<sup>9–12</sup>

The screening of unknowns was enabled by high-resolution mass spectrometry (HRMS) which allows the accurate detection of a broad range of masses with high resolving power in a short time interval necessary for chromatographic separation.<sup>13,14</sup>

To reduce raw HRMS data to plausible molecular candidates, here referred to as features, requires specialized and robust data evaluation workflows. The main challenge therefore is to identify relevant signals in an extensive set of complex data.

When querying online compound databases such as PubChem<sup>15</sup> with over 100 million listed compounds, a feature's accurate mass alone does not suffice as a search parameter. Therefore, additional amenable information on an investigated sample and a detected feature needs to be considered and can, for instance, be connected to the physicochemical properties of a candidate substance. Thus, consistently using mass spectrometric fragmentation patterns and/or retention behavior of a feature can help to significantly reduce the number of compounds assigned to a feature. Furthermore, relying on selective databases for compounds relevant for the aquatic environment could narrow down tentative annotations to a feature. Integrating such a selective compound database into a NTS workflow helps customizing it to its area of application and thus making it more feasible for a routine environment. However, there are other NTS workflow solutions, for instance when discovering novel environmentally relevant chemicals, which require more comprehensive databases. In each case, unambiguous identification of a feature can only be completed by confirmation with a reference standard.

Including polar molecules into an NTS-based monitoring strategy adds to the already existing challenges at the level of data evaluation and interpretation. As a consequence, available analysis tools need to be adjusted to the specific research question at hand, such as finding polar organic molecules in aqueous environmental samples.<sup>11</sup>

Key for a streamlined identification of polar molecules is a transparent and specialized feature extraction workflow followed by a compound database query. It should include filters for highly confident features which are worth validating with reference standards. This can be realized by using specific compound database queries and a ranking of retrieved candidates, on the basis of further information on the sample and analysis (meta-data).

In this study, a robust data evaluation workflow is presented with a specially designed prioritization strategy for the identification of polar molecules in samples from the Danube river basin, analyzed by polarity-extended chromatography coupled to tandem HRMS. The term "polar molecules" as it is used here describes small organic molecules (<1000 Da), which have a negative octanol–water partition coefficient (log *D* value) at a pH of 7.

## Experimental

## Chemicals

LC-MS grade water and acetonitrile were purchased from Supelco (Darmstadt, Germany) and Honeywell (Morristown, New Jersey, U.S.A), respectively. Ammonium acetate was obtained from Sigma Aldrich (St. Louis, Missouri, U.S.A). All target substances had a purity of ≥95% and were bought from ACROS organics (Thermo Fisher Scientific; Geel, Belgium), Alfa Aesar (Thermo Fisher Scientific; Karlsruhe, Germany), Cayman Chemical Company (Ann Arbor; Michigan, U.S.A), Fluka (Buchs, Switzerland), Merck KGaA (Darmstadt, Germany) and Sigma Aldrich (St. Louis, Missouri, U.S.A).

Standard compounds were handled as individual stock solutions in acetonitrile/water (50/50, v/v) at a concentration of 1 mM. A multicomponent standard of 100 components (listed in Table S1 of the ESI†) was prepared in acetonitrile at a concentration of 10 μM (0.7–4.4 mg L<sup>-1</sup>). A subset of 34 standard compounds (Table S2†) was diluted with tap water to obtain two so-called synthetic samples at a lower concentration level (10 nM; *c*<sub>1</sub> = 1.0–8.8 μg L<sup>-1</sup>) and a higher concentration level (100 nM; *c*<sub>1</sub> = 10.0–87.6 μg L<sup>-1</sup>). All solutions were refrigerated at 4 °C until use.

## Targeted analysis

To assess the instrumental performance and optimize the following non-target feature extraction method, a two-step targeted analysis was carried out. The standard compounds were selected to represent environmentally relevant and polar trace organic compounds. They covered compounds with log *D* values between –5.9 and 1.6 (pH 7) and a mass range of 74 Da to 440 Da. For the first step, three replicate injections of the multicomponent standard were performed, one after each pass of the sample batch, in order to evaluate the retention time (RT) repeatability.

In a separate analysis, both synthetic samples were measured in triplicates along with a tap water blank. Subsequently, the peak duration, full width at half maximum (FWHM), peak height and the respective deviations, RT precision, and mass precision as well as mass accuracy were determined for each compound. The precision measures the variability of experimental values around the mean and was expressed by the standard deviation (SD), relative standard deviation (RSD) and the maximum difference within a technical replicate. Assessing the precision of multiple replicate measurements made under similar conditions allows drawing conclusions on the short-term repeatability of an instrumental setup. The accuracy, in turn, is a measure of proximity of the experimental value, *i.e.* the detected mass, to the true value, *i.e.* the exact mass of a target compound, expressed in parts per million (ppm).

## Samples

The Danube and its major tributaries were sampled in the course of the fourth Joint Danube Survey (JDS4), conducted in 2019. Grab samples for direct injection were collected at 51 sites

(Table S3, ESI<sup>†</sup>) and 20 mL aliquots were sent to our laboratory.<sup>16</sup> The samples were stored at 4 °C and filtered (0.22 µM, PVDF; Berrytec, Gruenwald, Germany) shortly before analysis.

### RPLC-HILIC-ESI-QTOF-MS measurements

Chromatographic separation was performed on a serial coupling of RPLC and HILIC columns, a detailed description of which is presented in a previous study.<sup>17</sup>

In brief, two Agilent LC-systems of the 1260 Infinity series (Waldbronn, Germany) consisting of a binary pump, an online degasser and a mixing chamber were used. The RP analytical column was a Poroshell 120 EC-C18 (50.0 × 3.0 mm, 2.7 µm; Agilent Technologies). The respective mobile phase, delivered by the first pump, was a mixture of 10 mM ammonium acetate containing aqueous solution and acetonitrile at volumetric ratios of 90/10 and 10/90, respectively. The HILIC separation was carried out on a ZIC-HILIC column (150.0 × 2.1 mm, 5 µm, 200 Å; Merck Sequant, Umea, Sweden) and for the mobile phase acetonitrile and water were used. Both columns as well as the second binary pump were connected by a T-piece with mixing frit (Upchurch, IDEX Europe GmbH, Erlangen, Germany). The gradient elution method is published elsewhere.<sup>10,11</sup> The injection volume of each sample was 10 µL.

The chromatographic setup was connected to a quadrupole time-of-flight mass spectrometer (QTOF-MS; Sciex TripleTOF series 4600) equipped with a DuoSpray<sup>TM</sup> ion source with a TurboIonSpray<sup>®</sup> probe for electrospray ionization (Sciex, Darmstadt, Germany). Non-target screening data were obtained by screening a mass range of 65–1000 Da in full scan mode at a scan time of 1.10 s and an accumulation time of 0.25 s (survey scan). In order to gather fragmentation information, MS2 spectra were recorded using eight parallel product ion scans. They were triggered if an ion, monitored during the survey scan, exceeded a signal intensity increase threshold of 50 counts per second (cps), a method referred to as information-dependent acquisition (IDA). A maximum of eight candidate ions were monitored per cycle. The former product ion was excluded from IDA for 7 s. IDA experiments were conducted with a collision energy of 40 ± 20 eV and an accumulation time of 0.10 s. The ESI probe operated in positive ionization mode only, and the spray parameters were optimized in a preliminary study to the following values: nebulizer gas 44 psi, curtain gas 29 psi, heater gas 50 psi, ion spray voltage floating 200 V, temperature 650 °C and declustering potential 46 V.<sup>18</sup> The instrument was recalibrated automatically after five measurements using an atmospheric pressure chemical ionization (APCI) probe integrated into the same source housing as the ESI probe. The data were acquired using Analyst TF software (Sciex; version 1.7.1).

### Data handling

The HRMS raw data files were converted to the open mzML format by using the ProteoWizard's msConvert module (version 3.0.20229-f269cc95b).<sup>19</sup> Spectra were centroided using the "peakPicking" filter, whereas all MS levels were considered.

For both targeted and non-targeted data analysis, MZmine 2 (ref. 20) software was used.

The newly developed NTS data processing workflow for the 51 JDS4 samples is depicted in Fig. 1.

The first part of the NTS data analysis comprised the feature extraction from HRMS full scan data: for constructing extracted ion chromatograms (EICs) and deconvoluting chromatographic peaks, the algorithms of the "Automated Data Analysis Pipeline" (ADAP) workflow<sup>21</sup> were used. Furthermore, a Savitzky-Golay filter was applied for smoothing the EICs. Chromatographic peaks were aligned across the technical replicates and features which were recognized in less than three samples were filtered out. Subsequently, the feature list was reduced by isotopes as well as sodium, potassium and ammonium adducts belonging to a singly protonated molecular ion. The exact parameter settings of the feature extraction method are given in Table S4 of the ESI<sup>†</sup>. Blank samples were treated equally throughout the feature extraction process and were finally compared to the real samples for blank exclusion based on RT and accurate mass.

Detected features were annotated to chemical structures using the compound database STOFF-IDENT (SI).<sup>22</sup> MS2 spectra were predicted by using MetFrag (version 2010).<sup>23</sup> Both tools are implemented into the FOR-IDENT platform (FI).<sup>24</sup> A pH value of 7 and a mass tolerance of 5 ppm for precursor ions as well as fragment ions were specified as input parameters. The feature annotation process is shown schematically in Fig. 1.

Software used for further processing of feature and candidate lists included Microsoft Excel (version 2002), Notepad++ (version v7.8.9) and RStudio (version 1.3.959).

## Results and discussion

In this study, a data processing strategy was developed to identify polar, environmentally relevant and organic molecules. The concept was further optimized and deployed on real samples proving it to be a universal NTS workflow for a wide scope of applications. Therefore, 51 surface water samples of the Danube river and its tributaries were measured by polarity-extended chromatography coupled to HRMS. Features were extracted from the raw data in a non-targeted manner followed by a compound assignment step (Fig. 1). Afterwards, prioritized candidates were picked out of the final feature list to be first in line for confirmation *via* reference standards. In the following, the individual steps are detailed in a chronological order.

### NTS data processing workflow

The non-targeted feature extraction workflow was constructed according to the scheme in Fig. 1. Masses were detected and grouped together in order to build EICs and chromatographic peaks deconvoluted within the RT interval between 5 and 15 min. During this time period, polar compounds elute from the HILIC column as part of the polarity-extended chromatographic setup.

Features detected in less than three technical replicates of each sample were removed. Furthermore, features were excluded from a sample's feature list if they were present in the blank sample. After redundant peaks, namely isotopes and

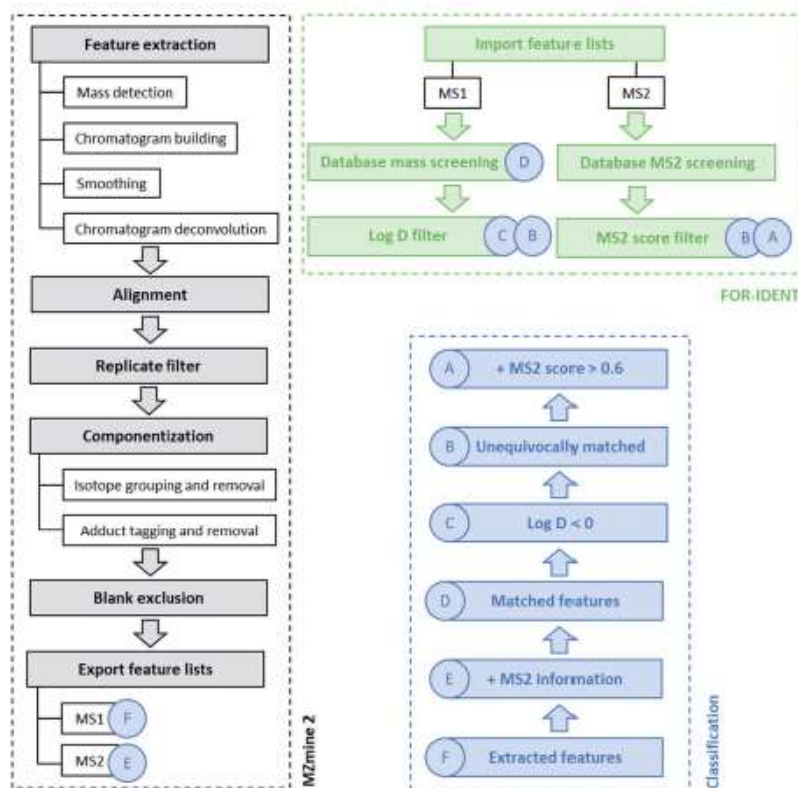


Fig. 1 Schematic display of the data processing workflow. The feature extraction is depicted in black boxes, the feature allocation process in green boxes and the classes in blue circles. Features were matched with candidate substances using the STOFF-IDENT compound database on the FOR-IDENT platform.

adducts, were removed, 45 to 146 different features were extracted from each sample.

The feature extraction from HRMS raw data was followed by the allocation of compound candidates, as depicted by the green boxes in Fig. 1. Initially, features were matched by accurate mass with organic compounds of anthropogenic origin stored in the SI compound database on the FI platform. That way, for each feature an elemental composition was proposed, plausible for the analytical scope of the aquatic environment. Secondly, if available, a feature's fragmentation pattern was compared to the counterpart predicted by MetFrag for the suggested molecule. In case of more than one hit for a single feature, an MS2 score was assigned to each hit which is calculated from a weighted fragment peak count and the bond dissociation energy. A score close to one indicates higher structural similarity between the feature and the proposed compound.<sup>23</sup>

In the following step, the resulting candidate lists were filtered for polar molecules. Polarity is herein described by the octanol-water partition coefficient ( $\log D$ ) at a pH of 7. Even though the  $\log D$  value cannot predict the partition variability between substance classes or different natural organic phases,<sup>25</sup> using a single coefficient facilitates automated data processing. It was favoured over  $\log P$  because there is a statistically

significant difference at a reference pH of 7.4 due to the ionization of compounds.<sup>26</sup> Features eluting from the HILIC column between 5 min and 15 min are expected to be polar as was defined for the applied chromatography in a former publication.<sup>10</sup> The polarity criterion was confirmed by the 34 target analytes eluting before 15 min of which 97% had a  $\log D$  value < 0. As a result, candidate lists were filtered for compounds with a  $\log D$  value < 0 at pH 7.

#### Setting critical parameters based on target screening data

A two-step targeted analysis was performed to gather information on the RPLC-HILIC-QTOF-MS system to

- Assess the quality of the instrumental performance in general and
- Optimize and validate the non-targeted data processing workflow.

The RT repeatability was assessed on the basis of three technical replicates of the multicomponent standard, one injection after each pass of the sample batch. The median RSD was as precise as 1% and the maximum RSD was found for histamine with a value of 5% considering 100 target compounds (compare Table S1†). We observed isolated cases where the RT of an analyte "jumps" between two distinct values. It is possible that switching from a water sample to a matrix-free

standard mixture or laboratory blank disturbs the equilibrium in the HILIC stationary phase due to unsaturated ionic interaction sites or instabilities in the water layer.<sup>27</sup>

In a second step, a targeted analysis of two synthetic samples was conducted comprising 34 HILIC standard compounds at a lower ( $c_1$ ) and a higher ( $c_2$ ) concentration level, respectively. The synthetic samples provided information on the performance of the instrumental setup necessary for setting the parameters of the feature extraction method. The median value for mass precision ( $n = 6$ ), meaning the closeness of observed masses to each other, was 3 ppm. The mass accuracy, meaning the closeness of observed masses to theoretical masses, was 14 ppm. An increased deviation of a detected mass from the target value compared to the mean value seems plausible since a continuous mass drift could be expected for the samples after each calibration, probably reinforced by the load of matrix species. Since there are no true values in an NTS approach, the precision was used to set the mass tolerance for the feature extraction method. The maximum mass difference was observed for acetyllysine and rounded up to 0.0026 Da (Table S2†). In the synthetic samples the RTs shifted less than 3% (triethylene glycol monomethyl ether) which corresponds to a RT difference of 0.61 min. However, the feature extraction method needs to account for the aforementioned kind of outlier in RT variability to reduce the risk of false negative features. Accordingly, for the tolerance threshold, a relatively conservative value of 1.60 min (which corresponds to the RT difference of histamine) was specified. Apart from the binning and alignment tolerances, other parameters critical to the feature extraction method such as the intensity threshold and the wavelet function scales for chromatogram deconvolution were optimized based on the target analytes contained in the synthetic samples (Table S2†). To this end, the total maxima and/or minima of the chromatographic peak height, peak duration and the full width at half maximum (FWHM) were determined, and the parameters were set accordingly. The more conservative approach of favouring total maxima and minima over mean values across technical replicates managed to reduce the number of false negative features by 73% in the higher concentration synthetic sample and by 63% in the lower concentration one. The different settings of the critical parameters applied for this comparison can be taken from Table S4 of the ESI†

For validation purposes, the optimized feature extraction method was applied to the synthetic samples. Looking at the final feature lists, >90% of the target compounds were recovered at the higher concentration level  $c_2$  and >60% at the lower  $c_1$  level. Then, the 34 individual analytes were tracked throughout the data processing steps and for false negative compounds the points of losses were determined (Table S5, ESI†). At the  $c_1$  level nine and at the  $c_2$  level two features tagged as targets were eliminated by the replicate filter. In all cases except for sotalol, the filter was triggered due to one or two replicate peaks of the target feature that could not be deconvoluted prior to the alignment step. These findings suggest that the difference in recovery rates originates from an increased variance in feature properties at lower concentrations. For the given non-targeted

feature extraction method, critical parameter settings were adjusted to the target analytes spiked into the synthetic samples. It should be noted that the parameter settings are an expression of a compromise considering different types of substances at different concentration levels in a complex matrix, as expected in real water samples. More stability data, including details on RPLC analytes were presented in former publications.<sup>10</sup>

### Prioritization by feature classification

After extracting features from non-targeted data, this study aims to select those feature-candidate pairs that are particularly relevant to the Danube river basin and have a high probability of further being validated successfully by a reference standard. Two main criteria for prioritization were applied in this situation:

- The class describing how confidently a feature is identified as a polar organic substance of anthropogenic origin
- The frequency of a feature occurring throughout the course of the river basin

To serve the first criterion, all features were divided into six classes, depending on how far along they had passed through the funnel of characterization certainty as shown in Fig. 1:

- Features which were unequivocally annotated by querying the compound database and were assigned an MS2 score >0.6.
- Features which were unequivocally allocated, either because the mass screening did not yield any database-stored isomers and/or differentiation by the MS2 score was possible.
- Features which were assigned at least one candidate substance with a log  $D$  value <0.
- Features which were matched with at least one compound stored in the database by accurate mass.
- Features extracted from the HRMS raw data with MS2 information available.
- Features which were extracted from the HRMS raw data following the non-targeted feature extraction workflow (black boxes in Fig. 1).

Class A as described above complies with a level 3 in identification confidence according to Schymanski *et al.*, since these features can be considered as “[...] top-ranked structures from *in silico* fragmentation of candidates from compound database searches, and/or suspects selected using additional information such as [...] retention behaviour”.<sup>28</sup> The presented workflow addresses the retention behaviour in the form of a polarity filter: in order to create meaningful feature-candidate compound pairs, the HILIC elution interval is connected to negative log  $D$  values. Thereby, class A features converge towards the more confident identification level 2.<sup>29</sup> Even though in case of this study, class E and F features were processed using the FI platform, the classification system from above is transferrable to other tools.

The classification system can be illustrated on a feature, characterized by its observed values for RT and accurate mass, as it was found in the sample JDS4-1: it was extracted from the raw data at 10.23 min and 201.1729 Da (class F) with an MS2

## Analytical Methods

spectrum assigned to it (class E). The SI database was screened for its accurate mass and returned three matches (class D): *N*-(2-hydroxyethyl)-3,5,5-trimethylhexanamide (InChIKey JECPTUXNSPVAST-UHFFFAOYSA-N), 4-hydroxy-2,2,6,6-tetramethylpiperidine-1-ethanol (STEYNUVPFMIUOY-UHFFFAOYSA-N) and 11-aminoundecanoic acid (GUOSQNAUYHMCRU-UHFFFAOYSA-N). Only the candidate 4-hydroxy-2,2,6,6-tetramethylpiperidine-1-ethanol had a negative log *D* value at a pH of 7; thus the feature qualified as class B. The list of fragment masses and respective relative intensities extracted for the feature (10.23 min/201.1729 Da) was uploaded to the FI platform. A MS2 score of 1.0 was calculated based on the *in silico* spectrum generated by the integrated MetFrag tool. With the score being >0.6, the feature-candidate compound pair met the criteria for class A.

Furthermore, Fig. 2 visualizes the number of features of the classes B–F detected in each Danube sample in relation to each other.

The differing amounts of features in the classes E and F reflect that on average 44% of features extracted by the non-targeted workflow had MS2 data available. This could be attributed to the fact that the information-dependent acquisition (IDA) method selects precursor ions for fragmentation from the survey scan based on their intensity. In this study, a minimum signal intensity of 50 cps was necessary to trigger an IDA experiment. That increases the chance for analytes with lower abundances to be sent for collision-induced dissociation. However, they compete with more matrix species present in real samples. The MS2 acquisition hit rate for IDA-based methods is

lower compared to other fragmentation methods which operate the Q1 quadrupole of the QTOF instrument at wider *m/z* precursor windows. On the other hand, the quality of MS2 spectra in terms of a high fraction of real product ions benefits from this selective fragmentation procedure.<sup>40</sup> Throughout this study, the precursor ions scheduled for IDA were frequently selected very near the beginning of a chromatographic peak. The resulting MS2 spectra were relatively low in abundance and sometimes hampered the assignment of candidate *in silico* spectra by the MetFrag tool on the FI platform. It was argued in a preceding publication and reconfirmed here that the full scan acquisition on the MS1 level is essentially the core of a non-target screening approach.<sup>11</sup> Nevertheless, of all unequivocally allocated features (class B), four candidates were confirmed by a MS2 matching, meaning that they scored an MS2 congruence of >0.6 (Table 1). The corresponding features were assigned to class A and were consequently attributed high priority for further validation.

## Binary trends along the Danube river

The spatial binary trends of the different classes are displayed in Fig. 2. Herein a binary trend describes the presence or the absence of a feature at a sampling site rather than the spatial development of a continuous variable attributed to a feature, such as its signal intensity. The binary trends along the Danube river of features classified as C or higher, which implicitly have a negative log *D*, could point to potential sources emitting polar trace organic substances. For example, a significant

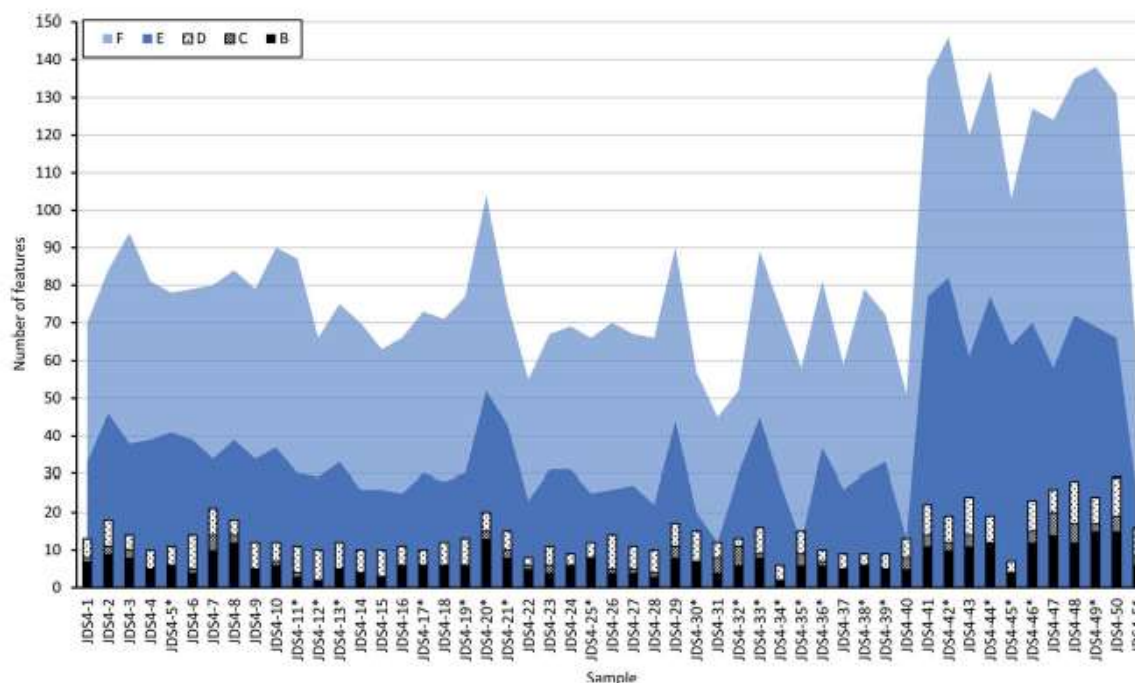


Fig. 2 The number of features of the classes B–F detected in each sampling site along the Danube river is displayed. Features were classified according to their identification confidence. Sample taken from the Danube's tributaries are marked with a star.

**Table 1** Several features of identification as class A are presented. Features are described by their mean RTs and accurate masses and MS2 scores across *n* samples. The properties of substances suggested by the compound database are also presented. Information on the source was gathered from the PubChem database<sup>11</sup>

Mean mass [Da]	Mean RT [min]	MS2 <i>n</i> score	Name	InChIKey	Elemental formula	Monoisotopic mass [Da]	log <i>D</i> (pH 7)	Source
187.1202 ± 0.0001	8.17 ± 0.04	2 1.0 ± 0.0	(3 <i>R</i> )-3-(2-Amino-2-oxoethyl)-5-methylhexanoic acid	NPDKTSLVWGFPOG-UHFFFAOYSA-N	C <sub>9</sub> H <sub>17</sub> NO <sub>3</sub>	187.1208	-1.5	Ambiguous
201.1728 ± 0.0002	10.14 ± 0.04	47 1.0 ± 0.0	4-Hydroxy-2,2,6,6-tetramethylpiperidine-1-ethanol	STEYNLUPFMIUOY-UHFFFAOYSA-N	C <sub>11</sub> H <sub>23</sub> NO <sub>2</sub>	201.1729	-2.6	Ambiguous
257.1024	13.80	1 0.7	Benserazide	BNQDGRGUHNAIGH-UHFFFAOYSA-N	C <sub>10</sub> H <sub>15</sub> N <sub>3</sub> O <sub>3</sub>	257.1012	-2.6	Pharmaceutical
267.0963	8.63	1 1.0	Vidarabine	OHRDTQYFTABQOQ-UHTZMRRCNSA-N	C <sub>10</sub> H <sub>13</sub> N <sub>5</sub> O <sub>4</sub>	267.0968	-2.1	Discontinued pharmaceutical

increase in class C features appeared at the sampling site JDS4-7 in Austria (rkm 2113), 8 km downstream of the WWTP Asten with a capacity of 950 000 population equivalents. There was another amplitude of polar features in the sample JDS4-20 of the Hron river in Slovakia at Danube confluence river kilometre 1716. This is in good accordance with Loos *et al.*, who showed that the highest concentrations of polar organic substances are usually found in the tributaries of the Danube river.<sup>11</sup> The discharge of tributaries is significantly lower compared to the Danube river itself, in which the afflux of polluted tributaries is diluted. That is evidenced for instance by the drop in the amount of detected polar features at JDS4-22 of the Danube river (rkm 1707). However, there was a local minimum of class C features at the Jantra mouth (JDS4-45). The highest number of class C features was detected at the sampling site JDS4-47 (rkm 488), which is located 9 km downstream of the WWTP Giurgiu in Romania with 62 895 population equivalents.

#### Features unequivocally assigned to polar candidate substances

Processing the data of the 51 JDS4 samples yielded 77 class B features, which could be assigned to 67 candidate substances as shown in Table S6.† Some substances were matched with multiple features with the same accurate mass but at different RTs. The listed compounds are described by a distinct name, InChIKey, elemental formula, the log *D* value at pH 7, potential source and whether experimental mass spectral data was available. Of the class B candidate compounds, 61% contain a hydroxy functional group, 60% a carbonyl group and 31% a carboxyl group. Additionally, primary and secondary amines are strongly represented in 36% and 25% of the proposed molecules, respectively. These functional groups can be expected to contribute to the interactions with the HILIC stationary phase. Thus, these findings are in good agreement with the polarity filter of log *D* < 0 (pH 7) applied to features annotated with database hits. Moreover, 45% of the 67 substances listed in Table S6† are heterocyclic. Nitrogen-containing heterocycles are among the most prevalent structural elements in small-molecule pharmaceuticals.<sup>12</sup> And indeed, at least nine candidate substances with the feature IDs 6, 12, 19, 38/39/40, 56, 64, 66, 73, and 75 supposedly contain a ring system with at least one nitrogen atom and are specified as pharmaceuticals or pharmaceutical related compounds by the PubChem database. At least 20% of the suspects contain substructures which indicate increased potential for mutagenicity:<sup>13</sup> aromatic-bound amine groups were identified in 12 tentative structures (feature IDs 1, 9, 10, 18, 20, 27, 53, 54, 73, 74, and 75). Aromatic-bound nitro groups were identified in two proposed structures corresponding to the features 66 and 70/71. Chlormequat (ID 7/8) contained an aliphatic halide group. These structural characteristics suggest that a considerable fraction of the molecules reported in Table S6† are toxicologically relevant. The numbers of candidate compounds containing the structural elements discussed in this section are graphically represented in Fig. 3.

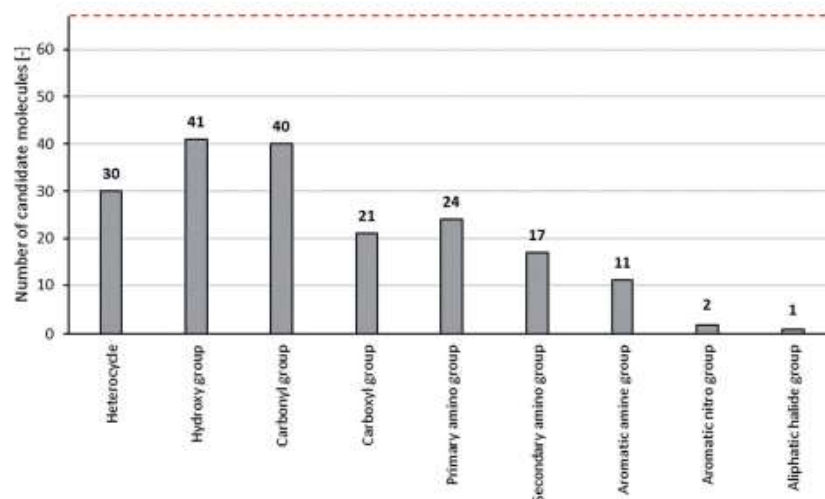


Fig. 3 Structural elements contained in the class B candidate molecules listed in Table S6†. The total number of candidates is indicated by the red dashed line. These substructures could contribute to the interactions with the HILIC stationary phase or indicate the toxicological potential of a compound.

The unambiguous allocation of these features was facilitated by using the SI database that on the one hand is specialized on anthropogenic substances relevant to the aquatic environment, and on the other hand able to connect the analytical information of a feature to the physicochemical properties of a suggested compound.

To get an idea of how thoroughly the suggested compounds have already been investigated and the amount of reference data available, a mass spectral database containing experimental spectra was queried. The European MassBank<sup>44</sup> database was therefore searched by InChIKey and spectra were considered comparable if they were acquired under similar instrumental conditions (Table S6†). For eight out of the 67 proposed

molecules, experimental MS2 spectra were found (Table S6†). These findings underline the need for further investigating these compounds and sharing data on the relevant platforms.

To sum up, the consequent NTS strategy followed by a compound database query proposed 67 polar organic compounds which are very likely to be plausible and relevant to the aquatic environment and may be validated by using reference materials.

#### Prioritization by the frequency of detection

Apart from ranking features according to the unambiguity of a compound allocation, they were prioritized based on how frequently they were found in the JDS4 sample batch. This

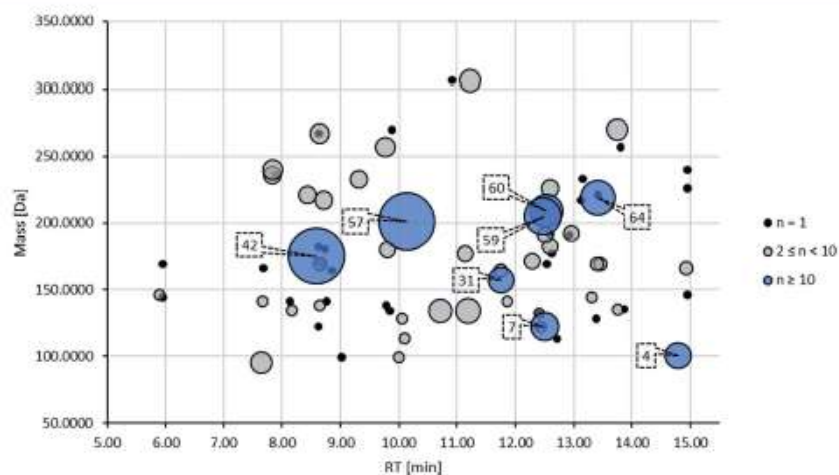


Fig. 4 Features are displayed which were unequivocally assigned to a compound with a  $\log D < 0$  at pH 7 (class B). They are defined by their location on the RT- $m/z$ -plane. The detection frequency  $n$  is expressed by the disc area. Features found in  $n \geq 10$  samples are highlighted in blue and the features' IDs are given (compare Table S6†).

prioritization strategy is well suited for large sampling campaigns, like the one investigated here with 51 different locations. In Fig. 4, all class B features are mapped according to their accurate mass and RT. The disc areas correspond to the frequency of detection ( $n$ ) throughout the course of the JDS4 and are scaled to the maximum ( $n = 47$  for feature 57). 33 class B features were detected at one and 36 class B features at two to nine different locations. Eight features (IDs 4, 7, 31, 42, 57, 59, 60, and 64) are highlighted in blue as they occurred in more than nine samples. These eight features were defined to be of high priority. The frequent detection of features suggests that they are particularly persistent and mobile in the aquatic environment and/or entered the water system *via* various sources. However, the 'frequency of detection' filter could just as well be applied at an earlier stage of the identification process, for instance to class E or F features. These were partly not matched with compounds stored in the SI database, but they could still be ecotoxicologically relevant judging from some of their functional groups. At this point other compound databases and annotation tools could be consulted in order to resolve the identities of such frequently detected features.

A selection of features characterized as high priority by 'frequency of detection' are listed in Table 2. All substances suggested for these features are highly polar with a  $\log D$  value  $\leq -1$  at pH 7 and are consequently expected to interact with the HILIC column. In addition to that, each candidate listed in Table 2 contains at least one of the aforementioned structural elements which could indicate a potential for toxicity as discussed in the previous section. Of the eight candidate molecules in Table 2, 1-methylpiperazine (for ID 5), 2,2,6,6-tetramethylpiperidin-4-ol (for ID 31), *m*-(1-cyanoethyl)benzoic acid (for ID 42) and 4-hydroxy-2,2,6,6-tetramethylpiperidine-1-ethanol (for ID 57) are registered under REACH (Registration, Evaluation, Authorisation and Restriction of Chemicals). *N,N*-bis(carboxymethyl)alanine (for ID 59) is pre-registered. Four features are assigned to chemicals directly or indirectly discharged from industrial sources. Miglustat was launched as a treatment for lysosomal storage diseases and was authorized for use in the European Union by the European Medicines Agency. It could have reached the Danube river basin through municipal WWTPs. Chlormequat has been approved as a pesticide by the European Union to be used on cereals and non-edible crops for a limited time period of 12 years under regulation 1107/2009/EC. It could have entered the Danube river basin through run-off from adjacent agricultural areas.

4-Hydroxy-2,2,6,6-tetramethylpiperidine-1-ethanol is a particularly significant suspect since the respective feature 57 was classified as class A in identification confidence (Table 1) and detected in 47 out of the 51 JDS4 samples (Table 2). It was described as acutely harmful to aquatic organisms by the European Chemicals Agency.<sup>35</sup> Arp *et al.* screened organic REACH chemicals and 4-hydroxy-2,2,6,6-tetramethylpiperidine-1-ethanol achieved the highest score for persistence in surface and ground water with a degradation half-life of >60 d and the highest mobility score with a  $\log D < 1$  and a water solubility of >10 g L<sup>-1</sup>. According to their system, it was classified among those compounds with the "[...] highest chance of permeating

**Table 2** Features which occurred in  $n \geq 10$  samples are listed below. Features are described by their mean RTs and accurate masses across  $n$  samples. The ID refers to Table S6 in the ESI. The properties of substances suggested by the compound database are also presented. Information on the source as well as toxicity was sourced from the PubChem database.<sup>31</sup> \* indicates that ecotoxicological quantitative data are available in the PubChem database and 'AT' stands for acute toxicity as specified by the Globally Harmonized System of Classification and Labelling of Chemicals

ID	Mean mass [Da]	Mean RT [min]	$n$	Suggested compound	InChIKey	Elemental formula	Monoisotopic mass [Da]	$\log D$ (pH 7)	Source
5	100.0997 ± 0.0001	14.79 ± 0.09	10	1-Methylpiperazine	PVOAHNGSUXLS-UHFFFAOYSA-N	C <sub>5</sub> H <sub>12</sub> N <sub>2</sub>	100.1000	-2.7	<sup>AT</sup> Industrial use (intermediates)
8	122.0727 ± 0.0001	12.50 ± 0.06	12	Chlormequat	JUZXDNPBRUJQR-UHFFFAOYSA-N	C <sub>5</sub> H <sub>13</sub> ClN	122.0731	-3.3	*Pesticide
31	157.1462 ± 0.0002	11.76 ± 0.02	10	2,2,6,6-Tetramethylpiperidin-4-ol	VDVUCLWJZJHFAV-UHFFFAOYSA-N	C <sub>9</sub> H <sub>19</sub> NO	157.1467	-2.3	Industrial use (intermediates)
42	175.0632 ± 0.0003	8.59 ± 0.05	45	<i>m</i> -(1-Cyanoethyl)benzoic acid	IRYTPWRXROPSX-UHFFFAOYSA-N	C <sub>10</sub> H <sub>9</sub> NO <sub>2</sub>	175.0633	-1.0	Ambiguous
57	201.1728 ± 0.0002	10.14 ± 0.04	47	4-Hydroxy-2,2,6,6-tetramethylpiperidine-1-ethanol	STEYNUVPFMIUOY-UHFFFAOYSA-N	C <sub>11</sub> H <sub>23</sub> NO <sub>2</sub>	201.1729	-2.6	Ambiguous
59	205.0587 ± 0.0004	12.46 ± 0.03	20	<i>N,N</i> -Bis(carboxymethyl)alanine	CIEZGWIJBXOTE-UHFFFAOYSA-N	C <sub>7</sub> H <sub>11</sub> NO <sub>6</sub>	205.0586	-9.9	Industrial use ( <i>i.e.</i> ion exchange agents), consumer use ( <i>i.e.</i> laundry and dishwashing products)
60	209.0719 ± 0.0002	12.53 ± 0.07	16	3-Morpholin-4-ylpropane-1-sulfonic acid	DVLFYONBTKHTER-UHFFFAOYSA-N	C <sub>7</sub> H <sub>13</sub> NO <sub>4</sub> S	209.0722	-2.7	Industrial use (laboratory chemicals and intermediates)
64	219.1470 ± 0.0003	13.41 ± 0.04	18	Miglustat	UQORRPFVSGFNRO-UTINFBMNSA-N	C <sub>10</sub> H <sub>21</sub> NO <sub>4</sub>	219.1471	-2.7	Pharmaceutical

drinking water resources if emitted into the environment".<sup>36</sup> In line with these findings, this study showed that the compound spread across the entire Danube river rather than transiently appearing after a point source.

The suspects presented in Table 1 as well as Table 2 were prioritized by their degree of identification confidence and frequency of occurrence, respectively. Therefore, they are worth being considered for validation by measuring the respective reference standards under the same chromatographic and mass spectrometric conditions. If available, reference standards may preferably be isotopically labelled in order to distinguish between isomers. In subsequent investigations, they could serve as internal standards for quantitative analysis.

## Conclusions

A NTS workflow followed by a compound database search was presented to determine and characterize novel polar and environmentally relevant trace organic compounds in the aqueous environment like the studied Danube river and its tributaries. NTS data were acquired using a polarity-extended chromatographic setup connected to a QTOF mass spectrometer. In order for it to record MS2 data in parallel to a full scan experiment, compromises need to be made. They could not only impair the hit rates or quality of MS2 spectra but might also affect the number of data points describing a chromatographic peak. For future investigations we suggest complementing the NTS run with specialized multiple reaction monitoring experiments based on predefined feature lists and tentatively identified polar molecules.

A data processing method is proposed that specializes in extracting polar features from HRMS raw data and connecting them to polar organic substances. The feature extraction workflow was optimized to HILIC peaks. The SI compound database (on the FI platform) was used to incorporate chromatographic information into the annotation process. As a result, 67 polar features were unequivocally matched with plausible trace organic substances. A non-target screening for polar features coupled to a specialized allocation process proved to be a valuable supplement to the routine monitoring of the Danube river basin. Moreover, the application of the method could be extended to other sample types.

Campaigns to comprehensively investigate a river system, such as the Joint Danube Survey, generate a vast amount of data leading to a multitude of features and candidate compounds. Confirmation with a reference standard is the inevitable last step to unequivocally identify a feature. It should, however, be feasible even when dealing with large data sets and if possible, have a high rate of success. Therefore, a dual prioritization strategy is presented based on the identification confidence and detection frequency. As a result, at least eleven feature-candidate compound pairs were selected which might have adverse effects on the aquatic environment of the Danube river and could even reach catchment areas for drinking water abstraction. However, another conceivable prioritization strategy could be an ecotoxicological evaluation of candidate substances. We urgently suggest a quantitative and effect-based

analysis of 4-hydroxy-2,2,6,6-tetramethylpiperidine-1-ethanol in Danube river water as well as drinking water sourced therefrom.

## Conflicts of interest

There are no conflicts of interest to declare.

## Acknowledgements

We thank all the colleagues in the NORMAN network for their impressive cooperation, support, and discussions (also regarding the implementation of the STOFF-IDENT/FOR-IDENT idea into the NORMAN-own platform). We acknowledge financial support of the "Westfälische Wasser- und Umweltanalytik GmbH" and especially thank Dr André Liesener for constructive discussions. We also thank Sciex for providing the TripleTOF mass spectrometer and Dr Axel Besa for very helpful discussions as well as valuable technical support. The authors thank Prof. J. Drewes and the colleagues of the Chair of Urban Systems Engineering of the Technical University of Munich for substantial support.

## Notes and references

- 1 R. P. Schwarzenbach, B. I. Escher, K. Fenner, T. B. Hofstetter, C. A. Johnson, U. von Gunten and B. Wherli, *Science*, 2006, **313**, 1072–1077.
- 2 D. J. Lapworth, N. Baran, M. E. Stuart and R. S. Ward, *Environ. Pollut.*, 2012, **163**, 287–303.
- 3 I. Liška, F. Wagner, M. Sengl, K. Deutsch and J. Slobodnik, *Joint Danube Survey 3: A Comprehensive Analysis of Danube Water Quality*, 2015.
- 4 German Environment Agency (UBA), *Protecting the sources of our drinking water – The criteria for identifying Persistent, Mobile, and Toxic (PMT) substances and very Persistent, and very Mobile (vPvM) substances under EU REACH Regulation (EC) No. 1907/2006*.
- 5 T. Reemtsma, S. Weiss, J. Mueller, M. Petrovic, S. Gonzalez, D. Barcelo, V. Francese and T. P. Knepper, *Environ. Sci. Technol.*, 2006, **40**, 5451–5458.
- 6 R. Loos, B. M. Gawlik, G. Locoro, E. Rimaviciute, S. Contini and G. Bidoglio, *Environ. Pollut.*, 2009, **157**, 561–568.
- 7 D. Zahn, I. J. Neuwald and T. P. Knepper, *Anal. Bioanal. Chem.*, 2020, **412**, 4763–4784.
- 8 K. Kiefer, A. Müller, H. Singer and J. Hollender, *Water Res.*, 2019, **165**, 1–20.
- 9 Y. Tang, Y. Xu, F. Li, L. Jmaiff, S. E. Hrudey and X. Li, *J. Environ. Sci.*, 2016, **42**, 259–266.
- 10 S. Bieber, G. Greco, S. Grosse and T. Letzel, *Anal. Chem.*, 2017, **89**, 7907–7914.
- 11 S. Minkus, S. Grosse, S. Bieber, S. Veloutsou and T. Letzel, *Anal. Bioanal. Chem.*, 2020, **412**, 4953–4966.
- 12 A. Kolkman, D. Vughs, R. Sjerps, P. J. F. Kooij, M. van der Kooij, K. Baken, J. Louisse and P. de Voogt, *ACS ES&T Water*, 2021, DOI: 10.1021/acsestwater.0c00237.
- 13 J. Hollender, E. L. Schymanski, H. P. Singer and P. L. Ferguson, *Environ. Sci. Technol.*, 2017, **51**, 11505–11512.

## Paper

## Analytical Methods

- 14 M. Krauss, H. Singer and J. Hollender, *Anal. Bioanal. Chem.*, 2010, **397**(3), 943–951.
- 15 Compound database PubChem of the National Center for Biotechnology Information, <https://pubchem.ncbi.nlm.nih.gov/>, accessed 9 December 2020.
- 16 J. Slobodnik and A. Höbart, in *Joint Danube Survey 4*, 2020, March, 1–17.
- 17 G. Greco, S. Grosse and T. Letzel, *J. Sep. Sci.*, 2013, **36**, 1379–1388.
- 18 S. Minkus, S. Bieber, S. Moser and T. Letzel, *AFIN-TS Forum*, 2020, March, 1–17.
- 19 R. Adusumilli and P. Mallick, *Proteomics*, 2017, **1550**, 339–368.
- 20 T. Pluskal, S. Castillo, A. Villar-Briones, *et al.*, MZmine 2: Modular framework for processing, visualizing, and analyzing mass spectrometry-based molecular profile data, *BMC Bioinf.*, 2010, **11**, 395.
- 21 O. D. Myers, S. J. Sumner, S. Li, S. Barnes and X. Du, *Anal. Chem.*, 2017, **89**, 8696–8703.
- 22 T. Letzel, A. Bayer, W. Schulz, A. Heermann, T. Lucke, G. Greco, S. Grosse, W. Schüssler, M. Sengl and M. Letzel, *Chemosphere*, 2015, **137**, 198–206.
- 23 S. Wolf, S. Schmidt, M. Müller-Hannemann, *et al.*, In silico fragmentation for computer assisted identification of metabolite mass spectra, *BMC Bioinf.*, 2010, **11**, 148.
- 24 Open Access Platform FOR-IDENT, <https://www.for-ident.org/>, accessed 27 November 2020.
- 25 K.-U. Goss and R. P. Schwarzenbach, *Environ. Sci. Technol.*, 2001, **35**(1), 1–9.
- 26 S. Knoll, T. Rösch and C. Huhn, *Anal. Bioanal. Chem.*, 2020, **412**, 6149–6165.
- 27 S. Wemisch and S. Pennathur, *Anal. Bioanal. Chem.*, 2016, **408**, 6079–6091.
- 28 E. L. Schymanski, J. Jeon, R. Gulde, K. Fenner, M. Ruff, H. P. Singer and J. Hollender, *Environ. Sci. Technol.*, 2014, **48**, 2097–2098.
- 29 T. Letzel, T. Lucke, W. Schulz, M. Sengl and M. Letzel, *Lab More Int.*, 2014, **4**, 24–28.
- 30 X. Zhu, Y. Chen and R. Subramanian, *Anal. Chem.*, 2014, **86**, 1202–1209.
- 31 R. Loos, S. Tavazzi, B. Paracchini and J. Fick, in *Joint Danube Survey 3: A Comprehensive Analysis of Danube Water Quality*, 2015, pp. 240–248.
- 32 E. Vitaku, D. T. Smith and J. T. Njardarson, *J. Med. Chem.*, 2014, **57**, 10257–10274.
- 33 J. Kazius, R. McGuire and R. Bursi, *J. Med. Chem.*, 2005, **48**, 312–320.
- 34 European MassBank mass spectral database of the NORMAN network, <https://massbank.eu/MassBank/>, accessed 1 February 2021.
- 35 European Chemicals Agency, *REACH registered substance factsheets*, <https://echa.europa.eu/de/registration-dossier/-/registered-dossier/13887/6/2/1>, accessed 29 November 2020.
- 36 H. P. H. Arp, T. N. Brown, U. Berger and S. E. Hale, *Environ. Sci.: Processes Impacts*, 2017, **19**, 939–955.

---

**Appendix A.3 Spotlight on mass spectrometric non-target screening analysis: Advanced data processing methods recently communicated for extracting, prioritizing and quantifying features**

The following review article has undergone a peer-review process and has been previously published as presented below.

Reference: Minkus S, Bieber S, Letzel T (2022) Spotlight on mass spectrometric non-target screening analysis: Advanced data processing methods recently communicated for extracting, prioritizing and quantifying features. *Anal Sci Adv* 3:103–112. <https://doi.org/10.1002/ansa.202200001>

Received: 1 January 2022

Revised: 22 March 2022

Accepted: 24 March 2022

# Spotlight on mass spectrometric non-target screening analysis: Advanced data processing methods recently communicated for extracting, prioritizing and quantifying features

Susanne Minkus<sup>1,2</sup> | Stefan Bieber<sup>1</sup> | Thomas Letzel<sup>1,2</sup><sup>1</sup>AFIN-TS GmbH, Augsburg, Germany<sup>2</sup>Technical University of Munich (Chair of Urban Water Systems Engineering), Munich, Germany**Correspondence**Thomas Letzel, AFIN-TS GmbH, Am Mittleren Moos 48, 86167 Augsburg, Germany.  
Email: t.letzel@afin-ts.de**Abstract**

Non-target screening of trace organic compounds complements routine monitoring of water bodies. So-called features need to be extracted from the raw data that preferably represent a chemical compound. Relevant features need to be prioritized and further be interpreted, for instance by identifying them. Finally, quantitative data is required to assess the risks of a detected compound. This review presents recent and noteworthy contributions to the processing of non-target screening (NTS) data, prioritization of features as well as (semi-) quantitative methods that do not require analytical standards. The focus lies on environmental water samples measured by liquid chromatography, electrospray ionization and high-resolution mass spectrometry. Examples for fully-integrated data processing workflows are given with options for parameter optimization and choosing between different feature extraction algorithms to increase feature coverage. The regions of interest-multivariate curve resolution method is reviewed which combines a data compression alternative with chemometric feature extraction. Furthermore, prioritization strategies based on a confined chemical space for annotation, guidance by targeted analysis and signal intensity are presented. Exploiting the retention time (RT) as diagnostic evidence for NTS investigations is highlighted by discussing RT indexing and prediction using quantitative structure-retention relationship models. Finally, a seminal technology for quantitative NTS is discussed without the need for analytical standards based on predicting ionization efficiencies.

**KEYWORDS**

environmental analysis, feature extraction, non-target screening, prioritization, semi-quantification

**1 | INTRODUCTION**

For several decades, the presence of anthropogenic organic chemicals in natural waters is reported. Many of them are known to cause adverse effects on aquatic and maybe even human health.<sup>1,2</sup> Important prerequisites for mitigating potential risks posed by these chemicals, are comprehensive analysis and monitoring efforts. Known constituents are routinely monitored in water bodies by (quantitative) target screen-

ing methods, mainly based on liquid chromatography (LC), coupled to tandem mass spectrometry (MS/MS), such as triple quadrupole MS. This technique is well established but can cover only a small fraction of the chemical constituents, namely those, which are already known and searched for.<sup>3</sup> In recent years, LC coupled with soft ionization techniques like electrospray ionization (ESI) hyphenated to high-resolution MS (HMRS), has become more and more important for the analysis of anthropogenic compounds in the aquatic environment. HMRS

This is an open access article under the terms of the [Creative Commons Attribution License](https://creativecommons.org/licenses/by/4.0/), which permits use, distribution and reproduction in any medium, provided the original work is properly cited.

© 2022 The Authors. *Analytical Science Advances* published by Wiley-VCH GmbH

instruments are able to accurately screen the entire mass range of small molecules with cycling times short enough to resolve even narrow chromatographic peaks. These technical advancements powered the evolution of non-target screening (NTS) methods for interrogating samples without any pre-selected substances.<sup>4,5</sup> NTS aims at filling the gaps or complementing target screening efforts by allowing to detect so far unexpected or unknown chemical compounds in water bodies as so-called features. A feature is usually described by the three coordinates accurate mass, retention time (RT) as well as signal intensity. Full scan HRMS measurements produce vast amounts of complex data that need rigorous and sophisticated processing and well-informed interpretation. The challenge for data evaluation is here to extract, align, filter and bin features that correspond to a real compound and distinguish them from artefacts or redundant signals. Therefore, tools are required to effectively extract, prioritize, annotate and interpret features. Nowadays, there are many examples of different software tools for NTS data evaluation, which help to set up such data processing. On the one hand, there is commercially available software, often marketed by MS vendors, such as Compound Discoverer (Thermo Fisher Scientific), Mass Profiler (Agilent), UNIFI (Waters) or others. On the other hand, there is a rapidly increasing variety of powerful open-source and/or open-access software (i.e. XCMS<sup>6</sup> or MZmine 2<sup>7</sup>), which can be used independently from the applied MS. In the following, the spotlight focuses on advances in such vendor-independent tools.

Typically, a core NTS data processing strategy includes data pretreatment, feature extraction, componentization, feature alignment and filtering. To use data in vendor-independent tools, data pretreatment often entails converting raw HRMS data files into open formats like mzML<sup>8</sup>, mzXML<sup>9</sup> or ANDI/netDCF (<https://www.astm.org/>). Additionally, the data can here be trimmed and simplified through an initial noise threshold or centroiding (i.e. by using the MSconvert tool of the ProteoWizard toolkit<sup>10</sup>). Feature extraction or peak picking often involves extracting ion chromatograms, followed by deconvoluting or integrating a chromatographic peak. There are algorithms taking on that task such as "centWave"<sup>11</sup> implemented in the XCMS tool<sup>6</sup> or the "ADAP" workflow<sup>12</sup> within the MZmine 2 framework.<sup>7</sup> Componentization refers to the binning of redundant ion traces that belong to the same compound such as isotopologues, adducts or in-source fragments. Features may be aligned across several technical replicates or samples of a batch if they are expected to be the same compound. Finally, filtering feature lists based on various quality criteria (e.g., present in all replicates, absent in the blank samples, minimum signal intensity, etc.) is intended to remove artefacts and false-positive features. Questions associated with NTS are diverse and require individual data processing solutions. Thus, the processing steps should be handled interchangeable and flexible.

After a feature list of sufficient quality<sup>13,14</sup> is generated, an NTS method could follow different objectives: Comparative analysis for process evaluation (a), trend analysis (b), or identification of unknown or unexpected substances (c). While objectives a, and b, mainly focus on the comparison of samples and might result in a statistical interpretation, objective c, aims to reveal the identity of specific features and annotate it.

The basis of feature annotation is querying chemical compound databases such as PubChem<sup>15</sup> (<https://pubchem.ncbi.nlm.nih.gov/>) or ChemSpider<sup>16</sup> (<https://www.chemspider.com/>) by accurate mass. When running MS2 experiments, another dimension of structural information is available in the form of characteristic fragmentation patterns. Spectral libraries like European MassBank<sup>17</sup> or MassBank of North America (MoNA; <https://mona.fiehnlab.ucdavis.edu/>) allow a comparison of MS2 spectra. If there are no experimental spectra available, in silico fragmentation prediction performed by i.e. MetFrag<sup>18</sup> or SIRIUS4 CSI:FingerID,<sup>19</sup> support tentative identification of features. How confidently a feature could be identified depends on the amount of evidence available and is usually communicated via a level system proposed by Schymanski et al.<sup>20</sup> A feature is considered unequivocally identified if the proposed structure is confirmed by matching MS1, MS2 and RT information with a reference compound. However, this step constitutes the bottleneck of the workflow as it is time-consuming and authentic standards can be expensive or even unavailable. To that end, it is necessary to prioritize features that are expected to be environmentally relevant. Criteria for that might be toxicity (T), persistence (P), mobility (M), all combined as PMT, bioaccumulation, endocrine disruption capabilities or the formation of new compounds in processes of biosystems.

To further support the interpretation of LC-MS data, sophisticated models are increasingly developed and applied. These models are able to mine information from large empirical data sets and describe complex relationships between a chemical structure and biological activity or chromatographic retention. Usually, the data set is split into multiple subsets, one called the training set for fitting the model and another one called the test set which is withheld for external validation of the predictive ability of the model. The training set itself is often submitted to resampling methods such as cross-validation or bootstrapping for internal validation and definition of the applicability domain.<sup>21,22</sup>

An assortment of recent and – according to the authors' assessment – noteworthy advancements is collected, related to feature extraction (Section 1), prioritization (Section 2) and quantification (Section 3) in NTS analysis. In Section 1, centroiding, as a data pretreatment step comes to fore and software platforms, are presented that combine various feature extraction tools for more effective processing of environmental NTS data. Furthermore, a multivariate chemometric method is discussed as an effective alternative for processing complex LC-MS data. In Section 2, suggestions are given on how to confine the chemical space in order to streamline the feature identification workflow. When dealing with feature prioritization, a focus lies on methods that take chromatographic information into account. From intensity-based prioritization, this review moves to a quantification method suited for NTS applications as it refrains from using analytical standards Section 3.

## 2 | FEATURE EXTRACTION

If not performed during data acquisition, centroiding is an integral part of LC-MS data pretreatment. Data size and density are reduced by converting the mass profile peak into a single data point described by

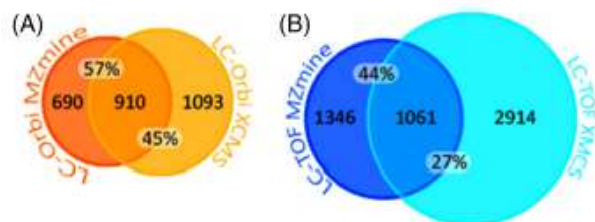


**FIGURE 1** Venn diagrams of the total number of features (areas of the circles) extracted with MZmine 2 and XCMS from data acquired on an LC-Orbitrap (A) setup and a liquid chromatography–time-of-flight (LC-TOF) setup (B). Reprinted and adapted with permission from Elsevier<sup>27</sup>

mass and intensity. To calculate centroid values, an appropriate peak shape model and the respective parameter settings need to be selected which could become even more complex if peaks are noisy, skewed or overlapping.<sup>23</sup> Open source centroiding approaches are often considered inferior to vendor approaches as some proprietary information might not be translated to open formats and information on mass peak widths is lacking.<sup>24,25</sup> The open-source tool Cent2Prof was developed to convert profile and centroided data in both directions.<sup>25</sup> Furthermore, a random forest regression model uses mass-to-charge ( $m/z$ ) values, relative intensities and retention factors to predict mass peak widths, which could be helpful information further down the feature extraction workflow. The model was internally validated via 500 bootstrapping samples and 5-fold cross-validation and the external validation yielded an average prediction error of 56%. However, the model is currently developed based on data acquired with quadrupole time-of-flight mass analyzers and needs to be extended for Orbitrap instruments.

As nowadays numerous software tools are available, many of them running on different (sometimes proprietary) algorithms, different results might be expected. Hohrenk et al. compared the four different processing tools *enviMass*, MZmine 2, XCMS online and the commercial software *Compound Discoverer* (Thermo Fisher Scientific).<sup>26</sup> They found that overlapping features constitute only 8%–12% of all extracted features. Even when the 100 most intense features were considered, the percentage of overlapping features did not significantly increase. In the course of finding biomarkers in bioreactor samples, Neusüß and coworkers compared MZmine 2 and XCMS online on two different instrumental setups: LC-Orbitrap and LC-TOF.<sup>27</sup> They found 45%–57% of commonly extracted features for LC-Orbitrap and 27%–44% for LC-TOF (see Figure 1). However, the overlap was significantly increased for features prioritized by a multivariate chemometric method. Therefore, partial least square regression was applied to build models for the prediction of gas yields based on feature intensity. Features were then ranked by their importance based on the variable importance in projection which describes a feature's contribution to the model. The small fraction of commonly extracted features underline the need for introducing quality control (QC) measures to an NTS data processing workflow. In both studies, parameters and filters for feature extraction were set to the same values (if possible)

for better comparison. Software-specific parameters were optimized based on the recovery of internal standards. Hohrenk et al. additionally considered verified suspects as well as the total number of features. Those are agreed upon QC criteria that aim at assessing and minimizing false negative and false positive rates, respectively.<sup>14,28</sup> Individually optimized parameter settings cannot be excluded as a source of variation between feature lists and Hohrenk et al. furthermore suspected varying effects of the blank and replicate filters as they are implemented differently in the investigated software tools. Moreover, the typical QC regime for NTS investigations of environmental samples currently lacks criteria to evaluate the componentization step. Nevertheless, there is reason to assume that the different operations of peak picking algorithms themselves lower the congruence between extracted feature lists.

The NTS investigator could counter these uncertainties by (a) a thorough QC and reporting routine for data processing (as proposed<sup>14,29</sup>), (b) a deeper understanding of algorithms and (c) orthogonally constructed tools like *patRoom*.<sup>30</sup> The open-source platform *patRoom* combines multiple established algorithms in an R interface.<sup>31</sup> As visualized in Figure 2, it covers the entire workflow from data pre-treatment, feature extraction and componentization, annotation, visualization and reporting. Many open-source and/or open-access software tools such as MZmine were originally developed for proteomic or metabolomic research. Consequently, they might lack specific functionalities necessary to meet the demands of environmental analysis such as detection of analytes at low or varying concentrations, trend recognition over longer time periods (i.e. surface water monitoring activities) or across diverse matrices (i.e. influents and effluents of wastewater treatment plants) and annotation of environmentally relevant compounds. Like *enviMass*,<sup>32</sup> *patRoom* was more specifically designed for processing environmental NTS data. By applying strategies for parallelization of processes or threads such as multiprocessing execution times were significantly reduced for several processing steps. For almost all integrated tools, execution times normalized to sequential results were reduced by approximately 200%–500% when increasing the number of parallel processes, with an optimum at the number equal to the number of physical CPU cores (here six). User-friendliness in *patRoom* is promoted by partially implementing a graphical user interface (GUI) and an installation script for Microsoft Windows and its dependencies. Furthermore, the results of previous processing steps are accessible at any point throughout the workflow and can be visualized. This is a helpful tool in the development of data evaluation workflows because it can be used to assess the impact of different workflow stages on the results. A noteworthy addition to the *patRoom* workflow is the adapted R package *IPO* for automatic optimization of data processing parameters based on the statistical design of experiments (DoE).<sup>33</sup> A similar functionality was included in another LC-MS data processing workflow named *SLAW*, presented by Delabriere et al.<sup>34</sup> It containerizes several tools to reduce computational time and memory consumption. Apart from the number of detected isotopic peaks as an optimization criterion for peak picking, in *SLAW* a score was added for the reliability of integration across pooled QC samples, which promotes reproducibility. Objectives, designs or instrumental stability can vary from one

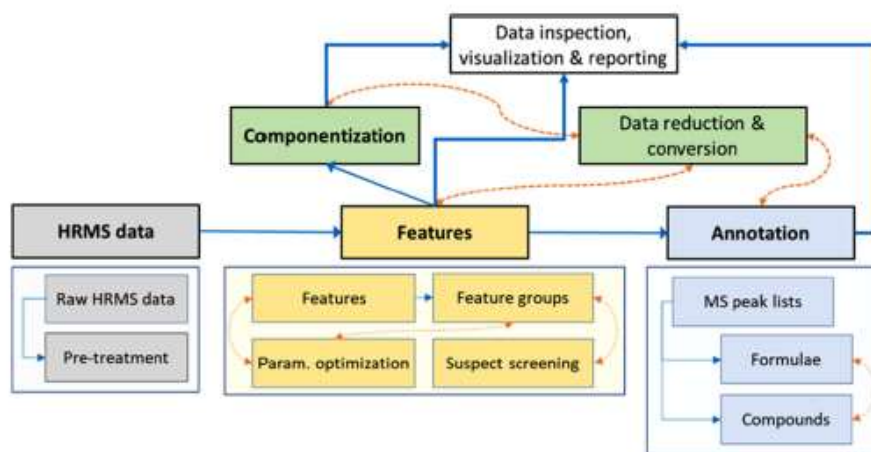


**FIGURE 2** patRoom workflow for processing environmental non-target screening (NTS) data. Reprinted<sup>30</sup>

NTS study to another which requires specific adjustment of parameter settings. Generally, an integrated optimization method based on DoE and response surface modelling constitutes a more systematic alternative to approaches like “trial and error” or “changing one factor at a time”, which heavily rely on the user’s experience, are prone to error (i.e. by not considering statistical interactions) and time-consuming. In SLAW just like in patRoom, one can choose from different peak picking algorithms. In patRoom, features or annotations derived from different algorithms (i.e. XCMS<sup>6</sup> or OpenMS<sup>35</sup>) can be compared and a consensus is created. Thereby it is possible to exclusively keep commonly found features or use complementary algorithms to increase feature coverage. This functionality could address the aforementioned concern of little correspondence between different algorithms.

Many feature extraction methods employ a strategy referred to as “binning” to compress LC-MS data and transform it into a matrix ( $x = RT$ ;  $y = m/z$ ). Thereby, the  $m/z$  axis is discretized into bins of a specific size. Yet, finding the appropriate bin size is complicated, chromatographic peaks might be overlaid or split between bins and the approach is prone to spectral inaccuracies.<sup>11</sup> An alternative strategy for filtering, compressing and resolving LC-MS data in regions of interest-multivariate curve resolution (ROIMCR), a method originally introduced to the field of metabolomics.<sup>36,37</sup> The approach employs two steps: First, data is compressed by searching for “regions of interest” (ROI) which describe areas of densely arranged data points followed by “data voids” as was initially introduced by Stolt et al.<sup>38</sup> and later on incorporated into the centWave algorithm as part of the XCMS tool.<sup>11</sup> In the second step, the compressed data is analyzed using multivariate curve resolution-alternating least squares (MCR-ALS). With MCR-ALS, pure spectral and elution profiles of analytes across different chromatographic runs can be recovered, even if they differ in RT and peak shape.<sup>39</sup> Thus, the MCR-ALS approach does not require chromatogram deconvolution (shape modelling peaks by i.e. fitting a Gaussian curve or its derivative) and peak alignment across multiple samples. However, MCR methods are not free of uncertainty, for which rotational ambiguity is a major source. It refers to multiple feasible

solutions for the bilinear decomposition of data matrices and needs to be reduced by introducing constraints.<sup>40</sup> Nevertheless, this chemometric approach has been recently picked up for the non-targeted analysis of proteins<sup>41</sup> and trace organic compounds in wastewater<sup>42</sup> due to its ability to overcome coelution problems in complex matrices. An MCR-ALS tool was implemented in the MATLAB environment with GUI features and is available on <http://www.mcrals.info/> (including background information).

### 3 | PRIORITIZATION

The enormous amount of information that can be retrieved from NTS data needs to undergo various data reduction steps that should result in a manageable number of relevant features. This process can be defined as prioritization in its broadest sense. A form of prioritization is already introduced into the feature extraction workflow when setting input parameters and applying filters to comply with certain quality standards. For instance, analyzing pooled samples as it is general practice in metabolomics since 2006,<sup>43,44</sup> has made its way into the QC regime of environmental studies as well.<sup>34,45,46</sup> Strategies downstream of feature extraction are often based on metadata, physicochemical properties, spatial and temporal trends, suspected occurrence, identification confidence or anticipated effects.

Especially when following an identification workflow, feature prioritization is crucial as compound annotation in the face of the chemical universe can become a daunting task. PubChem as one of the largest chemical inventories currently contains over 100 million compounds which could mean thousands of matches per mass query. Nevertheless, these compound databases are necessary for annotating features since they provide additional information on physicochemical properties and metadata of compounds for filtering or ranking. Narrowing the scope of expected compounds to a sub-group of major interest or relevance could be the first step in streamlining the identification process. Smaller and specialized compound databases, such as

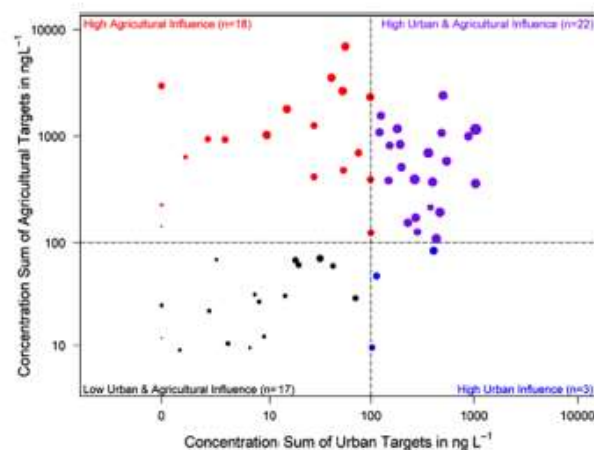


**FIGURE 3** Classification of 60 groundwater monitoring sites based on targets of urban and agricultural origin. The dot size corresponds to the number of targets and is scaled to a maximum of 74. Sum concentrations of  $100 \text{ ng L}^{-1}$  mark the thresholds (dashed lines) for the four classes. Reprinted with permission from Elsevier<sup>46</sup>

STOFF-IDENT<sup>47</sup> or CompTox,<sup>48</sup> could facilitate identifying environmentally relevant compounds. Recently, Schymanski et al. collapsed the PubChem database into PubChemLite by selecting relevant subcategories such as “Agrochemical Information” or “Drug and Medication Information”.<sup>49</sup> So far, the PubChemLite can be incorporated into workflows with MetFrag or patRoön. At the risk of missing some correct matches, it might streamline identification workflows by increasing computational efficiency as well as ranking performance.

Source-related prioritization is another approach for limiting the space of expected chemicals prior to structural elucidation. Kiefer et al. classified groundwater samples based on urban or agricultural influence. Therefore, they calculated the sum concentrations for target compounds of urban origin (i.e. sweeteners and industrial compounds) and for targets of agricultural origin (pesticides and their transformation products). If the sum concentration exceeded  $100 \text{ ng L}^{-1}$  a sample was considered to be highly influenced (see Figure 3). The classification system allowed to prioritize features for further structural elucidation based on suspected urban and/or agricultural origin.<sup>46</sup>

Accurate mass alone is not sufficient for excluding false compound candidates. Even if a mass spectrometer had a theoretical mass accuracy of 0.1 ppm, it would still result in multiple possible elemental compositions for features with masses  $>500 \text{ Da}$ .<sup>50</sup> Furthermore, a query of the PubChem database via MetFrag for the formula  $\text{C}_{17}\text{H}_{29}\text{NO}_4$  ( $311.4 \text{ g mol}^{-1}$ ) obtained 1304 candidate compounds (accessed on 21 December 2021). The manifold annotation possibilities suggest that additional diagnostic evidence is needed for ranking and filtering non-target features. Chromatographic parameters such as RT can be connected to the physicochemical properties of an analyte. Our group demonstrated the benefits of this relationship by filtering for polar compound candidates.<sup>51,52</sup> NTS measurements were carried out on a chromatographic setup comprising reversed-phase LC (RPLC) coupled in series to hydrophilic interaction liquid chromatography (HILC)

for the separation of analytes of an extended polarity range.<sup>53</sup> Features eluting from the HILC column were annotated using a compound database specialized in water analysis, namely the STOFF-IDENT<sup>47</sup> on the FOR-IDENT platform (<https://water.for-ident.org>). Only candidates with a negative  $\log D$  value (logarithmic distribution coefficient between water and octanol at pH 7) were further considered. The  $\log D$  filter reduced the number of plausibly annotated features per sample by on average 43%.

Retention time indexing, as originally introduced for gas chromatography by Kováts using *n*-alkanes,<sup>54</sup> allows comparing retention behaviour with different laboratories and libraries. The approach has gained traction in the field of LC-MS as well. By harmonizing the RT and thus making it more comparable, it becomes more accessible to NTS investigations, that is by using it as additional evidence to identify features. Usually, experimental RTs of features are normalized using a linear calibration curve based on a set of standard compounds. An approach implemented in the FOR-IDENT platform correlates RT indices (RTIs) with  $\log D$  values using experimentally determined calibrants. The observed  $\log D$  values are compared to those of compounds stored in one of the databases hosted by the platform. The difference  $\Delta \log D$  can be used to further evaluate the plausibility of compounds assigned to a feature.<sup>55,56</sup> Aalizadeh et al. introduced an RTI system as well as a prediction approach based on quantitative structure-retention relationship (QSRR) models.<sup>57</sup> For each ESI mode, they selected a set of 18 calibrants that represented the chemical space (here 2123 compounds) best based on chemical similarity and maximum overlap with RTs. These calibrants can be used to normalize experimental RTs to RTIs between 1 and 1000. Tests on different RPLC columns, under different chromatographic conditions and in different laboratories found the RTI system harmonize RTs reliably. However, the performance of the RTI systems was less accurate for a mobile phase composed of acetonitrile/ $\text{H}_2\text{O}$  compared to methanol/ $\text{H}_2\text{O}$  and the uncertainty was generally increased in ESI negative mode. Two QSRR models were built following previously reported workflows<sup>58,59</sup> with the objective of predicting RTIs based on one of the most representative molecular descriptors (i.e.  $\log D$  with the highest relative importance of approximately 68%). The non-linear model employing a support vector machine (SVM) algorithm outperformed the multiple linear regression algorithm. The external validation for ESI negative and positive mode returned  $R^2$  values of 0.833 and 0.868 and mean root mean square errors (RMSE) of 75.70 and 82.64, respectively. Comparing experimental RTI between laboratories or *in silico* predictions could increase the identification confidence in NTS workflows. Caution should be exercised if calibrants deviate considerably from linearity or compounds fall outside the applicability domain of the RTI model.

Julien Parinet compared various sets of molecular descriptors and five different machine learning algorithms in order to find the combination that most accurately and precisely predicts the RTs of pesticides on an RPLC system.<sup>60</sup> Six sets of molecular descriptors from four influential studies<sup>61–65</sup> were chosen and a seventh set was created by merging all variables. The molecular descriptors were calculated for roughly 800 pesticides. The model that predicted RTs best, used all 40 molecular descriptors and multi-layer perceptron regression. However, a less

complex model based on SVM regression showed no significant differences in performance. It only used eight molecular descriptors (Log P, log D, molecular weight, molecule volume, Molar refractivity, polar surface area, H-Donor and H-Acceptors) and thus seemed to be the best compromise. The results of the external validation returned an  $R^2$  of 0.85, an RMSE value of 0.69 min and a 6% percentage error.

The signal intensity is one dimension of a feature often used for prioritization as higher intensities often produce higher quality MS1 peaks and MS2 spectra and are assumed to be to some extent proportional to a compound's concentration.<sup>3</sup> Many prioritization efforts in non-targeted analysis serve the purpose of streamlining the workflow towards a (tentative) identification of features. As this approach heavily relies on chemical databases, it discriminates against so far unreported compounds even though they might be environmentally relevant. For assessing general patterns in technical or natural systems, such as evaluating the effectiveness of wastewater treatment or locating a spilling event in a river, following the entire identification regime may not be necessary or even cut important information. That is why intensity-based prioritization approaches are not only interesting for identification strategies but also for process evaluations or trend analysis. Non-linear response relationships and matrix effects like signal suppression or enhancement often hamper the comparison of samples with different matrices. Therefore, strategies need to be developed to scale features to equal intensities. One way of normalizing intensities is based on spiking isotopically labelled internal standards (ISTDs) into each sample that serve as chemical surrogates. An exemplary implementation would be to first calculate the median intensity per ISTD across all samples. Secondly, the deviation of each ISTD intensity in an individual sample from the median across all samples is determined. Finally, the median deviation is calculated for each sample which served as a normalization factor. The normalization factor is then applied to correct the signal intensities of non-target features.<sup>45,66,67</sup> Schollée et al. used normalized feature intensities to assign trends for the evaluation of different advanced wastewater treatments.<sup>45</sup> They, therefore, aligned features along with treatment steps and defined relative ranges of high (1), medium (0) and low (-1) intensities at 100%–60%, 60%–20% and <20% of the maximum intensity, respectively. These “barcode trends” indicated whether a feature was eliminated, formed or persistent. In a former process evaluation study by Bader et al. in 2017, fold changes of features between effluent and influent samples were determined and fold change intervals were defined for elimination, decrease, consistency, increase and formation.<sup>68</sup> Reymond et al. brought together intensity-based and target-guided prioritization approaches in order to find and identify features in wastewater samples that are related to the synthesis of illicit drugs.<sup>69</sup> Peak areas were normalized using the closest eluting ISTD and then compared to loads of known target drugs using similarity metrics (Pearson's correlation coefficient, Spearman's rank correlation coefficient, the distance correlation and maximum information coefficient). Thereby, 28 features were detected that were closely associated with the target drug patterns. It should be noted that deciding on the size and composition of a sufficient ISTD set for intensity normalization is difficult, as the compounds in the environmental sample are initially unknown to the inves-

tigator and a large structural variety can be expected. Moreover, the factors influencing the RT and the ionization efficiency are to some extent different.<sup>70,71</sup>

## 4 | QUANTIFICATION OF NON-TARGET FEATURES

Semi-quantitative prioritization methods attempt to overcome the qualitative focus of NTS studies by prioritizing features that are expected to be environmentally relevant as they are (a) present at comparatively high concentrations or (b) newly formed or emitted. These assumptions are based on relative interpretations of chemical abundance, derived from normalization over a sample set or calculation of fold changes for binary comparison. Still, risk assessment and regulatory decisions require absolute quantitative estimates.<sup>72</sup> As an example, there are well-known stressors such as steroid hormones that already have ecotoxicological effects on aquatic organisms at concentrations in the  $\text{ng L}^{-1}$  range or even below.<sup>73</sup> Moreover, analytical standards for newly identified compounds and transformations products might be commercially unavailable and their synthesis resource-intensive. Thus, quantification methods are desirable as they do not rely on calibration with an authentic standard. This proved to be a difficult task since the signal response in an LC-ESI-HRMS setup not only depends on concentration but also the compound, the sample matrix, the mobile phase composition and the instrument. To overcome these issues Ligand et al. proposed an approach for quantifying compounds based on predicted ionization efficiency.<sup>74</sup> Ion efficiency data was collected in ESI positive and negative mode from >450 compounds and >100 different mobile phase compositions. A model based on random forest regression was developed with the measured ionization efficiency values, structure-related chemical descriptors (PaDEL descriptors<sup>75</sup>) and empirical eluent descriptors. The external validation of the ESI positive and negative models, returned RMSE values of 3.0 times and 2.3 times for the test sets, respectively. The authors measured the ionization efficiency *IE* of a compound relative to an anchoring compound and the prediction error was defined as follows<sup>74</sup>:

$$\text{Prediction error} = \max \left\{ \begin{array}{l} \frac{\text{predicted IE}}{\text{measured IE}} \\ \frac{\text{predicted IE}}{\text{measured IE}} \end{array} \right.$$

Interestingly, the models revealed that the number of hydrogen and nitrogen atoms in a molecule as well as viscosity, pH and presence of ammonium ions in the mobile phase strongly influence the ionization efficiency. The authors were able to show that predicted ionization efficiency values are transferrable between different instruments. Specific instrumental parameters are not accounted for in the ionization efficiency predictions. Therefore, the universal values need to be converted by measuring a set of calibration compounds at defined concentration levels under the same conditions as the compound of interest. Besides compensating for instrumental differences, the authors expect this transformation to also account for matrix effects. Furthermore,

they were able to show a rather consistent prediction error across different matrices. The instrument-specific ionization efficiency value as well as the measured signal intensity of the compound of interest can then be used to estimate its concentration. In a recent study by Kruve et al.,<sup>70</sup> the aforementioned approach for quantification without analytical standards (a) was compared to two others using the response factors of parent compounds to quantify TPs (b) and of the closest eluting ISTD (c).<sup>76</sup> Therefore, 74 micropollutants were detected in real groundwater samples and quantified with analytical standards for reference. The quantification approach based on ionization efficiency exhibited the highest prediction accuracy and the narrowest error distribution. Its mean prediction error was a factor of 1.8 and all of the data points had an error below a factor of 10. It should be noted that the model is able to predict ionization efficiency for protonated and charged [M]<sup>+</sup> compounds in ESI positive mode and for deprotonated species in negative mode but not for sodium or ammonium adducts. The ionization efficiency prediction could complement NTS investigations by allowing estimation of the concentration of tentatively identified features. The semi-quantification approach could even be applied retrospectively to stored NTS data if calibration information (QC samples and ISTDs) is available.<sup>71</sup> However, if no SMILES code was putatively assigned to a feature, this method does not apply.

## 5 | CONCLUSION AND OUTLOOK

The interest in NTS has been constantly increasing in the last few years. This can be demonstrated by over 1200 publications (SCOPUS search for non(-)target/untarget\* screening/analysis published in the subjects environmental science and chemistry in 2021 and 2022), but also by recent events such as the "International Conference on Non-Target Screening 21" in the year 2021 in Germany. This review addressed recent and noteworthy studies concerning the processing and interpretation of NTS data acquired on LC-HRMS instruments with a focus on the analysis of environmental samples. The landscape of tools is fairly scattered, offering plenty of specialized or partial solutions. patRoom or SLAW is a comprehensive, fully-integrated workflow and still leave room for customization and optimization. Further efforts for making such tools more user-friendly like GUIs, thorough documentation and quick start workflows could promote a broader use. Consistent maintenance and support even for future user generations would be of great help to the community. Comparability of results generated by different data processing tools was identified as a problem here. Future works should address this issue by using multiple feature extraction algorithms, especially when using NTS for process evaluations. Some limitations of conventional feature extraction tools are met by multivariate chemometric methods such as ROIMCR which ensures full spectral resolution when compressing second-order LC-MS data and does not require chromatographic deconvolution or alignment. Prioritization of relevant features is of utmost importance for NTS analysis due to the sheer amount of complex data. Strategies are mostly governed by the level of identification confidence assigned

to a feature-compound pair. Approaches that limit the number of possible annotations as was intended by the PubChemLite project could improve the efficiency of identification workflows in the future. HRMS is a powerful tool for structural elucidation by giving information on accurate mass, isotopic abundance patterns, and often fragmentation behaviour of compounds. It is probably due to these strengths that chromatographic information was sometimes overlooked in NTS identification workflows. As the RT is closely connected to the physicochemical properties of a compound like its hydrophobicity, it can be exploited for ranking or filtering annotated features. RTI and prediction make chromatographic information amenable to screening workflows. RTI tools are available on platforms like FOR-IDENT (<https://water-for-ident.org>) and the RTIs Platform of the National and Kapodistrian University of Athens (<http://rti.chem.uoa.gr/>). The need for additional information to augment HRMS data is also reflected by the growing interest in ion mobility spectrometry (IMS) for environmental analysis. The drift time measured by IMS is added as a fourth dimension to describe a feature (besides *m/z*, RT and signal intensity) and supports the identification of chemicals of emerging concern in water samples.<sup>77,78</sup> Another obvious choice for prioritization of non-target features are intensity-based approaches. However, no direct proportionality to the analyte's concentration can be assumed due to i.e. matrix effects (signal enhancement or suppression). Normalization using ISTDs could still allow an interpretation of feature profiles along spatial or temporal axes. Finally, sophisticated predictions of ionization efficiencies are able to accurately predict a feature's concentration without the help of analytical standards. Future NTS investigations might consider shifting the focus from a primarily qualitative to a more quantitative approach which might allow a quick, provisional risk assessment of a multitude of annotated features without having to rely on reference standards. The NTS solutions became generally more applicable in our days presented in practical review articles of quantitative NTS,<sup>71</sup> or other topics like IMS<sup>79</sup> and GC-MS.<sup>80</sup>

## ACKNOWLEDGEMENT

Figure 2 is licensed under a Creative Commons Attribution 4.0 International License: <http://creativecommons.org/licenses/by/4.0/>. We acknowledge financial support of the "Westfälische Wasser- und Umweltanalytik GmbH" and especially Dr. André Liesener for constructive discussions.

Open access funding enabled and organized by Projekt DEAL.

## CONFLICT OF INTEREST

The authors declare that they have no conflict of interest.

## AUTHOR CONTRIBUTIONS

Susanne Minkus: Conceptualization (equal), writing – original draft (lead), writing – review and editing (lead); Stefan Bieber: Conceptualization (supporting), writing – original draft (supporting), writing – review and editing (supporting); Thomas Letzel: Conceptualization (equal), writing – original draft (supporting), writing – review and editing (supporting)

## DATA AVAILABILITY STATEMENT

Data sharing is not applicable – no new data are generated.

## REFERENCES

- Schwarzenbach RP, Escher BI, Fenner K, et al. The challenge of micropollutants in aquatic systems. *Science* (80-). 2006;313(5790):1072–1077.
- Bolong N, Ismail AF, Salim MR, Matsuura T. A review of the effects of emerging contaminants in wastewater and options for their removal. *Desalination*. 2009;239(1-3):229–246. <https://doi.org/10.1016/j.desal.2008.03.020>.
- Schymanski EL, Singer HP, Longré P, et al. Strategies to characterize polar organic contamination in wastewater: exploring the capability of high resolution mass spectrometry. *Environ Sci Technol*. 2014;48(3):1811–1818. <https://doi.org/10.1021/es4044374>.
- Hollender J, Schymanski EL, Singer HP, Ferguson PL. Nontarget screening with high resolution mass spectrometry in the environment: ready to go?. *Environ Sci Technol*. 2017;51(20):11505–11512. <https://doi.org/10.1021/acs.est.7b02184>.
- Hernández F, Pozo JÓ, Sancho JV, López FJ, Harin JM, Ibáñez M. Strategies for quantification and confirmation of multi-class polar pesticides and transformation products in water by LC-MS<sup>2</sup> using triple quadrupole and hybrid quadrupole time-of-flight analyzers. *Trends Anal Chem*. 2005;24(7):596–612. <https://doi.org/10.1016/j.trac.2005.04.007>.
- Smith CA, Want EJ, O'Maille G, Abagyan R, Siuzdak G. XCMS: processing mass spectrometry data for metabolite profiling using nonlinear peak alignment, matching, and identification. *Anal Chem*. 2006;78(3):779–787. <https://doi.org/10.1021/ac051437y>.
- Pluskal T, Castillo S, Villar-Briones A, MZmine Orešič M. 2: modular framework for processing, visualizing, and analyzing mass spectrometry-based molecular profile data. *BMC Bioinformatics*. 2010;11(395). <https://doi.org/10.1186/1471-2105-11-395>.
- Martens L, Chambers M, Sturm M, et al. mzML - A community standard for mass spectrometry data. *Mol Cell Proteomics*. 2011;10(1):R110.000133. <https://doi.org/10.1074/mcp.R110.000133>.
- Pedrioli PGA, Eng JK, Hubley R, et al. A common open representation of mass spectrometry data and its application to proteomics research. *Nat Biotechnol*. 2004;22(11):1459–1466. <https://doi.org/10.1038/nbt1031>.
- Chambers MC, MacLean B, Burke R, et al. A cross-platform toolkit for mass spectrometry and proteomics. *Nat Biotechnol*. 2012;30(10):918–920. <https://doi.org/10.1038/nbt.2377>.
- Tautenhahn R, Bottcher C, Neumann S. Highly sensitive feature detection for high resolution LC/MS. *BMC Bioinformatics*. 2008;9:1–16. <https://doi.org/10.1186/1471-2105-9-504>.
- Myers OD, Sumner SJ, Li S, Barnes S, Du X. One step forward for reducing false positive and false negative compound identifications from mass spectrometry metabolomics data: new algorithms for constructing extracted ion chromatograms and detecting chromatographic peaks. *Anal Chem*. 2017;89(17):8696–8703. <https://doi.org/10.1021/acs.analchem.7b00947>.
- Broadhurst D, Goodacre R, Reinke SN, et al. Guidelines and considerations for the use of system suitability and quality control samples in mass spectrometry assays applied in untargeted clinical metabolomic studies. *Metabolomics*. 2018;14(6):1–17. <https://doi.org/10.1007/s11306-018-1367-3>.
- Schulze B, Jeon Y, Kaserzon S, et al. An assessment of quality assurance/quality control efforts in high resolution mass spectrometry nontarget workflows for analysis of environmental samples. *TrAC - Trends Anal Chem*. 2020;133(October). <https://doi.org/10.1016/j.trac.2020.116063>.
- Kim S, Chen J, Cheng T, et al. PubChem in 2021: new data content and improved web interfaces. *Nucleic Acids Res*. 2021;49(D1):D1388–D1395. <https://doi.org/10.1093/nar/gkaa971>.
- Pençe HE, ChemSpider Williams A. An online chemical information resource. *J Chem Educ*. 2010;87(11):1123–1124. <https://doi.org/10.1021/ED100697W>.
- Horai H, Arita M, Kanaya S, et al. MassBank: a public repository for sharing mass spectral data for life sciences. *J Mass Spectrom*. 2010;45(7):703–714. <https://doi.org/10.1002/jms.1777>.
- Ruttkies C, Schymanski EL, Wolf S, Hollender J, Neumann S. MetFrag relaunched: incorporating strategies beyond in silico fragmentation. *J Cheminform*. 2016;8(1):1–16. <https://doi.org/10.1186/s13321-016-0115-9>.
- Dührkop K, Fleischauer M, Ludwig M, et al. SIRIUS 4: a rapid tool for turning tandem mass spectra into metabolite structure information. *Nat Methods*. 2019;16(4):299–302. <https://doi.org/10.1038/s41592-019-0344-8>.
- Schymanski EL, Jeon J, Gulde R, et al. Identifying small molecules via high resolution mass spectrometry: communicating confidence. *Environ Sci Technol*. 2014;48(4):2097–2098. <https://doi.org/10.1021/es5002105>.
- Gramatica P. Principles of QSAR models validation: internal and external. *QSAR Comb Sci*. 2007;26(5):694–701. <https://doi.org/10.1002/qsar.200610151>.
- Tropsha A, Gramatica P, Gombar VK. The importance of being earnest: validation is the absolute essential for successful application and interpretation of QSPR models. *QSAR Comb Sci*. 2003;22(1):69–77. <https://doi.org/10.1002/qsar.200390007>.
- Urban J, Afseth NK, Štys D. Mass assignment, centroiding, and resolution – fundamental definitions and confusions in mass spectrometry. *TrAC Trends Anal Chem*. 2014;53:126–136. <https://doi.org/10.1016/j.trac.2013.07.010>.
- Berger U, Ost N, Sättler, et al. *Assessment of Persistence, Mobility and Toxicity (PMT) of 167 REACH Registered Substances, Report No (UBA-FB) 002595, German Environment Agency*; 2018.
- Samanipour S, Choi P, O'Brien JW, Pirok BWJ, Reid MJ, Thomas KV. From centroided to profile mode: machine learning for prediction of peak width in HRMS data. *Anal Chem*. 2021;93(49):16562–16570. <https://doi.org/10.1021/acs.analchem.1c03755>.
- Hohrenk LL, Itzel F, Baetz N, Tuerk J, Vosough M, Schmidt TC. Comparison of software tools for liquid chromatography-high-resolution mass spectrometry data processing in nontarget screening of environmental samples. *Anal Chem*. 2020;92(2):1898–1907. <https://doi.org/10.1021/acs.analchem.9b04095>.
- Höcker O, Flottmann D, Schmidt TC, Neusüß C. Non-targeted LC-MS and CE-MS for biomarker discovery in bioreactor: influence of separation, mass spectrometry and data processing tools. *Sci Total Environ*. 2021;798:149012. <https://doi.org/10.1016/j.scitotenv.2021.149012>.
- "Non-Target Screening" expert committee of the German Water Chemistry Society. *Use of Non-Target Screening by Means of LC-ESI-HRMS in Water Analysis*; 2019. [https://www.wasserchemische-gesellschaft.de/images/HAI/NTS-Guideline\\_EN\\_s.pdf](https://www.wasserchemische-gesellschaft.de/images/HAI/NTS-Guideline_EN_s.pdf)
- Peter KT, Phillips AL, Knolhoff AM, et al. Nontargeted analysis study reporting tool: a framework to improve research transparency and reproducibility. *Anal Chem*. 2021;93(41):13870–13879. <https://doi.org/10.1021/acs.analchem.1c02621>.
- Helmus R, ter Laak TL, van Wezel AP, de Voogt P, Schymanski EL. patRoom: open source software platform for environmental mass spectrometry based non-target screening. *J Cheminform*. 2021;13(1):1–25. <https://doi.org/10.1186/s13321-020-00477-w>.
- R Core Team. R: a language and environment for statistical computing. R Foundation for Statistical Computing. 2019. <https://www.r-project.org/>
- Loos M, Schmitt U, Schollée JE. *enviMass* version 3.5. 2018. <https://doi.org/10.5281/zenodo.1213098>

33. Libiseller G, Dvorzak M, Kleb U, et al. IPO: a tool for automated optimization of XCMS parameters. *BMC Bioinformatics*. 2015;16(1):1–10. <https://doi.org/10.1186/s12859-015-0562-8>.
34. Delabriere A, Warmer P, Brennstiner V, Zamboni N. SLAW: a scalable and self-optimizing processing workflow for untargeted LC-MS. *Anal Chem*. 2021. <https://doi.org/10.1021/acs.analchem.1c02687>.
35. Röst HL, Sachsenberg T, Aeche S, et al. OpenMS: a flexible open-source software platform for mass spectrometry data analysis. *Nat Methods*. 2016;13(9):741–748. <https://doi.org/10.1038/nmeth.3959>.
36. Tauler R, Gorrochategui E, Jaumot J, Tauler R. A protocol for LC-MS metabolomic data processing using chemometric tools. *Protoc Exch*. 2015:1–28. <https://doi.org/10.1038/protex.2015.102>.
37. Gorrochategui E, Jaumot J, Tauler R. ROIMCR: a powerful analysis strategy for LC-MS metabolomic datasets. *BMC Bioinformatics*. 2019;20(1):1–17. <https://doi.org/10.1186/s12859-019-2848-8>.
38. Stolt R, Torgrip RJO, Lindberg J, et al. Second-order peak detection for multicomponent high-resolution LC/MS data. *Anal Chem*. 2006;78(4):975–983. <https://doi.org/10.1021/ac050980b>.
39. Tauler R. Multivariate curve resolution applied to second order data. *Chemom Intell Lab Syst*. 1995;30(1):133–146. [https://doi.org/10.1016/0169-7439\(95\)00047-X](https://doi.org/10.1016/0169-7439(95)00047-X).
40. de Juan A, Tauler R. Multivariate curve resolution: 50 years addressing the mixture analysis problem – a review. *Anal Chim Acta*. 2021;1145:59–78. <https://doi.org/10.1016/j.aca.2020.10.051>.
41. Perez-Lopez C, Ginebreda A, Carrascal M, Barcelò D, Abian J, Tauler R. Non-target protein analysis of samples from wastewater treatment plants using the regions of interest-multivariate curve resolution (ROIMCR) chemometrics method. *J Environ Chem Eng*. 2021;9(4). <https://doi.org/10.1016/j.jece.2021.105752>.
42. Hohrenk LL, Vosough M, Schmidt TC. Implementation of chemometric tools to improve data mining and prioritization in LC-HRMS for non-target screening of organic micropollutants in complex water matrices. *Anal Chem*. 2019;91(14):9213–9220. <https://doi.org/10.1021/acs.analchem.9b01984>.
43. Sangster T, Major H, Plumb R, Wilson AJ, ID Wilson. A pragmatic and readily implemented quality control strategy for HPLC-MS and GC-MS-based metabolomic analysis. *Analyst*. 2006;131(10):1075–1078. <https://doi.org/10.1039/b604498k>.
44. Godzien J, Alonso-Herranz V, Barbas C, Armitage EG. Controlling the quality of metabolomics data: new strategies to get the best out of the QC sample. *Metabolomics*. 2015;11(3):518–528. <https://doi.org/10.1007/s11306-014-0712-4>.
45. Schollée JE, Hollender J, McArdell CS. Characterization of advanced wastewater treatment with ozone and activated carbon using LC-HRMS based non-target screening with automated trend assignment. *Water Res*. 2021;200:117209. <https://doi.org/10.1016/j.watres.2021.117209>.
46. Kiefer K, Du L, Singer H, Hollender J. Identification of LC-HRMS nontarget signals in groundwater after source related prioritization. *Water Res*. 2021;196:116994. <https://doi.org/10.1016/j.watres.2021.116994>.
47. Letzel T, Bayer A, Schulz W, et al. LC – MS screening techniques for wastewater analysis and analytical data handling strategies : sartans and their transformation products as an example. *Chemosphere*. 2015;137:198–206. <https://doi.org/10.1016/j.chemosphere.2015.06.083>.
48. Williams AJ, Grulke CM, Edwards J, et al. The CompTox chemistry dashboard: a community data resource for environmental chemistry. *J Cheminform*. 2017;9(1):1–27. <https://doi.org/10.1186/s13321-017-0247-6>.
49. Schymanski EL, Kondić T, Neumann S, Thiessen PA, Zhang J, Bolton EE. Empowering large chemical knowledge bases for exposomics: PubChemLite meets MetFrag. *J Cheminform*. 2021;13(1):1–15. <https://doi.org/10.1186/s13321-021-00489-0>.
50. Kind T, Fiehn O. Metabolomic database annotations via query of elemental compositions: mass accuracy is insufficient even at less than 1 ppm. *BMC Bioinformatics*. 2006:1–10. <https://doi.org/10.1186/1471-2105-7-234>.
51. Minkus S, Grosse S, Bieber S, Veloutsou S, Letzel T. Optimized hidden target screening for very polar molecules in surface waters including a compound database inquiry. *Anal Bioanal Chem*. 2020;412(20):4953–4966. <https://doi.org/10.1007/s00216-020-02743-0>.
52. Minkus S, Bieber S, Letzel T. (Very) polar organic compounds in the Danube river basin: non-target screening workflow and prioritization strategy for extracting highly confident features. *Anal Methods*. 2021;13(17):2044–2054. <https://doi.org/10.1039/D1AY00434D>.
53. Greco G, Grosse S, Letzel T. Serial coupling of reversed-phase and zwitterionic hydrophilic interaction LC/MS for the analysis of polar and nonpolar phenols in wine. *J Sep Sci*. 2013;36(8):1379–1388. <https://doi.org/10.1002/jssc.201200920>.
54. Kováts E. Gas-chromatographische Charakterisierung organischer Verbindungen. Teil 1: retentionsindices aliphatischer halogenide, alkohole, aldehyde und ketone. *Helv Chim Acta*. 1958;41(7):1915–1932. <https://doi.org/10.1002/hlca.19580410703>.
55. Rostkowski P, Haglund P, Aalizadeh R, et al. The strength in numbers: comprehensive characterization of house dust using complementary mass spectrometric techniques. *Anal Bioanal Chem*. 2019. <https://doi.org/10.1007/s00216-019-01615-6>.
56. Wahman R, Moser S, Bieber S, et al. Untargeted analysis of lemna minor metabolites: workflow and prioritization strategy comparing highly confident features between different mass spectrometers. *Metabolites*. 2021;11(12):832. <https://doi.org/10.3390/metabo11120832>.
57. Aalizadeh R, Alygizakis NA, Schymanski EL, et al. Development and application of liquid chromatographic retention time indices in HRMS-based suspect and nontarget screening. *Anal Chem*. 2021;93(33):11601–11611. <https://doi.org/10.1021/acs.analchem.1c02348>.
58. Aalizadeh R, Thomaidis NS, Bletsou AA, Gago-Ferrero P. Quantitative structure-retention relationship models to support nontarget high-resolution mass spectrometric screening of emerging contaminants in environmental samples. *J Chem Inf Model*. 2016;56(7):1384–1398. <https://doi.org/10.1021/acs.jcim.5b00752>.
59. Aalizadeh R, Nika MC, Thomaidis NS. Development and application of retention time prediction models in the suspect and non-target screening of emerging contaminants. *J Hazard Mater*. 2019;363(September 2018):277–285. <https://doi.org/10.1016/j.jhazmat.2018.09.047>.
60. Parinet J. Prediction of pesticide retention time in reversed-phase liquid chromatography using quantitative-structure retention relationship models: a comparative study of seven molecular descriptors datasets. *Chemosphere*. 2021;275:130036. <https://doi.org/10.1016/j.chemosphere.2021.130036>.
61. Bade R, Bijlsma L, Miller TH, Barron LP, Sancho JV, Hernández F. Suspect screening of large numbers of emerging contaminants in environmental waters using artificial neural networks for chromatographic retention time prediction and high resolution mass spectrometry data analysis. *Sci Total Environ*. 2015;538(2015):934–941. <https://doi.org/10.1016/j.scitotenv.2015.08.078>.
62. Bade R, Bijlsma L, Sancho JV, Hernández F. Critical evaluation of a simple retention time predictor based on LogKow as a complementary tool in the identification of emerging contaminants in water. *Talanta*. 2015;139:143–149. <https://doi.org/10.1016/j.talanta.2015.02.055>.
63. Barron LP, McEneff GL. Gradient liquid chromatographic retention time prediction for suspect screening applications: a critical assessment of a generalised artificial neural network-based approach across 10 multi-residue reversed-phase analytical methods. *Talanta*. 2016;147:261–270. <https://doi.org/10.1016/j.talanta.2015.09.065>.

64. Norekdeen HAA, Liu X, Wang X, et al. Quantitative structure-retention relationships model for retention time prediction of veterinary drugs in food matrices. *Int J Mass Spectrom.* 2018;434:172–178. <https://doi.org/10.1016/j.ijms.2018.09.022>.
65. McEachran AD, Mansouri K, Newton SR, Beverly BEJ, Sobus JR, Williams AJ. A comparison of three liquid chromatography (LC) retention time prediction models. *Talanta.* 2018;182:371–379. <https://doi.org/10.1016/j.TALANTA.2018.01.022>.
66. Loos M. Mining of high-resolution mass spectrometry data to monitor organic pollutant dynamics in aquatic systems. 2015. <https://doi.org/10.3929/ethz-a-010645125> Rights
67. Albergamo V, Schollée JE, Schymanski EL, et al. Nontarget screening reveals time trends of polar micropollutants in a riverbank filtration system. *Environ Sci Technol.* 2019;53(13):7584–7594. <https://doi.org/10.1021/acs.est.9b01750>.
68. Bader T, Schulz W, Kümmerer K, Winzenbacher R. LC-HRMS data processing strategy for reliable sample comparison exemplified by the assessment of water treatment processes. *Anal Chem.* 2017;89(24):13219–13226. <https://doi.org/10.1021/acs.analchem.7b03037>.
69. Reymond N, Emke E, Boucheron T, et al. Retrospective suspect and non-target screening combined with similarity measures to prioritize MDMA and amphetamine synthesis markers in wastewater. *Sci Total Environ.* 2022;811:152139. <https://doi.org/10.1016/j.scitotenv.2021.152139>.
70. Krueve A, Kiefer K, Hollender J. Benchmarking of the quantification approaches for the non-targeted screening of micropollutants and their transformation products in groundwater. *Anal Bioanal Chem.* 2021;413(6):1549–1559. <https://doi.org/10.1007/s00216-020-03109-2>.
71. Malm L, Palm E, Souihi A, Plassmann M, Liigand J, Krueve A. Guide to semi-quantitative non-targeted screening using LC/ESI/HRMS. *Molecules.* 2021;26(12):3524. <https://doi.org/10.3390/molecules26123524>.
72. McCord JP, Groff LC, Sobus JR. Quantitative non-targeted analysis: bridging the gap between contaminant discovery and risk characterization. *Environ Int.* 2022;158:107011. <https://doi.org/10.1016/j.envint.2021.107011>. August 2021.
73. Richardson SD, Ternes TA. Water analysis: emerging contaminants and current issues. *Anal Chem.* 2021. <https://doi.org/10.1021/acs.analchem.1c04640>.
74. Liigand J, Wang T, Kellogg JJ, Smedsgaard J, Cech NB, Krueve A. Quantifying the unquantifiable: quantification for non-targeted LC/MS screening without standards. *Sci Rep.* 2020. <https://doi.org/10.1038/s41598-020-62573-z>. in press.
75. Yap CW. PaDEL-descriptor: an open source software to calculate molecular descriptors and fingerprints. *J Comput Chem.* 2010;32(7):1466–1474. <https://doi.org/10.1002/jcc.21707>.
76. Pieke EN, Granby K, Trier X, Smedsgaard J. A framework to estimate concentrations of potentially unknown substances by semi-quantification in liquid chromatography electrospray ionization mass spectrometry. *Anal Chim Acta.* 2017;975:30–41. <https://doi.org/10.1016/j.ACA.2017.03.054>.
77. Menger F, Gago-Ferrero P, Wiberg K, Ahrens L. Wide-scope screening of polar contaminants of concern in water: a critical review of liquid chromatography-high resolution mass spectrometry-based strategies. *Trends Environ Anal Chem.* 2020;28:e00102. <https://doi.org/10.1016/j.teac.2020.e00102>.
78. Hinnenkamp V, Balsaa P, Schmidt TC. Target, suspect and non-target screening analysis from wastewater treatment plant effluents to drinking water using collision cross section values as additional identification criterion. *Anal Bioanal Chem.* 2021. <https://doi.org/10.1007/s00216-021-03263-1>.
79. Capitain C, Weller P. Non-targeted screening approaches for profiling of volatile organic compounds based on gas chromatography-mobility spectroscopy (GC-IMS) and machine learning. *Molecules.* 2021;26(18):5457. <https://doi.org/10.3390/molecules26185457>.
80. Li X, Dorman FL, Helm PA, et al. Nontargeted screening using gas chromatography-atmospheric pressure ionization mass spectrometry: recent trends and emerging potential. *Molecules.* 2021;26(22):6911. <https://doi.org/10.3390/molecules26226911>.

**How to cite this article:** Minkus S, Bieber S, Letzel T. Spotlight on mass spectrometric non-target screening analysis: Advanced data processing methods recently communicated for extracting, prioritizing and quantifying features. *Anal Sci Adv.* 2022;1–10. <https://doi.org/10.1002/ansa.202200001>

## Appendix B: **Supporting information**

**Appendix B.1 Supplementary material - Optimization of electrospray ionization parameters in a RPLC-HILIC-MS/MS coupling by design of experiment**

Table S1: The design matrix on which the experimental plan depended. The lower and upper limit of the setting range is depicted by -1 and +1, respectively. Find the factor values in Table 1. Experiments 1 – 18 derived from a fractional factorial screening design with resolution IV. Experiments 19 – 21 were conducted to check for non-linearities if the factor ISV and 22 – 46 were a D-optimal complement.

Exp. No.	G1	G2	CUR	ISV	Temp	DP
1	-1	-1	-1	-1	-1	-1
2	1	-1	-1	-1	1	-1
3	-1	1	-1	-1	1	1
4	1	1	-1	-1	-1	1
5	-1	-1	1	-1	1	1
6	1	-1	1	-1	-1	1
7	-1	1	1	-1	-1	-1
8	1	1	1	-1	1	-1
9	-1	-1	-1	1	-1	1
10	1	-1	-1	1	1	1
11	-1	1	-1	1	1	-1
12	1	1	-1	1	-1	-1
13	-1	-1	1	1	1	-1
14	1	-1	1	1	-1	-1
15	-1	1	1	1	-1	1
16	1	1	1	1	1	1
17	0	0	0	-0.286	0	0
18	0	0	0	-0.286	0	0
19	0	0	0	-1	0	0
20	0	0	0	1	0	0
21	0	0	0	0	0	0
22	-1	-1	1	1	-0.333	1

---

<b>23</b>	-1	-1	0.333	1	-1	-1
<b>24</b>	-1	-1	-0.333	1	1	1
<b>25</b>	-1	1	-1	1	-0.333	1
<b>26</b>	-1	1	1	1	1	0.333
<b>27</b>	-1	-0.333	-1	-1	-1	1
<b>28</b>	-1	0.333	-1	-1	1	-1
<b>29</b>	1	-1	-1	1	0.333	-1
<b>30</b>	1	-1	1	1	1	-0.333
<b>31</b>	1	-1	-0.333	1	-1	1
<b>32</b>	1	1	-1	1	1	0.333
<b>33</b>	1	1	1	1	-1	0.333
<b>34</b>	1	1	0.333	1	1	-1
<b>35</b>	1	-0.333	1	-1	-1	-1
<b>36</b>	1	-0.333	1	-1	1	1
<b>37</b>	0.333	-1	-1	-1	1	1
<b>38</b>	-0.333	-1	1	-1	1	-1
<b>39</b>	-0.333	1	-1	-1	-1	-1
<b>40</b>	0.333	1	1	-1	-1	1
<b>41</b>	0	0	0	0	0	0
<b>42</b>	1	-0.333	1	-1	1	1
<b>43</b>	1	1	1	-1	1	-1
<b>44</b>	1	-1	1	1	1	-0.333
<b>45</b>	-1	1	-1	-1	1	1
<b>46</b>	1	1	1	-1	1	-1

---

Table S2: The 30 model substances below were chosen to check their response in signal intensity when varying the factor settings of the ESI source. In addition, the response specifications for each substance are listed. Responses that were logarithmically transformed in order to achieve a normal distribution are marked “~”.

Response	Name	InChi Key	Log D (pH 7)	Specification minimum [Cps]	Specification target [Cps]
1 ~	2,2,6,6-tetramethyl-4-piperidone	JWUXJYZVKZKLTJ-UHFFFAOYSA-N	-0.32	10000	320000
2 ~	2,4-Diamino-6-hydroxymethylpiperidine	CYNARAWTVHQHDI-UHFFFAOYSA-N	-1.37	10000	140000
3 ~	3-Dimethylaminopropionitrile	MTPJEFOSTIKRSS-UHFFFAOYSA-N	-0.30	2000	24000
4 ~	2-Morpholinoethanol	KKFDCBRMNNSAAW-UHFFFAOYSA-N	-1.13	10000	280000
5 ~	4-Methylumbelliferone	HSHNITRMYYLLCV-UHFFFAOYSA-N	1.72	10000	29000
6 ~	Candesartan	HTQMVQVXFRQIKW-UHFFFAOYSA-N	-0.12	10000	290000
7	Dapsone	MQJKPEGWNLWLTK-UHFFFAOYSA-N	1.27	10000	27000
8	DEET	MMOXZBCLCQITDF-UHFFFAOYSA-N	2.5	10000	540000
9	Dimethoate	MCWXGJITAZMZEV-UHFFFAOYSA-N	0.34	10000	53000
10 ~	Dorzolamide	IAVUPMFITXYVAFXPUUQOCRSA-N	-0.32	10000	98000
11 ~	Etilefrine	SQVIAVUSQAWMKL-UHFFFAOYSA-N	-1.42	10000	260000
12 ~	Panthenol	SNPLKNRPJHDVJAUHFFFAOYSA-N	-1.70	10000	100000
13 ~	Flufenacet	IANUJLZYFUDJIH-UHFFFAOYSA-N	3.22	20000	240000
14	Flurtamone	NYRMIJKDBAQCHC-UHFFFAOYSA-N	4.64	10000	2.5e+06
15 ~	Haloxypop	GOCUAJYOYBLQRH-UHFFFAOYSA-N	0.77	7000	30000

16 ~	Linuron	XKJMBINCVNINCA- UHFFFAOYSA-N	2.3	10000	55000
17	L-Phenylalanin	COLNVLDHVKWLR T-QMMMGPBSA- N	-1.19	2000	8000
18	Malathion	JXSJBGJIGXNWCI- UHFFFAOYSA-N	1.86	10000	133161
19 ~	Melamine	JDSHMPZPIAZGSV -UHFFFAOYSA-N	-1.97	10000	100000
20	Metazachlor	STEPQTYSZVCJPV -UHFFFAOYSA-N	2.98	10000	170000
21 ~	Metconazol	XWPZUHJBOLQNM N-UHFFFAOYSA-N	3.59	10000	520000
22 ~	Methylisothiazoli none	BEGLCMHJXHIJLR- UHFFFAOYSA-N	0.23	10000	110000
23 ~	Metobromuron	WLFdqEVORAMCI M-UHFFFAOYSA-N	2.24	10000	100000
24	Metolachlor	WVQBLGZPHOPPF O-UHFFFAOYSA-N	3.45	10000	260000
25 ~	Metribuzin	FOXfZRUHNHCZP X-UHFFFAOYSA-N	1.96	10000	290000
26 ~	Minoxidil	ZIMGGGWCDYVHO Y-UHFFFAOYSA-N	-2.25	10000	500000
27	Molinate	DEDOPGXGGQYY MW-UHFFFAOYSA- N	2.34	5000	30000
28	Monuron	BMLIZLVNXIYGCK- UHFFFAOYSA-N	1.93	10000	59000
29 ~	Moroxydine	KJHOZAZQWVKILO -UHFFFAOYSA-N	-5.43	10000	350000
30	N,N'- Trimethyleneure a	NQPJDJVGBDHCA D-UHFFFAOYSA-N	-1.03	10000	45000

---

**Appendix B.2 Electronic supplementary material - Optimized hidden target screening for very polar molecules in surface waters including a compound database inquiry**

**Analytical and Bioanalytical Chemistry**

**Electronic Supplementary Material**

**Optimized hidden target screening for very polar molecules in surface waters including a compound database inquiry**

Susanne Minkus, Sylvia Grosse, Stefan Bieber, Sofia Veloutsou, Thomas Letzel

**Table S1** Sample locations and coordinates. The relevance of the sampling location is explained in the comment. Each location was sampled during March, May and July of 2015. The samples 1, 7 and 10 of March and July were used for the DoE

ID	Location	Coordinates	Comment
1	Austria	47.395241, 11.265037	Estimation of the water quality before entering Germany
2	After Mittenwald	47.518692, 11.295976	Downstream of a wastewater treatment plant (WWTP) that discharges into the Isar river and a dam
3	Seinsbach river	47.473354, 11.279471	Pristine from the mountains
4	After Sylvenstein Lake	47.639632, 11.593347	Reservoir that creates long hydraulic retention times
5	Jachen river	47.639859, 11.576852	Carries water from a storage power plant
6	After Bad Tölz	47.781697, 11.545989	Sampling site is located 800 m downstream of a WWTP
7	Loisach river	47.933574, 11.428642	700 m downstream of a WWTP and 500 m upstream of the Loisach river entering the Isar
8	Before Munich	48.040292, 11.513920	Right before Isar enters the city of Munich
9	After Munich	48.313040, 11.699037	Located 2 km after a WWTP that treats water of Munich
10	After Freising	48.403349, 11.792101	2.2 km downstream of the WWTP that belongs to the town of Freising
11	Dingolfing	48.634222, 12.494877	Located downstream of the town of Landshut and a local power plant

**Table S2** Information on the gradients for the RPLC separation and the HILIC separation

RPLC			HILIC		
Time [min]	Flow rate [mL min <sup>-1</sup> ]	Solvent B [%]	Time [min]	Flow rate [mL min <sup>-1</sup> ]	Solvent D [%]
0	0.05	0	0	0.40	0
7	0.05	0	6	0.40	0
12	0.05	50	13	0.40	40
13	0.10	50	32	0.40	40
22	0.10	100	33	0.80	0
32	0.10	100	53	0.80	0
33	0.10	0	54	0.40	0
53	0.10	0	58	0.40	0
54	0.05	0			
58	0.05	0			

**Table S3** The 68 standard compounds shown below were measured four times over the course of the campaign. The mean values and the standard deviations (SDs) were calculated for the retention time (RT), the mass error (deviation of the observed mass from the monoisotopic mass), the full width at half maximum (FWHM) of the peak and its height. For the parameter RT, the relative standard deviation (RSD) is also provided. The entries are sorted in ascending order by mean RT

Compound Name	Formula	InChi Key	Monoisotopic Mass	Mean RT [min]	SD RT [min]	RSD RT [%]	Mean mass error [ppm]	SD mass error [ppm]	Mean FWHM [min]	SD FWHM [min]	Mean height [Counts]	SD height [Counts]
Dimethylsulfide	C2 H6 O S	IAZDPXIMUYVGZ-UHFFFAOYSA-N	78.0139	5.9	0.1	1.1	5.0	2.1	0.24	0.04	37291	63734
Methylurea	C2 H8 N2 O	XGEGHDBEHXKFP-X-UHFFFAOYSA-N	74.0480	6.0	0.1	1.4	7.8	1.3	0.20	0.03	491597	912742
2-pyrrolidinone	C4 H7 N O	HNJBEVLQSNELDL-UHFFFAOYSA-N	85.0528	6.1	0.1	1.7	3.0	1.4	0.14	0.02	105885	196125

Compound Name	Formula	InChi Key	Monoisotopic Mass	Mean RT [min]	SD RT [min]	RSD RT [%]	Mean mass error [ppm]	SD mass error [ppm]	Mean FWHM [min]	SD FWHM [min]	Mean height [Counts]	SD height [Counts]
Dicyandiamide	C2 H4 N4	QGBSISYHAICWAH-UHFFFAOYSA-N	84.0436	6.2	0.2	2.6	6.4	1.3	0.18	0.04	97936	169073
1-methylimidazole	C4 H6 N2	MCTWTZJPVLRJOU-UHFFFAOYSA-N	82.0531	6.3	0.1	1.1	5.7	3.4	0.17	0.07	4838967	8795216
6-Mercaptopurine	C5 H4 N4 S	GLVAUDGFNGKCSF-UHFFFAOYSA-N	152.0157	6.5	0.2	3.7	3.1	0.7	0.36	0.14	288785	406380
4(5)-Methylimidazole	C4 H6 N2	XLSZMDLNRCEUJ-UHFFFAOYSA-N	82.0531	6.7	0.1	1.2	5.6	2.2	0.26	0.06	5055221	6614692
Adenine	C5 H5 N5	GGFGBXGBJISGV-UHFFFAOYSA-N	135.0545	6.9	0.1	1.3	1.2	1.6	0.20	0.01	1037819	1839883
Melamine	C3 H6 N6	JDSHMPZPIAZGSV-UHFFFAOYSA-N	126.0654	7.0	0.1	0.8	2.2	2.4	0.34	0.06	1932888	3131122
Riboflavin	C17 H20 N4 O6	AUNGANRZJHGGP-Y-UHFFFAOYSA-N	376.1383	7.3	0.1	1.6	4.0	2.4	0.33	0.02	538360	848416
L-phenylalanine	C9 H11 N O2	COLNVLDHVWVLR-T-QMMMGPBSA-N	165.0790	10.3	0.2	1.5	4.4	3.8	0.25	0.17	162023	184999
Gabapentin	C9 H17 N O2	UGJMXCAKUNAIE-UHFFFAOYSA-N	171.1259	10.4	0.5	4.6	3.4	2.5	0.29	0.20	844230	1188812
Leucine	C6 H13 N O2	ROHFNLRQFUQHC-H-UHFFFAOYSA-N	131.0946	10.4	0.0	0.4	3.6	1.5	0.26	0.18	272597	371024
L-isoleucine	C6 H13 N O2	AGPKZVBTJNPAG-WHFBIKZSA-N	131.0946	10.8	0.1	0.7	2.2	1.7	0.20	0.12	263624	337823
L-tryptophan	C11 H12 N2 O2	QIVBCDUJAJPQS-VIFPVBQESA-N	204.0899	10.9	0.3	2.9	3.4	0.8	0.24	0.12	72993	88316
2,2',2''-nitrotriethanol	C6 H15 N O3	GSEJCLTVZPLZKY-UHFFFAOYSA-N	149.1067	11.4	0.2	2.0	8.8	7.1	0.31	0.30	825943	1515162
L-tyrosine	C9 H11 N O3	OUYCCASQSFEME-QMMMGPBSA-N	181.0739	11.6	0.1	1.0	3.1	0.3	0.23	0.07	55310	41879
Betaine	C5 H11 N O2	KWIUHFFTVRNATP-UHFFFAOYSA-N	117.0790	11.8	0.0	0.4	0.6	1.9	0.41	0.12	1238247	2295923
Atenolol	C14 H22 N2 O3	METKIMKYRPLGGS-UHFFFAOYSA-N	266.1630	12.0	0.5	3.8	3.9	2.3	0.36	0.14	2401537	3362767
Glutamate	C5 H9 N O4	WHUUTDBJXRKM-K-VKHYHEASA-N	147.0532	12.1	0.1	0.8	2.2	1.3	0.21	0.05	111016	164053
Vigabatrin	C6 H11 N O2	PJDFLNIOAUIZSL-UHFFFAOYSA-N	129.0790	12.7	0.0	0.3	2.1	0.8	0.28	0.09	616169	887394
L-asparagine	C4 H8 N2 O3	DCXYFEDJOCNFAF-REOHLBBSA-N	132.0535	13.1	0.1	1.0	2.6	1.9	0.44	0.20	80562	98645
Sotalol	C12 H20 N2 O3 S	ZBMZVLHJSJCTVON-UHFFFAOYSA-N	272.1195	14.5	0.6	4.2	3.5	1.8	1.13	0.43	726289	926508
Guanyurea	C2 H6 N4 O	SQSPRWMERUQXN-E-UHFFFAOYSA-N	102.0542	14.7	0.4	2.4	2.1	1.2	0.48	0.32	736194	1038678
Metformin	C4 H11 N5	XZWYZLIPXDOLR-UHFFFAOYSA-N	129.1014	17.0	0.8	4.4	1.8	1.3	0.99	0.72	997888	1229991
Primidone	C12 H14 N2 O2	DQMZLTXERSFNPB-UHFFFAOYSA-N	218.1055	23.7	0.2	0.7	5.4	1.5	0.21	0.09	25964	20892
Haloxyfop	C15 H11 Cl F3 N O4	GOCUAIJOYBLQRH-UHFFFAOYSA-N	361.0329	25.5	0.3	1.1	4.3	3.8	0.20	0.05	29582	26386
Diiclofenac	C14 H11 Cl2 N O2	DCOPUUMXTXDBNB-UHFFFAOYSA-N	295.0167	25.7	0.4	1.4	4.4	1.9	0.23	0.05	20882	22389
Carbetamide	C12 H16 N2 O3	AMRQXHFJXZFDCH-VIFPVBQESA-N	236.1161	25.8	0.2	0.9	5.6	1.7	0.15	0.09	1391259	2136834
Indomethacin	C19 H16 Cl N O4	CGIGDMFJXJATDK-UHFFFAOYSA-N	357.0768	25.9	0.4	1.7	5.1	1.6	0.13	0.00	109787	113961
Oxadixyl	C14 H18 N2 O4	UWVQIROCRJWDKL-UHFFFAOYSA-N	278.1267	26.3	0.3	1.0	2.2	4.8	0.14	0.04	1834928	2030737
Monuron	C9 H11 Cl N2 O	BMLZLVNXYGCK-UHFFFAOYSA-N	198.0560	26.3	0.2	0.9	3.9	1.0	0.16	0.01	951744	1623685
Carbamazepine	C15 H12 N2 O	FFGPTBGBLSHEPO-UHFFFAOYSA-N	236.0950	26.5	0.2	0.9	2.7	5.3	0.13	0.02	2349907	2997974
Phenytoin	C15 H12 N2 O2	CXOFVDLJLONNDW-UHFFFAOYSA-N	252.0899	26.5	0.2	0.9	5.1	1.2	0.13	0.01	75960	110426
Azamethiphos	C9 H10 Cl N2 O5 P S	VNKBTWQZTQIWDV-UHFFFAOYSA-N	323.9737	26.5	0.2	0.9	5.5	2.9	0.12	0.06	2878677	5067968
Atrazine	C8 H14 Cl N5	MXWJVTOOROXGIU-UHFFFAOYSA-N	215.0938	27.7	0.3	1.0	6.2	3.4	0.13	0.05	2477966	3226190
N,N-diethyl-m-toluamide (DEET)	C12 H17 N O	MMOXZBCLCQITDF-UHFFFAOYSA-N	191.1310	27.7	0.3	0.9	5.4	4.0	0.12	0.05	3132623	3800263
Carboxin	C12 H13 N O2 S	GYSSRZJHXQEHQUHFFFAOYSA-N	235.0667	27.8	0.2	0.8	3.4	1.0	0.16	0.01	902560	970027
Testosterone	C19 H28 O2	MUMGGOZAMZWBJJ-DYKIFRCSA-N	288.2089	28.0	0.3	1.0	3.5	3.9	0.16	0.02	115814	111034

Compound Name	Formula	InChi Key	Monoisotopic Mass	Mean RT [min]	SD RT [min]	RSD RT [%]	Mean mass error [ppm]	SD mass error [ppm]	Mean FWHM [min]	SD FWHM [min]	Mean height [Counts]	SD height [Counts]
Metobromuron	C9 H11 Br N2 O2	WLFDQEVORAMCI-M-UHFFFAOYSA-N	258.0004	28.2	0.2	0.7	2.7	6.5	0.12	0.07	40185	20351
Metazachlor	C14 H16 Cl N3 O	STEPQTYSZVCJPV-UHFFFAOYSA-N	277.0982	28.3	0.2	0.8	4.7	2.9	0.17	0.03	2946569	4054204
Diphenhydramine	C17 H21 N O	ZZVUWRFRHKOJYTH-UHFFFAOYSA-N	255.1623	28.8	0.6	2.0	3.9	2.3	0.29	0.14	3218370	3525887
Flurtamone	C18 H14 F3 N O2	NYRMIJKDBAQCHC-UHFFFAOYSA-N	333.0977	28.9	0.2	0.8	2.9	2.7	0.13	0.07	2183773	2057452
Tris(2-chloro-1-methylethyl) phosphate (TCPP)	C9 H18 Cl3 O4 P	KVMPUXDNESXNO-H-UHFFFAOYSA-N	326.0008	29.0	0.2	0.8	4.2	2.2	0.18	0.01	303175	203903
Diethofencarb	C14 H21 N O4	LNJNFVJKDJYTEU-UHFFFAOYSA-N	267.1471	29.2	0.2	0.8	3.8	0.7	0.16	0.02	239752	149112
Linuron	C9 H10 Cl2 N2 O2	XXJMBINCNVNINCA-UHFFFAOYSA-N	248.0119	29.3	0.2	0.8	2.0	1.9	0.18	0.00	73997	94418
Norfluoxetin	C16 H16 F3 N O	WQRCCHMSJFFON-W-UHFFFAOYSA-N	295.1184	29.5	0.6	2.1	3.6	2.5	0.30	0.15	959864	1503514
Chlorbromuron	C9 H10 Br Cl N2 O2	NLYNUTMZTCLNO-O-UHFFFAOYSA-N	291.9614	29.6	0.2	0.8	3.5	1.9	0.18	0.01	77590	103420
Boscalid	C18 H12 Cl2 N2 O	WYEMLYFITZORAB-UHFFFAOYSA-N	342.0327	29.8	0.2	0.8	3.1	1.9	0.16	0.01	141605	69289
Molinate	C9 H17 N O S	DEDOPGXGGQYYM-W-UHFFFAOYSA-N	187.1031	30.2	0.2	0.8	6.0	1.1	0.15	0.03	69840	97180
Methyl dihydrojasmonate	C13 H22 O3	KWWWIYGFBDJQC-UHFFFAOYSA-N	226.1569	30.3	0.2	0.7	4.7	6.2	0.15	0.02	31169	25586
Malathion	C10 H19 O6 P S2	JXSJBGJGXNWC-UHFFFAOYSA-N	330.0361	30.4	0.2	0.7	4.2	0.6	0.16	0.03	859644	684270
Fenoxycarb	C17 H19 N O4	HJUFUJJOISQSKQ-UHFFFAOYSA-N	301.1314	30.4	0.2	0.7	6.8	1.0	0.15	0.02	208143	174020
Metconazol	C17 H22 Cl N3 O	XWPZUHJBLQNM-N-UHFFFAOYSA-N	319.1451	30.5	0.2	0.7	4.4	2.8	0.14	0.05	3123646	3307415
Flufenacet	C14 H13 F4 N3 O2 S	IANJLZYFUDJIH-UHFFFAOYSA-N	363.0665	30.6	0.2	0.7	3.7	1.3	0.16	0.01	264444	112156
Metolachlor	C15 H22 Cl N O2	WVQBLGZPHOPPF-O-UHFFFAOYSA-N	283.1339	30.8	0.2	0.7	4.7	1.8	0.20	0.03	1727283	1622800
Alachlor	C14 H20 Cl N O2	XCSPAVHZFQHG-E-UHFFFAOYSA-N	269.1183	30.8	0.2	0.7	3.5	0.8	0.36	0.03	105024	69633
Tris(2-chloro-1-(chloromethyl)ethyl) phosphate (TDCPP)	C9 H15 Cl6 O4 P	ASLWPAWFJZCFK-F-UHFFFAOYSA-N	427.8839	31.0	0.2	0.7	3.4	2.4	0.15	0.00	41791	17891
Chlorfenvinphos	C12 H14 Cl3 O4 P	FSAVDKDHPDSC-T-UHFFFAOYSA-N	357.9695	31.1	0.2	0.8	5.4	1.5	0.13	0.03	955520	608441
Oxybenzone	C14 H12 O3	DXGLGDHPHMLXJ-C-UHFFFAOYSA-N	228.0786	31.1	0.2	0.6	4.0	1.3	0.18	0.01	194328	149481
Picoxystrobin	C18 H16 F3 N O4	IBSNKSODLGJUMQ-UHFFFAOYSA-N	367.1031	31.3	0.2	0.7	2.2	1.8	0.19	0.03	3929775	2355193
Pyraclostrobin	C19 H18 Cl N3 O4	HZRSNVGNWUDEF-X-UHFFFAOYSA-N	387.0986	32.1	0.2	0.7	-0.4	1.8	0.18	0.08	7563212	4124593
Triclocarban	C13 H9 Cl3 N2 O	ICUTUKXCWQYES-Q-UHFFFAOYSA-N	313.9780	32.3	0.2	0.6	-0.9	1.3	0.19	0.02	44608	6709
Diazinon	C12 H21 N2 O3 P S	FHIVAFMUCKRCQO-UHFFFAOYSA-N	304.1010	32.4	0.2	0.7	3.6	2.1	0.17	0.02	6467634	7187032
Profenofos	C11 H15 Br Cl O3 P S	QYMMJNLHFKGAN-Y-UHFFFAOYSA-N	371.9351	33.7	0.4	1.1	2.1	1.9	0.31	0.10	193587	206316
Prosulfocarb	C14 H21 N O S	NQLVQOSNDJXLKG-UHFFFAOYSA-N	251.1344	34.1	0.2	0.7	4.5	1.5	0.18	0.03	581161	684205
Quinoxifen	C15 H8 Cl2 F N O	WRPIRSINYZBGPK-UHFFFAOYSA-N	306.9967	34.5	0.2	0.5	1.5	1.4	0.17	0.07	3678364	1956188
Fenofibrat	C20 H21 Cl O4	YMTINGFKWWXKF-G-UHFFFAOYSA-N	360.1128	35.1	0.2	0.7	2.3	1.7	0.21	0.02	78572	77999

**Table S4** The eight quantitative factors were defined at two levels. Those minimum and maximum values either derived from the operational range given by the program or an estimation based on the initial raw data check. The objective of a design of experiment is to check a reduced set of factor value combinations. The experimental plan displayed below derives from a Plackett-Burman screening design (experiments 1-12) with a complete fold-over (experiments 13-24), two adjusted center-point runs (experiments 25, 26) and two runs to check for non-linearities of factor (experiments 27, 28)

Exp. No.	F1 [Counts]	F2 [-]	F3 [min]	F4 [ppm]	F5 [Counts]	F6 [Counts]	F7 [Counts]	F8 [ppm]
1	2000	1	1.0	5.0	0	5000	5000	10.0
2	2000	4	0.1	50.0	0	5000	0	10.0
3	0	4	1.0	5.0	5000	0	0	10.0
4	2000	1	1.0	50.0	0	0	0	500.0
5	2000	4	0.1	50.0	5000	0	5000	10.0
6	2000	4	1.0	5.0	5000	5000	0	500.0
7	0	4	1.0	50.0	0	0	5000	500.0
8	0	1	1.0	50.0	5000	5000	5000	10.0
9	0	1	0.1	50.0	5000	5000	0	500.0
10	2000	1	0.1	5.0	5000	0	5000	500.0
11	0	4	0.1	5.0	0	5000	5000	500.0
12	0	1	0.1	5.0	0	0	0	10.0
13	0	4	0.1	50.0	5000	0	0	500.0
14	0	1	1.0	5.0	5000	0	5000	500.0
15	2000	1	0.1	50.0	0	5000	5000	500.0
16	0	4	0.1	5.0	5000	5000	5000	10.0
17	0	1	1.0	5.0	0	5000	0	500.0
18	0	1	0.1	50.0	0	0	5000	10.0
19	2000	1	0.1	5.0	5000	5000	0	10.0
20	2000	4	0.1	5.0	0	0	0	500.0
21	2000	4	1.0	5.0	0	0	5000	10.0
22	0	4	1.0	50.0	0	5000	0	10.0
23	2000	1	1.0	50.0	5000	0	0	10.0
24	2000	4	1.0	50.0	5000	5000	5000	500.0
25	1000	2	0.6	27.5	2500	2500	2500	200.0
26	1000	2	0.6	27.5	2500	2500	2500	200.0
27	1000	3	0.1	27.5	2500	2500	2500	100.0
28	1000	3	1.0	27.5	2500	2500	2500	100.0

**Table S5** Below the mean values and standard deviations (SD) of the ten features are given which responses R5 and R6 are based on. The integration of all their EICs was manually checked based on the following criteria: The relative mass differences of the peaks within a compound group should not exceed an overall spread of  $\pm 10$  ppm. Furthermore, a peak is approximately Gaussian shaped and in its mass spectrum, the monoisotopic signal should be accompanied by at least one additional isotope ion

Feature	Mean RT [min]	SD RT [min]	Mean mass	SD mass
1	13.2	0.0	75.0326	0.0003
2	7.2	0.0	117.0789	0.0001
3	6.3	0.1	144.0906	0.0005
4	27.7	0.1	227.1898	0.0008
5	5.8	0.0	268.1523	0.0007
6	9.3	0.0	314.1945	0.0008
7	29.9	0.3	414.2073	0.0016
8	26.0	0.1	529.3828	0.0013
9	23.7	0.1	848.4306	0.0062
10	11.9	0.0	921.0027	0.0001

**Table S6** The responses were calculated after conducting the 28 experiments given in Table S4. Each set of six response values corresponds to the result of an experiment. At the bottom the specifications that were defined for the limit optimization are provided

Exp. No.	R1 [min]	R2 [%]	R3 [%]	R4 [ppm]	R5 [-]	R6 [-]
1	0.07	2.6	7.9	1.5	6	15
2	0.03	2.7	16.0	1.5	4	25
3	0.33	5.8	44.8	2.6	5	15
4	0.22	5.6	35.8	2.3	6	20
5	0.03	1.7	8.4	1.2	4	22
6	0.22	7.0	35.4	2.7	9	19
7	0.13	2.7	24.4	2.4	6	13
8	0.07	2.4	9.6	1.6	4	10
9	0.02	3.3	11.4	1.8	5	24
10	0.02	3.4	5.2	1.6	2	27
11	0.02	3.2	12.7	1.8	4	17
12	0.03	2.7	13.1	1.6	2	16
13	0.03	3.3	14.5	1.9	5	19
14	0.11	4.2	18.6	2.2	6	17
15	0.02	3.0	5.6	1.5	2	26
16	0.03	1.9	10.0	1.4	3	21
17	0.26	6.0	38.8	2.6	12	13
18	0.03	1.8	6.7	1.3	3	23
19	0.03	2.6	9.8	1.4	4	27
20	0.03	3.5	13.7	1.8	4	23
21	0.09	2.5	12.1	1.6	6	13
22	0.32	5.6	46.8	2.6	10	6
23	0.29	5.7	45.3	2.1	9	10
24	0.11	4.1	21.3	2.0	6	17
25	0.07	3.6	21.2	2.1	10	14
26	0.07	3.6	21.2	2.1	10	14
27	0.03	3.1	14.2	1.8	4	18
28	0.13	4.6	22.7	2.4	6	17
<b>Target</b>	0.01	1.0	10.0	1.0	3	7
<b>Maximum</b>	0.30	6.0	50.0	3.0	15	20

**Table S7** For each response variable (R1 – 6) the coefficients and the standard errors of the model terms that are included in the model are presented. The  $R^2$  and  $Q^2$  values measure the goodness-of-fit and goodness-of prediction for each response. The formulas are presented at the bottom of the table with the observed value  $y$ , the predicted value  $\hat{y}$ , the mean value  $\bar{y}$  and the predicted response  $\hat{y}_{-i}$  when leaving out the  $i$ -th object from the training set (cross-validation\*). A model with a value of 1 for both,  $R^2$  and  $Q^2$ , fits the data perfectly

	R1	R2	R3	R4	R5	R6
<b>Constant</b>	-1.185 ± 0.024	3.673 ± 0.135	1.351 ± 0.079	2.136 ± 0.123	10.000 ± 1.023	14.300 2.132
<b>F1</b>	-	-	-0.043 ± 0.023	-0.110 0.035	-	2.083 ± 0.614
<b>F2</b>	-	-	0.076 ± 0.023	0.091 ± 0.035	-	-
<b>F3</b>	0.385 ± 0.025	0.868 ± 0.140	0.186 ± 0.022	0.310 ± 0.034	1.731 ± 0.284	-3.962 ± 0.590
<b>F3<sup>L</sup></b>	-	-	-0.157 ± 0.082	-0.240 ± 0.127	-4.731 ± 1.062	3.959 ± 2.210
<b>F4</b>	-	-	-	-	-	-
<b>F5</b>	-	-	-	-	-	-
<b>F6</b>	-	-	-	-	0.458 ± 0.295	-
<b>F7</b>	-0.120 ± 0.026	-0.851 ± 0.145	-0.170 ± 0.023	-0.195 ± 0.035	-0.958 ± 0.295	-
<b>F8</b>	-	0.441 ± 0.143	-	0.161 ± 0.035	-	1.329 ± 0.605
$R^2 = 1 - \frac{\sum_{i=1}^n (y_i - \hat{y}_i)^2}{\sum_{i=1}^n (y_i - \bar{y})^2}; Q^2 = 1 - \frac{\sum_{i=1}^n (y_i - \hat{y}_{-i})^2}{\sum_{i=1}^n (y_i - \bar{y})^2}$						
<b>R<sup>2</sup></b>	0.913	0.775	0.868	0.880	0.753	0.739
<b>Q<sup>2</sup></b>	0.889	0.685	0.796	0.805	0.651	0.638

\* Golub GH, Heath M, Wahba G (1979) Generalized cross-validation as a method for choosing a good ridge parameter. *Technometrics* 21:215–223.

**Table S8** The table shows isotope ratios of the chromatographic peaks from the EICs displayed in the Figures S1-3. The highest mass spectrometric peak was scaled to 100%. When calculating isotope ratios mass spectrometric peaks with intensities < 1% were neglected. Deviations of one percentage point could occur for low-intensity peaks of molecules with more than five atoms of the same kind\*

	Peak	Intensity (expected) [%]	Intensity (reference) [%]	Intensity (samples) [%]
<b>Guanylurea</b>	First isotope	100.0	100.0	100.0
	Second isotope	3.7	3.1	3.0
<b>Melamine</b>	First isotope	100.0	100.0	100.0
	Second isotope	5.5	4.6	4.4
<b>1,3-dimethylimidazolidin-2-one</b>	First isotope	100.0	100.0	100.0
	Second isotope	6.3	5.8	3.3

\* Pfeilsticker D Isotopen-Muster-Rechner. <https://www.pfeilsticker.net/chemie/massen/>. Accessed 25 Jan 2020

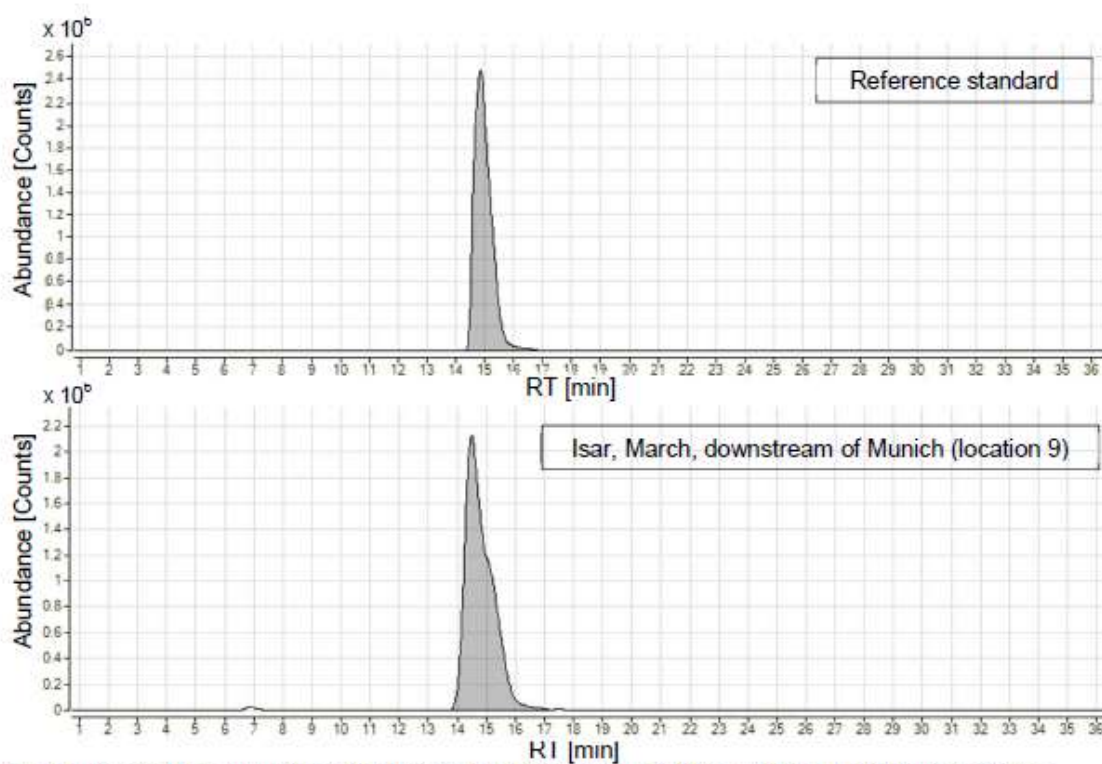


Fig. S1 Extracted ion chromatograms (EICs) of guanlyurea (ID 2) in the standard mix (top) and in the water sample (bottom)

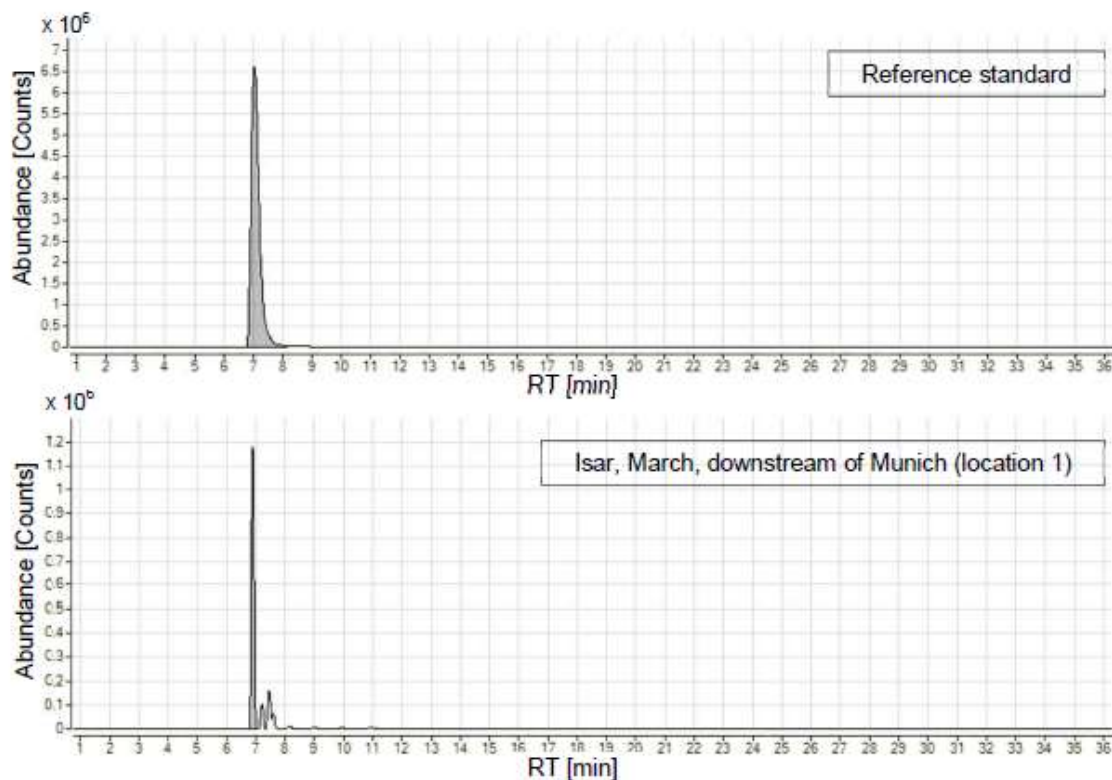
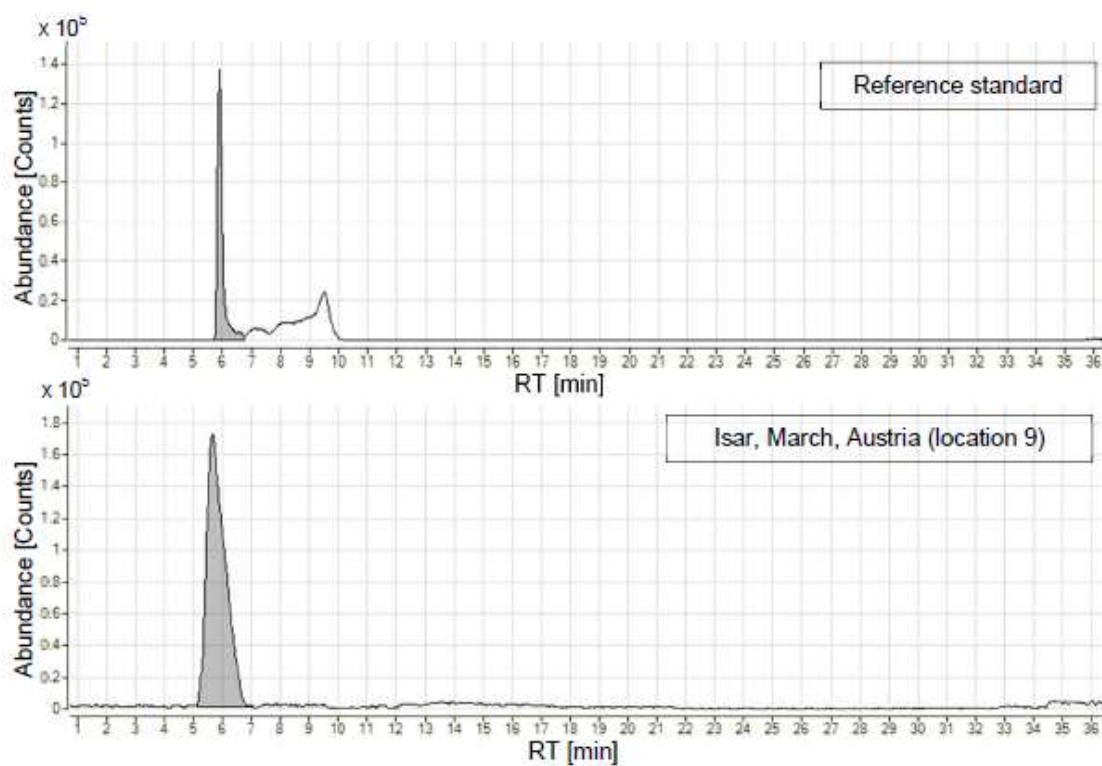


Fig. S1 Extracted ion chromatograms (EICs) of melamine (ID 11) in the standard mix (top) and in the water sample (bottom)



**Fig. S2** Extracted ion chromatograms (EICs) of 1,3-dimethylimidazolidin-2-one (ID 6) in the standard mix (top) and in the water sample (bottom)

---

**Appendix B.3 Electronic supplementary information - (Very) polar organic compounds in the Danube river basin: Non-target screening workflow and prioritization strategy for extracting highly confident features**

## Electronic supplementary information

(Very) polar organic compounds in the Danube river basin: Non-target screening workflow and prioritization strategy for extracting highly confident features

Susanne Minkus<sup>a,b</sup>, Stefan Bieber<sup>b</sup> and Thomas Letzel<sup>a,b\*</sup>

### Content:

Table S1: Targeted analysis to determine the RT tolerance.....	2
Table S2: Targeted analysis to optimize the non-targeted feature extraction method.....	6
Table S3: Detailed descriptions of the 52 samples taken from the Danube river and several of its tributaries.....	9
Table S4: The exact parameter settings of the feature extraction method.....	11
Table S5: Target compounds that were identified as false negative features and their points of losses in the feature extraction workflow.....	14
Table S6: The features-candidate compound pairs of class B.....	16

<sup>a</sup> Technical University of Munich (Chair of Urban Water Systems Engineering), Munich, Germany.

<sup>b</sup> Analytisches Forschungsinstitut für Non-Target Screening GmbH (AFIN-TS), Augsburg, Germany.

Table S1: Targeted analysis of the multicomponent standard: 100 reference compounds were measured in triplicates. The variation of parameter values is indicated by the standard deviation (SD) or the relative standard deviation (RSD). The maximum RT difference ( $\Delta$ RT) of 1.60 min was found for histamine and this value was set for the RT tolerance of the non-targeted feature extraction method.

Compound name	InChIKey	Log D (pH 7)	Mean RT [min]	SD RT [min]	RSD RT [%]	$\Delta$ RT (min)
1-(3-carboxypropyl)-3,7-dimethyl-xanthin	WKASGTGXOGALBG-UHFFFAOYSA-N	-3.6	7.91	0.10	1.29	0.20
1,2,2,6,6-Pentamethyl-4-piperidinol	NWHNXXMYEICZAT-UHFFFAOYSA-N	-2.1	11.82	0.14	1.22	0.28
1,2-Dimethylimidazole	GIWOSPTLQVMISG-UHFFFAOYSA-N	-0.3	9.37	0.16	1.65	0.31
1,3-Dimethyl-2-imidazolidinone	CYSGHNMQYZMIA-UHFFFAOYSA-N	-0.6	6.02	0.04	0.70	0.08
1-[N,N-Bis(2-hydroxyethyl)amino]-2-propanol	ZFECYLNALTEDE-UHFFFAOYSA-N	-3.2	9.47	0.08	0.86	0.16
1-Methylimidazole	MCTWTZJPVRIQIU-UHFFFAOYSA-N	-0.1	8.56	0.09	1.01	0.16
2-(Butylamino)ethanol	LIDSTRZHPWMDPG-UHFFFAOYSA-N	-2.4	11.55	0.08	0.72	0.15
2,2,6,6-Tetramethyl-4-piperidinol	VDVUCLWZJHFAV-UHFFFAOYSA-N	-2.3	11.67	0.13	1.14	0.27
2,2,6,6-tetramethyl-4-piperidone	JWUXJYZKZKLTJ-UHFFFAOYSA-N	-0.3	6.50	0.04	0.69	0.09
2,4-Diamino-6-(hydroxymethyl)pteridine	CYNARAWTVHQHDI-UHFFFAOYSA-N	-1.4	7.74	0.06	0.78	0.12
2,6-Dimethylmorpholine	HNVIQPOGUDBSU-UHFFFAOYSA-N	-1.3	10.81	0.11	0.99	0.19
2-Aminopyridine	ICSNLGPBYBMBD-UHFFFAOYSA-N	0.3	6.40	0.00	0.07	0.01
2-Butyne-1,4-diol	DLDJFOGPPSOZKI-UHFFFAOYSA-N	-0.7	11.67	0.12	1.04	0.24
2-Methylimidazole	LXBGSDVWAMZDD-UHFFFAOYSA-N	-0.6	10.09	0.38	3.77	0.71
2-Phenyl-5-benzimidazole	UVCIGUGAGLDPAA-UHFFFAOYSA-N	0.1	6.96	0.07	1.04	0.13
2-Pyrrolinone	HNJBEVLOSNELDL-UHFFFAOYSA-N	-0.6	6.27	0.10	1.63	0.18
3,4-Diaminobenzoic acid	HEMGTNNCNDNX-UHFFFAOYSA-N	-1.6	6.49	0.02	0.27	0.03
3-Aminobenzoic acid	XFDUJHPVKIXHO-UHFFFAOYSA-N	-1.4	8.12	0.13	1.62	0.26
3-Dimethylaminopropionitrile	MTPJEFOSTIKRSS-UHFFFAOYSA-N	-0.3	6.45	0.04	0.57	0.07
3-Pyridinemethanol	MVQVNTPHUGQQHK-UHFFFAOYSA-N	0.0	6.40	0.02	0.24	0.03
4-(2-Hydroxyethyl)morpholine	KKFDCBRMNSAAW-UHFFFAOYSA-N	-1.1	7.01	0.04	0.54	0.07
4-Formylmorpholine	LCEDQNDDFOCWGG-UHFFFAOYSA-N	-0.9	6.01	0.02	0.33	0.04
4-Methylimidazole	XLSZMDLNRCEUJ-UHFFFAOYSA-N	-0.3	9.21	0.20	2.21	0.39
4-Methylmorpholine	SJRIKPEHAURKC-UHFFFAOYSA-N	-0.7	8.31	0.02	0.23	0.03
4-Pyrimidinol	DNCYBUMDUBHJZ-UHFFFAOYSA-N	-0.6	6.85	0.14	2.11	0.29

6-Amino-1,3-dimethyl-5-(formylamino)uracil	ZNDGACBZGSJGU-UHFFFAOYSA-N	-2.0	6.92	0.05	0.70	0.09
Acamprosate	AFCGFAGUEYAMAO-UHFFFAOYSA-N	-4.1	7.30	0.07	0.98	0.14
Acetaminophen	RZVAJINKPMORJF-UHFFFAOYSA-N	0.9	6.39	0.12	1.82	0.21
Acetylcholine	OIPILEWXSMMKGL-UHFFFAOYSA-N	-4.2	11.66	0.08	0.72	0.15
Acetylslysine	DTERQVGMUDWAZ-UHFFFAOYSA-N	-3.2	13.04	0.30	2.26	0.58
Adenine	GFFGJBXBJISGV-UHFFFAOYSA-N	-0.6	7.75	0.06	0.78	0.12
Adenosine	OIRDTOYFTABOOQ-UHFFFAOYSA-N	-2.1	7.71	0.02	0.26	0.04
Allantoin	POIWDADGALRAB-UHFFFAOYSA-N	-2.4	10.46	0.03	0.32	0.06
Arecoline	HJJPSJXAXAIPN-UHFFFAOYSA-N	-0.6	6.85	0.02	0.28	0.04
Asulam	VGPYEKHOIGNJKV-UHFFFAOYSA-N	-0.6	6.10	0.07	1.16	0.12
Atenolol	METKIMKYRPLGS-UHFFFAOYSA-N	-2.1	11.38	0.05	0.47	0.11
Betaine	KWIUHFTVRNATP-UHFFFAOYSA-O	-3.7	14.94	0.44	2.96	0.77
Bisoprolol-M3	WONQRVASZHUNFS-UHFFFAOYSA-N	-1.2	12.54	0.02	0.18	0.04
Caffeine	RYVVLZVUVJVGH-UHFFFAOYSA-N	-0.6	6.05	0.01	0.18	0.02
Candesartan	HTOMVQVFRQIKW-UHFFFAOYSA-N	-0.1	7.18	0.10	1.33	0.18
Chlorsulfuron	VJYFXZLXQVHO-UHFFFAOYSA-N	1.6	5.92	0.08	1.28	0.14
Cimetidine	AOXAKUUQRKLNLD-UHFFFAOYSA-N	-0.3	7.24	0.07	0.92	0.13
Ciprofloxacin	MYSWGUAQZAJOK-UHFFFAOYSA-N	-0.8	6.98	0.04	0.53	0.07
Cytosine	OPTASPLRGRNAP-UHFFFAOYSA-N	-1.2	9.24	0.19	2.04	0.35
Dacarbazine	OMJKFYKNWZZTK-UHFFFAOYSA-N	-1.7	7.80	0.21	2.75	0.38
Dicyandiamide	QGBSISYHAICWAH-UHFFFAOYSA-N	-1.0	6.63	0.02	0.31	0.04
Disopropylamine	UAOMVDZISHZME-UHFFFAOYSA-N	-1.8	10.94	0.09	0.85	0.17
Dimethylsulfoxide	IAZDPXIOMIUVGZ-UHFFFAOYSA-N	-1.4	6.05	0.01	0.13	0.02
Dipropylamine	WEHWNAGRSTTBQ-UHFFFAOYSA-N	-1.6	10.58	0.07	0.71	0.15
Ectoine	WQXNXVJDBPYKBA-UHFFFAOYSA-N	-2.5	12.74	0.02	0.13	0.03
Etilefrine	SCVIAVUSOAWMKL-UHFFFAOYSA-N	-1.4	11.38	0.06	0.57	0.13
Famotidine	XUFQPHANEPEMU-UHFFFAOYSA-N	-3.0	7.30	0.06	0.83	0.11
Gabapentin	UGJMXCAKCUNAIE-UHFFFAOYSA-N	-1.3	9.98	0.02	0.18	0.03
Gamma-aminobutyric acid	BTCSZJIGUNDROE-UHFFFAOYSA-N	-2.9	13.75	0.04	0.26	0.07

Glycine ethyl ester	NTNZEONFHNYBC-UHFFFAOYSA-N	-1.0	6.69	0.04	0.54	0.07
Guanylurea	SQSPRWMERUOXNE-UHFFFAOYSA-N	-2.1	14.51	0.20	1.35	0.36
Histamine	NTYJOPFIAHURM-UHFFFAOYSA-N	-3.9	15.01	0.80	5.36	1.60
Isopentylamine	BMFVGAASNGQNM-UHFFFAOYSA-N	-1.8	10.92	0.07	0.66	0.14
L-Alanine	ONAYBMKLOCPYGI-UHFFFAOYSA-N	-2.8	13.23	0.08	0.60	0.16
Lenalidomid	GOTYRUGSSMKFN-UHFFFAOYSA-N	-0.7	13.35	0.09	0.66	0.16
Leucine	ROHFNLRQFUQHCH-UHFFFAOYSA-N	-1.6	11.07	0.07	0.64	0.14
Lisinopril	RLAWWYSOJDYHDC-BZSNMDCSA-N	-3.1	13.07	0.03	0.23	0.05
L-Isoleucine	AGPKZVBTJINPAG-WHFBIAKZSA-N	-1.5	11.31	0.06	0.55	0.13
L-Phenylalanine	COLNLVDHVKWLRT-UHFFFAOYSA-N	-1.2	10.98	0.08	0.76	0.14
L-Proline	ONIBWKKTOPOVIA-UHFFFAOYSA-N	-2.6	12.50	0.04	0.34	0.08
L-Threonine	AYFYIQAPQTCC-GBXJUSLDSA-N	-3.5	11.38	0.10	0.86	0.18
L-Tyrosine	OUYCCASQSFEME-QMMMGPBSA-N	-1.5	12.26	0.03	0.28	0.07
Melamine	JDSHMPZPIAZGSV-UHFFFAOYSA-N	-2.0	9.51	0.20	2.05	0.39
Metformin	XZWYZLUPXDOLR-UHFFFAOYSA-N	-3.7	15.04	0.76	5.04	1.45
Methacrylic acid	CEROIWHTDKMF-UHFFFAOYSA-N	-1.2	13.76	0.04	0.30	0.08
Methylisothiazolinone	BEGLCMHXHLR-UHFFFAOYSA-N	0.2	6.07	0.01	0.15	0.02
Metoprolol acid	PUQIRTNPIRRCZ-UHFFFAOYSA-N	-1.0	12.48	0.01	0.10	0.02
Miglitol	IBAQFQHRJAVAV-UJAWRXDOSA-N	-3.9	11.58	0.03	0.29	0.06
Moroxydine	KJHOZAZQWVKILO-UHFFFAOYSA-N	-5.4	13.89	0.73	5.23	1.45
N-(Hydroxymethyl)nicotinamide	JRFKIOFLCXKVT-UHFFFAOYSA-N	-0.8	6.49	0.02	0.27	0.03
N,N'-Ethylenebisacetamide	WNYIBZHOMJZDKN-UHFFFAOYSA-N	-1.8	6.23	0.03	0.56	0.07
N,N'-Trimethyleneurea	NQPIDIVGBDHCAD-UHFFFAOYSA-N	-1.0	6.70	0.03	0.40	0.05
N-[3-(dimethylamino)propyl]methacrylamide	GDFCSMGLZFNFY-UHFFFAOYSA-N	-1.9	12.21	0.31	2.58	0.62
N-Hydroxyethyl acrylamide	CNCOEDDPFOAUMB-UHFFFAOYSA-N	-0.6	6.21	0.01	0.21	0.02
N-Methylurea	XGEGHDBEHKFPX-UHFFFAOYSA-N	-1.1	6.24	0.02	0.35	0.04
Norphenylephrine	LRCRAABFLVAI-UHFFFAOYSA-N	-1.9	14.32	0.34	2.39	0.63
Omethoate	PZXOQEXFMICDPG-UHFFFAOYSA-N	-0.6	6.01	0.04	0.63	0.07
Oxaceprol	BAPRUDZDYCKSOQ-WDSKDSINSA-N	-4.7	11.93	0.07	0.55	0.12

Pantherol	SNPLKNRPJHDVJA-ZETCQYMHSA-N	-1.7	6.62	0.03	0.47	0.06
Piracetam	GMZVRMREEHGGF-UHFFFAOYSA-N	-1.7	6.36	0.05	0.73	0.08
Pregabalin	AYXPKUFHZROOJ-ZETCQYMHSA-N	-1.4	10.33	0.13	1.30	0.25
Pyridoxine	LXNHXLTXMVPWM-UHFFFAOYSA-N	-1.0	6.72	0.11	1.58	0.21
Riboflavin	AUNGANRZJHGGPY-UHFFFAOYSA-N	-1.2	7.77	0.06	0.77	0.12
Ritalinic acid	INGSNVSERUZOAK-UHFFFAOYSA-N	-0.4	8.58	0.02	0.18	0.03
Sarcosine	FSYKKLZXSHPZ-UHFFFAOYSA-N	-3.2	13.04	0.07	0.57	0.15
Sotalol	ZBMZVLHSICTVON-UHFFFAOYSA-N	-2.5	10.70	0.13	1.17	0.25
Taurine	XOAAWQZATWQOTB-UHFFFAOYSA-N	-2.6	12.79	0.20	1.53	0.34
Tetraethylene glycol	UWHCKJMYHZGTTT-UHFFFAOYSA-N	-1.4	6.26	0.04	0.56	0.07
Tetraethylene glycol dimethylether	ZUHZGEOXBKGPSW-UHFFFAOYSA-N	-0.1	6.19	0.07	1.19	0.13
Triethanolamine	GSEJCLTVZPLZKY-UHFFFAOYSA-N	-3.3	11.57	0.13	1.15	0.26
Triethylene glycol monomethyl ether	JLGLQAWTXGDEM-UHFFFAOYSA-N	-0.7	6.03	0.01	0.13	0.01
Trisopropanolamine	SLNHHMUFWFWMU-UHFFFAOYSA-N	-2.9	6.82	0.06	0.88	0.12
Tyramine	DZGWFCGIZJUFU-UHFFFAOYSA-N	-1.5	11.82	0.16	1.34	0.31
Vidarabine	OIRDQYFTABQOQ-UHTZMRCNSA-N	-2.1	8.48	0.08	0.95	0.16
Vigabatrin	PIDFLNIOAUJZSL-UHFFFAOYSA-N	-2.1	12.91	0.20	1.52	0.35

Table S2: Targeted analysis to optimize the feature extraction method: 34 reference compounds were measured at two concentration levels, three times in each case (n = 6). The variation of parameter values is indicated by the standard deviation (SD) or the relative standard deviation (RSD). Peak width was expressed by the full width at half maximum (FWHM).

Compound name	InChiKey	log D (pH 7)	Mean m/z [Da]	RSD m/z [ppm]	Mass error [ppm]	$\Delta$ Mass [Da]	Mean RT [min]	SD RT [min]	RSD RT [%]	$\Delta$ RT [min]	Mean peak height [cps/Da]	SD peak height [cps/Da]	Mean peak duration time [min]	SD peak duration time [min]	Mean FWHM [min]	SD FWHM [min]
1,1'-iminodipropan-2-ol	LVTYCIALWPMFN	-3.2	134.1199	1.5	17.2	0.0005	14.70	0.06	0.4	0.19	583	529	1.45	0.46	0.52	0.06
1,2,2,6-Pentamethyl-4-piperidinol	NW-HNXMYEICZAT-UHFFFAOYSA-N	-2.1	172.1720	2.8	13.8	0.0013	11.77	0.03	0.2	0.08	1065	923	2.32	0.80	0.24	0.04
1-[N,N-Bis(2-hydroxyethyl)amino]-2-propanol	ZFECCYLNALTEDE-UHFFFAOYSA-N	-3.2	164.1312	3.1	19.0	0.0013	9.93	0.05	0.5	0.14	3075	2525	2.03	0.47	0.61	0.15
2,2,6,6-Tetramethyl-4-piperidinol	VDVUCLWZJHFAV-UHFFFAOYSA-N	-2.3	158.1566	1.3	17.1	0.0005	11.57	0.02	0.2	0.05	869	684	0.84	0.30	0.18	0.02
2,4-Diamino-6-hydroxymethylpteridine	CYNARAWTVHQHD-UHFFFAOYSA-N	-1.4	193.0844	2.0	5.8	0.0006	9.03	0.02	0.2	0.06	871	741	1.29	0.48	0.43	0.10
2-Butylaminoethanol	LJDSTRZHPWMDPG-UHFFFAOYSA-N	-2.4	118.1246	1.8	16.9	0.0009	11.66	0.02	0.2	0.05	956	831	0.64	0.17	0.17	0.03
4-(2-Hydroxyethyl)morpholine	KKFDCBRMNSAAW-UHFFFAOYSA-N	-1.1	132.1020	0.6	1.0	0.0002	7.81	0.02	0.3	0.05	573	461	1.42	0.52	0.23	0.04
Acetyllysine	DTEROYGVUDWYAZ-UHFFFAOYSA-N	-3.2	189.1232	4.6	-0.9	0.0025	13.08	0.05	0.4	0.15	1792	1459	1.54	0.40	0.37	0.04
Adenine	GFFGIBXBJISGV-UHFFFAOYSA-N	-0.6	136.0641	2.1	17.1	0.0009	9.01	0.08	0.9	0.20	171	113	0.86	0.28	0.25	0.12
Adenosine	OIRDQYFTABQQ-UHFFFAOYSA-N	-2.1	268.1084	0.4	16.1	0.0003	9.04	0.05	0.5	0.13	9339	8182	1.72	0.31	0.44	0.02
Atenolol	METKIMKRPQLGS-UHFFFAOYSA-N	-2.1	267.1746	1.3	15.9	0.0010	13.87	0.09	0.7	0.24	4156	3705	2.73	0.64	0.87	0.05
Bisoprolol-H3	WONQVRSZJHNS-UHFFFAOYSA-N	-1.2	254.1427	1.4	15.6	0.0009	12.46	0.01	0.1	0.02	11724	10540	0.88	0.32	0.19	0.03
Creatinine	DDRIANPRUIHGJ-UHFFFAOYSA-N	-1.5	114.0681	6.9	16.7	0.0021	13.09	0.02	0.2	0.06	626	545	2.06	0.51	0.47	0.17
Ectoine	WQXNYUDBPYKBA-UHFFFAOYSA-N	-2.5	143.0839	3.7	16.8	0.0013	12.65	0.02	0.1	0.05	2177	1889	0.84	0.21	0.18	0.04

Glutathion	RWSXRVCMGQZ WBV- UHFFFAOYSA-N	0.0	308.091 9	2.1	2.7	0.001 7	12.59	0.03	0.2	0.09	297	224	0.24	0.06	0.10	0.05
Guanylurea	SQSPRWMERUOX NE-UHFFFAOYSA- N	-2.1	103.061 8	1.0	3.3	0.000 3	14.32	0.01	0.1	0.04	271	154	0.66	0.16	0.23	0.04
Hydroxyproline	PNMVEEVMWA SON- DMTCNVQSA-N	-3.7	132.067 6	2.9	15.9	0.001 1	13.49	0.03	0.2	0.07	531	514	0.67	0.36	0.17	0.03
L-Citrulline	RHGKRLROHJDJR -UHFFFAOYSA-N	-3.9	176.100 4	4.1	-14.5	0.002 0	13.88	0.03	0.2	0.07	854	698	1.20	0.52	0.28	0.16
Glutamate	WHJUUTDBJXJK MK- VKHMYHEASA-N	-5.9	148.060 4	3.2	-0.6	0.001 3	12.64	0.02	0.2	0.06	241	119	0.71	0.10	0.40	0.36
L-Glutamic acid	WHJUUTDBJXJK MK-UHFFFAOYSA- N	-5.9	148.063 0	5.3	1.6	0.002 2	12.57	0.02	0.2	0.06	320	192	0.53	0.23	0.19	0.04
Lisinopril	RLAWWYSOIDYH DC- BZSNMMDCSA-N	-3.1	406.233 2	2.0	-1.2	0.001 8	13.50	0.02	0.2	0.07	662	566	1.55	1.20	0.43	0.21
L-Proline	ONIBWKTPOVI A-UHFFFAOYSA-N	-2.6	116.073 1	2.5	21.3	0.000 9	12.51	0.09	0.7	0.25	336	281	0.89	0.62	0.20	0.12
L-Tyrosine	OUYCCASQSFEM E- QMMMGPOBSA- N	-1.5	182.082 7	3.9	8.2	0.002 0	12.52	0.05	0.4	0.13	258	162	0.54	0.25	0.20	0.08
Methyl-3-aminocrotonate	KKORCTIIRYKLLG- ONEGZINKSA-N	-0.2	116.072 0	4.7	12.1	0.001 4	12.53	0.04	0.3	0.11	166	118	0.73	0.17	0.28	0.08
Metoprolol acid	PUQIRTPIRFCZ -UHFFFAOYSA-N	-1.0	268.154 7	2.3	1.3	0.001 7	12.41	0.01	0.1	0.03	8854	7699	0.95	0.38	0.16	0.01
Miglitol	IBAQFQHRJAV V-UJLAWRXDQSA- N	-3.9	208.120 9	3.5	14.2	0.002 0	11.43	0.03	0.3	0.09	589	491	0.77	0.32	0.22	0.03
Moroxydine	KHOZAZQWVKIL O-UHFFFAOYSA-N	-5.4	172.119 4	1.2	0.5	0.000 6	13.61	0.02	0.1	0.05	1235	1108	3.12	1.14	0.79	0.21
N-Acetyethanolamine	PVCJKHXXKFRP -UHFFFAOYSA-N	-1.5	104.070 8	2.2	2.2	0.000 7	13.77	0.01	0.1	0.04	166	121	0.93	0.37	0.15	0.07
Panthenol	SNPLKNRPJHDVJA -UHFFFAOYSA-N	-1.7	206.139 2	1.9	2.5	0.000 9	8.35	0.02	0.3	0.06	496	413	1.30	0.42	0.42	0.08
Pyridoxine	LXNHLLTXMWWP M-UHFFFAOYSA- N	-1.0	170.084 4	5.4	19.0	0.002 5	7.60	0.01	0.1	0.03	3292	2548	1.19	0.53	0.29	0.07
Sotalol	ZBMZVLHSICTVO N-UHFFFAOYSA-N	-2.5	273.132 4	3.3	20.8	0.002 5	14.91	0.08	0.5	0.23	4081	3476	2.26	0.40	1.08	0.26

Tranexamic acid	GVDJEQRTZSCIOI-UHFFFAOYSA-N	-1.5	158.1204	3.2	17.9	0.0015	13.95	0.02	0.1	0.04	1581	1364	0.67	0.33	0.14	0.01
Triethylene glycol monomethyl ether <sup>1</sup>	JLGLQAWTXXGVE-M-UHFFFAOYSA-N	-0.7	165.1153	3.8	19.1	0.0017	9.55	0.29	3.0	0.61	666	181	1.82	0.43	0.60	0.14
Trisopropanolamine	SLINHMUJFWFWB-MU-UHFFFAOYSA-N	-2.9	192.1629	4.2	18.3	0.0022	8.64	0.02	0.2	0.04	2743	2250	2.85	0.83	0.76	0.16
Vidarabine	OIRDQVFTABOO-Q-UHTZMRCNSA-N	-2.1	268.1050	2.5	3.6	0.0017	9.79	0.06	0.6	0.14	1949	1667	1.58	0.62	0.43	0.03

Table S3: Detailed descriptions of the 51 samples taken from the Danube river and several of its tributaries are shown below. Geographical coordinates are presented in decimal degrees and the river kilometer of either the Danube or the respective tributary river is given.

Sample number	Location/Country	River	Latitude	Longitude	River kilometer	Sampling date	Comment
1	Böfinger Halde/DE	Danube	48.42405	10.02688	2581	06/29/2019	
2	Bittenbrunn/DE	Danube	48.73599	11.15507	2479	06/29/2019	700 m downstream power station
3	Kelheim/DE	Danube	48.91648	11.86462	2415	06/30/2019	Upstream gauging station
4	Niederaltreich/DE	Danube	48.77453	13.00914	2276	06/30/2019	
5	Passau/DE	Inn	48.55678	13.43575	4	07/01/2019	Downstream power station
6	Jochenstein Hindling/AT	Danube	48.58452	13.52854	2218	07/01/2019	
7	Enghagen/AT	Danube	48.24042	14.51204	2113	07/02/2019	
8	Oberloiben/AT	Danube	48.38832	15.52271	2008	07/02/2019	
9	Klosterneuburg/AT	Danube	48.33012	16.32987	1942	07/03/2019	
10	Hainburg/AT	Danube	48.16390	16.99168	1879	07/03/2019	Upstream Morava
11	Pohansko/CZ	Morava, Dyje	48.72349	16.88528	17	07/04/2019	
12	Lanzhot/CZ	Morava	48.68721	16.98931	79	07/04/2019	
13	Devín/SK	Morava	48.18768	16.97596	1	07/05/2019	
14	Bratislava/SK	Danube	48.14232	17.06576	1969	07/05/2019	
15	Čunovo, Gabčíkovo reservoir/SK	Danube	48.04025	17.23058	1855	07/03/2019	
16	Medvedov, Mečve/SK, HU	Danube	47.78952	17.65977	1806	07/03/2019	
17	Vének/HU	Moson Danube arm	47.73617	17.78158	0	07/04/2019	
18	Gönyű/HU	Danube	47.74265	17.84397	1790	07/04/2019	
19	Komárno/SK	Váh	47.76091	18.14233	3	07/04/2019	
20	Kamenica/SK	Hron	47.82608	18.72334	2	07/05/2019	
21	Salka/SK	Ipeľ	47.88596	18.76256	12	07/05/2019	
22	Szop/HU, SK	Danube	47.81340	18.86323	1707	07/06/2019	
23	Megyeri Bridge/HU	Danube	47.61603	19.10177	1660	07/06/2019	Budapest upstream
24	M0 bridge/HU	Danube	47.38830	19.00408	1630	07/07/2019	Budapest downstream
25	Tass/HU	Ráckevei-Soroksári	47.03398	18.97820	59	07/07/2019	
26	Dunaföldvár/HU	Danube	46.81707	18.92632	1560	07/08/2019	

27	Paksz/HU	Danube	46.63373	18.88042	1532	07/08/2019	
28	Baja/HU	Danube	46.20053	18.92350	1481	07/09/2019	
29	Hercegszanto, Batina, Bezdan/HU, HR, RS	Danube	45.91455	18.80593	1434	07/09/2019	
30	Drava/HR	Drava	45.55224	18.86460	5	07/10/2019	5 km upstream Danube confluence
31	Ilok, Backa Palanka/HR, RS	Danube	45.23158	19.36060	1300	07/09/2019	
32	Tiszaziget, Martonoš/HU, RS	Tisza	46.18552	20.10467	163	07/10/2019	
33	Tisza mouth	Tisza	45.14700	20.28087	1	07/09/2019	
34	Jesenice na Dolenjskem/SI	Sava	45.86092	15.69200	729	07/08/2019	
35	Jamena/RS, BA	Sava	44.87828	19.08364	205	07/08/2019	
36	Sava mouth/RS	Sava	44.79300	20.39607	7	07/07/2019	
37	Pancevo/RS	Danube	44.81447	20.64443	1151	07/07/2019	
38	Varvarin/RS	Velika Morava	43.74000	21.38000	154	07/06/2019	
39	Velika Morava mouth/RS	Velika Morava	44.70927	21.03570	1	07/06/2019	
40	Banatska Palanka, Bazias/RS, RO	Danube	44.80510	21.38380	1073	07/05/2019	
41	Radujevac, Gruia/RS, RO	Danube	44.26092	22.68498	847	07/05/2019	
42	Timok mouth/RS, BG	Timok	44.21492	22.67215	0	07/04/2019	
43	Pristol, Novo Selo Harbour/ RO, BG	Danube	44.17230	22.78217	837	07/04/2019	
44	Iskar mouth/ BG	Iskar	43.72990	24.44382	0	07/03/2019	
45	Jantra mouth/ BG	Jantra	43.63748	25.56987	1	07/03/2019	
46	Russenski Lom mouth/ BG	Russenski Lom	43.83482	25.93092	0	07/02/2019	
47	Ruse, Giurgiu/ BG, RO	Danube	43.91083	26.06696	488	07/02/2019	
48	Chiciu, Silistria/ RO, BG	Danube	44.13693	27.05112	375	07/01/2019	
49	Giurgulesti/ MD, RO	Prut	45.47187	28.19673	1	06/30/2019	
50	Reni/ RO, UA	Danube	45.45630	28.26013	132	06/29/2019	
51	Vilkova/ RO, UA	Danube	45.39455	29.58140	18	06/29/2019	

Table S4: The exact parameter settings of the feature extraction method executed with MZmine 2 software are shown. The RT and mass tolerances, the signal intensity threshold as well as the parameters for wavelet scaling (peak duration range and RT wavelet range) were set based on the target analysis of two synthetic samples (Table S2). When setting these parameters, absolute minima and/or maxima of all compounds and injections were favored over mean values across the six technical replicates (given in brackets) in order to reduce the number of false negative features.

Processing module	Description	Parameter	Setting	Comment
Mass detection	Generates a list of ions for each scan	Algorithm	Centroid	Only algorithm available for centroided data
		RT range	5 min – 15 min	Corresponds to the HILIC elution window
		MS levels	1+2	Scan as well as fragmentation experiments were included
		Polarity	+	MS data was acquired in positive ionization mode
		Spectrum type	Centroided	The raw data was centroided during conversion to mzML file format
		Noise level	1.0 cps Da <sup>-1</sup> , 0.0 cps Da <sup>-1</sup>	Corresponds to MS level 1 and 2, respectively
ADAP chromatogram builder	Constructs EICs using the ADAP algorithms <sup>1</sup>	Minimum group size in number of scans	5	Corresponds to the expected scan span of a chromatographic peak
		Group intensity threshold	10 cps Da <sup>-1</sup>	Data points below this threshold were excluded from EIC building
		Minimum highest intensity	49 (166) cps Da <sup>-1</sup>	Derived from targeted analysis of the synthetic samples (minimum peak height, Table S2)
		m/z tolerance	0.0026 (0.0014) Da	Derived from targeted analysis of the synthetic samples (maximum mass difference)
Smoothing	Applies Savitzky-Golay smoothing to EICs	Filter width	17	Number of data points necessary to smooth HILIC peaks with a FWHM up to 1.08 ± 0.26 min (n = 6)
Chromatogram deconvolution	Separates each chromatogram into	Algorithm	Wavelets (ADAP)	ADAP algorithms reduce the risk of false positives without compromising sensitivity <sup>1</sup>

individual peaks	S/N threshold	10	Reduces risk of deconvoluting noise
	Minimum feature height	45 (160) cps Da <sup>-1</sup>	Derived from targeted analysis of the synthetic samples considering smoothing effects
	Coefficient/area threshold	30	Filters out low-quality peaks by maintaining a recovery > 50% of target compounds at a lower concentration level
	Peak duration range	0.13 (0.23) min – 4.40 (3.13) min	Derived from target data of synthetic samples (peak duration time) and iteratively adjusted to increase recovery rates
	RT wavelet range	0.03 (0.10) min – 1.58 (1.09) min	Estimated from target data of synthetic samples (FWHM) and iteratively adjusted to increase recovery rates
	m/z center calculation	Median	
	m/z tolerance	0.0026 (0.0014) Da	
	Weight for m/z	1	
	RT tolerance	1.60 (0.20) min	Derived from target data of the multicomponent standard (maximum RT difference, Table S1)
	Weight for RT	1	
Isotopic peaks grouper	m/z tolerance	0.0026 (0.0014) Da	
	RT tolerance	1.60 (0.20) min	
	Maximum charge	1	Predominantly expected for small molecules
	Representative isotope	Lowest m/z	
Adduct search	RT tolerance	1.60 (0.20) min	
	Adduct m/z differences	21.9825 Da, 37.9559 Da,	Correspond to sodium, potassium and ammonium adducts

	17.0265 Da
m/z tolerance	0.0026 (0.0014) Da
Maximum relative adduct peak height	100% Full peak height of the adduct was accepted relative to the main peak
Feature list rows filter	Removes features from aligned list based on specified criteria Maximum peaks in a row 3 Used to filter out peaks found in less than three replicates

<sup>1</sup> O. D. Myers, S. J. Sumner, S. Li, S. Barnes and X. Du, Anal. Chem., 2017, 89, 8696–8703.

Table S5: Target compounds which were identified as false negative features at the end point of the feature extraction workflow are listed below. The standard compounds were contained in two synthetic samples, one at a lower concentration level (c1) and the other one at a higher concentration level (c2) (Table S2). The targets were tracked throughout the steps of the workflow and the points of losses were identified. Green boxes indicate the chromatographic peak or feature corresponding to the target was found, red boxes mean it was not found.

C1	Chromatogram building (1)	Chromatogram building (2)	Chromatogram building (3)	Smoothing (1)	Smoothing (2)	Smoothing (3)	Chromatogram deconvolution (1)	Chromatogram deconvolution (2)	Chromatogram deconvolution (3)	Alignment	Replicate filter	Isotope removal	Adduct removal
2,2,6,6-Tetramethyl-4-piperidinol	Green	Green	Green	Green	Green	Green	Green	Green	Green	Green	Green	Green	Green
Creatinine	Green	Green	Green	Green	Green	Green	Green	Green	Green	Green	Green	Green	Green
Glutathion	Green	Green	Green	Green	Green	Green	Green	Green	Green	Green	Green	Green	Green
L-Citrulline	Green	Green	Green	Green	Green	Green	Green	Green	Green	Green	Green	Green	Green
L-Glutamic acid	Green	Green	Green	Green	Green	Green	Green	Green	Green	Green	Green	Green	Green
Lisinopril	Green	Green	Green	Green	Green	Green	Green	Green	Green	Green	Green	Green	Green
L-Proline	Green	Green	Green	Green	Green	Green	Green	Green	Green	Green	Green	Green	Green
L-Tyrosine	Green	Green	Green	Green	Green	Green	Green	Green	Green	Green	Green	Green	Green
Methyl 3-aminocrotonate	Green	Green	Green	Green	Green	Green	Green	Green	Green	Green	Green	Green	Green
Miglitol	Green	Green	Green	Green	Green	Green	Green	Green	Green	Green	Green	Green	Green
N-Acetyethanolamine	Green	Green	Green	Green	Green	Green	Green	Green	Green	Green	Green	Green	Green
Sotalol	Green	Green	Green	Green	Green	Green	Green	Green	Green	Green	Green	Green	Green
Vidarabine	Green	Green	Green	Green	Green	Green	Green	Green	Green	Green	Green	Green	Green



Table S6: The features of category B defined by their accurate masses and RTs are listed below with the respective candidates suggested by the STOFF-IDENT database. Source indications were taken from the PubChem database<sup>1</sup>. “\*” symbolizes that ecotoxicological values are available on the PubChem database and “AT” indicates acute toxicity as specified by the Globally Harmonized System of Classification and Labeling of Chemicals. The candidate substances were searched by their InChIKeys in the MassBank database<sup>2</sup>. The criteria to consider an entry comparable to the observed data were: The MS2 spectra had to be recorded on a LC-ESI-QTOF instrument in positive ionization mode at a collision energy of 20 – 60 eV or ramps which touched that interval.

ID	Mean mass [Da]	Mean RT [min]	Sample number(s) with (amount n)	Name	InChIkey	Elemental formula	Monoisotopic mass	Log D (pH 7)	Source	MassBank entry
1	95.0479 ± 0.0000	10.00 ± 0.00	35, 40 (2)	2-aminopyrimidine	LXQPZWIHJMPQO-UHFFFAOYSA-N	C4H5N3	95.0483	-0.1	Ambiguous	No
2	97.9673 ± 0.0001	7.84 ± 0.15	1, 2, 3, 8, 24, 44 (6)	Sulfuric acid	QAOWNCQDCNUR-D-UHFFFAOYSA-N	H2O4S	97.9674	-5.6	*Industry use (i.e. pigments), consumer use (i.e. air care products)	No
3	99.0681	9.02	32 (1)	1-methyl-2-pyrrolidone	SEXSIVLOFMRIM-UHFFFAOYSA-N	C5H9NO	99.0684	-0.4	*Industry use (i.e. solvents), consumer use (i.e. cleaning and furnishing care products)	Yes
4	100.1002 ± 0.0004	11.75 ± 0.02	39, 43, 47 (3)	1-methylpiperazine	PVOAHINGSUIXLS-UHFFFAOYSA-N	C5H12N2	100.1	-2.8	AT Industry use (intermediates)	No
5	100.0997 ± 0.0001	14.79 ± 0.09	1, 2, 3, 4, 5, 6, 7, 8, 9, 10 (10)							
6	113.0584	12.71	7 (1)	2-imino-1-methylimidazolidin-4-one	DDRJAANPRIHGI-UHFFFAOYSA-N	C4H7N3O	113.0589	-1.5	Pharmaceutical related, human metabolite	Yes
7	122.0733	8.62	16 (1)	Chlormequat	JUZXDNPBRPUJIOR-UHFFFAOYSA-N	C5H13ClN	122.0731	-3.3	*Pesticide	No
8	122.0727 ± 0.0001	12.50 ± 0.06	15, 17, 19, 31, 33, 37, 43, 46, 48, 49, 50, 51 (12)							
9	126.0649 ± 0.0001	12.29 ± 0.05	47, 48, 49, 50 (4)	Melamine	JDSHMPZPIAZGSV-UHFFFAOYSA-N	C3H6N6	126.0654	-2.0	*Industry use (i.e. flame retardants), consumer use (i.e. adhesives)	Yes
10	127.0489 ± 0.0001	13.74 ± 0.08	43, 44, 46, 47, 48, 49, 50 (7)	Cyanurodiamide (=Atrazin-desethyl-desisopropyl-2-hydroxy)	MASBWURJOFLOO-UHFFFAOYSA-N	C3H5N5O	127.0494	-1.7	Hair conditioner, toys	No
11	128.0582	13.38	35 (1)	5,5-dimethylhydantoin	YROYDNZEPTFOL-UHFFFAOYSA-N	C5H8N2O2	128.0586	-0.5	*Industry use (i.e. intermediates),	No

12	128.1310 ± 0.0003	11.14 ± 0.05	41, 46, 47, 49 (4)	1-ethylpyrrolidin-2-ylmethylamine	UNRBEYLRYXCG-UHFFFAOYSA-N	C7H16N2	128.1313	-3.2	Pharmaceutical related	No
13	129.1261 ± 0.0001	11.22 ± 0.03	42, 44, 46, 47, 48, 49, 50 (7)	2-piperazin-1-ylethylamine	IMUDHTPIFBORV-UHFFFAOYSA-N	C6H15N3	129.1266	-5.6	*Industry use (i.e. adhesives), consumer use (i.e. paper products)	Yes
14	132.0781	12.39	49 (1)	2,2-dimethyl-1,3-dioxolan-4-ylmethanol	RNVQYLELCKWAN-UHFFFAOYSA-N	C6H12O3	132.0786	-0.1	Industry use (i.e. solvents)	No
15	134.0585	9.84	1 (1)	2,2-bis(hydroxymethyl)propionic acid	PTBDHRZVDMNKB-UHFFFAOYSA-N	C5H10O4	134.0579	-3.8	Industry use (i.e. lubricants), consumer use (i.e. adhesives)	No
16	134.0593 ± 0.0000	10.09 ± 0.00	35, 40 (2)	Nitrioltriacetonitrile	LJAIDEYQVJERM-UHFFFAOYSA-N	C6H6N4	134.0592	-1.2	Industry use (ion exchange agents)	No
17	134.0593 ± 0.0000	12.44 ± 0.00	35, 40 (2)							
18	135.0542	13.87	7 (1)	Adenine	GFFGBXGBJISGV-UHFFFAOYSA-N	C5H5N5	135.0545	-0.6	<sup>AT</sup> Dietary supplement, human metabolite	Yes
19	137.0585 ± 0.0001	9.81 ± 0.03	1, 2, 3, 19 (4)	Isoniazid	QRXWMOHMRWLF-EY-UHFFFAOYSA-N	C6H7N3O	137.0589	-0.7	Pharmaceutical	No
20	138.0790	9.78	1 (1)	4-amino-2-(aminomethyl)phenol	PZKNKZNLQYKXFV-UHFFFAOYSA-N	C7H10N2O	138.0793	-2.7	Prohibited/restricted hair dye	No
21	140.0835 ± 0.0001	8.71 ± 0.16	10, 16, 30, 33, 46 (5)	Octalynol	BODKCWCMDBMLE-H-UHFFFAOYSA-N	C8H12O2	140.0837	-0.4	Fatty acyls	No
22	141.0784	8.76	20 (1)	4-(1-oxo-2-propenyl)morpholine	XLPIHCZORXHG-UHFFFAOYSA-N	C7H11NO2	141.079	-0.1	Industry use (paint and coating additives)	No
23	141.1150	8.13	20 (1)	4-(diethylamino)-2-butyne-1-ol	ACGZBRWTWOZSFU-UHFFFAOYSA-N	C8H15NO	141.1154	-0.8	Pharmaceutical related	No
24	143.9740	5.95	20 (1)	Ethephon	UDPGUNMODCGORJ-Q-UHFFFAOYSA-N	C2H6ClO3P	143.9743	-2.9	<sup>AT</sup> *Pesticide	No
25	146.1049	14.95	41 (1)	Lysine	KDXKERNBXSRRK-UHFFFAOYSA-N	C6H14N2O2	146.1055	-5.3	Flavoring agent	Yes
26	148.0746 ± 0.0000	10.05 ± 0.00	35, 40 (2)	Propanenitrile, 2-[bis(cyanomethyl)amino]-	FILUFZGDWANGJE-UHFFFAOYSA-N	C7H8N4	148.0749	-0.6	<sup>AT</sup> Ambiguous	No
27	151.0744 ± 0.0003	9.76 ± 0.06	16, 17, 19, 38, 46, 49, 50 (7)	2,3-Diaminobenzamide	NAWIZCEYBOLUGY-UHFFFAOYSA-N	C7H9N3O	151.0746	-0.2	Ambiguous	No

28	152.0833 ± 0.0003	8.64 ± 0.06	2, 14, 25, 29, 30, 47 (6)	(3-chloro-2-hydroxypropyl)trimethylammonium	XIUCEANTZSXBQQ-UHFFFAOYSA-N	C6H15ClNO	152.0837	-3.9	Ambiguous	No
29	152.0835 ± 0.0004	12.59 ± 0.07	26, 36, 42, 46 (4)		GOHTUMIGOHRCB-UHFFFAOYSA-N	C9H16N2	152.1313	-1.6	*Industry use (intermediates, process regulators)	No
30	152.1307 ± 0.0002	11.19 ± 0.04	41, 42, 43, 44, 46, 47, 48, 49, 50 (9)	1,8-diazabicyclo[5.4.0]undec-7-ene	VDVUCLWZJHFV-UHFFFAOYSA-N	C9H19NO	157.1467	-2.3	Industry use (intermediates)	No
31	157.1462 ± 0.0004	11.76 ± 0.02	7, 24, 30, 41, 43, 47, 48, 49, 50, 51 (10)	2,2,6,6-tetramethylpiperidin-4-ol	YIOJMHVTEACTIC-UHFFFAOYSA-N	C6H9NO4	159.0532	-0.7	Ambiguous	No
32	159.0535 ± 0.0004	12.41 ± 0.02	3, 32 (2)	Methyl 2-hydroxy-2-(1-oxo-2-propenylamino)acetate	LRMSQVBRUNSOIL-UHFFFAOYSA-N	C3HF5O2	163.9897	-1.9	Ambiguous	No
33	163.9898 ± 0.0004	10.71 ± 0.07	41, 42, 43, 44, 45, 46, 47, 49 (8)	Pentafluoropropionic acid	JLGLQAWTXXGVEM-UHFFFAOYSA-N	C7H16O4	164.1049	-0.7	*Industry use (i.e. functional fluids), consumer use (i.e. automotive care products)	No
34	164.1044	8.85	7 (1)	2-(2-(2-methoxyethoxy)ethoxy)ethanol	GPLRAVKSUXZTP-UHFFFAOYSA-N	C6H14O5	166.0841	-2.5	Industry use (viscosity adjusters)	No
35	166.0849	7.68	42 (1)	Oxybispropanediol	BRMWTNUJHUMWMS-UHFFFAOYSA-N	C7H11N3O2	169.0851	-3.1	Ambiguous	No
36	169.0851 ± 0.0001	14.93 ± 0.03	48, 49, 50 (3)	1-Methyl-L-Histidin	WRPSPFHGNBMG-UHFFFAOYSA-N	C9H15NO2	169.1103	-1.9	Pharmaceutical	No
37	169.0854	8.70	25 (1)		UGIMXCAKUNAIE-UHFFFAOYSA-N	C9H17NO2	171.1259	-1.3	Pharmaceutical	Yes
38	169.1100	5.95	46 (1)	Acetclidine	IRYIYPWRXROPSX-UHFFFAOYSA-N	C10H9NO2	175.0633	-1.0	Ambiguous	No
39	169.1100 ± 0.0003	8.43 ± 0.31	8, 20, 29, 36, 44 (5)							
40	169.1098	12.54	18 (1)							
41	171.1253	8.61	7 (1)	1-(aminomethyl)cyclohexanecarboxylic acid						
42	175.0632 ± 0.0003	8.59 ± 0.05	1, 2, 3, 4, 5, 6, 7, 8, 9, 10, 11, 12, 13, 14, 15, 16, 17, 18, 19, 20, 21, 22, 23, 24, 25, 26, 27, 28, 29, 30, 32, 33, 36, 37, 38, 39, 41, 43, 44, 46, 47, 48,	m-(1-cyanoethyl)benzoic acid						

43	177.0643	12.62	49, 50, 51 (45)	2-hydroxyethyliminodiacetic acid)	JYXGKAKDAARW-UHFFFAOYSA-N	C6H11NO5	177.0637	-7.6	Adhesive, pesticide	No
44	180.0785 ± 0.0005	8.73	13 (1)	3-(4-Methoxyphenyl)propanoic acid	FIUFLSGGHNPSM-UHFFFAOYSA-N	C10H12O3	180.0786	-0.7	Ambiguous	No
45	182.0215 ± 0.0005	7.65 ± 0.27	5, 9, 10, 24, 26, 30, 33 (7)	Monoperoxyphthalate(2-)	GLVYLSKTCWWJR-UHFFFAOYSA-N	C8H6O5	182.0215	-2.1	Ambiguous	No
46	182.0923	8.62	25 (1)	Dacarbazine	OMJKYKNWZZKTK-LXBLZVNSA-N	C6H10N6O	182.0916	-1.7	Ambiguous	No
47	185.1047 ± 0.0002	12.51 ± 0.06	5, 8, 18, 20 (4)	Egonine	PHMBVCPLDPDES-MFKSUSPLISA-N	C9H15NO3	185.1052	-3.1	Narcotic	No
48	186.1365 ± 0.0001	12.59 ± 0.05	5, 8, 18, 20, 29 (5)	N,N'-methylenbis-morpholine	MIFZZKZNMWTHJK-UHFFFAOYSA-N	C9H18N2O2	186.1368	-0.1	Pesticide, disinfectant, lubricant, ...	No
49	187.1202 ± 0.0004	8.17 ± 0.04	20, 29 (2)	(3R)-3-(2-amino-2-oxoethyl)-5-methylhexanoic acid	NPDKTSLVWGFPOG-UHFFFAOYSA-N	C9H17NO3	187.1208	-1.5	Ambiguous	No
50	188.1156 ± 0.0004	13.75 ± 0.06	3, 8 (2)	Acetyllysine	DTEROYGMUDWYA-Z-UHFFFAOYSA-N	C8H16N2O3	188.1161	-3.2	Ambiguous	No
51	191.1163	12.92	32 (1)	1-o-tolylbiguanide	SOZCAOHYSOZCE-UHFFFAOYSA-N	C9H13N5	191.1171	-1.3	Industry use (paints and coatings), consumer use (paints and coatings)	No
52	191.1517 ± 0.0001	13.46 ± 0.07	41, 42, 44 (3)	1,1,1'-nitrioltriopropan-2-ol	SUNHMLUFWFBM-U-UHFFFAOYSA-N	C9H21NO3	191.1521	-2.9	Industry use (i.e. solvents), consumer use (building materials)	No
53	192.0751	12.59	31 (1)	(2,4-Diaminopteridin-6-yl)methanol	CYNARAWTVHQHDI-UHFFFAOYSA-N	C7H8N6O	192.076	-1.4	Ambiguous	No
54	194.0692 ± 0.0002	13.40 ± 0.01	4, 8, 20 (3)	3-Acetamido-5-aminobenzoic acid	SETVNZSWPLKAO-UHFFFAOYSA-N	C9H10N2O3	194.0691	-2.3	Ambiguous	No
55	194.1152 ± 0.0001	8.65 ± 0.54	7, 50 (2)	3,6,9-trioxundecane-1,11-diol	UWHCKJMYHZGTTI-UHFFFAOYSA-N	C8H18O5	194.1154	-1.4	Industry use (i.e. solvents), consumer use (i.e. lubricant)	No
56	199.9895 ± 0.0001	7.67 ± 0.34	47, 48 (2)	4-Thiazoleacetic acid, 2-(formylamino)-a-oxo-	JPJMBGVCGNFOD-UHFFFAOYSA-N	C6H4N2O4S	199.9892	-3.1	Pharmaceutical related	No
57	201.1728 ± 0.0002	10.14 ± 0.04	1, 2, 3, 4, 5, 6, 7, 10, 11, 12, 13, 14, 15, 16, 17, 18, 19, 20, 21, 22, 23, 24, 25, 26, 27, 29, 30, 32, 33, 34, 35, 36,	4-hydroxy-2,2,6,6-tetramethylpiperidine-1-ethanol	STEYNUVPFMIUOY-UHFFFAOYSA-N	C11H23NO2	201.1729	-2.6	Ambiguous	Yes

58	201.1729 ± 0.0003	12.95 ± 0.17	37, 38, 39, 40, 41, 42, 43, 44, 45, 46, 47, 48, 49, 50, 51 (47)	N,N-Bis(carboxymethyl)alanine	CIEZGWJIBXOTE-UHFFFAOYSA-N	C7H11NO6	205.0586	-9.9	Industry use (i.e. ion exchange agents), consumer use (i.e. laundry and dishwashing products)	No
59	205.0587 ± 0.0004	12.46 ± 0.03	8, 9, 28, 31 (4)	3-morpholin-4-ylpropane-1-sulfonic acid	DVLFVONBTKHTER-UHFFFAOYSA-N	C7H15NO4S	209.0722	-2.7	Industry use (laboratory chemicals, intermediates)	No
60	209.0719 ± 0.0002	12.53 ± 0.07	14, 16, 17, 18, 19, 22, 24, 25, 27, 29, 38, 39, 41, 43, 44, 45, 47, 48, 50, 51 (20)	Dimethipin	PHVNLCAQHGNKU-UHFFFAOYSA-N	C6H10O4S2	210.0021	-1.5	*Pesticide	No
61	210.0018 ± 0.0000	11.86 ± 0.00	2, 4, 11, 13, 20, 21, 22, 23, 25, 33, 37, 38, 42, 43, 49, 50 (16)	N-[(tert-butoxy)carbonyl]-L-valine	SZXBQTSZISFIAO-UHFFFAOYSA-N	C10H19NO4	217.1314	-1.0	Ambiguous	No
62	217.1312 ± 0.0003	8.65 ± 0.07	8, 20, 29 (3)	Miglustat	UQRORFVVSFNR0-UUTINFBMNSA-N	C10H21NO4	219.1471	-2.7	Pharmaceutical	No
63	217.1304	13.12	21 (1)	3,4-methylenedioxypropylamphetamine	LBXMOBTXOLBCCA-UHFFFAOYSA-N	C13H19NO2	221.1416	-0.3	* Ambiguous	No
64	219.1470 ± 0.0003	13.41 ± 0.04	7, 21, 22, 25, 27, 30, 32, 36, 37, 41, 42, 43, 44, 47, 48, 49, 50, 51 (18)	Nimorazole	MDJFHLTPRPZLY-UHFFFAOYSA-N	C9H14N4O3	226.1066	-0.1	Pharmaceutical	No
65	221.1420	13.41	41 (1)	Panthenyl ethyl ether	MRAMIP0PITCOOIN-UHFFFAOYSA-N	C11H23NO4	233.1627	-0.7	Hair conditioner	No
66	226.1065	14.95	21 (1)	2-Carboxy-ibuprofen	DIVLBVDYADZPL-UHFFFAOYSA-N	C13H16O4	236.1049	-2.4	Ambiguous	No
67	233.1621	13.15	6 (1)	(S)-4-amino-5-[(2-(1H-imidazol-4-yl)ethyl)amino]-5-oxopentanoic acid	FLEVPVPMJVEDN-QMVMGPOBSA-N	C10H16N4O3	240.1222	-3.9	Hair conditioner	No
68	236.1038	7.89	42 (1)	Benzoic acid, 4-(methylsulfonyl)-2-nitro-	QNOUJABNMRROS-L-UHFFFAOYSA-N	C8H7NO6S	244.9994	-3.1	Pesticide transformation product	No
69	240.1222	14.95	3, 36, 44, 45, 50 (5)	Benserazide	BNODCRGUHNALG-H-UHFFFAOYSA-N	C10H15N3O5	257.1012	-2.6	Pharmaceutical	No
70	244.9996 ± 0.0008	7.83 ± 0.27	8, 10, 20, 33, 34 (5)							
71	244.9992 ± 0.0007	9.31 ± 0.03	2 (1)							
72	257.1024	13.80								

73	267.0963	8.63	2 (1)	Vidarabine	OIRDTQYFTABOOQ- UHTZMRCNSA-N	C10H13N5O4	267.0968	-2.1	Discontinued pharmaceutical	No
74	270.1063	9.88	23 (1)	Tolonium	KZEUBCUXBNEMSQ -UHFFFAOYSA-O	C15H16N3S	270.1059	-1.0	Ambiguous	No
75	287.0789 ± 0.0003	13.30 ± 0.67	32, 33 (2)	Tenofovir	SGOIRFVHAKUTI- UHFFFAOYSA-N	C9H14N5O4P	287.0783	-3.5	Pharmaceutical	No
76	306.0013	10.92	39 (1)	2,2'-dithiodi(benzoic acid)	LBEMXWGHIXRA- UHFFFAOYSA-N	C14H10O4S2	306.0021	-2.8	Ambiguous	No
77	355.8745 ± 0.0004	5.90 ± 0.04	13, 17 (2)	2,5-dichloro-4,6-dicyano- benzene-1,3-disulfonic acid	KRIHZDRHCJOOQO -UHFFFAOYSA-N	C8H2Cl2N2O 6S2	355.8731	-3.5	Pesticide transformation product	No

<sup>1</sup> Compound database PubChem of the National Center for Biotechnology Information, <https://pubchem.ncbi.nlm.nih.gov/>, (accessed 9 December 2020).

<sup>2</sup> European MassBank mass spectral database of the NORMAN network, <https://massbank.eu/MassBank/>, (accessed: 1 February 2021).

**Appendix B.4 Supplementary material - Characterizing powdered activated carbon treatment of surface water samples using polarity-extended non-target screening analysis**

Table S1: Table of internal standards spiked into samples after treatment and prior to LC-MS analysis

Name	InChIKey	Chemical formula	Log <i>D</i> (pH 7)	Solvent stock	C(Stock) [μM]	Manufacturer
<b>6-amino-1,3-dimethyl-5-(formylamino)uracil</b>	ZNDGAXCBZGSJGU-UHFFFAOYSA-N	C7H10N4O3	-2.00	ACN/H2O (50/50)	1000	Sigma
<b>Etilefrine</b>	SQVIAVUSQAWMKL-UHFFFAOYSA-N	C10H15NO2	-1.42	ACN	1000	Sigma
<b>Sotalol</b>	ZBMZVLHSJCTVON-UHFFFAOYSA-N	C12H20N2O3S	-2.47	ACN	586	Sigma
<b>Vidarabine</b>	OIRDTQYFTABQOQ-UHTZMRCNSA-N	C10H15N5O5	-2.10	ACN/H2O (50/50)	337	
<b>Chloridazon</b>	WYKYKTKDBLFHCY-UHFFFAOYSA-N	C10H8ClN3O	1.11	ACN/H2O (50/50)	1000	Sigma
<b>Chlorbromuron</b>	NLYNUTMZTCLNOO-UHFFFAOYSA-N	C9H10BrClN2O2	2.85	Methanol	1000	Dr. Ehrenstorfer
<b>Chlortoluron</b>	JXCGFZXSOMJFOA-UHFFFAOYSA-N	C10H13ClN2O	2.44	ACN	1000	Sigma
<b>Metconazole</b>	XWPZUHJBOLQNMN-UHFFFAOYSA-N	C17H22ClN3O	3.59	Methanol	1000	Sigma
<b>Metobromuron</b>	WLFDQEVORAMCIM-UHFFFAOYSA-N	C9H11BrN2O2	2.24	ACN	1096	Sigma
<b>Monuron</b>	BMLIZLVNXYGCK-UHFFFAOYSA-N	C9H11ClN2O	1.93	Methanol	970	Sigma

Table S2: Polar standard compounds spiked into samples prior to PAC treatment.

Name	InChIKey	Chemical formula	Log <i>D</i> (pH 7)
<b>1,3-Dimethyl-2-imidazolidinone</b>	CYSGHNMQYZDMIA-UHFFFAOYSA-N	C5H10N2O	-0.64
<b>2,2,6,6-tetramethyl-4-piperidone</b>	JWUXJYZVKZKLTJ-UHFFFAOYSA-N	C9H17NO	-0.32
<b>2,4-diamino-6-(hydroxymethyl)pteridine</b>	CYNARAWTVHQHDI-UHFFFAOYSA-N	C7H8N6O	-1.37
<b>2-aminopyridine</b>	ICSNLGPSTRYBMBD-UHFFFAOYSA-N	C5H6N2	0.30
<b>3-pyridinemethanol</b>	MVQVNTPHUGQQHK-UHFFFAOYSA-N	C6H7NO	-0.01

<b>Ectoine</b>	WQXNXVUDBPYKBA- UHFFFAOYSA-N	C6H10N2O2	-2.53
<b>Famotidine</b>	XUFQPHANEAPEMJ- UHFFFAOYSA-N	C8H15N7O2S3	-3.04
<b>4-(2-hydroxyethyl)morpholine</b>	KKFDCBRMNNSAAW- UHFFFAOYSA-N	C6H13NO2	-1.12
<b>Miglitol</b>	IBAQFPQHRJAVAV- ULAWRXDQSA-N	C8H17NO5	-3.89
<b>N,N'-ethylenebisacetamide; (N,N'-ethylenedi(diacetamide))</b>	WNYIBZHOMJZDKN- UHFFFAOYSA-N	C6H12N2O2	-1.78
<b>Acamprosate</b>	AFCGFAGUEYAMAO- UHFFFAOYSA-N	C5H11NO4S	-4.10
<b>L-Leucine</b>	ROHFNLRQFUQHCH- UHFFFAOYSA-N	C6H13NO2	-1.59

Table S3: Parameter settings of each processing step of the non-target screening workflow for comparative analysis of an untreated and a treated sample. Parameters that were sufficiently optimized in a previous study<sup>1</sup> are highlighted in green. Parameters that were adapted to the circumstances of the present investigation are marked in red. In case there was no need to optimize default settings they are depicted in blue. If parameter settings differed for negative ionization mode, the values are given in brackets.

Processing step	Description	Parameter	Setting	Comment
Mass detection		Algorithm	Wavelet transform	Detects peaks using continuous wavelet transformation using “Mexican Hat” wavelet
		Noise level	10,000	Minimum intensity of a data point to be considered in chromatogram
		Scale level	6	Stretches or compresses the wavelet
		Wavelet window size	30 %	Window size used to calculate wavelet
		RT range	5 min – 33 min	Corresponds to the HILIC and RPLC elution intervals
		MS levels	1+2	
		Polarity	+(-)	

<sup>1</sup> Minkus S, Bieber S, Letzel T (2021) (Very) polar organic compounds in the Danube river basin: Non-target screening workflow and prioritization strategy for extracting highly confident features. Anal Methods 13:2044–2054. <https://doi.org/10.1039/D1AY00434D>

		Spectrum type	Profile	Adapted to the raw data format of the vendor (Thermo Fisher Scientific)
Chromatogram building	Constructs EICs using the ADAP algorithms[110]	Minimum group size in number of	5	
		Group intensity threshold	20,000	Optimized to minimize total number of features and processing time and maximize recall of standard compounds (n=20)
		Minimum highest intensity	50,000	Optimized to minimize total number of features and processing time and maximize recall of standard compounds (n=20)
		m/z tolerance	0.0012 Da	Derived from targeted analysis: Maximum m/z span over all sample injections (n=35) and standard compounds (n=20), rounded up to 4 <sup>th</sup> decimal
Smoothing	Applies Savitzky-Golay filter to EICs	Filter width	25	Adapted to noisier data
Chromatogram deconvolution	Separates each chromatogram into individual peaks	Algorithm	Wavelets (ADAP)	
		S/N threshold	10	
		Minimum feature height	100,000 (50,000)	Optimized to minimize total number of features and processing time and maximize recall of standard compounds (n=20)
		Coefficient/area threshold	30	
		Peak duration range (low)	0.13 min	
		Peak duration range (high)	8.00 min	Adapted to achieve full recall of standard compounds (n=20)
		RT wavelet range (low)	0.03 min	
		RT wavelet range (high)	2.00 min	Adapted to achieve full recall of standard compounds (n=20)
		m/z center calculation	Median	
Peak filter		Number of data points	2 – 1600	

	Eliminates peaks which do not meet the specified criteria	Tailing factor	0.40 – 8.30	Derived from targeted analysis: Minimum and maximum of all sample injections (n=35(36)) and standard compounds (n=20).
		Asymmetry factor	0.05 – 13.59	
Isotope grouping and removal	Recognizes isotopic patterns within defined RT and m/z ranges and removes all peaks except the highest isotope	m/z tolerance	0.0012 Da	Derived from targeted analysis: Maximum m/z span over all sample injections (n=35) and standard compounds (n=20), rounded up to 4th decimal
		RT tolerance	0.62 min	Derived from targeted analysis: Maximum RT span over replicate injections and standard compounds (n=20), rounded up to 2 <sup>nd</sup> decimal
		Maximum charge	1	
		Representative isotope	Lowest m/z	
Adduct tagging and removal	Recognizes adduct peaks within defined RT and mass range	RT tolerance	0.62 min	Derived from targeted analysis: Maximum RT span over replicate injections and standard compounds (n=20), rounded up to 2 <sup>nd</sup> decimal
		Adduct m/z differences	21.9825 Da, 37.9559 Da, 17.0265 Da	
		m/z tolerance	0.0012 Da	Derived from targeted analysis: Maximum m/z span over all sample injections (n=35) and standard compounds (n=20), rounded up to 4th decimal
		Maximum relative adduct peak	100 %	
Intra-sample alignment	Aligns peaks across technical replicates and corrects RT deviations based on RANSAC algorithm and non-linear regression model[68]	m/z tolerance	0.0015 Da	Adapted to achieve full recall of standard compounds (n=20)
		RT tolerance	1.00 min	Sets RT range to create the model for RT correction
		RT tolerance after correction	0.62 min	Derived from targeted analysis: Maximum RT span over replicate injections and standard compounds (n=20), rounded up to 2 <sup>nd</sup> decimal
		RANSAC iterations	2000	Maximum number of iterations to find model

		Minimum number of points	20 %	Minimum portion of points required for a valid model
		Threshold value	0.07 min	Threshold for a data point to fit the model
Duplicate filter	Finds features of which the m/z and RT difference is lower than the predefined tolerances	Filter mode	New average	Creates consensus feature from duplicates
		m/z tolerance	0.0015 Da	Adapted to achieve full recall of standard compounds (n=20)
		RT tolerance	0.62 min	Derived from targeted analysis: Maximum RT span over replicate injections and standard compounds (n=20), rounded up to 2 <sup>nd</sup> decimal
Replicate filter		Minimum peaks	3	
Inter-sample alignment	Aligns peaks across treated and untreated sample and corrects RT deviations based on RANSAC algorithm and non-linear	m/z tolerance	0.0015 Da	Adapted to achieve full recall of standard compounds (n=20)
		RT tolerance	1.00 min	Sets RT range to create the model for RT correction
		RT tolerance after correction	0.62 min	Derived from targeted analysis: Maximum RT span over replicate injections and standard compounds (n=20), rounded up to 2 <sup>nd</sup> decimal
		RANSAC iterations	2000	Maximum number to find model
		Minimum number of points	20 %	Minimum portion of points required for a valid model
		Threshold value	0.07 min	Threshold for a data point to fit the model
Gap filling	Searches for missing peaks using the m/z and RT range defined by the rest of the aligned peaks	m/z tolerance	0.0015 Da	Adapted to achieve full recall of standard compounds (n=20) and added to the m/z range constituted by the other peaks of the feature
Replicate filter		Minimum peaks	6	
Intensity normalization	The peak heights of a feature are normalized using internal standards	Normalization type	Weighted contribution of all standards	
		Peak measurement	Peak height	

	Standard compounds	Internal standards	N = 10, compare Table S1
--	--------------------	--------------------	--------------------------

Table S4: Means and standard deviations of  $\log_2(fc)$  values for the internal standards and the polar standard compounds measured in negative ionization mode. H118, H120 and H121 are the laboratory names of the different PAC types (Table 4) which were tested for surface water treatment at three different concentrations.

	H118	H120	H121
<b>Internal standards</b>	n = 10	n = 10	n = 10
2 mg L <sup>-1</sup>	0.07 ± 0.05	-0.24 ± 0.05	0.06 ± 0.07
7 mg L <sup>-1</sup>	0.14 ± 0.09	-0.32 ± 0.08	0.18 ± 0.07
30 mg L <sup>-1</sup>	0.04 ± 0.08	-0.37 ± 0.07	0.23 ± 0.07
<b>HILIC standards</b>	n = 2	n = 3	n = 5
2 mg L <sup>-1</sup>	-0.13 ± 0.12	-0.12 ± 0.24	-0.35 ± 1.16
7 mg L <sup>-1</sup>	0.20 ± 0.73	-0.25 ± 0.37	-2.16 ± 3.04
30 mg L <sup>-1</sup>	0.18 ± 0.86	-0.75 ± 1.19	-1.59 ± 2.94

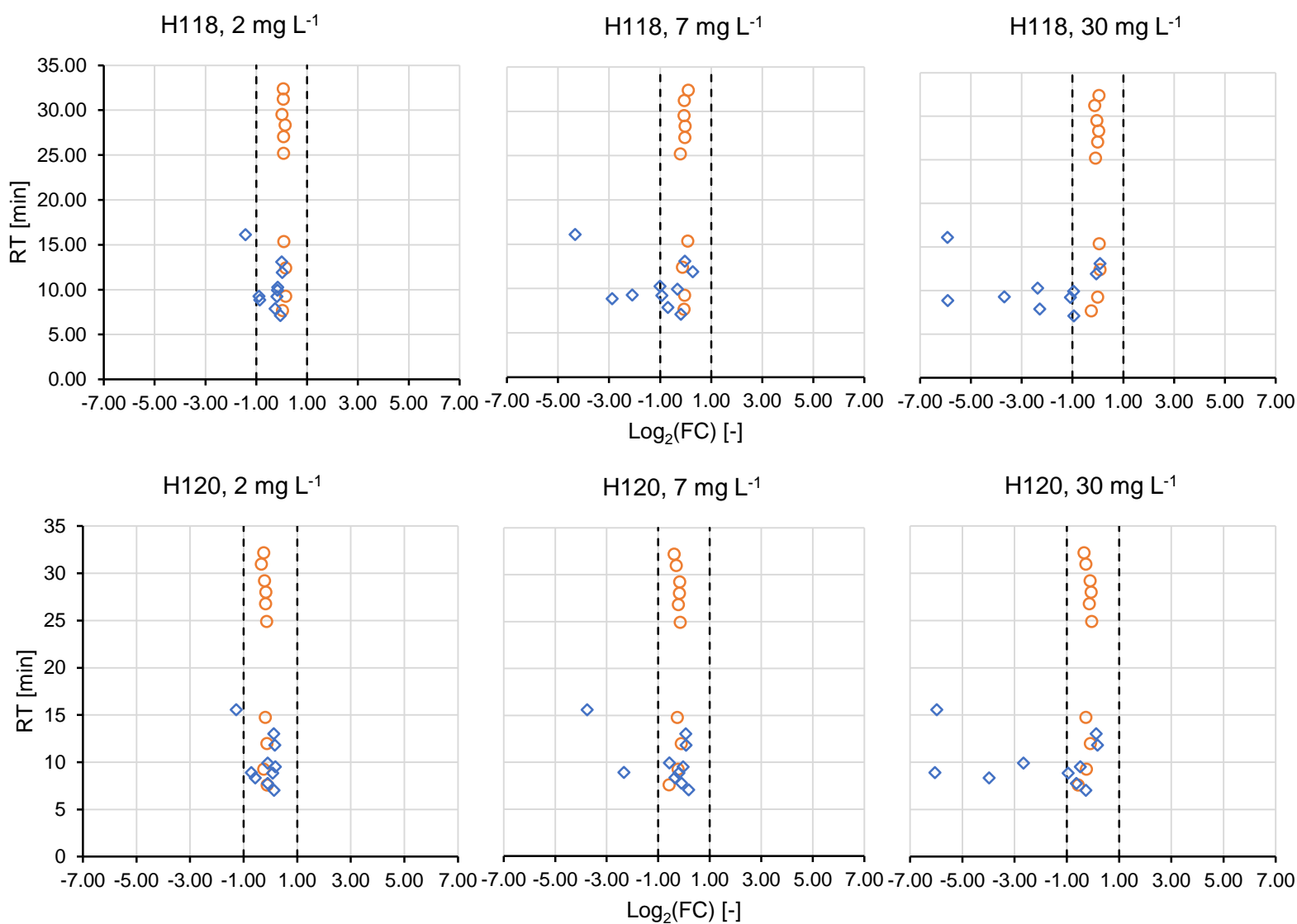


Figure S1: The base-2 logarithm of the fcs of the HILIC standards (blue diamonds) and the internal standards (orange circles) are plotted versus their retention times. The dashed lines mark the consistency interval where no compound removal is assumed. The data was recorded in positive ionization mode. The plots indicate that PAC H118 adsorbed the compounds famotidine, 2,4-diamino-6-(hydroxymethyl)pteridine, 3-pyridinemethanol, 2-aminopyridine and 4-(2-hydroxyethyl)morpholine. No decrease was observed for 4-(2-hydroxyethyl)morpholine when treating the sample with PAC H120.

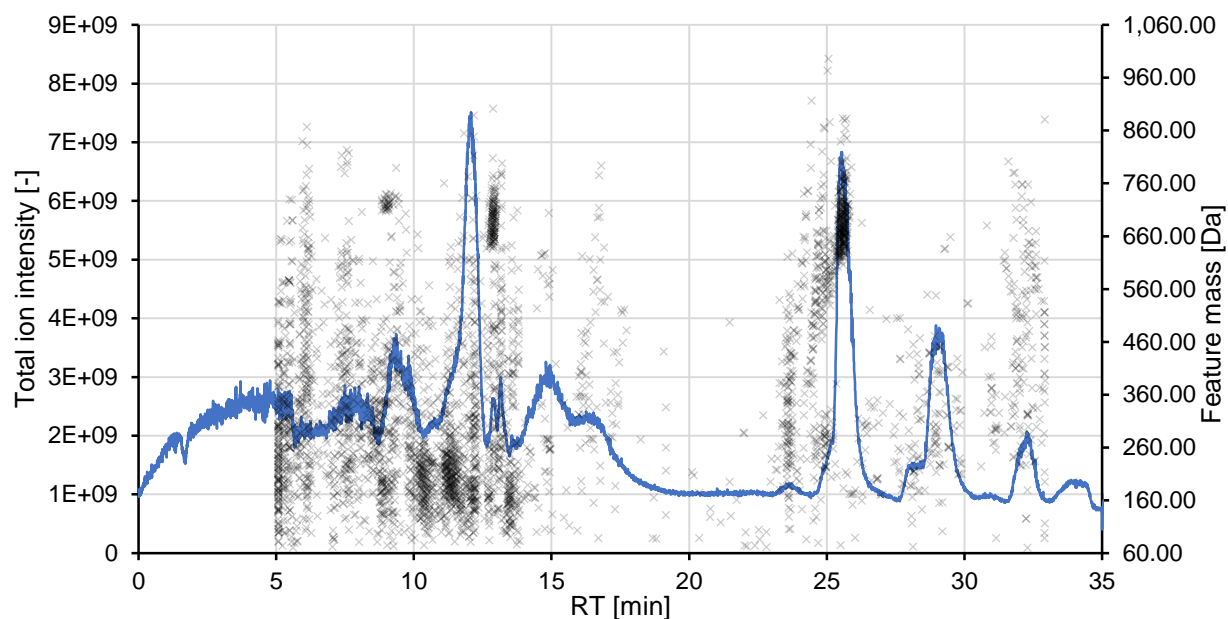


Figure S2: The total ion chromatograms (blue line, primary y-axis) and the non-target peaks (black crosses, secondary y-axis) are exemplarily displayed for the sample treated with the H118 PAC at 30mg L<sup>-1</sup>, third replicate.

Table S5: Means and standard deviations of  $\log_2(fc)$  values for the non-target features in negative ionization mode. H118, H120 and H121 are the laboratory names of the different PAC types (Table 4) which were tested for surface water treatment at three different concentrations.

	<b>Number of features</b>	<b>Mean <math>\log_2(fc)</math></b>	<b>Increasing/decreasing features [%]</b>	<b>Significant feature</b>
<b>H118</b>				
2 mg L <sup>-1</sup>	2318	-0.02 ± 0.31	0.3/0.5	0
7 mg L <sup>-1</sup>	2433	-0.13 ± 0.51	1.6/4.5	121
30 mg L <sup>-1</sup>	2482	-0.05 ± 0.55	2.6/3.7	118
<b>H120</b>				
2 mg L <sup>-1</sup>	2378	0.19 ± 0.34	2.9/0.0	17
7 mg L <sup>-1</sup>	2332	0.21 ± 0.36	3.5/0.2	50
30 mg L <sup>-1</sup>	2333	0.30 ± 0.38	6.7/0.2	125
<b>H121</b>				
2 mg L <sup>-1</sup>	2277	-0.03 ± 0.35	0.2/0.7	0
7 mg L <sup>-1</sup>	2357	-0.10 ± 0.37	0.2/1.6	0
30 mg L <sup>-1</sup>	2402	-0.06 ± 0.38	0.1/1.3	4

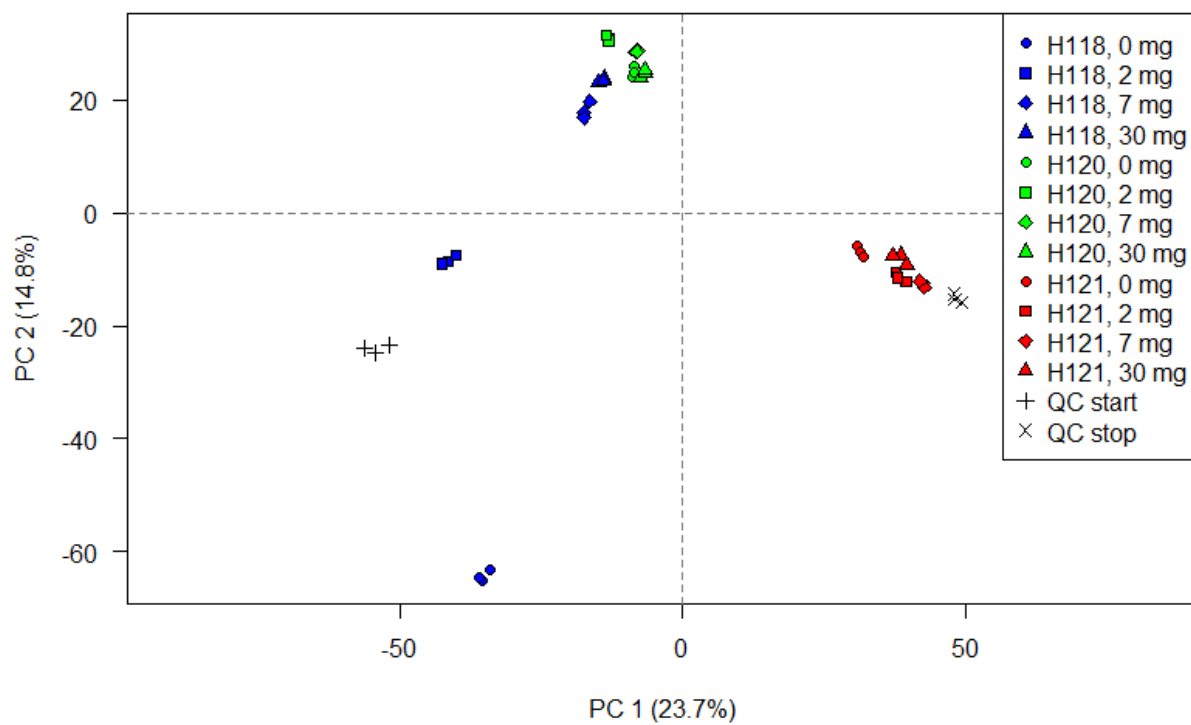


Figure S3: Scores plot of the PCA based on the normalized peak heights of the features extracted from each individual measurement in negative ionization mode.